SOME ASPECTS OF THE MATHEMATICAL MODELLING OF FIXED BED CHEMICAL REACTORS

by

William Richard Paterson

Thesis submitted for the degree of Doctor of Philosophy

UNIVERSITY OF EDINBURGH

1975

I declare that the work in this thesis is

my own, and that the thesis has been

composed by me.

11th June '78.

ACKNOWLEDGEMENTS

I should like to express my heartfelt thanks to Dr. D.L. Cresswell, but for whose advice, encouragement and enthusiasm this thesis might never have been completed.

I must further thank Mr. D. Ketchin and his workshop staff - particularly Mr. A. Donachie and Mr. K. Fee - for their help in the laboratory; Kate French, who proof-read with me; Graham Reed, by whose hands my rude diagrams were transformed; Jane Gorrie, who worked similar feats on my manuscript, Alan MacEwan, who took the photographs, and whoever it was who defined research as an attempt to unscrew the inscrutable.

CONTENTS PAGE

Chapter 1	Introduction	1
Chapter 2	The development of a simple, rapid and accurate method for the calculation of effectiveness factors	28
Chapter 3	Introduction to parameter estimation	64
Chapter 4	The development of approximate methods for parameter estimation in ordinary differential equations	87
Chapter 5	Applications of weighted residual methods to parameter estimation	122
Chapter 6	Extension of weighted residual methods to partial differential equations	146
Chapter 7	An introduction to the heat transfer investigation	165
Chapter 8	Heat transfer in beds of low 'aspect ratio'	216
Chapter 9	Concluding remarks	250
Appendix 1	Matters relating to effectiveness factor calculations	254
Appendix 2	Matters relating to parameter estimation	265
Appendix 3	Matters pertaining to the heat transfer investigation	286
Appendix 4	Experimental measurements for the flow case, arranged by angle	309
Appendix 5	Mathematical modelling of the exothermic packed bed reactor: application to o-xylene partial oxidation	325
References		336

Summary

Three aspects of the mathematical modelling of fixed bed chemical reactors are considered: the rapid solution of model equations, parameter estimation and model identification.

A novel method for the rapid solution of certain of the model equations - those describing reaction with diffusion in a catalyst pellet - is devised, based on the introduction of the concept of an "effective reaction zone", and on use of the orthogonal collocation technique.

Parameter estimation methods appropriate to the analysis of integral kinetic data are reviewed. New "weighted residual" methods are presented, their advantages - great convenience, low bias and acceptable efficiency - are demonstrated, and their extension to partial differential equation models is effected.

An experimental investigation of heat transfer in fixed beds of low tube to particle diameter ratio is reported and, following an examination of experimental error, it is concluded that the widely accepted two-dimensional quasi-homogeneous model is inadequate. It is also established that higher values of bed effective thermal conductivity obtain than are predicted by most available correlations.

CHAPTER 1:- Introduction

1.0 Introductory remarks.

1.1 Mathematical Modelling.

1.2 The Packed Bed Catalytic Reactor.

1.3 The Interaction of Physical and Chemical Processes.

1.4 Short range gradients: physical processes and their rates.

1.4.1 Flow of heat within the catalyst pellet.

1.4.2 Transport of material within the catalyst pellet.

1.4.3 Interphase transport.

1.5 Chemical Process Rates.

1.5.1 Experimental measurement.

1.5.2 Rate equations.

1.5.3 Incorporation of the rate equation into the reactor model.

1.6 Long Range Gradients.

1.6.1 The quasi-homogeneous model.

1.6.2 The heterogeneous model.

1.6.3 Cell models.

1.6.4 Remarks on models.

1.7 The pattern of the remainder of the thesis.

Explanation of symbols and terms.

Introductory Remarks

The subject of this work is the mathematical modelling of the steady-state behaviour of packed bed catalytic reactors. In this first chapter the nature of a mathematical model is reviewed, and three problems to be considered are listed. That is followed by a description of the packed bed reactor, with emphasis laid on the areas of uncertainty in its description. Finally the pattern of the remainder of the thesis is summarised.

1.1 Mathematical Modelling

The engineer is frequently faced with the problem of predicting the performance of equipment which is as yet unbuilt; or, if built, which must be operated under conditions not experienced previously. A powerful aid to such prediction is a mathematical model; that is, a set of relationships amongst dependent variables, whose values one seeks to calculate, and independent variables, whose values one may specify. The intention is that the values of the dependent variables predicted by the model be in good accord with the corresponding values observed experimentally. Such a comparison should be effected before a model is used.

Consider, for instance, a packed bed catalytic reactor. One might wish to compute the temperature and reactant concentrations (dependent variables) at some point in the bed i.e. for some specified set of values of, perhaps, axial, radial and angular co-ordinates (the independent variables).

Mathematical models will typically contain another type of entity, namely parameters, to which values must be assigned before

the model can be used predictively, but whose values are often established by suitable application of the model itself (or at least of some reduced form of the model) to the analysis of experimental results. Thus, one might use a simplified model to determine the values of chemical rate constants from the results of experiments in a laboratory-scale packed bed reactor, and then use these values of the rate constants (parameters) in predicting the behaviour of an industrial reactor.

A model will usually account for several different physical or chemical processes occurring within the equipment, and so a sub-model or "model component" will be required to represent each of these processes.

The work reported herein is addressed to three problems which arise in attempting to construct a useful mathematical model, or model component:-

Problem 1 - to devise a suitable model form. This problem is sometimes called "model building". One is concerned to find a set of equations with which to simulate the behaviour of the system under investigation. In Chemical Engineering the equations are usually derived from the Conservation Laws and relevant Rate Equations (1). G.E.P. Box (2) has proposed a scheme whereby some model is "tentatively entertained" and its appropriateness tested by the comparison of its predictions with the results of a suitably designed experiment. The model can then be rejected, improved or further entertained and, if necessary, new experiments may be performed, the model again tested, and the sequence continued until a model deemed adequate is found.

During this procedure one might wish to decide which of several models best represents the system - this task is called "model discrimination".

Problem 2 - to find suitable values for the model parameters, the so-called "parameter estimation" problem. Since, as explained earlier, we cannot use the model without parameter values, it is necessary to perform parameter estimation prior to each comparison of model predictions with experimental observations. Parameter estimation is thus a sub-problem of model building.

Problem 3 - to solve the model equations. Clearly the equations must be solved whenever the model is used. Equally, they must be solved prior to every comparison step in the model-building procedure, and further must usually be solved one or more times in performing parameter estimation. Economic considerations therefore motivate the development of rapid methods of performing such calculations. Since the model equations will often be nonlinear differential equations, then resort must often be made to approximate or numerical methods.

1.2 The Packed Bed Catalytic Reactor

Before carrying the above discussion farther, attention will be paid to the system which is the subject of this work viz. the packed bed catalytic reactor.

The word "catalysis" was first used by Berzelius in 1836 (3) to describe a number of experimental observations which included the discovery that ammonia was decomposed by metals, without the

metals apparently undergoing any change. Berzelius suggested that reactions could occur at the surfaces of solids provided that the latter possessed a "catalytic force". Although this last concept has long since been discarded, the conclusion that heterogeneous catalysis is a surface phenomenon has been well substantiated, and modern explanations use the concept of adsorption at "active sites" on the catalyst surface. Since the rate of catalytic reactions thus depends on the number of active sites available to the reactant molecules, it follows that catalysts can be made more active by arranging that a maximum of surface area is exposed to the (gaseous) reactants. So the catalyst, metal or non-metal, is spread thinly over the surface of some support material, or dispersed over the surface of the pores within that material. A packed bed reactor consists of a tube packed with pellets of such coated support. Through the packed bed so formed are pumped the reactant gases.

There has been, since the Second World War, a considerable research effort devoted to the study of such reactors, and progress may be gauged from a series of review publications (4-10). The difficulties associated with the modelling of such reactors stem from the interaction of the chemical and physical processes within them, and from the imperfect understanding of each of these types of process.

1.3 The Interaction of Physical and Chemical Processes

Consider a packed bed reactor effecting an exothermic reaction, with heat being removed from the system by a coolant flowing on the outside of the tube. Clearly there will be established axial concentration profiles, since the extent of reaction increases along

the tube. Additionally, an axial temperature profile will exist, with temperature initially rising as the reaction generates heat faster than heat can escape at the wall. If the bed is long enough, the temperature will eventually fall again as the heat generation rate declines below the heat removal rate; the former diminishing with decrease of reaction rate with decreasing reactant concentration, and the heat removal rate increasing with increase in the difference between bed and coolant temperature.

Moreover, there will of necessity be a radial temperature profile associated with the flux of heat from the bed centre to the wall, such that the former is at a higher temperature than the latter. Further, since chemical reactions generally proceed faster at higher temperatures, the reaction rate will tend to be greater in the centre, causing a depletion of reactants at the centre and the establishment of a radial concentration profile.

Although packed beds of square cross-section have occasionally been exploited industrially, tubes of circular cross-section are normally used. In these, cylindrical symmetry is assumed to obtain, so that 'angular' profiles need not be considered.

In short, there exist within packed beds gross axial and radial gradients of temperature and concentration.

However, there also exist gradients on a finer scale; different values of temperature and concentration pertain to the solid in the bed and to the gas flowing through the interstices of the bed. There is generally a sufficient "film resistance" or "boundary layer resistance" to heat and material flow at the surface of the solid particles to ensure that the surface is at higher temperature than

the gas, and that the reactant concentration there is lower than in the gas. Additionally, for a porous particle, the finite rate at which reactant can diffuse through the pores gives rise to intra-particle concentration profiles, and considerations similar to those concerning the bed radial temperature profile reveal that there exists also an intraparticle temperature profile.

The contents of this section are summarised in figure 1.1.

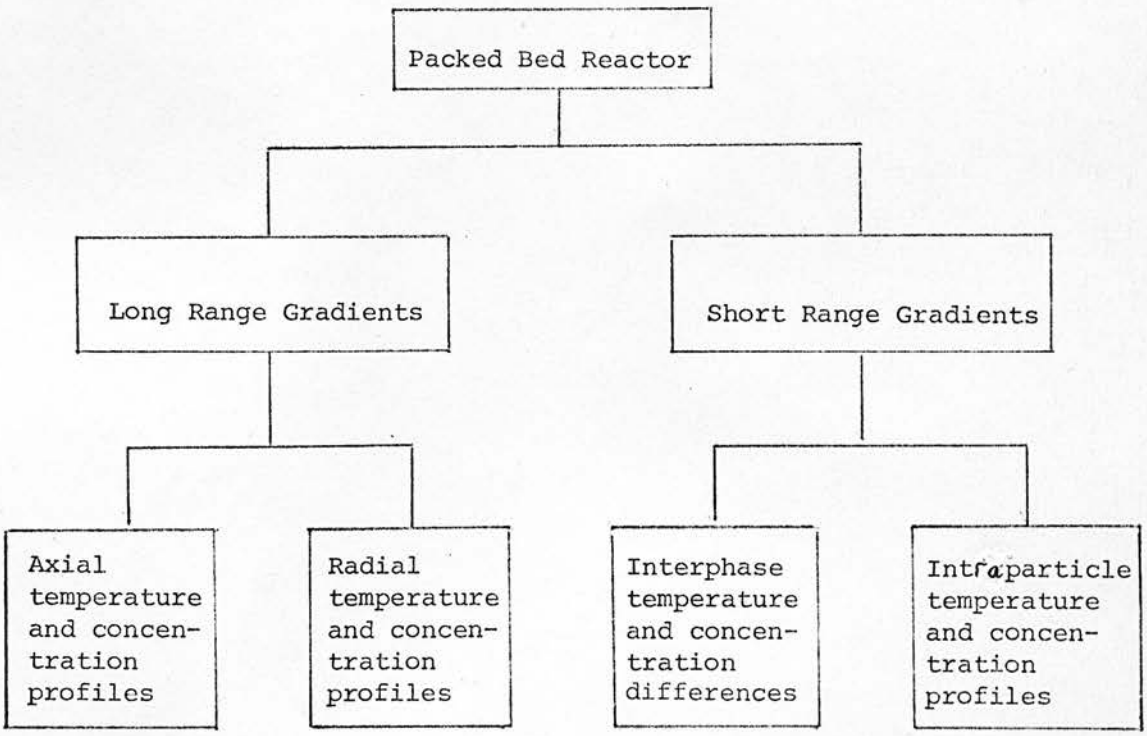

Figure 1.1 : The Scale of Gradients Within a Fixed Bed Reactor

1.4 Short-range Gradients: Physical Processes and their Rates

1.4.1 Flow of heat within the catalyst pellet

Catalyst supports are often manufactured by compaction of small particles, within each of which there is a network of very small pores called "micropores". Between the compacted particles there will normally be larger pores - "macropores". The pore structure largely determines many of the properties of the pellet. Clearly, heat flow through the pellet will involve conduction in the solid, convection within the gas-filled pores and radiation across the pores, and these mechanisms operate in series and in parallel. Nevertheless, workers in the field have universally described the heat flow by Fourier's Law using an effective thermal conductivity (K), based on the complete cross-section area of the pellet, not merely on that fraction which is solid.

The effect of the porous structure is to reduce the conductivity of the support far below that of the solid of which the support is composed - by an order of magnitude or more. Smith (11) has reviewed the difficulties involved in predicting K, but has pointed out that it is possible to choose a reasonable value because the possible range of values (excluding vacuum conditions) is narrow, approximately 0.15 to 0.70 W/m deg K. Tables of K values for various supports and a useful discussion are included in Satterfield's text (12).

The difficulty of predicting K accurately is not as serious as it might appear for two reasons:-

(i) The value is easy to measure, using one of Sehr's methods (13).

(ii) The prediction of a reactor model will usually be insensitive to K, because, firstly, the true value of K may often be sufficiently high that the catalyst pellets are essentially isothermal, so that the rate of reaction in the pellets is independent of the value of K; and secondly, the value of K has only a minor effect on the calculated values of the bed heat transfer parameters, and so again has little effect on the predictions of the model.

It would seem, then, that the estimation of a value of K should cause little difficulty for the modeller.

1.4.2 Transport of Material Within the Catalyst Pellet

The pressure drop accompanying gas flow through a packed bed causes a pressure differential across each catalyst pellet, leading to a tendency for gas flow through the pellet's pores. However, this flow is quite negligible compared to that due to diffusion (12). Material transport may also be affected by pressure difference due to change in the number of moles in reaction (14). However, if attention is restricted to equimolal reactions or to reactions carried out with considerable dilution by inert gas or an excess reactant, then the effect is negligible.

The major transport mechanisms within the pellet are diffusive. In large pores, ordinary or "bulk" diffusion occurs, whilst in pores of diameter comparable with the molecular mean free path, Knudsen diffusion predominates - a process wherein molecules collide with the pore wall, are momentarily adsorbed and are then ejected in random directions ("diffusely reflected"). Lastly, there can occur surface diffusion, an ill-understood mechanism whereby there is a flow

of mobile adsorbed molecules down a surface concentration gradient. Unfortunately, it is possible for this mechanism to interact with Knudsen diffusion (15) and potentially with catalytic reaction, thus complicating analysis of the effect.

In practice, diffusive transport is described using Fick's Law and an effective diffusivity (16), and various "theories" or models have been advanced to permit calculation of this quantity from a knowledge of the pellet pore structure, and of the bulk and Knudsen diffusion coefficients. (Consideration of surface diffusion is usually omitted on grounds of lack of understanding). These models are important because it is much easier to measure the properties of the pore structure than to measure the effective diffusivity directly. In recent reviews of such models (17,18) it has been concluded that the predicted diffusivities are reliable at best within a factor of two, and can be much worse.

A further question arises, namely, is the effective diffusivity measured under non-reactive conditions (D_{NR}) equal to that obtaining when chemical reaction is occurring (D_R)? Stoll and Brown (17) cite five systems where D_R was found to be considerably less, by up to a factor of 3, than D_{NR}, and only one case where the two agreed well. However, three other cases of good agreement have been reported, although none are apparently particularly representative. Kadlec et al (19) claimed good accordance for SO_2 oxidation in a pellet of simple pore structure, Hawtin (20) for the diffusion of O_2 and N_2 with gas/solid non-catalytic reaction in graphite and in porous non-graphitic carbon and Raja Rao and Smith (21), (who used an admittedly insensitive technique) for ortho-para H_2 conversion over Ni supported in a Vycor glass of particularly simple pore structure.

On the other hand, Wakao (21) has claimed, as a result of simulation and experiment, that under suitable circumstances D_R and D_{NR} should differ by up to a factor of five, due to the differing importance of the role of the micropores under reactive and non-reactive conditions. Other Japanese workers (23) have presented persuasive evidence that one source of the discrepancy between the two effective diffusivities, in certain pellets, is the non-uniformity of the pore structure; specifically, the occurrence of a high degree of blockage of macropores near the pellet surface. This discovery implies that a modeller would need to know the effective diffusivity as a function of position within the pellet, a formidable requirement.

In the face of such difficulties, it might seem best to measure the effective diffusivity in the presence of reaction, but this demands, inter alia, a good understanding of the reaction kinetics, which is itself difficult to come by.

In summary, the calculation of the rate of transport of material within the pellet is a major source of uncertainty in reactor modelling. Happily, work continues in an attempt to rectify this situation (24).

1.4.3 Interphase Transport

The transport of material and heat between the pellet and the gas flowing past it is described using the familiar mass and heat transfer coefficients. It is assumed that instead of point transfer coefficients, the more easily measured and used mean coefficients can be adopted without introducing substantial error (25). Further, the dependence of the coefficients upon the position of the pellet within the bed is ignored.

Appropriate values for the heat transfer coefficient are calculated from experimentally determined dimensionless correlations involving (usually) a j_H group related to a Reynold's Number (Re_p). Barker (26) has compared a large number of correlations and states that there is general agreement within a factor of two for predicted values of the heat transfer coefficient. More recently, Whitaker (27) devised a correlation which he claimed to be accurate to better than 25%. However, he surveyed a smaller field of data than did Barker. Lately, an attempt has been made to improve correlative success by introducing into the correlation an Archimedes number, which involves the pellet density and is used to account for the 'compactness' of the bed. Although success is claimed, figure 6 of (28) suggests a systematic discrepancy from the results of earlier workers, a conclusion not drawn by the authors.

Values of the mass transfer coefficient are calculated from j_D correlations. Early work was erroneous because of an unrecognised axial dispersion effect, but corrected correlations now exist (29) of accuracy presumably comparable with that of their heat transfer equivalents.

An indirect measure of correlation accuracy stems from examination of the predicted ratio of j_H to j_D: this ratio is reported variously as unity (4), 1.076 (believed to be wrong (30)), and 1.37 (30).

The scatter in the predictions of the correlations is due not only to difficulties of measurement, different experimental techniques and the overlooked presence of intraparticle temperature gradients, but probably reflects real differences in coefficient values in different investigations due, for example, to different packing patterns and surface roughnesses.

Apparently, then, one can make more accurate predictions of transfer coefficients than one can of, for instance, intraparticle effective diffusivity. It would seem that significantly better correlations, based on a mean coefficient, are unlikely to be devised, since those already existing have an accuracy comparable with other convective transfer correlations.

1.5 Chemical Process Rates

There is no theory which permits adequate prediction of the rates of heterogeneous catalytic reactions of interest to the engineer; expressions relating the rate of reaction to the concentration of the species involved and the temperature must be derived from experiment.

1.5.1 Experimental Measurement

Rate measurement equipment is designed to avoid (i) short-range gradients, which would distort the kinetics, (ii) mechanical complexity, which often leads to poor reliability, (iii) undue difficulty in interpreting the results, (iv) long-range temperature gradients which, if observed, lead to (iii) and if not, to falsified kinetics. The apparatus used is usually a variant of one of three types discussed below, although others have been tried (31).

a) The integral reactor: wherein some appreciable degree of conversion is obtained in a small-diameter tubular packed bed reactor cooled at the wall. Since it is an integral conversion which is measured rather than a rate, analysis of the results is often difficult, even more so if the bed is non-isothermal, a condition which it is often difficult to avoid even using catalyst dilution (32).

The avoidance of short-range gradients is difficult. Direct calculation using available correlations may suggest that gradients external to the pellet are insignificant, and this may be confirmed in suitable circumstances (33) by varying Re_p while holding reactor residence time constant. The significance of internal gradients is usually judged from experiments using different sizes of pellets.

b) The differential reactor is typically a short packed bed with a degree of conversion, and concomittant temperature rise, so small that the whole reactor may be viewed as operating at the same value of concentration and temperature. The measured conversion can readily be used to calculate a rate of reaction (which is held to appertain at that set of values), and so data analysis is simple. Short-range gradients are dealt with as above. The reactor may be used to investigate different concentration ranges either by placing it in series after an integral reactor, or by using a synthetic feed.

The major disadvantage of the differential reactor is that if conversion is low enough for the 'differential' concept to be used, then the change in composition will be so low as to be difficult to measure accurately.

c) The perfectly mixed reactor is designed to operate with concentrations and temperature uniform throughout, so that the rate corresponding to those concentrations and temperature is easily computed. The reactor takes one of three forms. First, there is the tubular reactor with external recycle loop. This device has the interphase transport resistance problems associated with a tubular reactor,

and often has problems associated with the recycle compressor. Secondly, one can use the 'spinning catalyst basket reactor' (34,35), an arrangement where a basket containing catalyst pellets is spun at high speed in a chamber full of reaction mixture. There are three important disadvantages - it appears (36) that the spinning basket sets the reaction mixture spinning too, so that the pellet/gas relative velocity is low enough for interphase resistances to be important; the reaction vessel often has enough free space and exposed solid surface for an appreciable degree of homogeneous reaction or vessel-surface catalysed reaction to occur; and the mixing may be imperfect (37).

Thirdly, there is the 'internal recycle stationary bed reactor', where a fixed bed of catalyst is operated with a high recycle rate of gas within the vessel in which the bed is located. This arrangement is intended to avoid the mechanical troubles of the external recycle loop and the transport resistance problems of the spinning basket (38,39).

In all the perfectly mixed reactors, the problems of pellet internal gradients are dealt with as in the integral reactor.

1.5.2 Rate Equations vary from entirely empirical forms (40), to power law kinetics analogous to the "mass-action" kinetics of homogeneous reactions and finally to such semi-theoretical forms as those of Hougen and Watson(4). The rates of reaction ought properly to be defined in terms of surface area of catalyst, but are more often written in terms of mass of catalyst pellet. It follows that the specific surface area of pellets ought to be determined and reported with the rate data.

Hougen-Watson (H-W) equations are derived from an (approximate) adsorption theory of catalysis based on the work of Langmuir and Hinshelwood. One proceeds by postulating a reaction mechanism and then invokes various simplifying assumptions (4,41) to arrive at a rate law, which Sawyer (42) has dubbed a 'model', to distinguish it from the mechanism. There has been some argument on the merits of H-W kinetics; arguments relevant also to the other 'theoretical' rate expressions sometimes used in heterogeneous catalysis (43,44).

It has been shown that the assumptions of the theory are frequently wrong (42,45,46,47) and that power-law kinetic expressions often fit experimental data better than H-W forms (47,48). Against this, it has been argued that H-W theory has some measure of validity, and that a theory casting any light on the subject is useful and should become more so as its shortcomings are discovered and remedied (49).

There does seem to be agreement that some published work includes unreasonable claims of having established a mechanism merely on grounds of a model yielding a good fit to experimental data. There are three flaws in such claims. First, different mechanisms can, under appropriate assumptions, lead to the same form of model and one mechanism can be reduced to the same model under various quite different sets of assumptions. Secondly, various untested models might fit the experimental data as well as, or better than, the favoured model. Thirdly, the proposed mechanism will often involve intermediates whose very existence has not been observed. These flaws are not unique to catalytic kinetics (50).

An important disadvantage of H-W kinetics is the proliferation of parameters in the rate equations. The value of these parameters (typically adsorption equilibrium constants) are estimated from the kinetic data and are not measured separately. Indeed, values of the adsorption constants obtained from kinetic and independent experiments often disagree (51), and values deduced from kinetic experiments may be physically implausible (48).

Computer methods have made it possible to generate (52) and screen large numbers of H-W (and other) models to see which best fit the data. Modern statistical methods are available to help the experimenter plan new experiments to discriminate between, and estimate parameters in, the models (45), although these are not without their pitfalls (53).

The unsatisfactory state of catalytic kinetics may be appreciated from the fact that there is no agreement on the best form of model (52) for such an intensively studied reaction as iron catalysed NH_3 synthesis. Among the techniques advocated to better our understanding of the subject are programmed temperature desorption studies (42), the use of marked atoms and of the stoichiometric number concept (44), and the use of pulsed microcatalytic reactors (54), which might allow discrimination between power-law and H-W models which fit steady-state data equally well (55). Other advanced techniques are described by Yates (56).

There is one other difficulty plaguing catalytic kinetics viz. the activity of catalysts will often change substantially during experimentation and from one manufacturing batch to another (57). When that source of uncertainty is added to that of ill-established model form and the poor confidence in parameter estimates due to the number of parameters to be established and the scatter in the data,

it will be seen that the kinetic equation will often contribute a considerable measure of uncertainty to the mathematical model of the reactor, especially if the rate equation is used for extrapolation.

1.5.3 Incorporation of the Rate Equation into the Reactor Model

For this purpose, resort is frequently made to the effectiveness factor, defined as the ratio of the rate of reaction associated with a catalyst pellet to the rate which would occur if all the catalytic surface in the pellet were exposed to gas of the same composition and temperature as the gas flowing past the pellet. Then, in the reactor model one uses the chemical rate expression multiplied by the effectiveness factor to calculate the local reaction rate.

It will be seen that the definition above introduces another idealisation viz. that there is a simple set of concentrations and temperature attributable to the gas passing the pellet, whereas in practice that gas will be non-uniform due to the long-range gradients in the bed. Petersen et al.(58) calculate that this approximation is satisfactory.

The behaviour of this somewhat idealised pellet - which one might call a "pseudo-pellet" - is described by a set of boundary value non-linear ordinary differential equations (o.d.e.'s), the solution of which is often difficult. The title 'pseudo-pellet' may be further justified by noting that when the packed bed equations are solved, the pseudo-pellet equations will often be solved for conditions corresponding to a position in the bed which bears no particular relationship to the location of the real catalyst pellets, and further, that the

quasi-homogeneous description of the bed assumes that the pellet may be treated as being of negligible size, whereas the very existence of intrapellet gradients reveals that this description is inadequate.

1.6 Long Range Gradients

Three different approaches to the problem of accounting for the long-range gradients are next examined.

1.6.1 The quasi-homogeneous model

Here the bed is treated as a quasi-phase, as if it were homogeneous "in the large". The detailed location of pellets and the shape, size and direction of the interstices of the bed are alike ignored. The bulk flow of gas in the axial direction is (almost always) assumed to be "plug flow" (11). Imposed on that there may be radial and axial dispersion of heat and material, described by Fourier's and Fick's Laws respectively, with use made of bed-effective radial and axial thermal conductivity and mass diffusivity. Experiments on packed beds in the absence of reaction reveal that radial rates of heat transfer in the centre of the bed are much greater than in the region close to the wall. The usual way of allowing for this increased resistance near the wall is to use an effective wall heat transfer coefficient, although an alternative is simply to define a zone near the wall with effective thermal conductivity much lower than the central zone (59). Further, it is assumed that temperature and composition vary smoothly within the bed, in spite of their known sharp change at the pellet surface. The model is, then, no more than a hopefully adequate compromise between the desire to faithfully describe

reality and the necessity that the model be useful, in the sense that its parameters may be estimated and its equations solved.

A report of what is known about the values of these parameters is now in order:-

i) Bed effective axial diffusivity. The value of this quantity has been much studied, and the findings are best summarised (60,8) by taking the value of the axial Peclet number for mass to lie between 1 and 2, probably nearer 2.

ii) Bed effective axial conductivity. This parameter has received much less attention, but a value of between 1 and 2 for axial Peclet number for heat appears to characterise it adequately (61).

iii) Bed effective radial diffusivity. Again resort is made to a Peclet number description; the range 8 to 11 appears to have been well confirmed (8).

iv) Bed effective radial conductivity. Froment's (8) figure 5 showing the correlations of several workers does suggest that the approximate linear dependence on Re_p is generally accepted, and that the magnitude of the conductivity at any value of Re_p is tolerably well established ($\sim \pm 30\%$), although a plot of the original experimental data would doubtless show more scatter.

v) Effective wall heat transfer coefficient. As Froment's figure 6 and Beek's (6) figure 4 demonstrate, the value of this parameter is poorly established. Neither its magnitude at given Re_p nor its dependence on Re_p is agreed upon. At $Re_p = 100$, the upper and lower predicted values of the coefficient differ by a factor of three. This range might well widen if more workers' correlations were included in the comparison.

The values of the axial dispersion parameters (in (i) and (ii) above) are such that axial dispersion effects are normally neglected, being small relative to the bulk flow, although recently it has been suggested (62) that the effects may be more important than has been imagined.

If this usual simplification is retained, then the quasi-phase is described by non-linear parabolic partial differential equations (p.d.e.'s), coupled with the equations of the pseudo-pellet. The resulting set of equations is mathematically intractable and requires numerical solution.

1.6.2 The heterogeneous model

In this case the reactor is regarded as containing two continuous phases, solid and gas. The model is not easily visualised geometrically, but is claimed to better represent reality (63). However, as no comparison has been effected with experimental results from a packed bed reactor, the claim is as yet unsubstantiated.

1.6.3 Cell models describe the behaviour of a packed bed as equivalent to that of an array of perfectly mixed cells, and thus provide an alternative representation of axial and radial dispersion phenomena. The relationships between cell and diffusive models have been extensively analysed (e.g. 64), and it has been shown that dispersion effects are predicted similarily by suitable cell models and by diffusive models with axial Peclet number ~ 2 and radial ~ 10.

Two cell models have been used in reactor modelling: Deans and Lapidus (65) used an arrangement in which the cell size was determined by heat and mass transfer considerations, whereas Caldwell (66) used a 'matrix model' such that each mixing cell contained exactly one catalyst pellet.

These models will not be further examined because

i) Gunn and Pryce (67) concluded that dispersion in a random packed bed is better described by a diffusive than a cell model.

ii) Caldwell (66) judged that the disadvantages of his cell model outweighed its advantages.

Lastly, note that the relationship between cell models and the finite difference equations which arise in the customary solution methods for the p.d.e.'s of the diffusive models has been examined by Rosenbrock and Storey (68), and that related comparisons have attracted the interest of Greenspan (69).

1.6.4 Remarks

The quasi-homogeneous model is currently the most widely used; there are estimates of the values of its parameters, and of their accuracy, available, and computational techniques for its solution are well developed. One of its features is its well known 'parametric sensitivity'; that is predictions can change greatly due to a small change in parameter values. Ironically, the model predictions tend to be most sensitive to the values of the least well established parameters. A summary of the position is shown in Table 1.

Table 1: The importance and accuracy of parameter values in the quasi-homogeneous reactor model.

Parameter	Relative Importance	Approximate accuracy of prediction (as a factor)
Intraparticle effective diffusivity	High	3
Interphase mass transfer coefficient	Low	0.3
Bed-effective radial diffusivity	Low	0.2
Pellet effective thermal conductivity	Low	2
Interphase heat transfer coefficient	High	0.3
Bed-effective radial thermal conductivity	Low	0.3
Effective wall heat transfer coefficient	High	2
Chemical Kinetics	High	-

1.7 The pattern of the remainder of the thesis

Recall the three problems listed in section 1.1.

First, model-building. The remarks of section 1.6 on the models, and parameters, describing the long-range gradients in packed bed reactors relate to those beds which have received considerable attention viz. those with tube to particle diameter ratio > 10. Much less is known about the industrially important beds of lower 'aspect ratio', and it might appear, a priori, that a diffusive model is unlikely to succeed (70). Chapters 7 and 8 report an experimental examination of this problem.

Secondly, parameter estimation. Parameter estimation in differential equations is important in heat transfer studies and in the analysis of integral kinetic data. Current methods are expensive, both of man-hours of programming and of CPU time, and sometimes ineffective. New algorithms designed to rectify these faults are presented in chapters four and five (o.d.e.'s) and chapter six (p.d.e.'s). A successful application to (non-isothermal)integral kinetic data is reported in chapter five, and some success in related model discrimination is also reported there.

Finally, equation solving. The solution of the bed equations is predicated on the solution of the pellet equations. Chapter two contains the development of a successful new method devised for the latter task. A description of the solution of a packed bed reactor model (for the partial oxidation of o-xylene to phthalic anhydride over vanadia) will be found in the paper appended to this thesis - appendix 5 - along with an examination of the sensitivity of predictions to the values of intraparticle effective diffusivity and interphase transport coefficients.

In short, this thesis presents some contribution to advance in each of the three problem-areas central to mathematical modelling.

Explanation of Symbols and Terms

K - effective thermal conductivity of the pellet

D_{NR} - effective diffusivity of the reactant through the pellet, measured in the absence of reaction

D_R - effective diffusivity of the reactant through the pellet, measured in the presence of reaction

Re_p - Reynold's number, based on pellet diameter $\equiv \frac{Gd_p}{\mu_f}$

j_H - Chilton and Colburn's j-factor for heat transfer $\equiv \frac{h}{GC_p} Pr^{2/3}$

j_D - Chilton and Colburn's j-factor for mass transfer $\equiv \frac{k_G P_t}{G_m} Sc^{2/3}$

Peclet number - a dimensionless group discriptive of diffusion parameters

$Pe_{H,r}$ - Peclet number for heat transport in the radial direction

$$\equiv \frac{GC_{pf} d_p}{k_{er}}$$

$Pe_{m,r}$ - Peclet number for mass transport in the radial direction

$$\equiv \frac{Gd_p}{D_{b,r} \rho_f}$$

$Pe_{H,a}$ - Peclet number for heat transport in the axial direction

$$\equiv \frac{GC_{pf} d_p}{k_{ea}}$$

$Pe_{m,a}$ - Peclet number for mass transport in the axial direction

$$\equiv \frac{Gd_p}{D_{b,a}\rho_f}.$$

Archimedes number $Ar \equiv \frac{d_p^3 g\rho_f(\rho_p-\rho_f)}{\mu_f^2}$

G - mass flux through bed i.e. mass flow rate of gas per unit of cross section area of the bed

d_p - pellet diameter

μ_f - viscosity of gas mixture

h - gas/pellet heat transfer coefficient

C_p - specific heat of the transferring species

Pr - Prandtl number of the transferring species $\equiv \frac{C_p\mu}{k}$

μ - viscosity of the transferring species

k - thermal conductivity of the transferring species

k_G - gas/pellet mass transfer coefficient (defined for a driving force of partial pressure difference)

P_t - total pressure

G_m - molal flux through bed i.e. molar flow rate of gas per unit cross section area of the bed

Sc - Schmidt number of the transferring species $\equiv \frac{\mu}{\rho D_m}$

ρ - density of the transferring species

D_m - diffusivity of the transferring species

C_{pf} - Specific heat of gas mixture

k_{er} - bed effective thermal conductivity in the radial direction

$D_{b,r}$ - bed effective mass diffusivity in the radial direction

$k_{e,a}$ - bed effective thermal conductivity in the axial direction

$G_{b,a}$ - bed effective mass diffusivity in the axial direction

g - local acceleration due to gravity

ρ_f - density of gas mixture

ρ_p - density of pellet

CHAPTER 2:- The Development of a Simple, Rapid and Accurate Method for the Calculation of Effectiveness Factors

2.1 A brief review of research on catalytic reaction in the presence of transport resistances - the steady state case.

2.2 The need for a rapid method for effectiveness factor calculations.

2.3 The model equations and the assumptions used in their derivation.

2.4 Numerical solution methods.

2.5 The Method of Weighted Residuals (M.W.R.).

2.6 The concept of the "Effective Reaction Zone", and its application.

2.7 The utility of the method and its possible extensions.

2.8 Notation.

Note: part of the contents of this chapter has been published:-

Paterson W.R. and Cresswell D.L., "A simple method for the calculation of effectiveness factors", in Chemical Engineering Science, Volume 26 pp 605-16, 1971.

2.1 A Brief Review of Research on Catalytic Reaction in the Presence of Transport Resistances - the Steady State Case

According to Aris (71), the analysis of diffusion and reaction began with Juttner in 1909, although his efforts were ignored for sixty years. Research restarted independently in the late nineteen-thirties in Germany, the U.S.S.R. and the U.S.A., and continued until, by the late nineteen-sixties, an extensive body of knowledge had accumulated. Since that knowledge has been well reviewed (12,16), only a brief account is included here. Broadly, the work progressed through the four stages shown in table 2, although there were also publications on such topics as diffusion with reaction in pellets with bi-disperse pore structures (e.g.72).

In stage one, the degree to which diffusion restricted the rate of reaction was examined, and a dimensionless group known as the "Thiele modulus" (Ω) was introduced as a measure of the relative rates of reaction and diffusion. In stage three, account was taken of the finite rate at which heat could be conducted through the pellet to its surface, and so two more groups were introduced:- β, the thermicity factor, a dimensionless measure of the relative rates of heat release by reaction and heat removal by conduction; and γ, a dimensionless activation energy, measuring the sensitivity of reaction rate to temperature. Table 3 shows approximate values of β and γ for some industrial reactions. Two important discoveries were made concerning exothermic reactions. First, it was found that values of the effectiveness factor (η) greater than unity are possible: that is, the transport resistances can enhance the rate of reaction. This situation occurs when the rise in temperature within the pellet

Table 2: Progress in the Analysis of the Interaction of Catalytic Reaction and Transport Resistances - the Steady State Case

Topic Investigated	Stage Number
Isothermal, irreversible, first-order reaction with pore diffusion	1
Reaction type extended to include reversible reaction, and power-law and H-W kinetics Analysis extended to include pellets of a variety of shapes	2
Extension to non-isothermal reactions where the pellet thermal conductivity assumes some importance	3
Extension to account for interphase resistances to heat and material transport	4

Table 3: a) Approximate Values of β and γ for some Industrial Reactions (adapted from (92))

Reaction	γ	β
NH_3 synthesis	29	6×10^{-5}
Synthesis of higher alcohols from CO and H_2	28	8×10^{-4}
Methanol oxidation	16	0.01
Vinylchloride Synthesis	7	0.25
Ethylene Hydrogenation	25	0.04 - 0.1
Oxidation of H_2	7	0.03 - 0.3
Ethylene Oxidation	13	0.1
Dissociation of N_2O	22	0.05 - 0.1
Benzene Hydrogenation	15	0.1
SO_2 oxidation	15	0.01

Table 3: b) Approximate Range of Parameter Values of Interest (Adapted from (93))

β	< 0.5
γ	< 40
Q	0.1 - 10
Sh	20 - 20,000
Nu	1 - 200

Note that Carberry (94) has suggested that Nu will rarely exceed 10, and may be less than unity in some cases. He further suggests that $Sh/_{Nu}$ may vary from 20 to 50,000

Table 4: Relative Importance of Physical Resistances (93,95,96)

Resistance	Importance
Interphase heat transfer	High
Intrapellet diffusion	High
Interphase mass transfer	Intermediate
Intrapellet conduction	Low

increases the reaction rate by more than it is decreased by the fall in reactant concentration. Secondly, it was found that for certain combinations of values of β, γ and Q, a pellet can exhibit three steady states. It was already known (73) that reaction at a non-porous surface, in the presence of interphase transport resistances, could yield three steady states.

Stage four involved combining the effects of interphase transport resistances with those of intra-pellet resistances, leading to the introduction of two more dimensionless groups to describe the relative rates of interphase and intrapellet transport of material and heat - the Sherwood (Sh) and Nusselt (Nu) numbers. The combination was found to be capable of giving rise to a multiplicity of steady states: Hatfield and Aris (74) found that five could exist in suitable circumstances. Another finding of stage four was the elucidation of the relative importance of the different transport resistances for industrially important ranges of parameter values - see table 4.

After stage four, work has progressed in two different directions. One line is the investigation of the multiplicity problem: to establish regions of parameter space where the steady state is unique, and investigate the number and stability of steady states elsewhere (e.g. 75-81), and further to establish bounds on the value of η. Of particular interest is a paper of Varma and Amundson (82), who provided a method for calculating maximum and minimum values of η: in cases where the two coincide, of course, only a unique steady state can exist.

The second line of work is the exploration of the assumptions on which previous work is based. The most intensively studied is the question of the symmetry of solutions. Consider an exothermic reaction carried out in a uniform slab of catalyst, of finite width and infinite length: the temperature and composition of the gas on each side of the slab are equal, as are the interphase transport coefficients. In stages one through four, the reasonable assumption was made that temperature and concentration profiles in the slab would be symmetrical. However, this is not necessarily true for a non-porous slab with reaction limited to the surface (83), - which, upon reflection, is not unreasonable (84). But, more surprising, Horn, Jackson et al. (85) discovered that for a porous slab asymmetric profiles were possible. This phenomenon, and the associated stability problem, has since been further investigated (86-89). It must be distinguished from asymmetry arising from differences in local coefficients of heat and mass transfer (90).

However, a yet more fundamental re-assessment of assumptions has been carried out by Jackson (91) who shows that the conventional o.d.e.'s used to describe binary diffusion with isothermal reaction are of restricted applicability, and should in general be replaced by an integro-differential equation. The new formulation reduces to the conventional one only in special circumstances such as steady states in highly symmetric geometries e.g. the sphere, the infinite cylinder and the semi-infinite slab, while "it should also be noted that the integral terms appear in steady-state calculations, even for geometries as simple and realistic as a cylinder of finite length, whenever the reaction is accompanied by a change in the number of molecules". This new approach casts doubt on previous work on stability,

uniqueness and symmetry, although no numerical results have yet been reported to show the extent of error in previous results. Happily, Jackson's discovery does not invalidate much of the work up to stage four of table 2, and, in particular, does not falsify the contents of this chapter and of appendix 5, involving, as they do, steady states in a sphere.

2.2 The need for a rapid method for effectiveness factor calculations

Consider a tubular reactor 3 m long by 2.5 cm diameter, packed with catalyst pellets 0.5 cm in diameter: such a bed will normally contain rather more than ten thousand pellets. The behaviour of each pellet is described by a set of o.d.e.'s, from whose solution the pellet effectiveness factor may be calculated. Although in simulating the reactor the equations need not necessarily be solved for every real pellet, still the effectiveness factor must be calculated many times. Since the pellet equations are intractable analytically and numerical solution is excessively time-consuming and occasionally unreliable, two approaches have been adopted to simplify the calculations:-

i) The effectiveness factor is computed under a range of conditions covering those likely to occur in a reactor. The results are then correlated empirically with the pellet parameters Q, β, γ. (97-100). A related technique consists of storing the effectiveness factor values, and using table look-up and interpolation as necessary (101). Jouven and Aris (99) report a reduction in computer time, compared with numerical solution, by a factor of fifty, with an error of less than 10%, and an even greater time-saving has been claimed by other workers (100).

This approach suffers from the disadvantage that the results will pertain only to a single class of reactions - typically irreversible first-order - and to a single type of pellet - usually a sphere of uniform properties i.e. with effective diffusivity (D_e) and pellet conductivity (K) independent of position. As was remarked in section 1.4.2, the latter restriction might be of consequence.

However, the first restriction is clearly the major shortcoming of the method. Not only would a different reaction order necessitate the construction of a new correlation, but a H-W kinetic expression would contain too many parameters to permit a correlation to be constructed at all.

ii) Alternatively, approximate solutions to the relevant o.d.e.'s are developed - see Table 5.

Further to the work shown there, Cresswell (95) compared Petersen's method - extended to include finite Sh and Nu (107) - with an approximate method of his own, the "lumped thermal resistance model" (108) {applicable only to first and zeroth order reactions}, which exploits the near-isothermality of the pellet under a wide range of parameter values (95, 104). He found the latter to be the more useful, and proposed an extension to allow for a small temperature rise within the pellet.

However, this work, and that of table 5, leans heavily on the use of various simplifying assumptions which are applicable over a limited and not easily-identifiable range of conditions, and are thus unsatisfactory. In section 2.6 an alternative technique is developed.

Table 5: Approximate solutions to the effectiveness factor problem

Workers	Method	Case Treated	Success (Exothermic reactions)
Schilson and Amundson (102)	Approximation of the heat generation function by one or two straight lines	$Sh = \infty = Nu$	Only when pellet centre temperature ≃ maximum possible
Beek (96)	Linearisation of reaction rate as a function of temperature and concentration	General	Only under mildly reactive conditions ($\eta \sim 1$)
Tinkler and Pigford (103)	Perturbation technique	Nu finite, $Sh = \infty$ First order irreversible reaction	Only under mild non-isothermality
Petersen (104)	Asymptotic method, with concentration of reactant assumed to be zero at pellet centre.	$Sh = \infty = Nu$	Useful for $Q > 3$, if β and γ not too large
Gunn (105)	Taylor series expansion of rate constant as a function of radial position in the catalyst sphere	First-order reaction $Sh = \infty = Nu$	Useful if reaction is only mildly exothermic
Hlavacek and Marek (106)	Simplification of Arrhenius temperature dependency	Zeroth order reaction $Sh = \infty = Nu$	Successful for a wide range of values of γ, β, Q, but the case is too restrictive for general use.

2.3 The model equations, and the assumptions used in their derivation

The interaction of in-pore diffusion, heat conduction and a single chemical reaction is described by the system of second order ordinary differential equations

$$\frac{d^2c}{dy^2} + \frac{a}{y}\frac{dc}{dy} = Q^2 \exp\{\gamma(1 - \frac{1}{t})\} f(c) \qquad (2.1)$$

$$\frac{d^2t}{dy^2} + \frac{a}{y}\frac{dt}{dy} = -\beta Q^2 \exp\{\gamma(1 - \frac{1}{t})\} f(c) \qquad (2.2)$$

where c, t and y are respectively the dimensionless concentration, temperature and distance from the centre of symmetry. Q, β and γ represent the familiar Thiele modulus, Thermicity and Activation Energy Parameter. The geometry of the catalyst pellet is described by 'a' - the values 0, 1 and 2 corresponding to the semi-infinite slab, infinite cylinder and sphere, respectively. The function f(c) describes the kinetic rate expression e.g. n^{th} order, or a more complicated Hougen-Watson form. It is assumed that the solutions of equations (2.1) and (2.2) are symmetrical about y = 0, hence

$$\text{At } y = 0, \frac{dc}{dy} = 0 = \frac{dt}{dy} \qquad (2.3)$$

At the surface of the catalyst pellet, the finite rates of convective mass and heat transfer lead to the conditions

$$c = 1 - \frac{1}{Sh}\frac{dc}{dy} \qquad (2.4)$$

$$\text{at } y = 1$$

$$t = 1 - \frac{1}{Nu}\frac{dt}{dy} \qquad (2.5)$$

where Sh and Nu are the modified Sherwood and Nusselt numbers.

Interest centres on evaluating the effectiveness factor η, which is the ratio of the overall observable rate of reaction to that rate which would be observed in the absence of heat and mass transport effects. From this definition, it follows that

$$\eta = (a + 1) \int_0^1 y^a \exp\{\gamma(1 - \tfrac{1}{t})\} f(c)\, dy \qquad (2.6)$$

The equations are sufficiently familiar to state without derivation. Some of the assumptions inherent in them have been discussed already in Chapters 1 and 2, but others must be examined now.

It has been assumed that D_e and K are independent of concentration and temperature, yet bulk diffusivity is proportional to $T^{1.5}$ and Knudsen to $T^{0.5}$: if follows that D_e must be a function of temperature. So also is K. Further, D_e may be a function of concentration, for instance in the case of molecular sieve catalysts (109). It has also been assumed that the heat of reaction is independent of temperature - which, strictly, it will not be.

Another assumption is rather less obvious.

If there is no change in the number of moles on reaction, then

$$N_R = -N_P$$

i.e. the diffusion fluxes of reactant and product are equal and opposite. But Fick's Law for binary diffusion yields (110):

$$N_R - \chi_R(N_R + N_P) = -C_t\, D_{PR}\, \nabla\chi_R$$

where χ_R is the mole fraction of reactant, D_{PR} the effective binary diffusivity and C_t the total concentration.

Combining the two equations, $N_R = -C_t D_{PR} \nabla \chi_R$

But, in deriving equation (1),

it was assumed that $N_R = -D_{PR} \nabla C_R$

Since $C_R = \chi_R . C_t$, the two equations immediately above are inconsistent unless C_t is constant. However $C_t = {}^{P_t}/_{RT}$, and thus is not constant {P_t is the total pressure, R the universal gas constant and T the absolute temperature}. Here, then, is another approximation in the treatment.

The error involved in these assumptions is likely to be small compared with the error in the parameter values - indeed this is known to be true of the temperature dependencies (14). One last assumption might be remarked upon - that the catalyst is uniformly dispersed throughout the support, so that f(c) is independent of y. This will not always be the case (111).

2.4 Numerical Solution Methods

Before developing the new approximate method, a variety of numerical solutions were computed, for two reasons. First, it was thought that one numerical method might be established as distinctly superior to others - no such conclusion was finally drawn - and secondly, accurate numerical solutions were needed to compare with the approximate solutions to be developed.

Table 6: Numerical Methods Used for the Catalyst Pellet Problem

(Zeroth order reaction)

Method	Comments
a. Quasilinearisation (112), implemented using central differencing with equidistant nodes	Robust i.e. converged from poor starting approximation
b. Cubic splines (Appendix 1)	Robust
c. Shooting method (113)	Robust
d. Integral equation (Appendix 1)	Not Robust: required much too good an approximation to obtain convergence
e. Variable transformation (Appendix 1)	Excellent, but unsuitable for design calculations, as it does not involve direct calculation of η for given Q

The methods listed in table 6 were all capable of yielding solutions in good agreement and therefore presumably of high accuracy. The three methods - a,b,c - suitable for design calculations often had comparable computing times (a few seconds on a IBM 360): appreciable differences in performance occurred only when there were steep

gradients near the pellet surface, which required the use of a large number of nodes in method (a), leading to a higher computing time. This difficulty was overcome in method (b) by concentrating nodes near the surface, and in method (c) by using a numerical integration technique with an adjustable step-length.

None of the methods were fast enough for use in reactor simulation.

2.5 The Method of Weighted Residuals (M.W.R.)

M.W.R. (114) is actually a family of techniques used to obtain approximate solutions to differential equations. It is particularly useful for boundary value problems.

Consider an o.d.e. formulated over a domain D of the independent variable s:

$$g\{Z\} = f(s)$$

$$B_i\{Z\} = b_i(s) \qquad i = 1,2, \ldots\ldots N_{bc}$$

where g is a non-linear differential operator, f and b_i are functions, and B_i represents the N_{bc} boundary conditions.

An approximate solution, Z_A, is sought as a linear combination of "trial functions", $\Phi_j(s)$, chosen by the user:

$$Z_A = \Phi_o(s) + \sum_{j=1}^{N} C_j \Phi_j(s)$$

where the C_j are constants or "adjustable parameters" whose values are, as yet, unknown. These values are determined by demanding that the approximate solution satisfy the o.d.e. (and boundary conditions)

in some approximate way. First, one notes that the approximate solution may be substituted into the o.d.e. and, since it is not the exact solution, it will not satisfy the equation exactly; that is to say, there will be a "residual" or "equation error"

$$g\{Z_A\} - f(s) \neq 0$$

This difference is a function of the Φ's, of the C_j's and of s, and so may be written as $R(C_j, \Phi_j, s)$.

M.W.R. consists of requiring that R should vanish "on the average" i.e. that a weighted average of R over the domain D should be zero:

$$\boxed{\int_D W_j(s)\, R(C_j, \Phi_j, s)\, ds = 0 ; \qquad j = 1,2....N}$$

where the W_j's are weighting functions.

This provides N equations for the determination of the N C_j's.

The techniques in the family differ in their choice of W_j's.

Thus, if the W_j's are chosen as the successive powers of s{ 1,s, s^2...} the Method of Moments is being implemented.

If W_j is chosen to equal $\partial R/\partial C_j$, then the Method of Least Squares is in use, so called because this choice of W_j corresponds to minimising the integral of the square of the residual w.r.t. the C_j

$$\left\{ \frac{\partial}{\partial C_j} \int_D R^2\, ds = \text{minimum} \rightarrow \int \frac{\partial R}{\partial C_j} R\, ds = 0 \right\}$$

In Galerkin's method, the W_j's are just the trial functions originally chosen i.e. $W_j = \Phi_j$.

The Sub-domain method involves splitting D into a set of N smaller sub-domains D_j, and choosing

$$W_j = \begin{cases} 1 \text{ if s is in } D_j \\ 0 \text{ otherwise} \end{cases}$$

and so results in $\int_{D_j} R(C_j, \Phi_j, s)ds = 0 ; \quad j = 1,2 ..... N$

Finally, the Collocation Method sets $W_j = \delta(s-s_j)$, where the delta function is defined by

$$\delta (S - S_j) = 0 \quad \text{if } S \neq S_j$$

$$\int_{-\infty}^{\infty} \delta (S - S_j)\, dS = 1$$

This, then involves the residual being forced to zero at the N selected points s_j in D.

These five are the best known of the M.W.R. techniques. Note that for N = 1, the moment method and the sub-domain method are exactly equivalent, both requiring $\int_D R(C_j, \Phi_j, s)ds = 0$. The application of this latter equation is sometimes known as the integral method.

M.W.R. can provide powerful techniques, but one disadvantage is immediately obvious; all but collocation require the evaluation of integrals which, for non-linear problems, can be difficult. A major advantage of M.W.R. is that the trial functions may be chosen by the user to suit the problem to hand - but this renders M.W.R. awkward to automate, for which shortcoming it has been criticised (115). However, this shortcoming has been overcome by Villadsen and Stewart (116), in their valuable "orthogonal collocation" method (O.C.). The name comes from the use of certain orthogonal polynomials (Jacobi polynomials) as trial functions, and of their roots as the selected points at which the residuals are set to zero.

Since the method is discussed at length in the literature (114, 116,117), and demcnstrated in use in section 2.6, only a brief introduction is necessary. The method can be explained as a computationally convenient analogue of Galerkin's method, which is well known to be of wide use (114), and it may be shown that the two methods are identical for linear problems with constant coefficients. Further, for other

problems O.C. is identical to Galerkin's method if the integrals arising in the latter are evaluated by suitable quadrature formulae.

Alternatively, one can explain the method by starting from the simple idea of collocation, and enquiring as to the best place to locate the collocation points or selected points. It is known (117) that an equal spacing would be inappropriate. It may be argued that a convenient spacing would be that which allowed the most efficient evaluation of integrals of the solution, since in many problems {such as the catalyst pellet problem}, it is such integrals, rather than the solution per se, which are of interest. This argument leads to the same O.C. method.

Villadsen (117) has placed the technique in the context of approximation theory, and progress has been made in the analysis of error bounds (118), convergence (119), the use of different families of polynomials (119,119a), the accurate calculation of relevant constants (120) and new ways of generating "problem-specific" polynomials (121). A review of all reported applications would be inappropriate. Rather, one might note that Finlayson has recently emphasised its wide usefulness (122), and that no fewer than five papers exploiting its advantages appeared in the March 1974 issue of "Chemical Engineering Science", which is indicative of its considerable utility.

2.6 The Concept of the "Effective Reaction Zone" and its Application

Consider the distributions of temperature and concentration which are established by the occurrence of an exothermic reaction within the pellet. Extensive calculations by numerous investigators show that, under conditions of high reactivity, the concentration of reactant may typically fall to almost zero at some point within the pellet and that the temperature will rise steeply in a zone near the outer surface, there-

after remaining almost constant. In particular, for the zeroth order reaction, the concentration may decline to exactly zero at some point - the "reaction interface". The temperature reaches its highest value at the reaction interface, and thereafter remains constant. Reaction occurs only in the outer "reaction zone". The zeroth order reaction thus exhibits a behaviour which is a limiting case of the behaviour of the general reaction.

Suppose that in the general case there exists an "effective reaction zone", similar to that of the zeroth-order reaction. Reaction occurs only in the effective reaction zone. $y_I \leq y \leq 1$, where y_I represents the position of a hypothetical reactive interface.

$$\text{By definition, } c(y_I) = 0 \tag{2.7}$$

Also, in order to preserve differentiability,

$$\frac{dt}{dy} = 0 = \frac{dc}{dy}; \quad y = y_I \tag{2.8}$$

By consideration of the fluxes of mass and heat at the pellet surface

$$t(1) = 1 + \beta \frac{Sh}{Nu} (1-c(1)). \tag{2.9}$$

Prater's relationship (123) between temperature and concentration obtains within the pellet:-

$$t(y) = t(1) - \beta(c(y) - c(1)). \tag{2.10}$$

Combining equations (2.9) and (2.10)

$$t(y) = (\beta + \frac{Nu}{Sh}) + (1 - \frac{Nu}{Sh})t(1) - \beta c(y) \qquad (2.11)$$

Equation (2.11) is independent of pellet geometry and kinetic rate law.

The effective reaction zone assumption is now invoked by combining equations (2.11) and (2.7) to yield

$$t(y_I) = (\beta + \frac{Nu}{Sh}) + (1 - \frac{Nu}{Sh})t(1) \qquad (2.12)$$

It is advantageous to define a new radial co-ordinate

$$\xi = \frac{y-y_I}{1-y_I} \qquad (2.13)$$

so that at $y = 1$, $\xi = 1$; at $y = y_I$, $\xi = 0$.

$$\text{From equation (2.8), at } \xi = 0, \frac{dt}{d\xi} = 0 = \frac{dc}{d\xi} \qquad (2.14)$$

thus preserving geometrical symmetry.

Using equations (2.11) and (2.13), equation (2.2) may be written as

$$\frac{1}{(1-y_I)^2}\frac{d^2t}{d\xi^2} + \frac{a}{y_I + (1-y_I)\xi}\left(\frac{1}{1-y_I}\right)\frac{dt}{d\xi} = -\beta\varphi^2 \exp\{\gamma(1-\frac{1}{t})\}g(t) \qquad (2.15)$$

where $$g(t) = f(1 + \frac{Nu}{\beta Sh} + \frac{1}{\beta}\{1 - \frac{Nu}{Sh}\}t(1) - \frac{1}{\beta}t) \qquad (2.16)$$

Assuming now that the temperature profile in the "effective" reaction zone $0 \leq \xi \leq 1$ is described by the n^{th} approximation

$$t^{(n)}(\xi) = t^{(n)}(1) + (1 - \xi^2) \sum_{i=0}^{i=n-1} a_i^{(n)} p_i(\xi^2) \qquad (2.17)$$

where the $p_i(\xi^2)$ are Jacobi polynomials, tabulated by Villadsen and Stewart, (116), and the $a_i^{(n)}$ are adjustable parameters. Note that Eqn. (2.17) satisfies the boundary condition (2.14).

A relationship between the $a_i^{(n)}$ and the surface temperature $t^n(1)$, can be found by requiring that Eqn. (2.17) satisfy condition (2.12):-

$$\sum_{i=0}^{i=n-1} a_i^{(n)} p_i(0) = (\beta + \frac{Nu}{Sh}) - \frac{Nu}{Sh} t^{(n)}(1) \qquad (2.18)$$

Similarly, the position of the "interface" $y_I^{(n)}$, can be found in terms of the $a_i^{(n)}$ and $t^{(n)}(1)$ by substituting Eqns. (2.13) and (2.17) into Eqn. (2.5):-

$$y_I^{(n)} = 1 + \frac{2 \sum_{i=0}^{i=n-1} a_i^{(n)} p_i(1)}{Nu\{1 - t^{(n)}(1)\}} \qquad (2.19)$$

Combining Eqns. (2.18) and (2.19) gives $y_I^{(n)}$ in terms of the $a_i^{(n)}$

$$y_I^{(n)} = 1 + \frac{2 \sum_{i=0}^{i=n-1} a_i^{(n)} p_i(1)}{Sh\{\sum_{i=0}^{i=n-1} a_i^{(n)} p_i(0) - \beta\}} \qquad (2.20)$$

The n adjustable coefficients $a_i^{(n)}$ are determined by substituting Eqns. (2.17), (2.18) and (2.20) into Eqn. (2.15), requiring that the differential equation residual should vanish at the n collocation points $\xi_1, \xi_2 \ldots \xi_n$. This leads to a set of n simultaneous algebraic equations in the unknowns $a_i^{(n)}$. The respective collocation points up to n=3 are given in Tables (2-4) of reference (116) for slab, cylindrical, and spherical geometry.

For example, the single parameter approximation used in most of the following examples leads to the following simple relationships:

$$t^{(1)}(\xi) = t_2 + a_o^{(1)}(1-\xi^2) \tag{2.21}$$

$$a_o^{(1)} = \beta - \frac{Nu}{Sh}(t_2-1) \tag{2.22}$$

$$y_I^{(1)} = 1 + \frac{2}{Sh} - \frac{2\beta}{Nu} \cdot \frac{1}{(t_2-1)} \tag{2.23}$$

where $t_2 \equiv t^{(1)}(1)$.

Consider a single first order reaction by way of illustration of the method. In this case,

$$f(c) = c$$

and g(t) in Eqn. (2.16) is given by

$$g(t) = 1 + \frac{Nu}{\beta Sh} + \frac{1}{\beta}\left(1 - \frac{Nu}{Sh}\right) t(1) - \frac{1}{\beta}t. \tag{2.24}$$

On substituting Eqns. (2.21) to (2.24) into Eqn. (2.15), setting the equation residual equal to zero at the point ξ_1, the following algebraic equation in $a_o^{(1)}$ is obtained

$$\alpha^2 \left\{\frac{1-\xi_1(1+a) - \alpha}{1 - \xi_1 - \alpha}\right\} = \frac{\xi_1^2}{2} \Omega^2 \exp\left(\frac{\gamma W}{1+W}\right) \qquad (2.25)$$

where $$\alpha = \frac{Sh}{2}\left(\frac{\beta - a_o^{(1)}}{a_o^{(1)}}\right)$$

and $$W = a_o^{(1)}\left(\frac{2\alpha}{Nu} + 1 - \xi_1^2\right).$$

Eqn. (2.6) defining the effectiveness factor, now becomes

$$\eta = (a+1)\int_{y_I}^{1} y^a \exp\{\gamma(1 - \tfrac{1}{t})\}\cdot g(t)\,dy$$

$$= (a+1)(1-y_I)\int_{0}^{1} \{y_I+(1-y_I)\xi\}^a \exp\{\gamma\ (1 - \tfrac{1}{t})\}\cdot g(t)\,d\xi. \qquad (2.26)$$

In the case of a sphere (a=2), for example, Eqn. (2.26) takes the form

$$\eta = 3(1-y_I)\{y_I^2 \int_{0}^{1} f(t)\,d\xi + 2y_I(1-y_I)\int_{0}^{1} \xi f(t)\,d\xi$$

$$+ (1-y_I)^2 \int_{0}^{1} \xi^2 f(t)\,d\xi\} \qquad (2.27)$$

where $f(t) = \exp\{\gamma(1 - \frac{1}{t})\} \cdot g(t)$.

Each of the integrals in Eqn. (2.27) may be simply evaluated by using the appropriate Gaussian integration formula (116). The function values required in the first two integrals are obtained by interpolating along the temperature profile.

Computational procedure

n=1

For given values of the parameters Q, γ, β, Sh and Nu, Eqn. (2.25), or its equivalent, was solved by Cox's method (124), which is particularly suited to algebraic problems having several possible roots. Only positive roots in the range $0 < a_o^{(1)} \leq \beta Sh/(2+Sh)$ are consistent with the twin requirements that the internal temperature be greater than the surface temperature and the position of the interface y_I lies in the range $0 \leq y_I \leq 1$. Having obtained the required root(s), the temperature profile, the surface temperature and the position of the interface are calculated from Eqns. (2.21)-(2.23). The effectiveness factor is then calculated from Eqn. (2.26), for given pellet geometry 'a' and rate expression f(t), by the procedure outlined previously.

If no root can be found within the acceptable range, the reaction zone approach is discarded and the mixed collocation method is applied directly to Eqns. (2.2), (2.5) and (2.11), as described by Villadsen and Stewart. This is normally the case at low values of the Thiele modulus when reaction is occurring throughout the pellet.

n > 1

The single parameter approximation (n=1) requires the solution of a single algebraic problem and as such is relatively straightforward. This solution represents a convenient starting point in a boot-strap technique for solving cases containing more than one parameter. For example, this solution can be used in a two parameter approximation to provide an estimate of the second parameter. An iterative Newton-Raphson type scheme (e.g.Davidenko-Broyden (125)) can then be used to find more accurate estimates of both parameters. The same strategy extends to the three parameter approximation, by using as a starting solution the case of (n=2), and so on.

DISCUSSION. A completely comprehensive study of the general problem is impossible, because of the number of parameters involved, but several cases are examined in detail which highlight the essential features of behaviour.

Comparison of Methods

(i) Zeroth order reaction

A test of the method is provided by the zeroth-order reaction which, for given system parameters, leads to the largest internal temperature and concentration gradients.

Fig. 2.1 shows the effectiveness factor for a catalyst slab (a=0) over a range of Thiele modulus covering the entire region of interest. Curve (a) was constructed by assuming a parabolic trial function for the temperature profile within the reaction zone, while

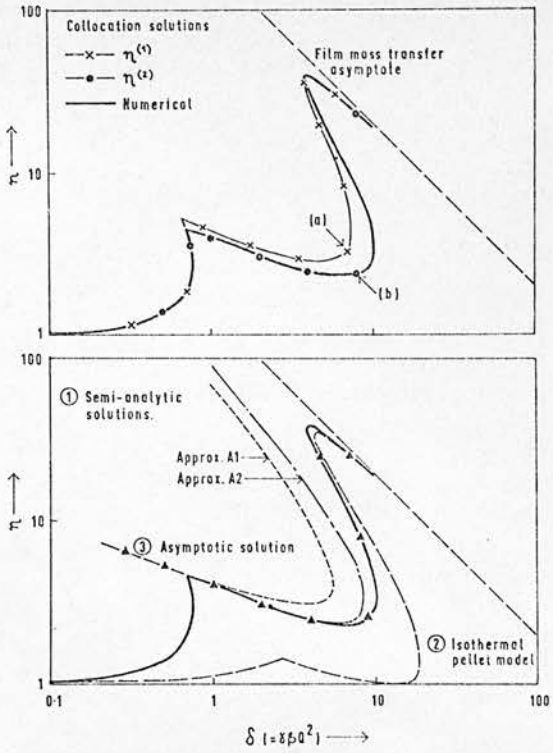

γ = 20
β = 0.1
Nu = 10
Sh = 100

Figure 2.1 Zeroth order reaction in a catalyst slab
Comparison of various approximation methods

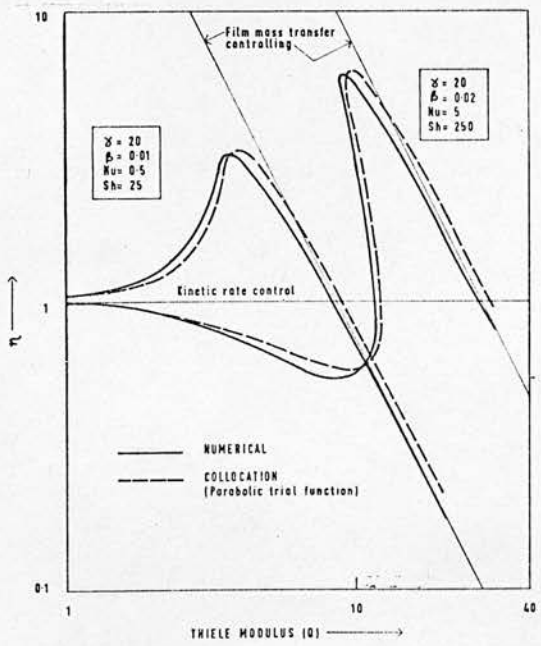

Figure 2,2 First order reaction in a catalyst sphere

the points marked on curve (b) were calculated from a more refined quartic trial function, containing two adjustable parameters. The results are compared with three alternative schemes which also avoid the encumbrance of numerical integration in this particular example, and are of the types discussed in Section 2.2

(1) semi-analytical procedures based on the use of simpler non-linear approximations to the Arrhenius rate constant,

(2) a simpler physical model which assumes the pellet to be isothermal, the resistance to heat transfer being confined to the external film,

(3) an asymptotic solution valid for conditions in which the reactant is completely consumed.

These methods, due to Cresswell, are developed in the appendices of reference 126. The numerical computations are the work of the present writer.

The results show that all the essential characteristics of the problem are reproduced by the simple computational method already described. A parabolic approximation (curve a) requires the solution of a single algebraic equation and, at any point outside the multiple solution region, gives an effectiveness factor within 10% of the 'exact' value. The regions of multiple steady states are also properly located. If more accuracy is required, a greater number of parameters must be used. Curve (b) represents a two parameter trial function, requiring the solution of a pair of simultaneous algebraic equations. It is accurate to within 0.5% in predicting both the effectiveness factor and the bounds of Thiele modulus between which multiple solutions occur. In view of the uncertainty involved in the experimental determination of both the physical and chemical data, the simplest single parameter trial function is probably sufficiently accurate for engineering design purposes.

Each of the alternative methods has some utility over a limited range of conditions. However, the establishment of analytical criteria which cover these regions would seem to be a most difficult undertaking. Moreover, the full advantages of these methods are only realised if certain integrals appearing in the solutions can be evaluated analytically. This necessarily limits their utility to all but the most idealised cases. The approach described here avoids evaluation of such complex integrals and is therefore applicable to a much wider class of reaction rate expressions.

(ii) First order reaction

Fig. 2.2 compares the proposed method with a full numerical solution for the case of a single first order reaction occurring within a catalyst sphere. Two examples are considered; one with a low value of the Nusselt number (Nu=0.5) leading to an initial steep rising arm in the effectiveness factor; the second with a higher value of the Nusselt number (Nu=5) in which the effectiveness factor falls initially below unity, as a result of internal mass diffusion limitation, and then shows a steeply inclined arm, which rises almost to the asymptotic bound imposed by the finite rate of film mass transfer. This second example also contains a region of multiple solutions. In both examples, the agreement is satisfactory over the entire range of Thiele modulus, even with only a single parameter trial function for the temperature profile within the reaction zone.

Multiple steady states

An indication of the power of this method of approach is provided in an example studied by Hatfield and Aris (74). For the particular data $\gamma=27$, Nu=10, Sh=60 and $\beta=1/3$, which represent an extremely

exothermic reaction, the effectiveness factor was found to change by over four orders of magnitude for $Q < 0.1$. Two peaks were found in the effectiveness factor curve with the second peak overtopping the first.

An attempt was made to reproduce this type of behaviour with the simple method employing only a single parameter trial function. The result is shown in Fig.2.3. Not only are the important features correct in gross aspect, but the location of the various regions of multiple steady states, and the number of steady states in each region, are accurately determined, as is indicated in Table 7.

Table 7: Comparison of Multiple Steady State Regions

Q^*	$Q^{(1)}$	number of steady states
< 0.06	< 0.055	1
$0.06 < Q < 0.12$	$0.055 < Q < 0.14$	3
$0.12 < Q < 0.17$	$0.14 < Q < 0.23$	5
$0.17 < Q < 0.3$	$0.23 < Q < 0.32$	3
$Q > 0.3$	$Q > 0.32$	1

Q^* (Fig. 2.3)

$Q^{(1)}$ Hatfield and Aris (74).

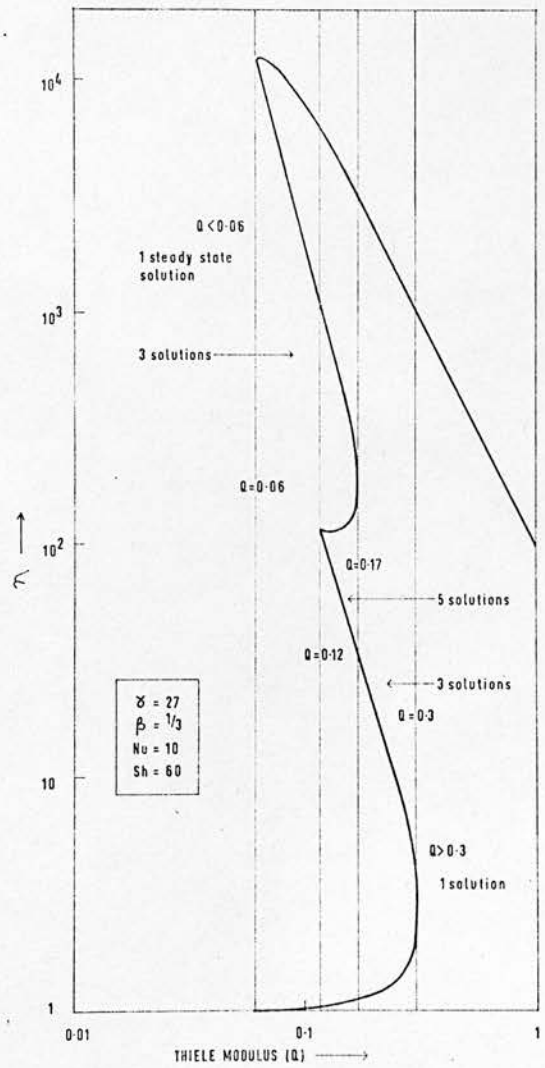

Figure 2.3 First order reaction in a catalyst slab
Approximate solution using a single parameter trial function.

2.7 The Utility of the Method and its Possible Extensions

The method developed above allows the approximate prediction of effectiveness factors to an accuracy sufficient for engineering use. By taking advantage of the physics of the problem, the mathematical difficulties of solving a non-linear boundary value set of o.d.e.'s are overcome. The method developed required, in most cases, solution of a single transcendental equation. Its reliability has been established by testing on several examples over a range of conditions. It reduces computation time by two or three orders of magnitude and appears to eliminate all convergence difficulties. It is effective over the entire range of rate-controlling steps and will predict accurately the bounds on the region of multiple solutions represented on an effectiveness factor versus Thiele modulus diagram. Moreover, it is possible to test the accuracy of the method in use, by utilising two different orders of collocation formulae.

As suggested by figure 2.2, the method can be improved marginally by using the "film mass transfer controlling" asymptotic solution i.e. whenever a calculated η exceeds the limiting value, replace it by the said value ($= (a+1)Sh/Q^2$). The resulting discontinuity in the slope of the η versus Q curve would be of no importance. Extension of the method to reversible reactions is straightforward - one would merely postulate that the reaction interface corresponds to the establishment of chemical equilibrium.

A major strength of the method is that it will deal with any kinetic form and any of the commonly used pellet geometries. Moreover, by appropriate adaption of the original o.d.e.'s (equations (2.1) and (2.2)), the method can cope with such situations as non-uniform catalyst dispersion, and the position, temperature and composition dependence of D_e and K.

In cases (such as those of appendix 5) where the pellet may confidently be expected to be isothermal, the method offers little advantage over Cresswell's "lumped thermal resistance model" (108) if the reaction is of zeroth or first order. If it were of some other order, the assumption of pellet isothermality combined with solution of the material balance o.d.e. by O.C. might offer an attractive approach.

The remarks of other workers on the method, since its publication, deserve some mention. Karanth and Hughes (127) described it as "simple and reliable" and elsewhere provided an alternative physical interpretation, suggesting the case where the interface arises from the exhaustion of one of the reactants whose concentration does not appear in the "rate law" of the reaction(128).Van den Bosch and Padmanabhan (129) examined the ability of the method to predict regions of multiplicity, and compared its results with those of two other methods, linearisation (92,130) and high-order O.C. (116). They found that the method presented here was much the best, but recommended a modification to it; namely, that in the situation where no "effective interface" is established, the family of orthogonal polynomials used (and hence collocation point(s)) should be different from that used when there is an "effective interface". This alternative version of the method is claimed to improve the accuracy of the prediction of the multiplicity region, although the authors do not present their evidence for the claim. The same authors (131) comment that the method, by its very nature as a low-order approximation, will not extend to the analysis of the stability of the steady states which it predicts.

Finally, Finlayson (122) describes the method as an example of "orthogonal collocation on finite elements", commends its merits to his readers, and remarks on its ability to successfully predict regions of multiplicity. However, he also points out that the method, as developed above, involves the use of polynomials symmetric in ξ, which symmetry "cannot be justified". He admits that his proposed remedy for this inconsistency reduces the accuracy of the method and imposes a discontinuity on the η versus Q curve. It is an open question whether this is a price worth paying for mathematical propriety. The gain in accuracy on using a not-quite-appropriate polynomial has been discovered independently by Villadsen (135).

2.8 Notation

a geometric parameter

$a_i^{(n)}$ the i^{th} adjustable parameter in the n^{th} approximation to the temperature profile

C point concentration of reactant

D_e effective diffusivity of reactant in the porous catalyst

E_a activation energy of the reaction

h fluid/particle heat transfer coefficient

$-\Delta H$ heat of reaction; positive for an exothermic reaction

k_g fluid/particle mass transfer coefficient

K effective thermal conductivity of the catalyst particle

L characteristic length of the particle: the radius if the particle is a sphere or cylinder; the half-thickness if a slab

r reaction rate

R gas constant

T point temperature

x co-ordinate measuring distance from the centre of symmetry

Reduced variables

c dimensionless reactant concentration, C/C_f

t dimensionless temperature, T/T_f

t_s dimensionless pellet temperature, isothermal model

y dimensionless co-ordinate, x/L

y_I position of the hypothetical reaction interface

y_1 position of the reaction interface, zero order reaction

Dimensionless groups

Nu modified Nusselt number hL/K

Sh modified Sherwood number $k_g L/D_e$

β thermicity $(-\Delta H)D_e C_f/KT_f$

γ activation energy parameter E_a/RT_f

δ $\gamma\beta Q^2$

η effectiveness factor, defined by equation (2.6)

ξ normalised co-ordinate in the effective reaction zone, defined by equation (2.13)

ξ_1, ξ_2 first and second collocation points

Q Thiele modulus, $L(r_f/D_e C_f)^{\frac{1}{2}}$

Subscripts

m at the interface, zero order reaction

f fluid phase

Superscript

(n) pertaining to the n^{th} approximation.

CHAPTER 3:- Introduction to Parameter Estimation

3.1 Experimental error.

3.2 Statistical properties of experimental error.

3.3 Desirable properties in a parameter estimation method.

3.4 Parameter estimation methods.

3.5 Parameter estimation in ordinary differential equations: the analysis of integral data.

3.6 Approximate methods.

3.7 A worked example: the oxidation of NO.

3.1 Experimental Error

A mathematical model will often take the form

$$y = f(\underline{x},\underline{\theta}) \tag{3.1}$$

where $\underline{x}$ is a vector of n_i independent variables

$\underline{\theta}$ is a vector of n_p parameters

y is the dependent variable

and the functional form f is known.

The experimenter seeks an estimate $\hat{\underline{\theta}}$ of the unknown value of $\underline{\theta}$. He proceeds by setting various different values to $\underline{x}$, and measuring the corresponding values of y. If all measurements were free of error, he would need only to take n_p measurements of y at different $\underline{x}$'s, and calculate $\underline{\theta}$ from a manipulated form of eqn. (3.1)

$$\underline{\theta} = f_1(\underline{x},y) \tag{3.2}$$

However, it is accepted as inevitable that, even if measurement of $\underline{x}$ may involve negligible error, the measurement of y will not. The measured value Y will be the sum of the "true value" y and an experimental error e.

$$Y = y + e \tag{3.3}$$

$$= f(\underline{x},\underline{\theta}) + e \tag{3.4}$$

This error may have two components: a systematic error, which it is the duty of the experimenter to eliminate, and a chance or random error, whose value cannot be known, but which may be described

by a probability distribution function. It is the presence of this unknown random error which renders useless eqn. (3.2), because the appropriate value of y in the R.H.S. will not be known, and necessitates the development of a theory of parameter estimation. The statistical properties of the error distribution largely determine the parameter estimation method to use, and the degree of confidence which may be attached to its results.

In a more general case there may be several (n_d) dependent variables in the model:

$$\underline{Y} = \underline{f}(\underline{x},\underline{\theta})$$

Those dependent variables whose values are measured are called 'observed variables' or 'responses', and the measured values will, of course, depend on a vector of experimental error $\underline{e}$.

If all the dependent variables are measured,

$$\begin{aligned} \underline{Y} &= \underline{y} + \underline{e} \\ &= \underline{f}(\underline{x},\underline{\theta}) + \underline{e} \end{aligned} \qquad (3.5)$$

and a similar equation applies if only certain of the dependent variables are measured (i.e. if $n_r < n_d$).

3.2 Statistical Properties of Experimental Error

Consider, for instance, an integral multi-response kinetic experiment, with $n_r \leq n_d$ responses being measured on each of m occasions $n_r.m > n_p$. Some important error properties are considered in Table 8. Property II is particularly difficult to confirm, although a useful guide comes from the analysis of residuals.

Table 8: Error Properties $i = 1,2....n_r$; $u = 1,2....m$

Number	Property	Symbolically	Remarks
I	Mean value of the error in each response is zero i.e. no systematic error	$E(e_{iu}) = 0$ all i,u	Necessary assumption
II	Errors in responses are not serially correlated i.e. independence of observation sets	$E(e_{iu}e_{jv}) = 0$ all $i,j,u \neq v$	Almost universal assumption, although implausible when measurements are made in time sequence on the same system. If serially correlated errors are present and their existence is ignored, one is likely at best to place too great a confidence in the parameter estimates, and at worst to draw erroneous conclusions on the adequacy of the model (136-138)
III	Errors have common form of distribution	$f(e_{iu}) \sim f(e_{jv})$ all i,j,u,v	Invariably assumed for simplicity. Impossible to confirm without a large amount of replicate data
IV	Variance of errors on each response are known	$E(e^2_{iu}) = \sigma_{iiu}$	Can be estimated from replicate data or perhaps from residual analysis. It is particularly convenient if the error variance on each response is constant ($\sigma_{iiu} = \sigma^2_i$), and a minor simplification if the error variances on different responses are equal ($\sigma^2_i = \sigma^2_j$, all i,j)
V	Co-variances of errors are known	$E(e_{iu}e_{ju}) = \sigma_{iju}$	In principle, but rarely in practice, is calculated from replicate data. The simplifying assumption of zero co-variance ($\sigma_{iju} = 0$, $i \neq j$, all u) is usually made.
VI	The error distribution is Normal	$f \sim f_N$	There is rarely enough replicate experimental data to confirm this assumption, although it is often true(139). It is certainly plausible in view of the Central Limit Theorem.
VII	The independent variable is measured with negligible error	$e_{\text{indep var}} = 0$	Usually assumed, and leads to great simplification. However, in many Chemical Engineering examples, it is not true (140,141). Only a little work has been performed on the case where the assumption is invalid (140,138)

(A residual is the difference between the observed value of the response and its value predicted by the model, using the estimated values of the parameters.) Violation of the property is very difficult to deal with, although some success has been obtained for simple cases (136, 137, 138). The property can often, in principle, be established by suitable experimental design, but the consequent amount of experimental effort may be prohibitive - see section 3.7.

3.3 Desirable Properties in a Parameter Estimation Method

i) Lack of bias

If an experiment were repeated n times, yielding the set of parameter estimates $\hat{\theta}_i$; i = 1,2...n, then the estimation method is said to be unbiased if

$$E(\hat{\theta}_i) = \theta_i \qquad (3.6)$$

where θ_i is the true value. Desirable as this property is, one might tolerate biased estimates (142) if they were to have a sufficiently small variance (see (ii) below). The degree of bias ascribable to a method must generally be calculated by computer simulation of the experimental system, although results can be established for linear systems (i.e. systems where f is linear in the θ_j) under ideal error assumptions.

ii) Efficiency

Because of the error in the data, there will be uncertainty associated with the parameter estimates, and the most efficient parameter estimation method is the one which minimises the amount of uncertainty.

Consider the problem of estimating a single parameter (true value θ_j) from n replicate experiments. The parameter variance is

$$\sigma^2_{\hat{\theta}_j} \equiv \frac{\sum_{i=1}^{n} (\hat{\theta}_{j,i} - \theta_j)^2}{n} \tag{3.7}$$

Since θ_j will be unknown, eqn. (3.7) will be approximated by

$$\sigma^2_{\hat{\theta}_j} = \frac{\sum_{i=1}^{n} (\hat{\theta}_{j,i} - \overline{\theta}_j)^2}{(n-1)} \tag{3.8}$$

$$\text{where } \overline{\theta}_j \equiv \frac{\sum_{i=1}^{n} \hat{\theta}_{j,i}}{n} \tag{3.9}$$

The most efficient method is one which yields the minimum value for $\sigma^2_{\hat{\theta}_j}$.

For multi-response problems, the most efficient method yields the minimum volume of parameter joint confidence region, i.e. it should minimise det($\underline{\underline{C}}$), where $\underline{\underline{C}}$ is the parameter variance-covariance matrix.

iii) Consistency

A method is consistent if, as the number of data used increases, each parameter estimate approaches its true value.

$$\lim_{n\to\infty} \{P(\hat{\theta}_j - \theta_j) = 0\} = 1, \quad \text{all } j. \tag{3.10}$$

iv) Convenience

As will be shown below, the use of classical parameter estimation methods may require a considerable amount of effort, even when using a digital computer. Tukey (143) has remarked:-

"Most data analysis is going to be done by people who are not sophisticated data analysts and who have very limited time: if you do not provide them with tools, the data will be even less studied."

Thus to encourage experimenters to examine their data, convenient methods should be devised.

The parameter estimation methods to be described in this chapter and the next will be judged according to these four desirable properties.

3.4 Parameter Estimation Methods

Table 9 presents a hierarchy of methods, with each one (from 2 to 5) a special case of one above. On proceeding down the table as far as 5, the amount of a priori information required decreases, and the number of assumptions made increases. Entries 6 and 7 are essentially empirical techniques, although method 7 has been justified by relating it to MLE for errors of Laplacian distribution. There is no compelling reason to assume that errors will follow such a distribution.

The fourth column shows the properties of the method for the linear case, when the model is linear in the parameters. For the non-linear case the same properties will usually hold approximately, while the computations required will typically render the method much less convenient.

Table 9: Heirarchy of Parameter Estimation Methods (144,145) Note: for simplicity, error property VII is assumed throughout

Method	Criterion	Assumptions and a priori information	Properties (linear case)	Remarks
1. Bayesian 'Minimum Risk'	$\min_{\underline{\theta}} \left(\int_{n_p} c(\hat{\underline{\theta}}, \underline{\theta}) \, p(\underline{\theta}\mid\underline{Y}) \, d^{n_p}\underline{\theta} \right)$	a) a priori probability density function (pdf) of errors: $p(\underline{\varepsilon}) \Rightarrow p(\underline{Y}\mid\underline{\theta})$ b) a priori pdf of parameter values c) a cost function $c(\hat{\underline{\theta}}, \underline{\theta})$, measuring the loss due to using wrong values of the parameters in a subsequent application	As the method is with a particular application in mind, method properties (i) to (iii) are unnecessary Very inconvenient	A rational criterion which, in this form, requires much more information than an engineer is likely to have
2. Maximum Likelihood Estimation (M.L.E.)	$\max_{\underline{\theta}} (p(\underline{Y}\mid\underline{\theta}))$	Common form (III) of error distribution known a priori. Absence of serial correlation almost invariably assumed, to render the calculations tractable (II)	Consistent. Asymptotically unbiased and efficient. Slightly inconvenient	Widely accepted method (146). A suitable standard with which to compare new methods (147).
3. Generalised Least Squares (Markov or Aitken Method)	$\min_{\underline{\theta}} (\underline{r}^T \underline{\underline{M}}^{-1} \underline{r})$	Error joint distribution assumed Normal (VI), of mean zero (I), with known variance-covariance matrix $\underline{\underline{M}}$ (IV and V) No serial correlation (II)	Convenient, unbiased. Most efficient linear unbiased estimator. Consistent.	Much used method (148,149) N.B. $\underline{r}$ is the vector of residuals
4. Box and Draper Method (150)	$\min_{\underline{\theta}} (\det(\underline{\underline{V}}))$	As above, but $\underline{\underline{M}}$ unknown	Less convenient than least squares. Consistent, unbiased efficient	$v_{ij} = \sum_{u=1}^{n} \{Y_{iu} - f_i(\underline{x}_{iu}, \underline{\theta})\} \times \{Y_{ju} - f_j(\underline{x}_{ju}, \underline{\theta})\}$
5. Least Squares	$\min_{\underline{\theta}} (\underline{r}^T \underline{r})$	Error joint distribution still Normal with zero mean, but with covariances assumed zero and variances equal. No serial correlation (II)	Consistent, convenient, unbiased and linear	If errors are uncorrelated, of mean zero, and from a common distribution, method yields consistent, unbiased, convenient estimates, even if error distribution is non-Normal
6. Chebyshev Norm	$\min_{\underline{\theta}} (\max_{i,u} \lvert r_{iu} \rvert)$	Justification largely intuitive	No properties established except inconvenience	Used on rare occasions (151,152)
7. Gershgorin Norm	$\min_{\underline{\theta}} \left(\sum_{\text{all } i} \sum_{\text{all } u} \lvert r_{iu} \rvert \right)$	M.L.E. for independent (II) errors, from Laplacian distribution, mean zero (I), zero covariance, constant variance.	As M.L.E. if assumptions correct.	Used rarely (151). Can be ambiguous (153).

Advice on the examination of data prior to parameter estimation has been offered by Box et al (154). All the methods are based on the assumption that the model is 'correct'. Its adequacy ought therefore to be tested by analysis of residuals (136,148,155) performed after parameter estimation.

3.5 Parameter Estimation in Ordinary Differential Equations: the Analysis of Integral Data

A kinetic model is generally of the form

$$\frac{d\underline{y}}{dt} = \underline{f}(\underline{y},\underline{\theta}) \qquad (3.11)$$

with observations of the state $\underline{y}$, but not of $\frac{d\underline{y}}{dt}$, available.

One approach is to perform graphical or numerical differentiation of the data to provide values of $\frac{d\underline{y}}{dt}$ for use as response variables in appropriate estimation methods for $\underline{\theta}$. Although appropriate differentiation techniques have been devised (156,157), it is known (158) that they are by nature inaccurate, especially for sparse data. Thus integral data should be recognised as corresponding to a differential equation model and analysed accordingly. If the o.d.e.'s are soluble analytically then familiar methods can be used. If not, then appropriate methods must be devised. Such methods have been reviewed (159, 145), but with emphasis on the typical equations of control engineering - high order linear o.d.e.'s. In reaction engineering, interest centres on methods suitable for sets of first order non-linear initial-value equations. Some suitable methods

are shown in table 10 - all designed for the digital computer, all iterative, all usually invoking a least-squares criterion, although adaptable to use other criteria from table 9, and all requiring repetitive integration of o.d.e.'s.

Disappointingly few comparisons of these methods have been reported. Berger (166) tested two gradient methods and found modified Gauss-Newton generally superior to Fletcher-Powell-Davidon. Schlossmacher (164) found the Gauss-Newton method to possess a larger convergence region and faster computation time than QLLS, while Medler and Hsu (167) reported comparable computation times.

There is no guarantee that any method will converge from an arbitrary starting point. Modifications to QLLS have been proposed (168,169) to increase its convergence region at the expense of speed of convergence. Donnelly and Quon (170) proposed an effective 'data perturbation' method to increase the convergence region of QLLS: an idea akin to Davidenko's for the iterative solution of non-linear equations (125).

Any minimisation method may fail when there exist multiple minima, as can arise in parameter estimation (171, 172). Hwang and Seinfeld (166) have suggested that an effective maneouvre to test whether a minimum is global is to alter the weighting function in the least squares criterion, whilst Bremermann (173) has reported his attempt to contrive an optimisation procedure which will locate the global minimum.

All the methods may suffer difficulty due to 'stiff' equations (174). Denis and Daubert (175) have discussed suitable numerical integration schemes to alleviate the problem, without apparently considering those based on orthogonal collocation (117).

Table 10: Parameter Estimation Methods for o.d.e.'s

Method	Algorithms	Convergence Region	No.of iterations required for convergence	No.of equations to integrate per iteration	Relative implementation difficulty
Hill-climbing (direct)	Powell (160) Nelder and Mead (161) and others	Large	Many	Only the model equations: n_d	Small: the search and integration routines are widely available and the other routines are trivial
Hill-climbing (gradient)	Steepest descent) Gauss-Newton) Marquardt) (162) and others	Often large	Intermediate, sometimes many	The model eqns. plus the 'parameter influence' or 'sensitivity' eqns. $(n_d + n_d n_p)$	Large: the derivation of the sensitivity equations can be tedious
Quasi-linearisation/ least squares (QLLS) (163)	See section 3.7	Small	Few (Quadratic convergence)	Assuming that care is taken to avoid solving trivial eqns.: $(n_d + n_d n_p)$	Large: see section 3.7
Other methods	Hwang and Seinfeld (165) Schlossmacher (164)	These methods are re-derivations of the Gauss-Newton method (see above)			

The 'number of equations to integrate' entry applies to the case of a single set of profiles, corresponding to a single set of initial conditions (which are assumed to be known exactly), for which $n_r = n_d$

n_d: number of dependent variables; n_p: number of parameters;

n_r: number of responses.

Broekhoven and Watts (176) have commented that, in non-linear least squares, convergence difficulties can arise when there are high correlations between parameters, when poor starting values are used and where there are many parameters. They have suggested a 'partitioning' method which could doubtless be exploited for o.d.e. problems, where the difficulties they describe arise (175, 177).

Hwang and Seinfeld (166) have proposed a scheme to cope with 'ill-posedness' - where large changes in the parameter values cause only small changes in the least squares criterion, leading to difficulties due to round-off and truncation error in the integration procedure. However, the best solution is probably to gather more data from suitably designed experiments (178,179).

In summary, there exist several methods, prone to difficulties of excessive computing time and poor convergence, which might be avoided if sufficiently good 'starting values' were available.

3.6 Approximate Methods

There is a need, then, for an approximate method to supply such good 'starting values' of the parameters. To be rapid, the method would have to avoid repetitive numerical integration of o.d.e.'s. Preferably, it would provide estimates which were themselves adequate for engineering applications. Ideally, it would furnish a measure of the degree of uncertainty attached to the estimates i.e. an 'error analysis', for parameter confidence intervals, cross-correlation coefficients and so forth. In the next chapter two such methods are developed: in this section the work of others is reviewed.

A method which has found practical applications (180-183) was first proposed by Himmelblau, Jones and Bischoff (184) and rediscovered by Foss (185). The procedure involves formally integrating the equations, and calculating the integrals so arising by replacing the 'true' values of the dependent variables by their measured values, followed by application of a four-point quadrature formula. The problem then becomes a regression problem to be solved using standard computer routines.

A second method is due to Tanner (186) who has used it to study enzyme kinetics (187). First an approximate solution to the o.d.e.'s is obtained, in the form of polynomials in the independent variable, by use of Picard's iteration. These polynomials have coefficients which involve the initial conditions and the unknown rate constants. Then the observed responses are fitted by orthogonal polynomials in the independent variables, using a least squares method. The rate constant values are found by equating the numerical coefficients of the orthogonal polynomials with their counterparts in the approximate solution to the o.d.e.'s. Tanner suggests that the results are sufficiently accurate to provide good starting values for iterative search methods.

Buzzi Ferraris and Donati (188) have developed a method for use with H-W kinetic laws. They transform the problem by treating the responses (concentrations) as being error free, and the independent variable (residence time) as being subject to experimental error, and therefore suitable for inclusion in an appropriately weighted sum-of-squares criterion. Parameter estimation is performed using an

ordinary non-linear least squares approach, the problem having been simplified because the definite integrals which appear can be evaluated once-and-for-all, rather than at each iteration.

Van den Bosch and Hellinckx (189) have presented a method which reduces the problem to linear regression, if the o.d.e. is linear in the parameters, and non-linear regression otherwise. The workers replace the sum-of-squares criterion by one involving 'equation residuals', and then evaluate that using a collocation technique. The method requires that the experimental measurements be made at prescribed values of the independent variable viz. at the collocation points. The authors state:- "slight errors indeed may cause rather large deviations for the estimates as compared to results obtained by the least squares method, which normally makes use of a larger number of data."

Of these methods, that of Himmelblau et al. has been most widely used, largely on problems where the o.d.e.'s are linear in the parameters. It appears to provide adequate 'point estimates' but seriously misleading 'interval estimates' (182). The method of Tanner has one clear advantage over Himmelblau's in that the former does not require measurement of all the dependent variables while the latter does. Buzzi Ferraris et al (52) have observed their method to have a particularly useful property, namely that although its parameter estimates do not coincide exactly with those obtained by least squares, the two techniques do lead to the same conclusions in model discrimination. The method of Van den Bosch and Hellinckx is rather complicated, and very restrictive in its demand for appropriate location of data points. It appears to offer no compensatory advantage.

None of the methods has been analysed in terms of properties (i) to (iii) listed in section 3.2, nor has an error analysis been reported for any of them.

Finally, it might be noted that approximate methods have been devised by Gavalas (190) and by Wei and Prater (191), but that they are not suitable for general application, being restricted to a small class of problems viz. linear o.d.e.'s with constant coefficients and systems of isothermal first order reversible reactions, respectively.

3.7 A Worked Example: The Oxidation of NO

The problem is to estimate the values of the two rate constants k_1, k_2 for the non-equimolar batch reaction

$$2NO + O_2 \rightleftharpoons 2NO_2$$

from Bodenstein and Lindner's (192) observed values of decrease in total pressure versus time (Table 11, top three rows).

Table 11: Y_i : observed decrease in pressure (mm Hg)

t_i : time (seconds)

y_i : decrease in pressure predicted by the model using the estimated values of k_1, k_2.

i	0	1	2	3	4	5	6	7	8	9	10	11	12	13	14
t_i	0	1	2	3	4	5	6	7	9	11	14	19	24	29	39
Y_i	0	1.4	6.3	10.5	14.2	17.6	21.4	23.0	27.0	30.5	34.4	38.8	41.6	43.5	45.3
y_i	0	4.6	8.5	12.0	15.9	17.9	20.4	22.6	26.5	29.7	33.6	38.2	41.3	43.5	46.1

Note: the value of Y_{11} is corrected from a misprint in the original.

The data were gathered at a temperature of 341.3°C.

Using conservation of mass and simple mass-action kinetics, the appropriate o.d.e. is readily derived:-

$$\frac{dy}{dt} = k_1(126.2 - y)(91.9 - y)^2 - k_2 y^2 \qquad (3.12)$$

where the original partial pressures (at t = 0) of NO and O_2 were 183.8 and 126.2 mm Hg respectively. These are assumed to be known precisely.

As discussed earlier, before analysing the data one should first consider the nature of the experimental errors.

First, assume property VII of table 8 - which here implies that the elapsed time is measured with negligible error - and property I, implying that the decrease in pressure is free from systematic measurement error.

Consider next property II. There are two reasons why the Y_i are unlikely to be independent. First, the decrease in pressure is calculated from the difference of the initial pressure and the time-varying pressure. Any error in the initial pressure measurement will therefore pass into all the Y_i, and so they will be correlated. This source of correlation could be avoided by working directly with the measured pressure, but is anyway unlikely to be important if, as already assumed, the two initial partial pressures are known to very high accuracy. The second source of correlation is likely to be more important, and it stems from the likely correlation among the measured pressures themselves, simply because of the particular sequential nature of the observations. To obtain independent measurements, one would have had to prepare a sample of reaction mixture, take a pressure

reading after one second, reject that mixture, prepare another, allow that to react for two seconds, take a reading, and so on. Since such a procedure was not followed, one can at best hope to test for serial correlation after the parameters have been estimated, by examining the residuals (136,137).

The error in Y_o will be assumed to be zero, which is both reasonable and convenient; property III will be assumed, as will be equality of the error variances. In such a case, it is reasonable to choose an unweighted least squares method - see table 9. To perform a confidence region analysis or 'error analysis', one must add properties IV and VI, and estimate the error variance from the residual sum-of-squares in the usual way (193).

The calculations were performed using direct hill-climbing (flexible simplex search (166)) and QLLS. Since the former method is straightforward, only the latter will be described here.

The QLLS technique treats the parameters as state variables, and adjoins to the original o.d.e.('s) supplementary o.d.e.'s describing their variation, or rather lack of variation.

Thus, writing

$$y_2 \equiv k_1, \text{ and } y_3 \equiv k_2 \tag{3.13}$$

then, since the parameters are constants

$$\frac{dy_2}{dt} = 0 = \frac{dy_3}{dt} \tag{3.14}$$

The initial value for eqn. (3.12) is

$$y(0) = Y_o = 0 \tag{3.15}$$

since Y_o is assumed to be error-free.

The initial values for eqn. (3.14) are the unknown parameter values, written as

$$y_{2,o} \text{ and } y_{3,o}$$

Write eqns. (3.12) and (3.14) in vector form,

$$\frac{d\underline{y}}{dt} = \underline{f}(\underline{y}) \tag{3.16}$$

where the elements of $\underline{y}$ are y_1 - formerly the scalar y - and y_2 and y_3, defined in eqn. (3.13).

The initial conditions are

$$\underline{y}(o) = \begin{bmatrix} o \\ y_{2,o} \\ y_{3,o} \end{bmatrix} \tag{3.17}$$

From eqns. (3.12) and (3.14), it is easy to identify

$$\begin{aligned} f_1 &\equiv y_2(126.2 - y_1)(91.9 - y_1)^2 - y_3 y_1^2 \\ f_2 &\equiv o \quad ; \quad f_3 \equiv o \end{aligned} \tag{3.18}$$

Using quasilinearisation (112), eqn. (3.18) is linearised about some 'first guess' solution $\underline{y}^{(o)}$, yielding a set of linear o.d.e.'s in a better approximate solution $\underline{y}^{(1)}$.

$$\frac{d\underline{y}^{(1)}}{dt} = \underline{f}^{(o)} + \underline{\underline{J}}^{(o)}(\underline{y}^{(1)} - \underline{y}^{(o)}) \tag{3.19}$$

where the Jacobian matrix

$$\underline{\underline{J}} \equiv \frac{\partial \underline{f}}{\partial \underline{y}} \equiv \begin{bmatrix} \frac{\partial f_1}{\partial y_1} & \frac{\partial f_1}{\partial y_2} & \frac{\partial f_1}{\partial y_3} \\ \frac{\partial f_2}{\partial y_1} & \frac{\partial f_2}{\partial y_2} & \frac{\partial f_2}{\partial y_3} \\ \frac{\partial f_3}{\partial y_1} & \frac{\partial f_3}{\partial y_2} & \frac{\partial f_3}{\partial y_3} \end{bmatrix} \tag{3.20}$$

The elements of $\underline{\underline{J}}$ are calculated from eqn. (3.18)

$$\frac{\partial f_1}{\partial y_1} = -2y_2(126.2 - y_1)(91.9 - y_1) - y_2(91.9 - y_1)^2 - 2y_3y_1$$

$$\frac{\partial f_1}{\partial y_3} = -y_1^2 \tag{3.21}$$

$$\frac{\partial f_2}{\partial y_1} = 0 = \frac{\partial f_2}{\partial y_2} = \frac{\partial f_2}{\partial y_3} = \frac{\partial f_3}{\partial y_1} = \frac{\partial f_3}{\partial y_2} = \frac{\partial f_3}{\partial y_3}$$

The complete solution of the linear eqn. (3.19) can be written, using the Principle of Superposition, as the sum of a particular solution and of multiples of the homogeneous solutions

$$\underline{y}^{(1)}(t) = \underline{P}^{(1)}(t) + \sum_{j=2}^{3} c_j^{(1)} \underline{h}_j^{(1)} \tag{3.22}$$

In a typical boundary value problem, the multipliers c_j would be chosen such that $\underline{y}^{(1)}$ satisfied the boundary conditions. Here they are chosen to minimise the objective function appropriate to the parameter estimation criterion used; in this case the simple sum-of squares- function

$$\Phi \equiv \sum_{i=1}^{14} \{Y_i - y_{1,i}\}^2 \tag{3.23}$$

$$= \sum_{i=1}^{14} \{Y_i - p_1^{(1)}(t_i) - c_2^{(1)} h_{2,1}^{(1)}(t_i) - c_3^{(1)} h_{3,1}^{(1)}(t_i)\}^2 \tag{3.24}$$

The appropriate values of the c_j's therefore follow from

$$\frac{\partial \Phi}{\partial c_2} = 0 = \frac{\partial \Phi}{\partial c_3} \tag{3.25}$$

which yield

$$c_2^{(1)} \sum_{i=1}^{14} \{h_{2,1}^{(1)}(t_i)\}^2 + c_3^{(1)} \sum_{i=1}^{14} h_{2,1}^{(1)}(t_i) h_{3,1}^{(1)}(t_i) = \sum_{i=1}^{14} h_{2,1}^{(1)}(t_i)\{Y_i - p_1^{(1)}(t_i)\}$$

$$c_2^{(1)} \sum_{i=1}^{14} h_{2,1}^{(1)}(t_i) h_{3,1}^{(1)}(t_i) + c_3^{(1)} \sum_{i=1}^{14} \{h_{3,1}^{(1)}(t_i)\}^2 = \sum_{i=1}^{14} h_{3,1}^{(1)}(t_i)\{Y_i - p_1^{(1)}(t_i)\} \tag{3.26}$$

which are simply a pair of linear algebraic equations for the c_j's, and thus simply solved.

The algorithm then becomes:-

1. Make a first guess at k_1 and k_2 ($y_{2,0}^{(0)}$ and $y_{3,0}^{(0)}$).

2. Integrate eqn. (3.12) with initial condition eqn. (3.15), to obtain $y_1^{(0)}$.

3. Obtain the particular solution $p^{(1)}$ by integrating eqn. (3.19) with initial values $\underline{p}^{(1)}(0) = \underline{0}$. Note that this step involves integrating only one member of the set of eqns. (3.19), since the solution to the other two equations is trivial, viz.

$$p_2^{(1)}(t) = 0 = p_3^{(1)}(t) \tag{3.27}$$

4. Obtain the homogeneous solutions from the homogeneous form of eqn. (3.19) viz.

$$\frac{d\underline{h}^{(1)}}{dt} = \underline{\underline{J}}^{(0)}\underline{h}^{(1)} \tag{3.28}$$

With the two sets of initial values

$$h_{jk}^{(1)}(0) = \delta_{jk} = \begin{cases} 0 & j \neq k \\ 1 & \text{otherwise} \end{cases} \tag{3.29}$$

for $j,k = 2,3$

5. Solve eqn. (3.26) for $c_2^{(1)}$ and $c_3^{(1)}$

6. Use eqn. (3.22) to compute $\underline{y}^{(1)}$, and use it in place of $\underline{y}^{(0)}$ in step 2. Repeat until convergence is obtained.

This is the recommended procedure for QLLS. However experience suggested an attractive alternative. The integration step 2 should be performed simultaneously with steps 3 and 4, and then one should perform step 5, before returning to step 1. Clearly this involves one more integration per iteration than the other procedure, but it leads to a more clear-cut convergence, with negligible oscillation or 'wander' near the solution. The re-integration of eqn. (3.12) clearly yields a more satisfactory $\underline{y}^{(0)}$ than does the use of eqn. (3.22), presumably because the latter may involve the combination of components of very different magnitudes. Further, this alternative procedure does not require use of the same integration nodes in each iteration - as the other procedure does - thus simplifying the programming and making it possible to use an adjustable step-length integration method.

A typical convergence sequence is shown in table 12.

Table 12: Convergence of QLLS

$\Phi \times 10^{-1}$	$k_1 \times 10^{6}$	$k_2 \times 10^{4}$
409	1	1
4.28	3.4128	25.535
2.63	4.5887	3.6826
2.194	4.5775	2.8078
2.187	4.5772	2.7966
2.187	4.5772	2.7966

The values predicted by the model with these parameter values are shown in table 11. The fit is clearly good. A confidence region analysis was also performed - see Appendix 2 and fig. 5.4.

It was found that QLLS had a smaller convergence region than simplex search, but that the latter required 83 equation integrations. The 'alternative procedure' QLLS required 24 equation integrations in all, but the integrations were easily programmed to economise on computer time, since 4 equations were integrated simultaneously at each iteration.

This example makes it clear that the QLLS method requires considerable manipulation to set up the basic equations, even for a single response system. Although the difficulties of convergence of the algorithm are not unduly troublesome here, it is shown in chapter five that this is not always the case.

CHAPTER 4:- The Development of Approximate Methods for Parameter Estimation in Ordinary Differential Equations

4.1 Weighted Residual Methods.

4.2 The sub-domain method (SDM).

4.3 The residual least squares method (RLSM).

4.4 Simplifications.

4.5 Statistical properties of the weighted residual estimators: a single response example.

4.6 Statistical properties of the weighted residual estimators: a multi-response example.

4.7 Simulation studies with non-zero error covariance.

4.8 Development of a Taylor Series analysis for efficiency and bias calculations.

4.9 Summary.

Note: the principles of the new methods were described by the writer at the First Annual Research Meeting of the Institution of Chemical Engineers, London, 1974.

4.1 Weighted residual methods

In this chapter two techniques are proposed for parameter estimation in first-order o.d.e.'s. They are developed as analogues of certain of the methods of weighted residuals used for the approximate solution of o.d.e.'s (section 2.5).

Consider first some single response model, with a single parameter θ:

$$\frac{dy}{dt} = f(y,\theta) \tag{4.1}$$

$$y(0) = y_o \tag{4.2}$$

where y is the dependent variable, t is the independent variable and f is, in general, a known non-linear function of y and θ.

Suppose the data to consist of directly observed pairs of values of y and t. The observations of t are assumed to contain negligible error (Table 8, property VII), while those of y are described by

$$Y_i = y_i + e_i \qquad (i = 0,1....m)$$

where Y_i is the observed value of y, y_i the 'true' value, and e_i the error associated with the i^{th} observation.

By analogy with M.W.R., an equation residual R may be defined by

$$R \equiv \frac{dy}{dt} - f(y,\theta) \tag{4.3}$$

Clearly the solution of eqns. (4.1) and (4.2) satisfies the condition

$$R = 0$$

identically for all $t > 0$. Therefore that solution satisfies the integral condition

$$\int_{t_B}^{t_F} Rg(y)\,dt = 0 \qquad (4.4)$$

where $g(y)$ is an arbitrary finite weighting function and t_F and t_B are any $t > 0$. The analogy between eqn. (4.4) and the fundamental equation of MWR is obvious. One can combine eqns. (4.3) and (4.4) to yield

$$\int_{t_B}^{t_F} f(y,\theta)g(y)\,dt = \int_{y_B}^{y_F} g(y)\,dy \qquad (4.5)$$

The important step in the new techniques is that one seeks to satisfy eqn. (4.5) with the integrals being approximated using the <u>observed values</u> Y_i. A simple approximation is the trapezoidal rule:-

$$\int_{t_B}^{t_F} G\,dt \doteq \sum_{i=b}^{f-1} \tfrac{1}{2}\{G(t_i) + G(t_{i+1})\}\{t_{i+1}-t_i\} \qquad (4.6)$$

Substituting eqn. (4.6) into eqn. (4.5), one finds

$$\sum_{i=b}^{f-1} \{f(Y_i,\theta)g(Y_i) + f(Y_{i+1},\theta)g(Y_{i+1})\}\{t_{i+1}-t_i\} = \sum_{i=b}^{f-1} \{g(Y_i)+g(Y_{i+1})\}\{Y_{i+1}-Y_i\} \qquad (4.7)$$

Note that θ is the only unknown in eqn. (4.7), and so the estimate $\hat{\theta}$ is found by requiring that eqn. (4.7) be satisfied exactly. The great advantage of this approach is that an estimate of θ is obtained much more easily from eqn. (4.7) than from the <u>least squares criterion</u>:

N.B. The limits b,f on the counting integer i are such that $t_b = t_B$, $t_f = t_F$

$$\min_{\theta}\{\Phi(\theta) \equiv \sum_{i=1}^{m}(Y_i - y_i)^2\} \qquad (4.8)$$

where the y_i must be obtained by solution of eqns. (4.1) and (4.2).

Equation (4.7) forms the basis of parameter estimation by weighted residual methods. Various techniques might be proposed, differing only in their choice of weighting function g(y). Here only two of the more obvious methods of choosing g(y) are examined, but it should be borne in mind that there are other plausible choices.

4.2 The sub-domain method (SDM)

Perhaps the most obvious choice of weighting function is:

$$g(y) = 1$$

This reduces eqn. (4.7) to the simple form

$$\tfrac{1}{2}\sum_{i=b}^{f-1}\{f(Y_i,\theta) + f(Y_{i+1},\theta)\}\{t_{i+1} - t_i\} = Y_m - Y_o \qquad (4.9)$$

This criterion is referred to as the 'sub-domain method' since it corresponds to the MWR variant of the same name, which requires that the equation residual disappear <u>on average</u> over suitable sub-domains of t.

4.3 The residual least squares method (RLSM)

$$\text{Here one chooses} \quad g(y) = \frac{\partial R}{\partial \theta} = -\frac{\partial f}{\partial \theta} \equiv -f'(\theta) \tag{4.10}$$

Substitution into eqn.(4.7) yields the estimator equation

$$\sum_{i=b}^{f-1} \{f(Y_i,\theta)f'(Y_i,\theta)+f(Y_{i+1},\theta)f'(Y_{i+1},\theta)\}\{t_{i+1}-t_i\} = \sum_{i=b}^{f-1} \{f'(Y_i,\theta)+f'(Y_{i+1},\theta)\} \{Y_{i+1} - Y_i\} \tag{4.11}$$

This is referred to as 'the residual least squares method', because the choice of g(y) corresponds to that used in the 'least squares' variant of M.W.R. Note that substitution of eqn. (4.10) into eqn. (4.4) yields

$$\int_{t_B}^{t_F} R \frac{\partial R}{\partial \theta}\, dt = 0 \quad \Rightarrow \quad \min_{\theta} \{ \int_{t_B}^{t_F} R^2\, dt\} \tag{4.12}$$

4.4 Simplifications

In chemical kinetic studies it is often possible to write $f(y,\theta)$ in the simpler form

$$f(y,\theta) = \theta\, q(y) \tag{4.13}$$

where θ represents a rate constant. In this case eqns. (4.9) and (4.11) become explicit in θ, yielding

$$\hat{\theta} = \frac{Y_m - Y_o}{\tfrac{1}{2} \sum_{i=b}^{f-1} \{q(Y_i) + q(Y_{i+1})\}\{t_{i+1} - t_i\}} \quad : \text{SDM} \tag{4.14}$$

$$\hat{\theta} = \frac{\sum_{i=b}^{f-1} \{q(Y_i) + q(Y_{i+1})\}\{Y_{i+1} - Y_i\}}{\sum_{i=b}^{f-1} \{q^2(Y_i) + q^2(Y_{i+1})\}\{t_{i+1} - t_i\}} \quad : \text{RLSM} \qquad (4.15)$$

The choice of the summation limits b and (f-1) will often be perfectly obvious: since one wants to use all the measurements Y_i (i=0,1....m), one should choose b=0 and f=m, for this single response problem.

It is clear that these new methods offer potentially striking computational advantages over conventional techniques which require repetitive numerical integration of the model equations as part of an iterative function minimisation. However, it is important to determine their statistical properties - bias, efficiency and consistency - as defined in Chapter 3.

4.5 Statistical properties of the weighted residual estimators: A single response example

It is accepted (143) that the performance of data analysis procedures must often be assessed by 'simulation' or 'experimental sampling'. A suitable test example is the constant volume, isothermal, irreversible, first-order reaction effected in the batch mode or in a plug-flow reactor: the appropriate model is

$$dy/dt = -ky$$

$$y(o) = y_o \qquad (4.16)$$

where the rate constant k is the parameter to be estimated, y represents the reactant concentration and t the elapsed time or residence time. Pseudo-experimental data is generated using

$$Y_o = y_o \; ; \quad Y_i = y(t_i) + \text{GAUSS}(0,S), \; i=1,2....m \qquad (4.17)$$

where GAUSS(0,S) is a Normally distributed random variable with zero mean and standard deviation S (see section A2.2), representing experimental error, and $y(t_i)$ is calculated from the analytical solution to eqn. (4.16)

$$\text{viz.} \quad y(t) = y_o \exp(-kt) \qquad (4.18)$$

with $k = 1$, $y_o = 1$.

In addition to the weighted residual estimates, the maximum likelihood estimate of k is also calculated, which, for the 'error' imposed here (Table 8, numbers I, II, III, IV, VI and constant error variance), equals the estimate computed by classical unweighted least squares.

The value of k estimated by any method is itself a random variable because it corresponds to one particular set of experimental errors. To obtain statistically significant results, five hundred simulated experiments were performed, and the mean ($\bar{\hat{k}}$) and variance ($\sigma_{\hat{k}}^2$) of the distribution of parameter estimates were calculated.

The estimators: the weighted residual estimators follow from eqns. (4.13) and (4.14) with $q(y) = y$

SDM

$$\hat{k} = \frac{Y_o - Y_m}{\frac{1}{2}\sum_{i=o}^{m-1}(Y_i+Y_{i+1})(t_{i+1}-t_i)}$$

RLSM

$$\hat{k} = \frac{Y_o^2 - Y_m^2}{\sum_{i=o}^{m-1}(Y_i^2+Y_{i+1}^2)(t_{i+1}-t_i)}$$

Classical least squares

$$\hat{k} : \min_k \{ [Y_i - y(t_i, k)]^2 \} \qquad (4.19)$$

The simulations: the effect of the level of measurement error was studied using 25 data points (m=25), with a time between successive measurements of 0.1 minutes. The results for $S = 10^{-2}$ and $10^{-3/2}$ are shown in table 13.

Table 13: Parameter Estimates and the Effect of the Level of Measurement Error

S		Classical Least Squares	Weighted Residual Methods		True value of k
			SDM	RLSM	
10^{-2}	$\bar{\hat{k}}$	1.000	0.999	0.996	1.000
	$\sigma_{\hat{k}} / \bar{\hat{k}}$	0.006	0.012	0.008	-
$10^{-3/2}$	$\bar{\hat{k}}$	1.000	1.000	0.990	1.000
	$\sigma_{\hat{k}} / \bar{\hat{k}}$	0.020	0.039	0.026	-

It will be seen that none of the methods is particularly sensitive to the level of measurement error. The classical least squares method and SDM both recover the true value of k and so are both approximately unbiased, whereas RLSM underpredicts k, the bias

increasing with the level of measurement error. However the bias error is less than 1%, which would certainly be acceptable in practice.

Classical least squares is the most efficient estimator, since it has the smallest variance $\sigma^2_{\hat{k}}$, but the new methods show promisingly small variances, especially RLSM.

Next the effect of the number of data points was studied. The range 0-2.5 minutes was divided into 10, 25 and 50 equal intervals, with $S = 10^{-3/2}$

Table 14: The Effect of the Number of Observations

m		Classical Least Squares	Weighted Residual Methods		True value of k
			SDM	RLSM	
10	$\overline{\hat{k}}$	1.000	0.995	0.975	1.000
	$\sigma_{\hat{k}}/\overline{\hat{k}}$	0.031	0.044	0.038	-
25	$\overline{\hat{k}}$	1.000	1.000	0.990	1.000
	$\sigma_{\hat{k}}/\overline{\hat{k}}$	0.020	0.039	0.026	-
50	$\overline{\hat{k}}$	1.000	1.000	0.993	1.000
	$\sigma_{\hat{k}}/\overline{\hat{k}}$	0.015	0.035	0.020	-

The accuracy of the weighted residual methods, particularly RLSM, deteriorates a little for small m, as a result of loss in accuracy of trapezoidal rule integration. This deterioration could be avoided by using a higher order integration formula, or by trying to locate the data points at optimal Gaussian quadrature points.

Table 14 demonstrates the consistency of the methods; as the number of data gathered increases, $\hat{k}$ approaches the true value of 1.

In summary, the weighted residual methods are shown to exhibit acceptable statistical properties, and to compare well with the calssical least squares method.

4.6 Statistical properties of the weighted residual estimators: A multi-response example

In the previous section discussion was restricted to a problem involving a single response. Attention is now turned to a multi-response system - a sequence of first order reactions

$$A \xrightarrow{k_1} B \xrightarrow{k_2} C$$

Under the assumptions mentioned in section 4.5, a suitable model is:

$$\frac{dy_1}{dt} = -k_1 y_1 \quad ; \quad y_1(o) = y_{1o}$$

$$\frac{dy_2}{dt} = k_1 y_1 - k_2 y_2 \quad ; \quad y_2(o) = o \tag{4.20}$$

where y_1 and y_2 represent the concentrations of A and B respectively. This system of equations has the solution

$$y_1(t) = y_{1o} \exp(-kt)$$

$$y_2(t) = \frac{k_1 y_{1o}}{k_1 - k_2} (\exp(-k_2 t) - \exp(-k_1 t)) \tag{4.21}$$

which will be used to generate simulated experimental data, and to perform maximum likelihood estimation for comparison with the results obtained using the weighted residual estimators.

The simulated data is generated using

$$Y_{1O} = y_{1O} \quad ; \quad Y_{1i} = y_1(t_i) + e_{1i} \quad ; \quad i = 1,2...m$$

$$Y_{2O} = y_{2O} = O \; ; \quad Y_{2i} = y_2(t_i) + e_{2i} \quad ; \quad i = 1,2...m \tag{4.22}$$

where $y_1(t_i)$ and $y_2(t_i)$ are calculated using eqns. (4.21) with the values shown in Table 15.

Table 15

Quantity	k_1	k_2	y_{1O}	y_{2O}	t_i	m
Value	1.0 min^{-1}	0.5 min^{-1}	1	O	0.1 i; i = 1,2...m	25

The 'errors' imposed are free from serial correlation, and follow a bi-variate Normal distribution with zero mean, and with marginal variances and covariance independent of t, so that

$$f(\underline{e}_i) = \frac{1}{\sqrt{2\pi}} (|\underline{\underline{U}}|)^{-\frac{1}{2}} \exp\{ -\tfrac{1}{2} \underline{e}_i^T \underline{\underline{U}} \underline{e}_i \} \qquad i = 1,2....m \tag{4.23}$$

where

$$\underline{e}_i^T \equiv (e_{1i} \quad e_{2i})$$

and $\underline{\underline{U}}$ is the error variance- covariance matrix

$$\underline{\underline{U}} \equiv \begin{bmatrix} \sigma_1^2 & \sigma_{12} \\ \sigma_{21} & \sigma_2^2 \end{bmatrix} = \begin{bmatrix} \sigma_1^2 & \rho_E \sigma_1 \sigma_2 \\ \rho_E \sigma_1 \sigma_2 & \sigma_2^2 \end{bmatrix} \tag{4.24}$$

where σ_1^2 and σ_2^2 are the marginal variances of e_{1i} and e_{2i} respectively

σ_{12} $(= \sigma_{21})$ is the covariance of e_{1i} and e_{2i}

and ρ_E is the error cross-correlation coefficient $(-1 \leq \rho_E \leq 1)$

If $\rho_E = 0$, the 'errors' e_{1i} and e_{2i} are <u>independent</u>. The algorithm used for generating the pseudo-error is described in appendix A2.3.

<u>The Estimators</u>

<u>a) SDM</u> After inspection of eqn. (4.20), equation residuals are defined by

$$R_1 \equiv \frac{dy_1}{dt} + k_1 y_1$$

$$R_2 \equiv \frac{dy_2}{dt} - k_1 y_1 + k_2 y_2 \tag{4.25}$$

and the criterion is invoked that

$$\int_o^{t_m} R_1 dt = 0 = \int_o^{t_m} R_2 dt \tag{4.26}$$

After a little manipulation, one obtains the estimator equations

$$\hat{k}_1 = \frac{Y_{1o} - Y_{1m}}{\tfrac{1}{2} \sum_{i=o}^{m-1} \{Y_1(t_i)+Y_1(t_{i+1})\}\{t_{i+1}-t_i\}}$$

$$\hat{k}_2 = \frac{(Y_{1o} + Y_{2o}) - (Y_{1m} + Y_{2m})}{\tfrac{1}{2} \sum_{i=o}^{m-1} \{ Y_2(t_i)+Y_2(t_{i+1})\}\{t_{i+1}-t_i\}} \tag{4.27}$$

Note that the estimate of k_1 depends only on the measured response $Y_1(t_i)$ and is <u>independent</u> of $Y_2(t_i)$, whilst the estimate of k_2 depends on $Y_2(t_i)$ and is independent of $Y_1(t_i)$, apart from the initial and final values Y_{1O} and Y_{1m}.

b) RLSM

First the integrals of the squared residuals are written down

$$S_1 \equiv \int_o^{t_m} \left(\frac{dy_1}{dt} + k_1 y_1 \right)^2 dt \qquad (4.28)$$

$$S_2 \equiv \int_o^{t_m} \left(\frac{dy_2}{dt} - k_1 y_1 + k_2 y_2 \right)^2 dt$$

Next an overall integrated squared residual S_o is defined as the weighted sum of the individual integral squared residuals

$$S_o \equiv W_1 S_1 + W_2 S_2 \qquad (4.29)$$

where W_1 and W_2 are weighting factors which may be chosen to give greater weight to that response which is measured with greater accuracy. The estimates are now obtained by requiring - in analogy with eqn. (4.12)- that S_o be minimised w.r.t. k_1 and k_2

$$\frac{\partial S_o}{\partial k_i} = 0 \quad ; \quad i=1,2 \qquad (4.30)$$

There follows

$$\begin{aligned} a_1 \hat{k}_1 + a_2 \hat{k}_2 &= a_3 \\ b_1 \hat{k}_1 + b_2 \hat{k}_2 &= b_3 \end{aligned} \qquad (4.31)$$

where $$a_1 \equiv (1 + \frac{W_2}{W_1}) \tfrac{1}{2} \sum_{i=o}^{m-1} \{Y_1^2(t_i) + Y_1^2(t_{i+1})\}\{t_{i+1} - t_i\}$$

$$a_2 \equiv -\frac{W_2}{W_1} \tfrac{1}{2} \sum_{i=o}^{m-1} \{Y_1(t_i)Y_2(t_i) + Y_1(t_{i+1})Y_2(t_{i+1})\}\{t_{i+1} - t_i\}$$

$$a_3 \equiv \frac{W_2}{W_1} \tfrac{1}{2} \sum_{i=o}^{m-1} \{Y_1(t_i) + Y_1(t_{i+1})\}\{Y_2(t_{i+1}) - Y_2(t_i)\} + \tfrac{1}{2}(Y_{1o}^2 - Y_{1m}^2) \qquad (4.32)$$

$$b_1 \equiv -\frac{W_1}{W_2} a_2 \; ; \quad b_3 \equiv \tfrac{1}{2}(Y_{2m}^2 - Y_{2o}^2)$$

$$b_2 \equiv -\tfrac{1}{2} \sum_{i=o}^{m-1} \{Y_2^2(t_i) + Y_2^2(t_{i+1})\}\{t_{i+1} - t_i\}$$

Eqns. (4.31) yield the estimators

$$\hat{k}_1 = \frac{a_2b_3 - a_3b_2}{a_2b_1 - a_1b_2} \quad ; \quad \hat{k}_2 = \frac{a_3b_1 - a_1b_3}{a_2b_1 - a_1b_2} \qquad (4.33)$$

Note that the entire data space is used in estimating each of k_1 and k_2.

c) Maximum likelihood method

For the error properties assumed here (Table 8, properties I to VII), maximum likelihood estimates correspond to those obtained by the use of Generalised Least Squares (G.L.S.) - Table 9, method 3 - as presented by Hunter (194). For the example under consideration, GLS may be written as

$$\min_{k_1, k_2} \{S_G\} \qquad (4.34)$$

where $$S_G \equiv \sigma^{11} \sum_{i=1}^{m} (Y_{1i} - y_{1i})^2 + 2\sigma^{12} \sum_{i=1}^{m} (Y_{1i} - y_{1i})(Y_{2i} - y_{2i})$$

$$+ \sigma^{22} \sum_{i=1}^{m} (Y_{2i} - y_{2i})^2 \qquad (4.35)$$

and the weighting factors are defined by

$$\sigma^{11} \equiv \frac{1}{\sigma_1^2(1-\rho_E^2)} \; ; \quad \sigma^{12} \equiv \frac{-\rho_E}{\sigma_1\sigma_2(1-\rho_E^2)} \; ; \quad \sigma^{22} \equiv \frac{1}{\sigma_2^2(1-\rho_E^2)} \tag{4.36}$$

The simulations

The parameter estimation methods are applied to each of 500 data sets constructed by simulation. Distributions of the estimates are thus obtained: examples are shown in figs. 4.1 and 4.2.

Bias. Simulations performed over many sets of error variance in the range $10^{-4} < \sigma_1^2, \sigma_2^2 < 10^{-2}$ suggested that SDM is unbiased whilst RLSM is biased: figs. 4.3 and 4.4 show some detailed results.

For the case of equal variances, $\sigma_1^2 = \sigma_E^2 = \sigma_2^2$, and zero cross-correlation, $\rho_E = 0$, the bias in the RLSM estimates is displayed in Table 16.

Table 16: Bias in the RLSM estimates

σ_E^2	% error in $\hat{k}_1$	% error in $\hat{k}_2$
10^{-4}	-0.7	-1.4
10^{-3}	-1.3	-2.8
10^{-2}	-7.3	-16.2

Inspection of figs. 4.3 and 4.4 reveals that RLSM consistently under predicts the values of k_1 and k_2, but that for accurate data ($\sigma_E^2 \leq 10^{-3}$) the bias is negligibly small. However, above a certain theshold, $\sigma_E^2 \sim 10^{-3}$, the bias tends to increase exponentially with σ_E^2,

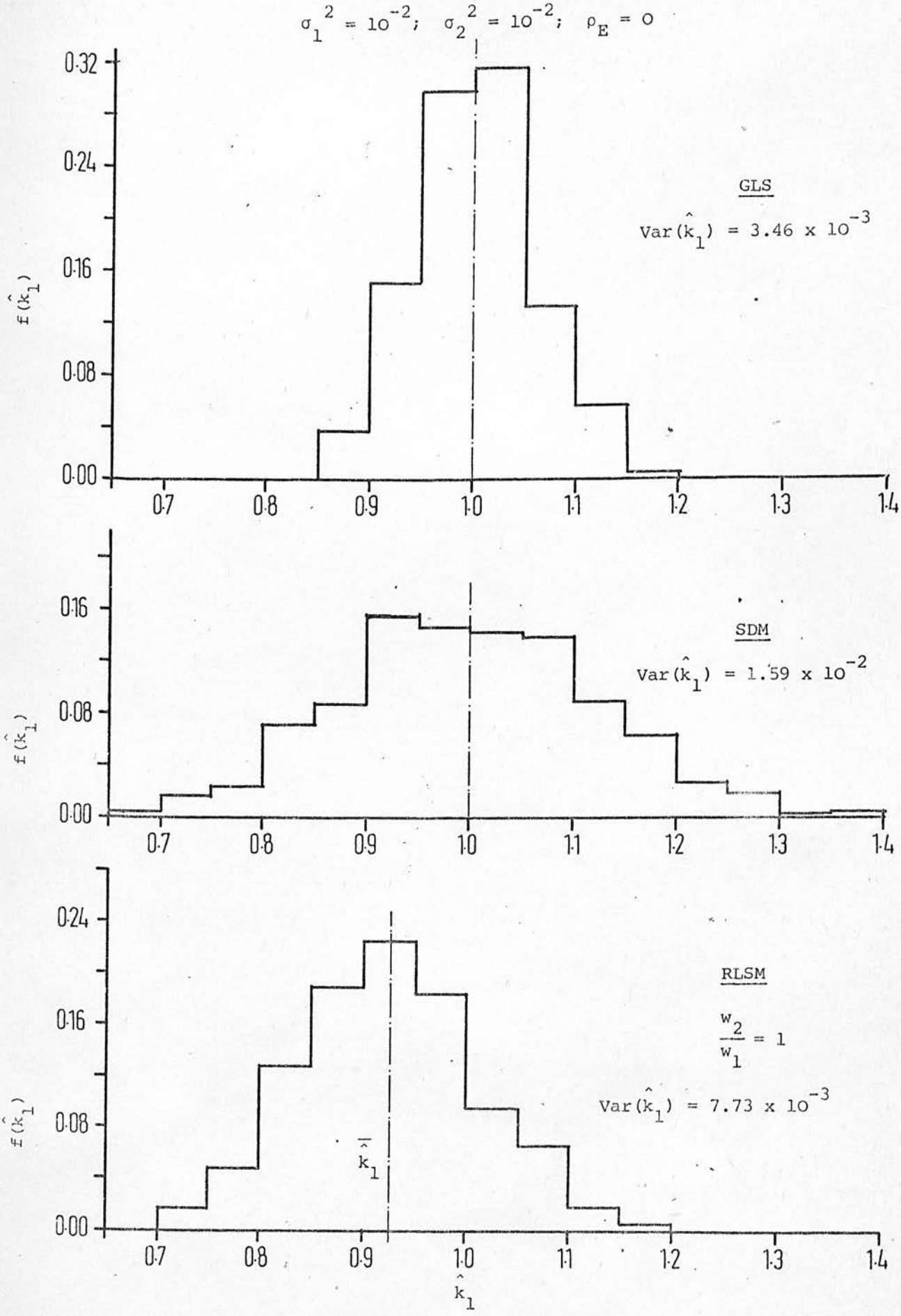

FIGURE 4.1 Marginal Distributions Of $\hat{k}_1$

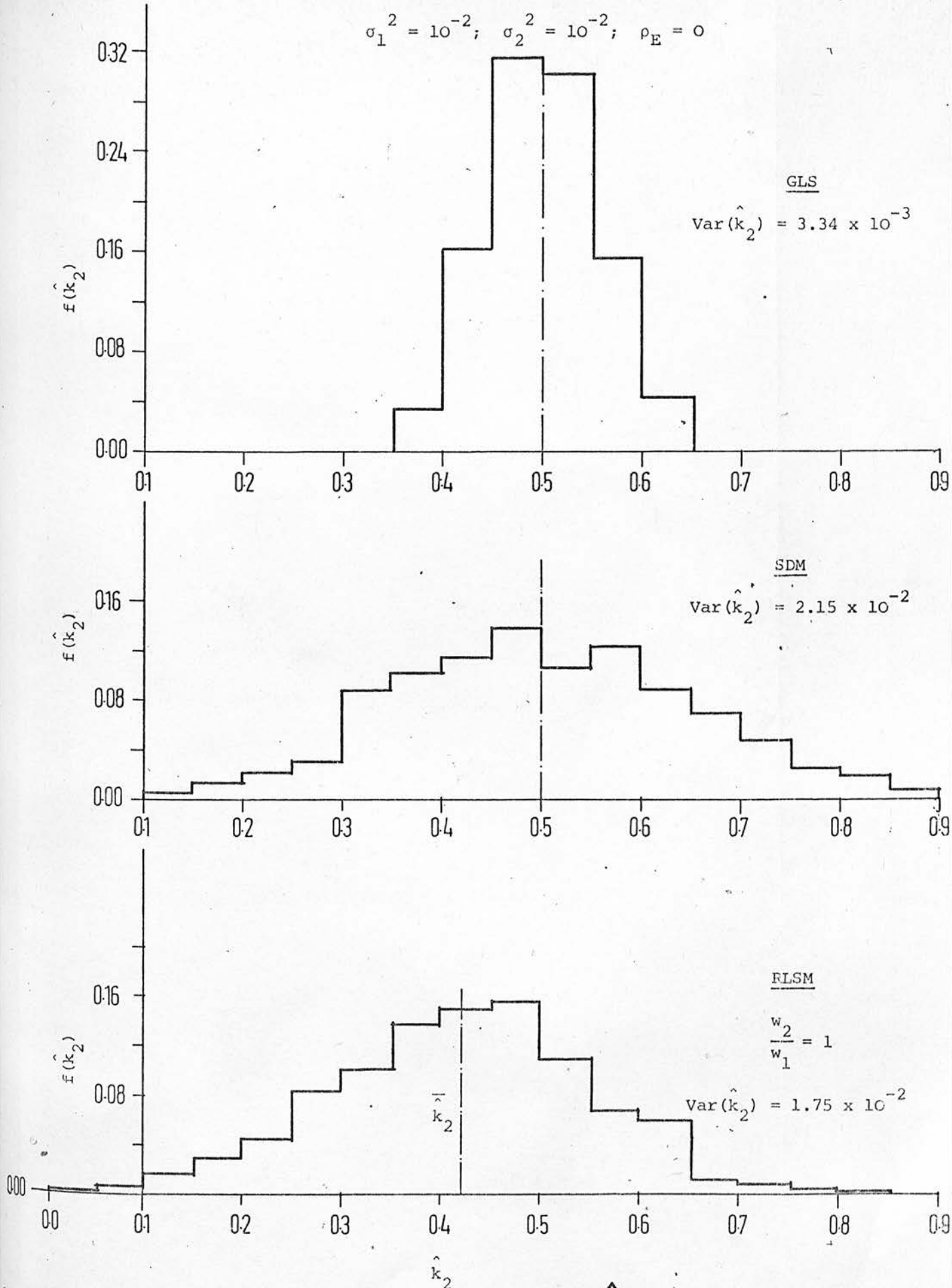

FIGURE 4.2 Marginal Distributions Of $\hat{k}_2$

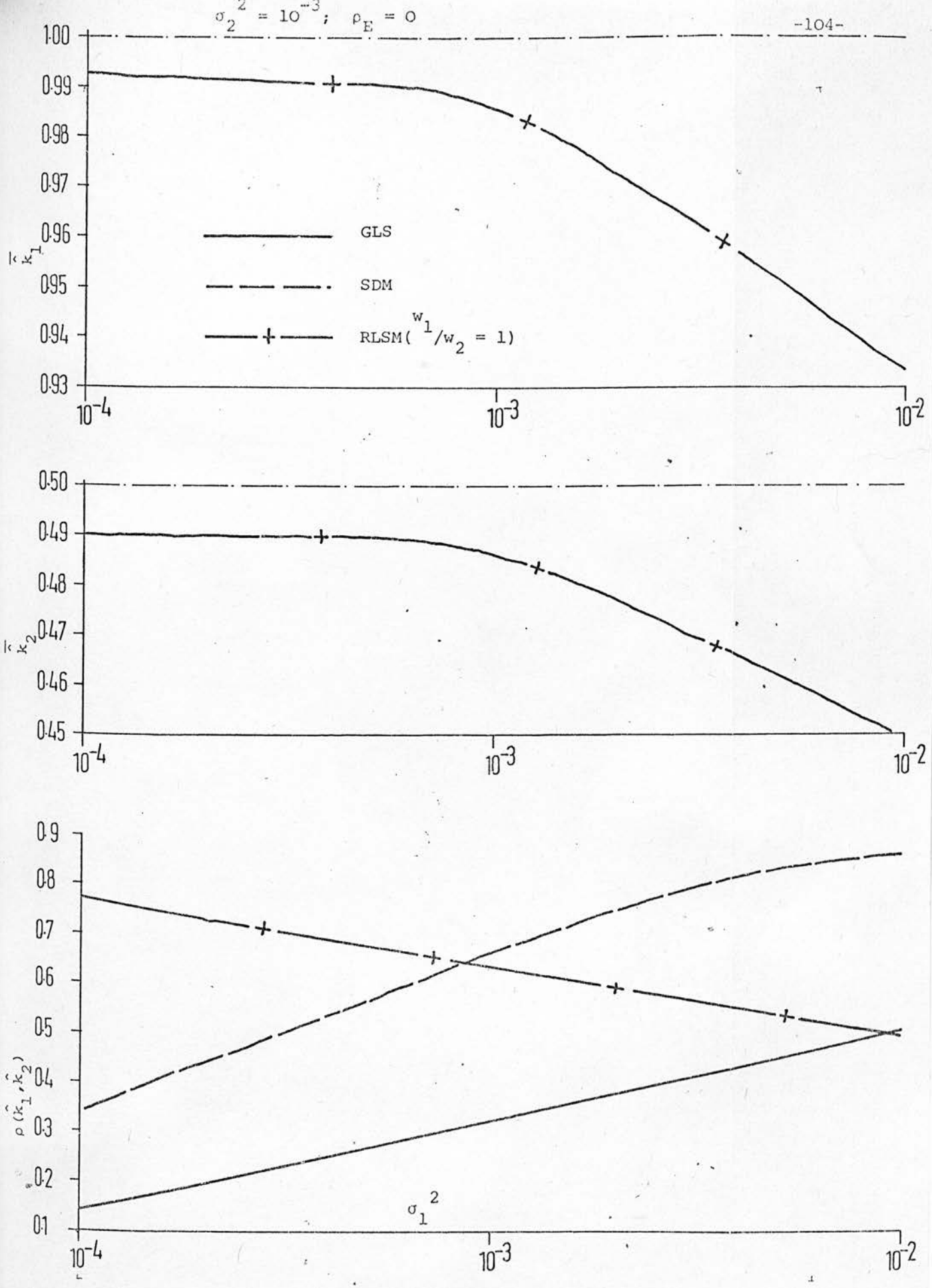

FIGURE 4.3 Bias As A Function Of σ_1^2

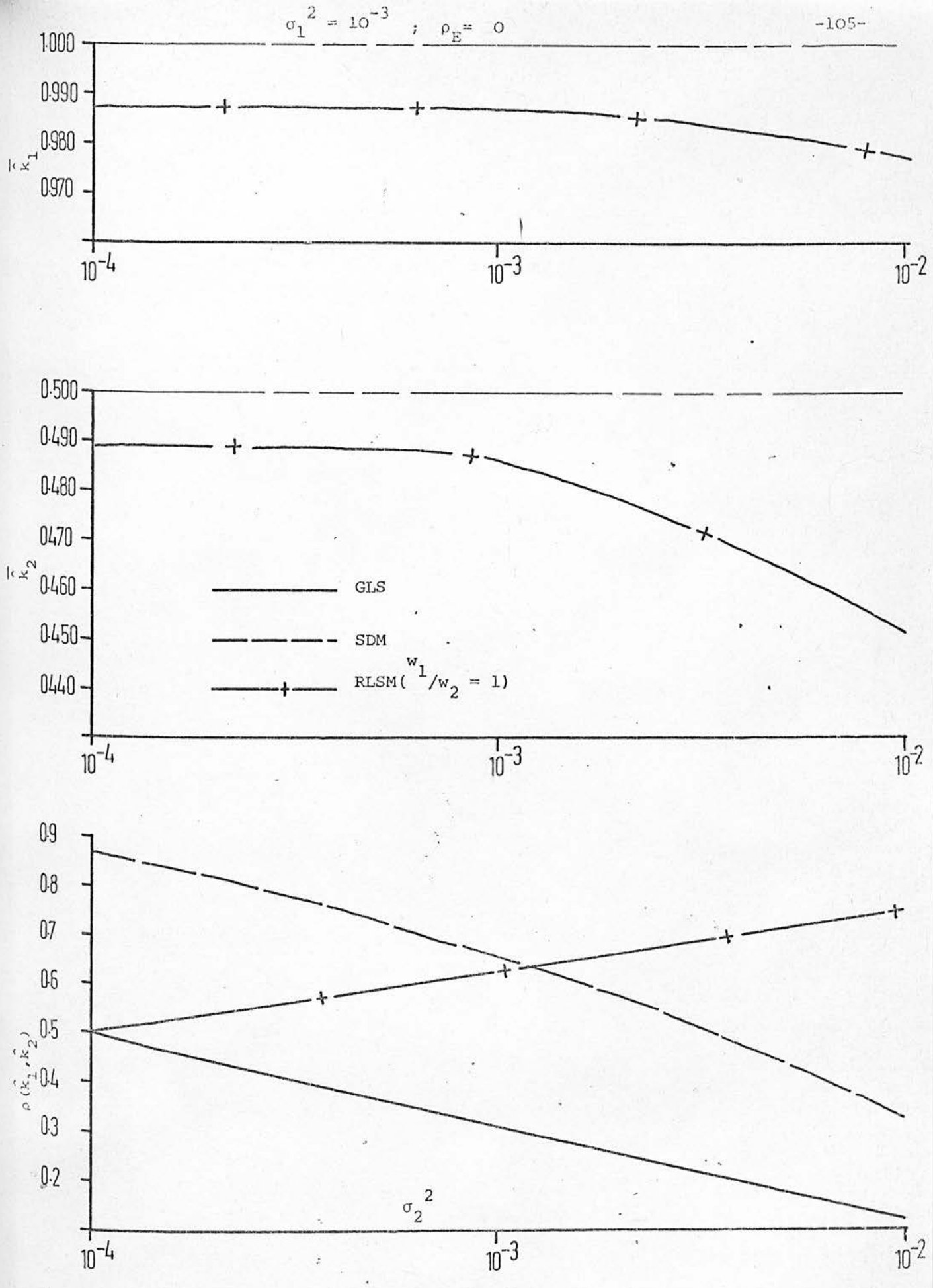

FIGURE 4.4 Bias As A Function Of σ_2^2

and the degree of bias seriously limits the usefulness of the RLSM method. Note, though, that this threshold corresponds to large proportional errors on the measurements

$$(\sigma_{E/\underline{y}_1} \sim 7\%; \quad \sigma_{E/\underline{y}_2} \sim 15\%)$$

Efficiency. The parameter variances and covariances may be calculated from the simulations: some results for the case of zero error covariance are shown in figures 4.3 to 4.6. Clearly the weighted residual methods are less efficient than GLS.

As may be inferred from 'probability paper' plots, such as those of figure 4.7, the probability estimates from all three methods display approximately Normal marginal distributions. Consequently the estimates of k_1 and k_2 for each method approximately follow a bi-variate Normal joint distribution with variance-covariance matrix $\underline{\underline{C}}$, where

$$C_{ij} = E\left\{ \left[\underline{\hat{k}} - E(\underline{\hat{k}})\right] \cdot \left[\underline{\hat{k}} - E(\underline{\hat{k}})\right]^T \right\}$$
$$\text{and } \underline{\hat{k}} \equiv (\hat{k}_1 \quad \hat{k}_2)^T; \quad E \text{ is the expectation operator.} \tag{4.37}$$

It follows that a 95% joint confidence region for the parameters may be calculated using the χ^2 distribution: such a region, for each of the three estimation methods, is shown in figure 4.8. The calculation method is demonstrated in section 5.6 and appendix A2.1.

Moreover, the relative efficiencies of the methods may be computed by comparing the volumes of their joint confidence regions, which corresponds to comparing $|\underline{\underline{C}}|^{\frac{1}{2}}$ for each method.

Such relative efficiencies are displayed in table 17, using the definitions

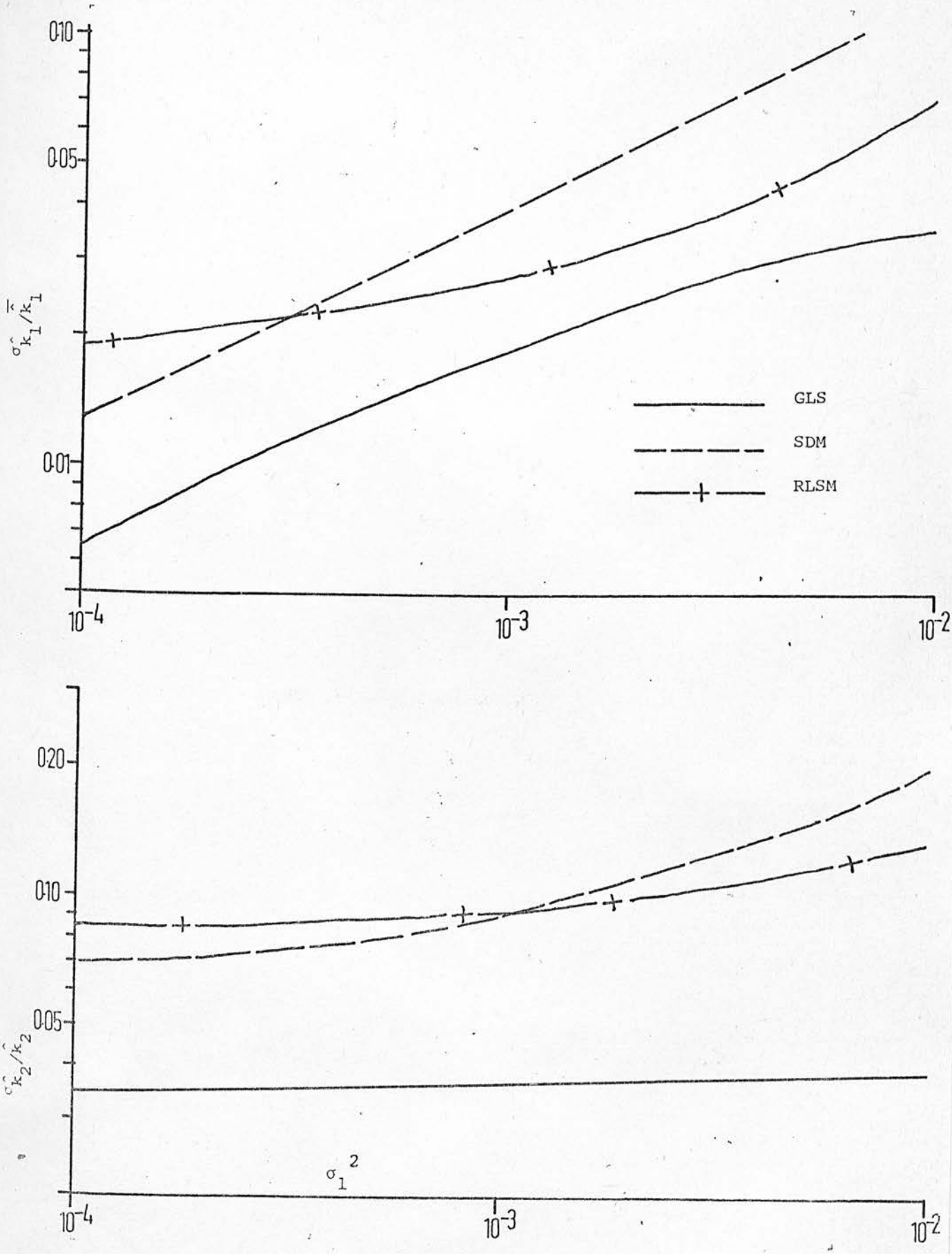

FIGURE 4.5 Efficiency As A Function Of σ_1^2

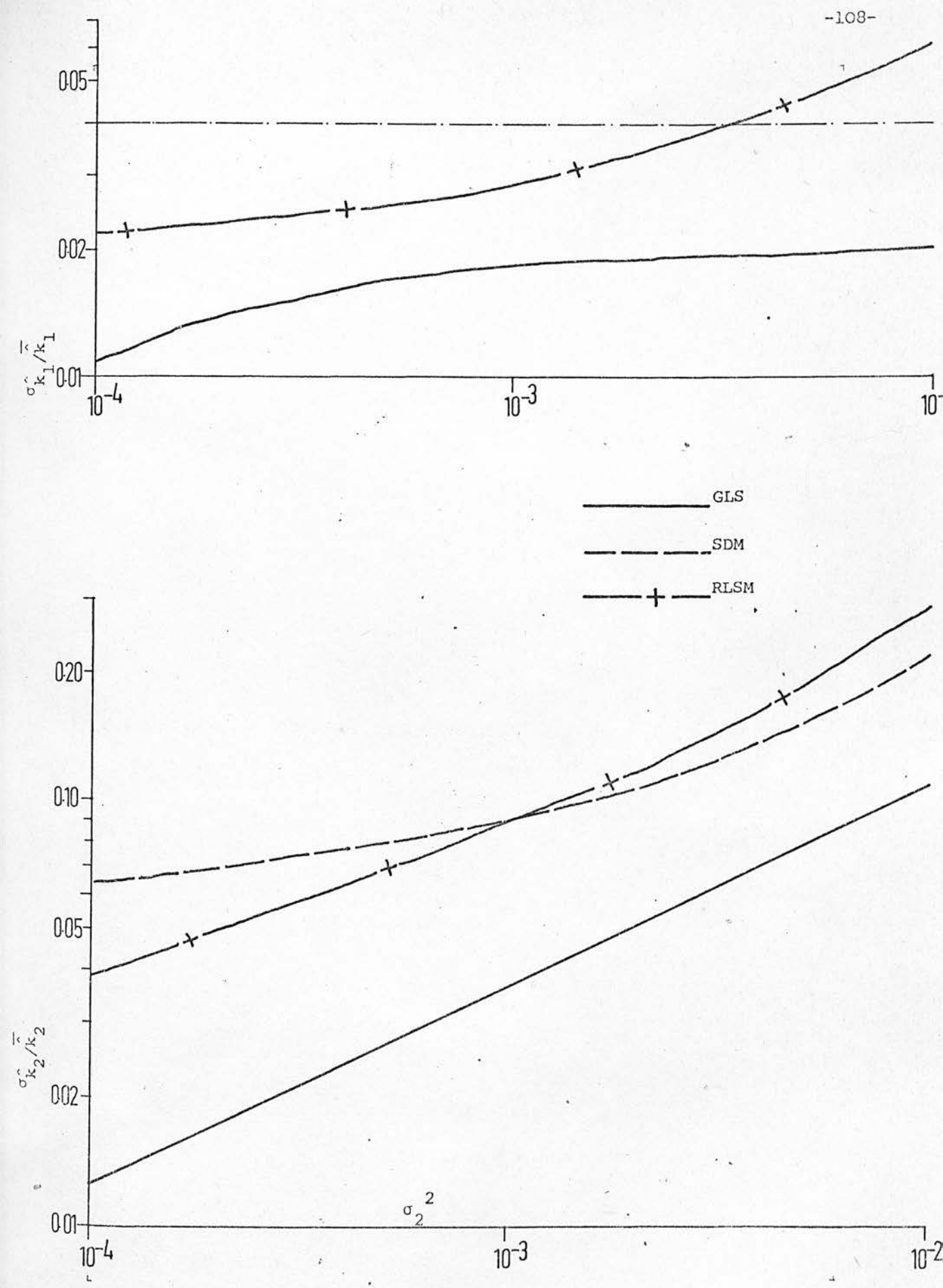

FIGURE 4·6 Efficiency As A Function Of σ_2^2

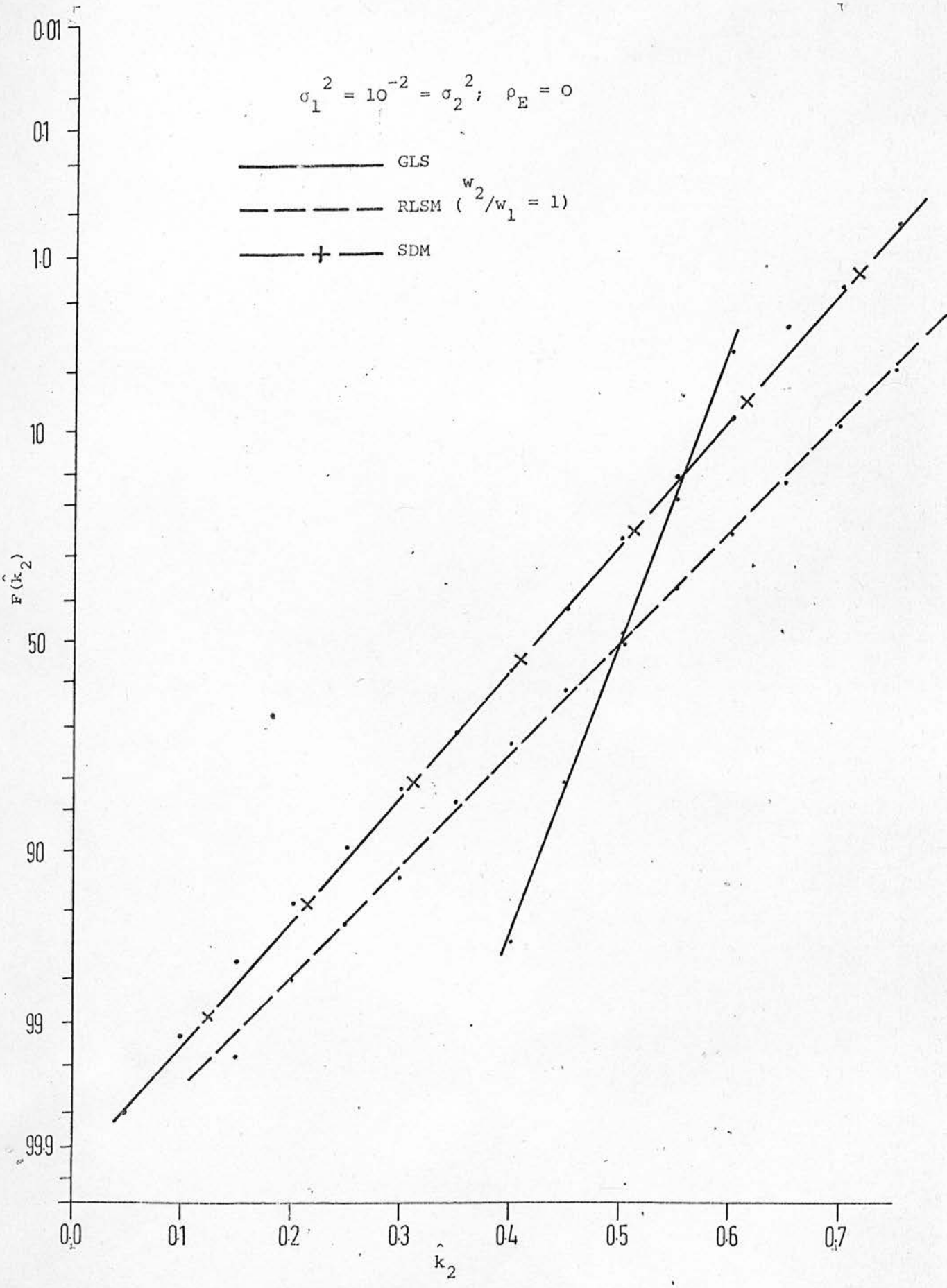

FIGURE 4.7 Cumulative Marginal Distributions Of $\hat{k}_2$

$\sigma_1^2 = 10^{-2} = \sigma_2^2$; $\rho_E = 0$

\+ $(\bar{\hat{k}}_1, \bar{\hat{k}}_2)$, SDM and GLS

o $(\bar{\hat{k}}_1, \bar{\hat{k}}_2)$, RLSM

GLS

RLSM ($w_2/w_1 = 1$)

SDM

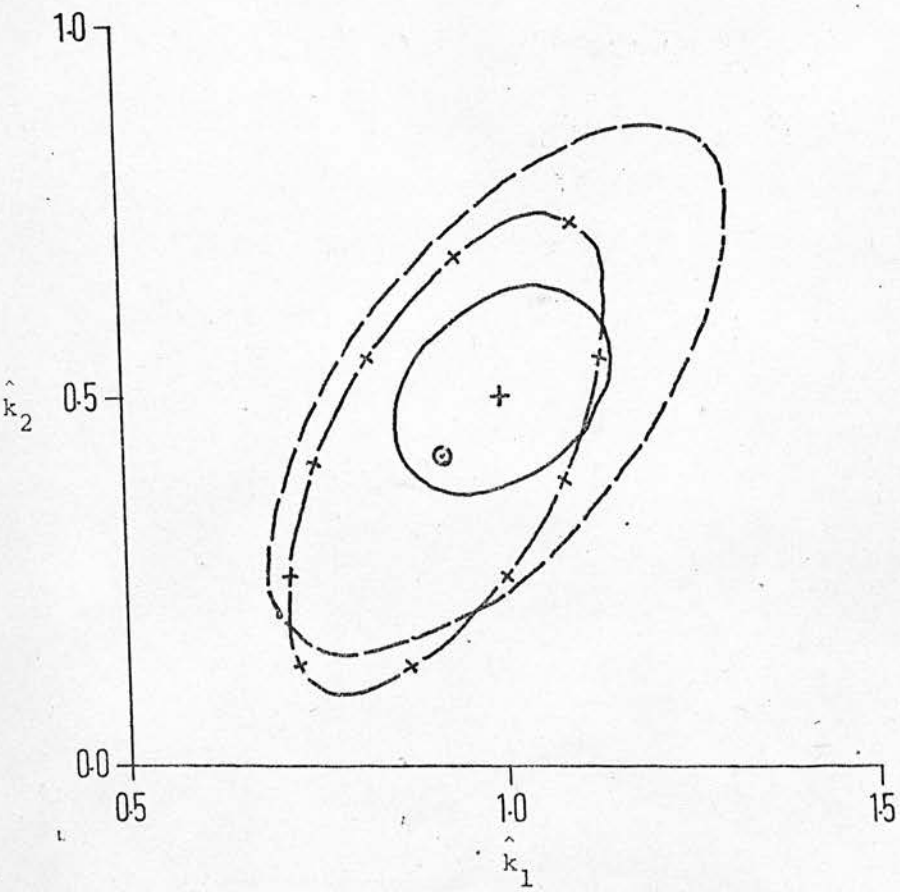

FIGURE 4.8 95% Confidence Regions

$$\eta_1 = \frac{|\underline{\underline{C}}|^{\frac{1}{2}}_{GLS}}{|\underline{\underline{C}}|^{\frac{1}{2}}_{SDM}} \quad ; \quad \eta_2 = \frac{|\underline{\underline{C}}|^{\frac{1}{2}}_{GLS}}{|\underline{\underline{C}}|^{\frac{1}{2}}_{LSRM}}$$

Table 17: Relative efficiencies of the estimation methods ($\rho_E = 0$)

σ_1^2	σ_2^2	η_1	η_2
10^{-2}	10^{-2}	0.23	0.16
10^{-3}	10^{-3}	0.23	0.33
10^{-4}	10^{-4}	0.23	0.32
10^{-3}	10^{-2}	0.27	0.23
10^{-3}	10^{-4}	0.09	0.16
10^{-2}	10^{-3}	0.09	0.18
10^{-4}	10^{-3}	0.27	0.22

For a wide range of error variancies, the efficiency of the SDM method falls within about 10%-30%, whilst for LSRM the range is circa 15% to 35%. These results are considered to be sufficiently good to encourage further development of the weighted residual methods.

The ability of LSRM to cope with the case $\sigma_1^2 \neq \sigma_2^2$ is demonstrated in table 18 below.

Table 18: Application of LSRM to the multiresponse problem:

$$\sigma_1^2 \neq \sigma_2^2; \quad \rho_E = 0$$

σ_1^2	σ_2^2	W_2/W_1	$\bar{\hat{k}}_1$	$\bar{\hat{k}}_2$	$Var(\hat{k}_1)$	$Var(\hat{k}_2)$	$\rho(\hat{k}_1, \hat{k}_2)$
10^{-3}	10^{-4}	10	0.987	0.489	4.822×10^{-4}	3.657×10^{-4}	0.501
10^{-4}	10^{-3}	0.1	0.993	0.490	3.516×10^{-4}	1.751×10^{-3}	0.773
10^{-3}	10^{-2}	10	0.978	0.452	3.430×10^{-3}	1.605×10^{-2}	0.762
10^{-2}	10^{-3}	0.1	0.933	0.449	4.113×10^{-3}	3.478×10^{-3}	0.502

4.7 Simulation studies with non-zero error covariance

The results reported so far have been for the case $\rho_E = 0$, and so next the more realistic case $\rho_E \neq 0$ is examined. Four different parameter estimation techniques were used:-

i) Generalised Least Squares (G.L.S.), as described in section (4.6). Recall that this method requires values of the error marginal variances and cross correlation coefficient.

ii) Weighted Least Squares (W.L.S.), wherein the sum-of-squares function is

$$S_W \equiv \frac{1}{\sigma_1^2} \sum_{i=1}^{m} (Y_{1i} - y_{1i})^2 + \frac{1}{\sigma_2^2} \sum_{i=1}^{m} (Y_{2i} - y_{2i})^2,$$

which follows from eqn. (4.35) if the error marginal variances are known, and their cross correlation coefficient is unknown, and assumed equal to zero.

iii) The method of Box and Draper (B-D). The criterion to be minimised is defined in table 9: the method is designed for cases where neither the error marginal variances nor the cross correlation coefficient is known. This method is equivalent to GLS with the error marginal variances and their covariance replaced by their maximum likelihood estimates.

iv) LSRM, for which only the error marginal variances are required - as with WLS.

Tables 19 and 20 below show the results for the case of large proportional errors ($\sigma_1^2 = \sigma_E^2 = \sigma_2^2 = 10^{-2}$) and small errors ($\sigma_1^2 = \sigma_E^2 = \sigma_2^2 = 10^{-4}$).

For the case of large error, LSRM provides estimates whose bias decreases with increase in ρ_E. Only for large negative ρ_E does the

Table 19: Parameter estimates with non-zero error cross-correlation, and $\sigma_E^2 = 10^{-2}$

		GLS	B-D	WLS	LSRM	
$\rho_E = 0.1$	$\bar{\hat{k}}_1$	1.002	1.001	1.001	0.930	$\rho_E > 0$
	$\bar{\hat{k}}_2$	0.501	0.500	0.501	0.425	
	$Var(\hat{k}_1)$	3.316×10^{-3}	3.447×10^{-3}	3.335×10^{-3}	7.368×10^{-3}	
	$Var(\hat{k}_2)$	3.391×10^{-3}	3.431×10^{-3}	3.433×10^{-3}	1.742×10^{-2}	
	$\rho(\hat{k}_1, \hat{k}_2)$	0.362	0.376	0.368	0.629	
$\rho_E = 0.5$	$\bar{\hat{k}}_1$	1.001	1.000	1.001	0.942	
	$\bar{\hat{k}}_2$	0.501	0.500	0.501	0.451	
	$Var(\hat{k}_1)$	2.437×10^{-3}	2.565×10^{-3}	2.775×10^{-3}	5.400×10^{-3}	
	$Var(\hat{k}_2)$	3.174×10^{-3}	3.263×10^{-3}	3.918×10^{-3}	1.634×10^{-2}	
	$\rho(\hat{k}_1, \hat{k}_2)$	0.546	0.561	0.612	0.652	
$\rho_E = 0.9$	$\bar{\hat{k}}_1$	1.001	1.000	1.001	0.954	
	$\bar{\hat{k}}_2$	0.500	0.500	0.501	0.478	
	$Var(\hat{k}_1)$	7.137×10^{-4}	7.505×10^{-4}	2.188×10^{-3}	2.538×10^{-3}	
	$Var(\hat{k}_2)$	1.107×10^{-3}	1.149×10^{-3}	4.184×10^{-3}	1.342×10^{-2}	
	$\rho(\hat{k}_1, \hat{k}_2)$	0.704	0.715	0.909	0.704	

Table 19 (contd.)

		GLS	B-D	WLS	LSRM
$\rho_E = -0.1$	$\bar{\hat{k}}_1$	1.002	1.001	1.002	0.924
	$\bar{\hat{k}}_2$	0.501	0.501	0.501	0.412
	$Var(\hat{k}_1)$	3.611×10^{-3}	3.725×10^{-3}	3.607×10^{-3}	8.050×10^{-3}
	$Var(\hat{k}_2)$	3.141×10^{-3}	3.173×10^{-3}	3.135×10^{-3}	1.749×10^{-2}
	$\rho(\hat{k}_1, \hat{k}_2)$	0.255	0.266	0.253	0.617
$\rho_E = -0.5$	$\bar{\hat{k}}_1$	1.002	1.001	1.002	0.912
	$\bar{\hat{k}}_2$	0.501	0.501	0.501	0.387
	$Var(\hat{k}_1)$	4.040×10^{-3}	4.115×10^{-3}	4.146×10^{-3}	8.870×10^{-3}
	$Var(\hat{k}_2)$	2.208×10^{-3}	2.219×10^{-3}	2.413×10^{-3}	1.687×10^{-2}
	$\rho(\hat{k}_1, \hat{k}_2)$	-0.030	0.024	0.018	0.584
$\rho_E = -0.9$	$\bar{\hat{k}}_1$	1.001	1.002	1.002	0.899
	$\bar{\hat{k}}_2$	0.501	0.501	0.500	0.360
	$Var(\hat{k}_1)$	4.305×10^{-3}	4.395×10^{-3}	4.663×10^{-3}	9.069×10^{-3}
	$Var(\hat{k}_2)$	9.127×10^{-4}	9.146×10^{-4}	1.895×10^{-3}	1.567×10^{-2}
	$\rho(\hat{k}_1, \hat{k}_2)$	-0.630	-0.631	-0.251	0.536

$k_1 = 1.00$
$k_2 = 0.50$
$\rho_E < 0$

Table 20: Parameter estimates with non-zero error cross-correlation, $\sigma_E^2 = 10^{-4}$

		GLS	B-D	WLS	LSRM
$\rho_E = 0.1$	$\bar{\hat{k}}_1$	1.000	1.002	1.000	0.993
	$\bar{\hat{k}}_2$	0.500	0.502	0.500	0.493
	$Var(\hat{k}_1)$	3.264×10^{-5}	2.162×10^{-5}	3.302×10^{-5}	7.159×10^{-5}
	$Var(\hat{k}_2)$	3.300×10^{-5}	2.292×10^{-5}	3.398×10^{-5}	1.901×10^{-4}
	$\rho(\hat{k}_1, \hat{k}_2)$	0.361	-0.448	0.375	0.619
$\rho_E = 0.5$	$\bar{\hat{k}}_1$	1.000	1.001	1.000	0.994
	$\bar{\hat{k}}_2$	0.500	0.502	0.500	0.494
	$Var(\hat{k}_1)$	2.391×10^{-5}	1.267×10^{-5}	2.750×10^{-5}	4.885×10^{-5}
	$Var(\hat{k}_2)$	3.149×10^{-5}	1.517×10^{-5}	3.833×10^{-5}	1.749×10^{-4}
	$\rho(\hat{k}_1, \hat{k}_2)$	0.552	-0.347	0.617	0.636
$\rho_E = 0.9$	$\bar{\hat{k}}_1$	1.000	1.000	1.000	0.994
	$\bar{\hat{k}}_2$	0.500	0.500	0.500	0.494
	$Var(\hat{k}_1)$	7.180×10^{-6}	1.425×10^{-6}	2.183×10^{-5}	2.416×10^{-5}
	$Var(\hat{k}_2)$	1.136×10^{-5}	2.128×10^{-6}	4.215×10^{-5}	1.423×10^{-5}
	$\rho(\hat{k}_1, \hat{k}_2)$	0.705	0.303	0.908	0.677

$k_1 = 1.000$
$k_2 = 0.500$
$\rho_E > 0$

Table 20 (contd.)

		GLS	B-D	WLS	LSRM
$\rho_E = -0.1$	$\bar{\hat{k}}_1$	1.000	1.002	1.000	0.993
	$\bar{\hat{k}}_2$	0.500	0.501	0.500	0.493
	$Var(\hat{k}_1)$	3.578×10^{-5}	2.431×10^{-5}	3.517×10^{-5}	8.237×10^{-5}
	$Var(\hat{k}_2)$	3.099×10^{-5}	2.459×10^{-5}	3.104×10^{-5}	1.940×10^{-4}
	$\rho(\hat{k}_1, \hat{k}_2)$	0.259	-0.477	0.253	0.612
$\rho_E = -0.5$	$\bar{\hat{k}}_1$	1.000	1.002	1.000	0.993
	$\bar{\hat{k}}_2$	0.500	0.501	0.500	0.493
	$Var(\hat{k}_1)$	3.977×10^{-5}	2.770×10^{-5}	4.072×10^{-5}	1.029×10^{-4}
	$Var(\hat{k}_2)$	2.182×10^{-5}	2.465×10^{-5}	2.505×10^{-5}	1.976×10^{-4}
	$\rho(\hat{k}_1, \hat{k}_2)$	-0.029	-0.575	0.015	0.599
$\rho_E = -0.9$	$\bar{\hat{k}}_1$	1.000	1.002	1.000	0.993
	$\bar{\hat{k}}_2$	0.500	0.500	0.500	0.492
	$Var(\hat{k}_1)$	4.337×10^{-5}	1.661×10^{-5}	4.503×10^{-5}	1.224×15^{4}
	$Var(\hat{k}_2)$	9.270×10^{-6}	8.679×10^{-6}	1.914×10^{-5}	2.036×10^{-4}
	$\rho(\hat{k}_1, \hat{k}_2)$	-0.629	-0.545	-0.243	0.582

$k_1 = 1.000$
$k_2 = 0.500$
$\rho_E < 0$

bias become intolerably large. For the case of small error, the bias is always negligible. Given the size of the imposed error, the LSRM estimate variances look reasonably good, although inferior to those of the classical least squares methods.

Appendix A2.12 contains some remarks on the relative performance of GLS and the Box-Draper method.

4.8 Development of a Taylor Series analysis for efficiency and bias calculations

The efficiency and bias results presented so far have been obtained by simulation. It would clearly be useful to develop analytical formulae relating the parameter distributions to the distributions of the experimental error. This can be accomplished using a Taylor series analysis, and the error assumptions of section 3.7.

First, the estimator equations (4.27) and (4.33) are written in the general form

$$\hat{k}_1 = \Phi_1(\underline{e}_1, \underline{e}_2) \; ; \quad \hat{k}_2 = \Phi_2(\underline{e}_1, \underline{e}_2) \tag{4.39}$$

where $\underline{e}_1$ and $\underline{e}_2$ are the m-vectors of errors in the measurement of y_1 and y_2 respectively, and Φ_1 and Φ_2 are known functional forms. For instance, for SDM

$$\Phi_1 = \frac{y_{1o} - y_{1m} + e_{1o} - e_{1m}}{\tfrac{1}{2}\sum_{i=o}^{m-1}\{y_1(t_i)+y_1(t_{i+1})\}\{t_{i+1}-t_i\} + \tfrac{1}{2}\sum_{i=o}^{m-1}(e_{1i}+e_{1,i+1})(t_{i+1}-t_i)} \tag{4.40}$$

$$\Phi_2 = \frac{y_{1o} + y_{2o} - y_{1m} - y_{2m} + e_{1o} + e_{2o} - e_{1m} - e_{2m}}{\tfrac{1}{2}\sum_{i=o}^{m-1}\{y_2(t_i)+y_2(t_{i+1})\}\{t_{i+1}-t_i\} + \tfrac{1}{2}\sum_{i=o}^{m-1}(e_{2i}+e_{2,i+1})(t_{i+1}-t_i)}$$

Next, the R.H.S. of eqn. (4.39) is expanded in Taylor series about $\underline{e}_1 = \underline{0} = \underline{e}_2$

$$\hat{k}_j = \Phi_j(\underline{0},\underline{0}) + \sum_{i=0}^{m} \left(\frac{\partial \Phi_j}{\partial e_{1i}}\Big|_{\underline{0},\underline{0}}\right) e_{1i} + \sum_{i=0}^{m} \left(\frac{\partial \Phi_j}{\partial e_{2i}}\Big|_{\underline{0},\underline{0}}\right) e_{2l}$$

$$+ \tfrac{1}{2} \sum_{i=0}^{m} \left(\frac{\partial^2 \Phi_j}{\partial e_{1j}^2}\Big|_{\underline{0},\underline{0}}\right) e_{1i}^2 + \tfrac{1}{2} \sum_{i=0}^{m} \left(\frac{\partial^2 \Phi_j}{\partial e_{2i}^2}\Big|_{\underline{0},\underline{0}}\right) e_{2i}^2 + \sum_{i=0}^{m} \left(\frac{\partial^2 \Phi_j}{\partial e_{1i} \partial e_{2l}}\Big|_{\underline{0},\underline{0}}\right)$$

$$e_{1i}\, e_{2i} + \cdots\cdots \qquad j = 1,2 \qquad (4.41)$$

Truncating after the first order terms and taking variances there follows

$$\mathrm{Var}(\hat{k}_j) \doteq \sigma_1^2 \sum_{i=0}^{m} \left(\frac{\partial \Phi_j}{\partial e_{1i}}\Big|_{\underline{0},\underline{0}}\right)^2 + \sigma_2^2 \sum_{i=0}^{m} \left(\frac{\partial \Phi_j}{\partial e_{2i}}\Big|_{\underline{0},\underline{0}}\right)^2$$

$$+ 2\sigma_{12} \sum_{i=0}^{m} \left(\frac{\partial \Phi_j}{\partial e_{1i}} \frac{\partial \Phi_j}{\partial e_{2i}}\right)\Big|_{\underline{0},\underline{0}} ; \quad j = 1,2 \qquad (4.42)$$

The covariance is similarily found to be

$$\mathrm{Covar}\,(\hat{k}_1,\hat{k}_2) \doteq \sigma_1^2 \sum_{i=0}^{m} \frac{\partial \Phi_1}{\partial e_{1i}} \frac{\partial \Phi_2}{\partial e_{1i}} + \sigma_2^2 \sum_{i=0}^{m} \frac{\partial \Phi_1}{\partial e_{2i}} \frac{\partial \Phi_2}{\partial e_{2i}}$$

$$+ \sigma_{12} \sum_{i=0}^{m} \left\{\frac{\partial \Phi_1}{\partial e_{1i}} \frac{\partial \Phi_2}{\partial e_{2i}} + \frac{\partial \Phi_1}{\partial e_{2i}} \frac{\partial \Phi_2}{\partial e_{1i}}\right\} \qquad (4.43)$$

When eqn. (4.41) is truncated after the second order terms and expectations are taken, there results

$$E(\hat{k}_j) \doteq \Phi_j(\underline{0},\underline{0}) + \tfrac{1}{2}\sigma_1^2 \sum_{i=0}^{m} \left(\frac{\partial^2 \Phi_j}{\partial e_{1i}^2}\Big|_{\underline{0},\underline{0}}\right) + \tfrac{1}{2}\sigma_2^2 \sum_{i=0}^{m} \left(\frac{\partial^2 \Phi_j}{\partial e_{2i}^2}\Big|_{\underline{0},\underline{0}}\right)$$

$$+ \sigma_{12} \sum_{i=0}^{m} \left(\frac{\partial^2 \Phi_j}{\partial e_{1i} \partial e_{2i}}\Big|_{\underline{0},\underline{0}}\right) ; \quad j = 1,2 \qquad (4.44)$$

Eqns. (4.42) and (4.43) permit calculation of the parameter variances and co-variance, and thus of the joint confidence region. The derivatives required are calculated from eqn. (4.40) or its counterpart for LSRM.

Eqn. (4.44) allows an approximate calculation of the bias in the estimates, since it is of the form

$$E(\hat{k}_j) \doteq k_{j,true} + k_{j,bias} \tag{4.45}$$

Indeed, 'bias compensation' could be effected by writing eqn. (4.45) in the form

$$k_{j,true} = \hat{k}_j - k_{j,bias}(\hat{\underline{k}}) \tag{4.46}$$

An example is shown in Appendix A2.4.

The accuracy of these Taylor series approximations is established by comparison with simulation results: see Tables 21 and 22 for examples.

Table 21: Expected values of the parameter estimates:

SDM ($\rho_E = 0$)

		Taylor Series		Simulation	
σ_1^2	σ_2^2	$E(\hat{k}_1)$	$E(\hat{k}_2)$	$E(\hat{k}_1)$	$E(\hat{k}_2)$
10^{-2}	10^{-2}	1.003	0.502	1.003	0.501
10^{-2}	10^{-3}	1.003	0.500	1.003	0.501
10^{-3}	10^{-2}	1.000	0.502	0.999	0.501

Table 22: Parameter variances and cross-correlation: SDM ($\rho_E = 0$)

		Taylor Series			Simulation		
σ_1^2	σ_2^2	$Var(\hat{k}_1) \times 10^2$	$Var(\hat{k}_2) \times 10^2$	$\rho(\hat{k}_1,\hat{k}_2)$	$Var(\hat{k}_1) \times 10^2$	$Var(\hat{k}_2) \times 10^2$	$\rho(\hat{k}_1,\hat{k}_2)$
10^{-2}	10^{-2}	1.59	2.04	0.62	1.59	2.15	0.65
10^{-2}	10^{-3}	1.59	1.07	0.86	1.59	1.05	0.87
10^{-3}	10^{-2}	0.159	1.17	0.26	0.157	1.23	0.34

4.9 Summary

Simulation studies show that the weighted residual methods have satisfactory statistical properties. They are much more convenient than the classical alternatives since both iterative function minimisation and the necessity of solving the model equations are avoided. The new methods also permit straightforward calculation of parameter estimate joint confidence regions. Moreover, the methods do not require the use of a digital computer: the parameter estimates and their confidence regions can be obtained rapidly on a modern pocket calculator.

The multi-response example worked above involved an equal number of responses and parameters: $n_r = n_p$. LSRM can easily cope with the case $n_r \neq n_p$: for SDM some modification is required, as will be demonstrated, for the case $n_r < n_p$, in chapter five, and for $n_r > n_p$ in chapter 6.

CHAPTER 5:- Applications of Weighted Residual Methods to Parameter Estimation

5.1 Identification of a rate law by interpreting temperature transients in an adiabatic reactor: an introduction.

5.2 Development of the model equations.

5.3 Application of the weighted residual methods.

5.4 Analysis of experimental data.

5.5 Advantages in using weighted residual methods.

5.6 Application of SDM to the NO oxidation problem.

5.7 Application of LSRM to the NO oxidation problem.

5.8 Summary

Note: part of the contents of this chapter has been published:-

Paterson W.R. and Cresswell D.L., "Kinetic rate modelling and parameter estimation by transient response measurements in exothermic reaction systems", Collected Papers, Series A, The First Annual Research Meeting of the Institution of Chemical Engineers, London 1974.

Other parts of the chapter were described by the writer at that meeting.

N.B. In this chapter, A represents an activation energy and not a pre-exponential factor.

5.1 Identification of a rate law by interpreting temperature transients in an adiabatic reactor: an introduction

As an experimental technique, the deliberate use of non-isothermal reactors dates back at least to 1924 (195). Adiabatic reactors have been used for heterogeneous catalytic rate studies (196,197), and for the examination of liquid phase reaction kinetics (198,199). The technique offers advantages when it is difficult to effect isothermal operation (e.g. 200), or when the measurement of concentration is much more difficult than the measurement of temperature - as is the case in the example considered at length below. Williams (201) has recommended the adiabatic reactor as an experimental tool, pointing out that the heat of reaction and reaction stoichiometry can be determined along with the kinetics.

A disadvantage of the technique is that the analysis of the data is difficult. Aris and co-workers (202,203) devised an approximate method for this task, but it met with little success.

The problem to be examined here is the interpretation of temperature transients in an adiabatic batch reactor using weighted residual and least squares methods.

Experimental arrangements. The reaction chosen for study was the exothermic batch acid-catalysed hydrolysis of propylene oxide (204) to propylene glycol:

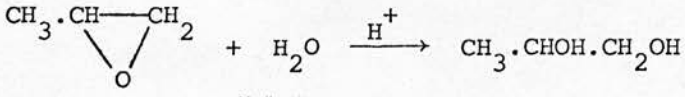

In a typical experiment, 700 ml of distilled water, 100 ml of propylene oxide (1,2 epoxypropane) and 14 ml of N sulphuric acid were placed in

reservoirs and held at constant temperature in a thermostatic bath. The reactants were then transferred to the reactor, which comprised a lidded Dewar flask, and thoroughly mixed. The acid catalyst was added and the mixture stirred. The changing temperature of the reaction mixture was measured with a calibrated Cr/Al thermocouple (Pyrotenax Ltd.) inserted through a small hole in the lid, and readings were taken from a Comark Electronic Thermometer Type 1604. Continuous mixing was achieved by gently 'swirling' the flask by hand. The adequacy of the mixing was tested by moving the thermocouple within the reaction mixture: the temperature therein was uniform.

Separate experiments using hot water alone in the flask had confirmed that the reactor could be assumed adiabatic over the time period of the reaction (less than thirty minutes), and that the container wall had a negligible heat capacity. Preliminary reaction experiments in an open beaker had shown that the concentrations of reactants and catalyst used would produce a convenient temperature rise over a convenient time interval. The choice of initial temperature was constrained below by the necessity that the water be liquid and by the heat of mixing of the reactants, and constrained above by the volatility of the propylene oxide. The reaction stoichiometry shown above is that reported by Furusawa et al (204), and has since been confirmed by other workers (205).

5.2 Development of the model equations

Let C(t) represent the concentration of propylene oxide, and C_o its initial concentration. The reaction is assumed to be irreversible, of zeroth order in concentration of water (due to its great excess) and of n^{th} order in concentration of propylene oxide. The rate constant is denoted by k, and is assumed to follow an Arrhenius temperature dependence

$$k(T) = k_o \exp(-A/RT) \qquad (5.1)$$

where k_o is the 'pre-exponential factor', A is the 'activation energy', R is the Universal Gas Constant, and T the absolute temperature of the reaction mixture.

Then, assuming the reaction mixture to be of constant volume, a material balance yields

$$-\frac{dC}{dt} = k(T)C^n \quad ; \quad C(0) = C_o \qquad (5.2)$$

Assuming the reactor to be adiabatic and letting T(t) represent the absolute temperature of the reaction mixture and T_o its initial temperature, then an energy balance yields

$$\rho_L C_p \frac{dT}{dt} = (-\Delta H)k(T)C^n \quad ; \quad T(0) = T_o \qquad (5.3)$$

where ρ_L = density of the reaction mixture
C_p = specific heat of the reaction mixture — assumed independent of T and C
$(-\Delta H)$ = heat of reaction

Defining

$$J \equiv (-\Delta H)/\rho_L C_p \qquad (5.4)$$

then eqn. (5.3) may be written as

$$\frac{dT}{dt} = Jk(T)C^n \qquad (5.5)$$

Manipulation of eqns. (5.2) and (5.5) results in

$$C = (C_o - \frac{T-T_o}{J}) \qquad (5.6)$$

When the reaction has proceeded to completion, so that C = 0 and $T = T_m$, then eqn. (5.6) becomes

$$C_o = \frac{T_m - T_o}{J} \qquad (5.7)$$

Substitution of eqns. (5.1), (5.6) and (5.7) into eqn. (5.5) yields

$$\frac{dT}{dt} = k_o \exp(-\frac{A}{RT})(T_m - T)^n J^{1-n} \quad ; \quad T(0) = T_o \qquad (5.8)$$

Re-parametrisation. It is well-known (206) that the activation energy and pre-exponential factor present great difficulties in estimation, and that these may often be ameliorated by 're-parametrisation':-

A dimensionless temperature is defined by

$$\theta \equiv \frac{T - T_b}{T_b} \tag{5.9}$$

where T_b is some chosen 'base temperature'. Note that since eqn.(5.9) is linear in T, then if the measurement errors in T are Normally distributed, so are the errors in θ.

Introducing the definition of θ into eqn. (5.1) there results

$$k = k_1 \exp(A_1 \frac{\theta}{1+\theta}) \tag{5.10}$$

$$\text{where } k_1 \equiv k_o \exp(-{}^{A}/_{RT_b}) \tag{5.11}$$

$$A_1 \equiv {}^{A}/_{RT_b} \tag{5.12}$$

Substituting eqns. (5.9) to (5.12) into eqn. (5.8) yields the

model equation

$$\frac{d\theta}{dt} = (\frac{J}{T_b})^{1-n} (\theta_m - \theta)^n k_1 \exp(\frac{A_1\theta}{1+\theta}) \quad ; \quad \theta(O) = \frac{T_o - T_b}{T_b} \tag{5.13}$$

in which the values of k_1, A_1 and n are to be found using the measured values T_i ; $i = O,1 \ldots .m$.

In the experiments which were performed, $(t_{i+1} - t_i)$ was equal to thirty seconds, although with suitable equipment a continuous trace of temperature could have been obtained.

Note, that, in eqn. (5.13), the value of J is known, having been calculated from eqn. (5.7). Thus, for the quantities of reagent cited earlier and from measured initial and final temperatures from six experimental runs, J is calculated to be 18.9×10^3 deg K ml/gmol. The value of T_b is chosen by the experimenter: for instance, it might be chosen equal to T_o.

The problem is treated by posing it as a problem in model discrimination: it is arbitrarily assumed that n should take one of the values ($\frac{1}{2}$, 1, 2), so that eqn. (5.13) yields three different models. Then for each model it is necessary to estimate the parameters k_1 and A_1.

5.3 Application of the weighted residual methods

i) SDM. Since there are two parameters and only one response, the domain $0\text{-}t_m$ is divided into two sub-domains $0\text{-}t_h$ and $t_h\text{-}t_m$. Y_i is used to represent the values of θ which are calculated from the observed values of T using eqn. (5.9). Application of SDM to the model eqn. (5.13) yields

$$Y_h - Y_o = k_1 \left(\frac{J}{T_b}\right)^{1-n} \tfrac{1}{2} \sum_{i=o}^{h-1} \{f(Y_i, A_1) + f(Y_{i+1}, A_1)\}\{t_{i+1} - t_i\}$$

$$Y_m - Y_h = k_1 \left(\frac{J}{T_b}\right)^{1-n} \tfrac{1}{2} \sum_{i=h}^{m-1} \{f(Y_i, A_1) + f(Y_{i+1}, A_1)\}\{t_{i+1} - t_i\} \quad (5.14)$$

where $$f(Y_i, A_1) \equiv (Y_m - Y_i)^n \exp\left(\frac{A_1 Y_i}{1+Y_i}\right)$$

From eqns. (5.14) there comes

$$(Y_m - Y_h) \sum_{i=o}^{h-1} \{f(Y_i, A_1) + f(Y_{i+1}, A_1)\}\{t_{i+1} - t_i\} - (Y_h - Y_o) \sum_{i=h}^{m-1} \{f(Y_i, A_1) + f(Y_{i+1}, A_1)\}\{t_{i+1} - t_i\} = 0 \quad (5.15)$$

$$k_1 = \frac{Y_m - Y_h}{\frac{1}{2}\sum_{i=h}^{m-1}\{f(Y_i,A_1)+f(Y_{i+1},A_1)\}\{t_{i+1}-t_i\}} \left(\frac{J}{T_b}\right)^{n-1} \qquad (5.16)$$

Equations (5.15) and (5.16) are the estimator equations: the non-linear equation (5.15) may be solved iteratively for A_1, and then k_1 may be found from equation (5.16)

ii) LSRM. Define

$$I_a \equiv \sum_{i=0}^{m-1}\{f(Y_i,A_1) + f(Y_{i+1},A_1)\}\{Y_{i+1}-Y_i\}$$

$$I_b \equiv \sum_{i=0}^{m-1}\{f^2(Y_i,A_1) + f^2(Y_{i+1},A_1)\}\{t_{i+1} - t_i\} \qquad (5.17)$$

$$I_c \equiv \sum_{i=0}^{m-1}\{\frac{Y_i}{1+Y_i} f(Y_i,A_1) + \frac{Y_{i+1}}{1+Y_{i+1}} f(Y_{i+1},A_1)\}\{Y_{i+1}-Y_i\}$$

$$I_d \equiv \sum_{i=0}^{m-1}\{\frac{Y_i}{1+Y_i} f^2(Y_i,A_1) + \frac{Y_{i+1}}{1+Y_{i+1}} f^2(Y_{i+1},A_1)\}\{t_{i+1}-t_i\}$$

It is easily shown that application of LSRM to eqn. (5.13) results in the estimator equations

$$I_a I_b - I_c I_d = 0 \qquad (5.18)$$

$$k_1 = \left(\frac{J}{T_b}\right)^{n-1} \frac{I_a}{I_b} \qquad (5.19)$$

Eqn. (5.18) is solved iteratively for A_1, and k_1 may then be calculated from eqn. (5.19).

Simulation results. Before applying the methods to experimental data, they were tested on simulated data. These tests were satisfactory - the methods appeared to show insignificant bias. Some typical results are shown in table 23.

Table 23: Application of SDM to simulated data

Simulation data	σ_E imposed on T (deg K)	$\hat{A}$	$\hat{k}_1 \times 10^4$
$n = 1$			
$J = 20 \times 10^3$ ml degK/gmol	0	20.0	2.932
$A = 20$ kcal/gmol	0.01	20.03	2.927
$k_o = 1.5 \times 10^{11}$ sec^{-1}	0.1	20.10	2.952
($k_1 = 2.932 \times 10^{-4}$)	0.2	20.19	2.977
$t_{i+1} - t_i = 50$ seconds	0.5	20.59	3.030
$m = 40$; $h = 17$			

There is one disadvantage to SDM: as described so far it is ambiguous in that the value of h, determining the sub-domain 'split', is arbitrary. In this problem, the matter is resolved by choosing a few plausible values of h, calculating the parameter estimates for each, and then calculating the corresponding temperature profile and comparing it with the observations. The value of h resulting in the smallest sum of squared discrepancies was chosen as 'best'.

5.4 Analysis of experimental data

Three near-replicate experiments were performed using the quantities of reagents described above, and having similar values of T_o. Assuming n = 1, values of k_1 and A_1 were estimated, and from these values of k_o and A were calculated (see Appendix 2.5) so that they could be compared with values obtained by Furusawa et al (204), who determined their values using isothermal CSTR experiments. As will be seen in table 24, the experiments yielded reasonably consistent results which agreed well with the results of Furusawa.

The estimates of k_1 and A_1 so obtained were then used as starting points for the application of quasilinearisation-least squares (QLLS), which yielded estimates agreeing very well with the starting values. Agreement is poorer but still acceptable when the untransformed parameters are compared: see table 25. Parameter estimates obtained assuming other reaction orders also agreed tolerably well: see table 26.

Table 24: Comparison of weighted residual parameter estimates with those of Furusawa et al. (n = 1)

			SDM		LSRM	
Run No.	T_o (°C)	h	$\hat{k}_o \times 10^{-9}$ sec^{-1}	$\hat{A}$ kcal/gmol	$\hat{k}_o \times 10^{-9}$ sec^{-1}	$\hat{A}$ kcal/gmol
1	23.53	27	4.91	17.85	4.84	17.85
2	24.18	24	4.22	17.76	4.29	17.78
3	23.58	25	4.84	17.81	5.25	17.88
	Mean		4.66	17.81	4.79	17.81
	Furusawa et al		4.71	18.0		

Table 25: A comparison of parameter estimates from Run 1 (n = 1)

Method	$\hat{k}_1 \times 10^{4}$	$\hat{A}_1 \times 10^{-1}$	$\hat{A}$	$\hat{k}_o \times 10^{-9}$
QLLS	3.2851	2.9974	17.6	3.38
SDM	3.3114	3.0328	17.9	4.91
LSRM	3.2336	3.0337	17.9	4.84

Table 26: Parameter estimates from Run 1 ($n \neq 1$)

Method	n	$\hat{k}_1 \times 10^{5}$	$\hat{A}_1 \times 10^{-1}$	n	$\hat{k}_1 \times 10^{1}$	$\hat{A}_1 \times 10^{-1}$
QLLS	0.5	1.709	1.840	2.0	1.190	5.338
SDM	0.5	1.747	1.683	2.0	1.447	5.140
LSRM	0.5	1.787	1.703	2.0	1.228	5.204

Model discrimination. On the basis of the estimates shown in tables 24 and 26, it is difficult to choose a 'best model' from the set $n = \frac{1}{2}, 1, 2$. Although $n = 1$ results in the smallest sum of squared discrepancies, the difference in the predicted profiles is not great - see Fig. 5.1. This similarity of prediction reflects the great flexibility of a model combining n^{th} order kinetics with an Arrhenius temperature dependence, and implies that considerable care is necessary in interpreting non-isothermal data.

A suitable test of the models is to compare their powers of extrapolation - a procedure involving no adjustable parameters.

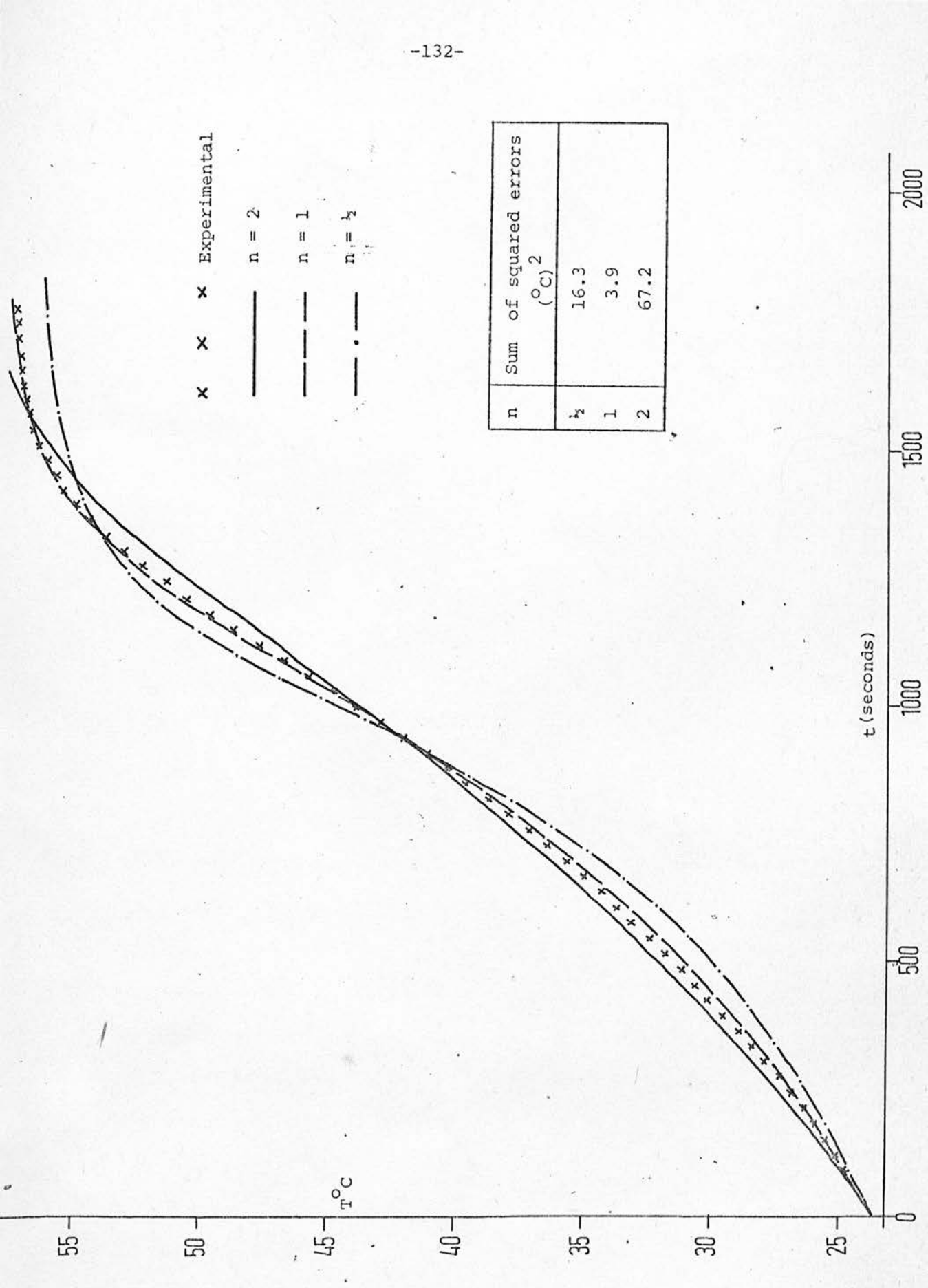

n	Sum of squared errors $(^{o}C)^{2}$
½	16.3
1	3.9
2	67.2

FIGURE 5-1 SDM: Run 1.

Model discrimination was therefore effected by using each set of parameter estimates to predict the temperature profiles which would result in an experiment carried out with a different initial temperature. It was found that the predicted profiles differed widely for $T_o > 30^oC$: predicted and observed profiles for Run 7 ($T_o = 31.6^oC$) are shown in fig. 5.2. From this figure (and others like it), it is clear that n = 1 is the 'best' choice of reaction order. This conclusion agrees with that of Furusawa et al. It should be noted that this same conclusion on reaction order was reached whichever parameter estimation method was used.

5.5 Advantages in using weighted residual methods

Two least squares methods were programmed for this problem: QLLS and hill-climbing by Simplex search. It was found that both least squares methods had very small convergence regions, that of Simplex search being slightly larger than that of QLLS. Part of the convergence region is shown in fig. 5.3: it will be seen that one would need to guess a combination of starting values for k_o and A within a very narrow band for convergence to occur. This is a great disadvantage of these least squares methods, and implies that a worker using them might well fail to obtain converged parameter estimates unless he used enormous amounts of computing time (and indeed of his own time) in trying different sets of starting values.

By comparison, the weighted residual methods required only a guess at upper and lower bounds on A (0 and 50 kcal/gmol were the physically reasonable values used), and convergence to $\hat{A}_1$ using a simple root-finding method (124) was easily effected. The computing time required was at least two orders of magnitude less than for a successful application of QLLS.

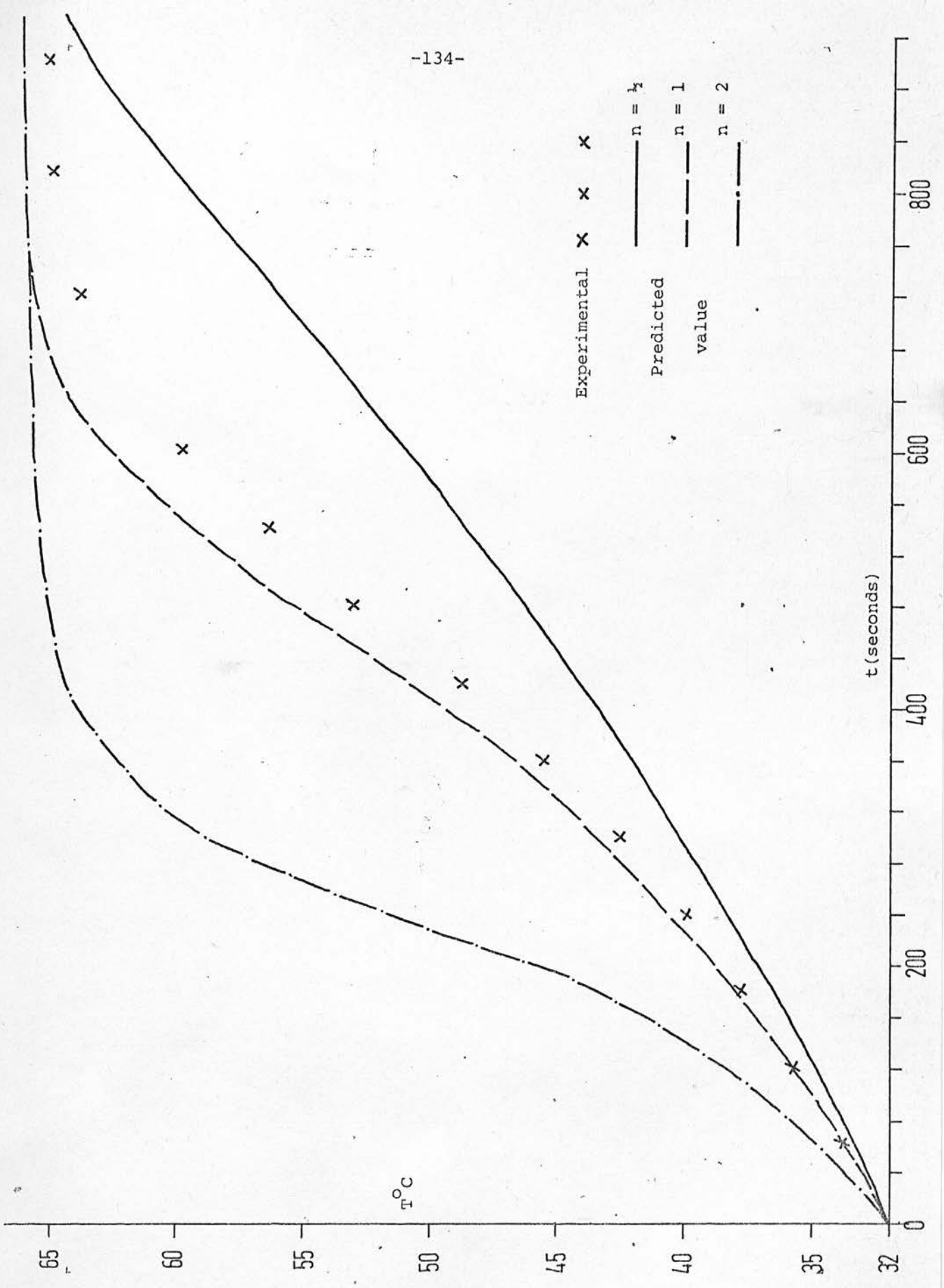

FIGURE 5.2 Predicted And Experimental Temperature Profiles

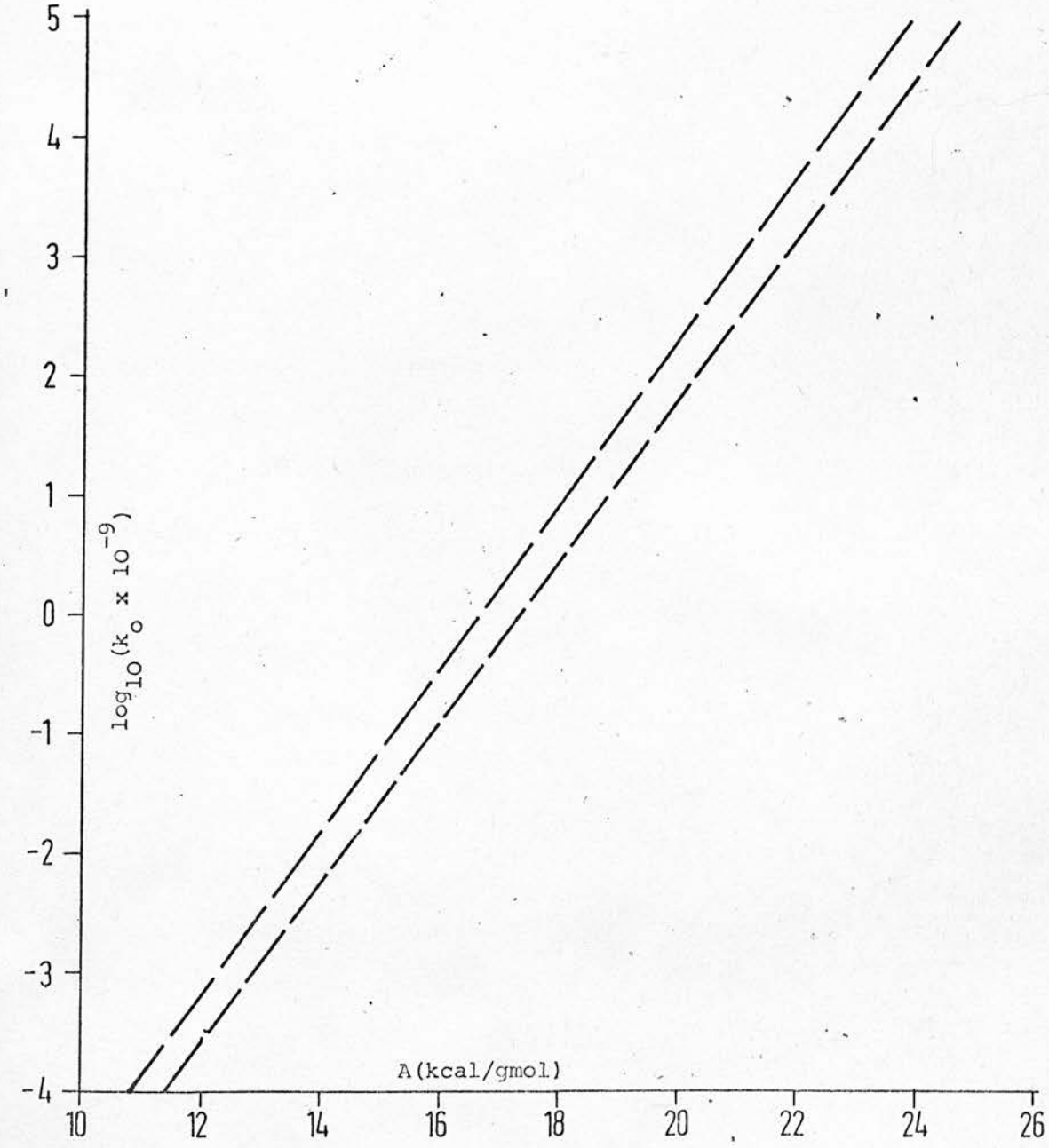

FIGURE 5.3 Region Of Convergence Of Quasilinearization Scheme

It is remarkable that both the weighted residual methods provided estimates within that narrow QLLS convergence band for all seven experimental runs and three reaction orders examined, thus permitting subsequent trouble-free least squares parameter estimation. This may be claimed as a major success for the weighted residual methods.

In addition to the difficulties of using the least squares methods, it must be emphasised their implementation is no trivial task. The QLLS method does not lend itself to being easily provided as a program package and therefore a potential user would need to study and understand the method and program it himself (see appendix A2.6). Even using standard library sub-routines for numerical integration and linear equation solving, a program of several hundred statements will be required. The writing of such a program might present considerable difficulties to an experimenter with a limited background in computing and numerical methods. The hill-climbing method is simpler to program, since it exploits a standard library Simplex search sub-routine, but might still pose some problems for a worker with limited computing experience. Moreover, whilst QLLS converged in a few (<6) iterations, when it converged at all, Simplex search required many more (>80) iterations. Its use does therefore consume large amounts of computing time - between two and five times as much as QLLS. By contrast, the weighted residual methods are notably simple to understand and program.

Since experimental workers will often find themselves with little time for, or interest in, programming tasks, and with limited computer time at their disposal, the weighted residual methods appear to offer substantial advantage since they rapidly provide accurate parameter estimates and yield acceptable results when used in model discrimination.

Remarks. From the shape of the convergence region shown in fig. 5.3, one might infer that the correlation coefficient for $\hat{k}_1$ and $\hat{A}_1$ was very high: in fact a value $\rho = 0.99$ was found by least squares variance-covariance analysis; see Appendix 2.6. This high value is attributed to the Arrhenius form of the temperature dependency of reaction rate, and similarily high values have been found on similar problems by other workers (207). It should be noted that a Taylor series method of confidence analysis has been developed in Appendix 2.7 for weighted residual estimators of the type arising here.

5.6 Application of SDM to the NO oxidation problem

SDM is next applied to the NO oxidation problem of section (3.7) i.e. the estimation of k_1 and k_2 in eqn. (3.12).

i) SDM: Define, for convenience

$$g_1 \equiv (126.2 - y)(91.9 - y)^2 \quad \text{and} \quad g_2 \equiv y^2$$

so that eqn. (3.12) may be written as

$$\frac{dy}{dt} - k_1 g_1 + k_2 g_2 = 0 \tag{5.20}$$

Whence one may write

$$k_1 \int_0^{t_h} g_1 dt - k_2 \int_0^{t_h} g_2 dt = y_h - y_o$$

$$k_1 \int_{t_h}^{t_m} g_1 dt - k_2 \int_{t_h}^{t_m} g_2 dt = y_m - y_h$$

and the corresponding estimator equations are

$$\hat{k}_1 \sum_{i=o}^{h-1} \{G_{1,i}+G_{1,i+1}\}\{t_{i+1}-t_i\} - \hat{k}_2 \sum_{i=o}^{h-1} \{G_{2,i}+G_{2,i+1}\}\{t_{i+1}-t_i\} = Y_h - Y_o$$

$$\hat{k}_1 \sum_{i=h}^{m-1} \{G_{1,i}+G_{1,i+1}\}\{t_{i+1}-t_i\} - \hat{k}_2 \sum_{i=h}^{m-1} \{G_{2,i}+G_{2,i+1}\}\{t_{i+1}-t_i\} = Y_m - Y_h \qquad (5.21)$$

where $G_{1,i} \equiv (126.2-Y_i)(91.9-Y_i)^2$; $G_{2,i} \equiv Y_i^2$

Note that eqns. (5.21) are linear in $\hat{k}_1$ and $\hat{k}_2$, corresponding to the simplification described in section 4.4.

Eqns. (5.21) may be written, in an obvious notation

$$\hat{k}_1 A_{11} - \hat{k}_2 A_{12} = C_1$$
$$\hat{k}_1 A_{21} - \hat{k}_2 A_{22} = C_2$$

to which the solutions are

$$\hat{k}_1 = \frac{A_{22}C_1 - A_{12}C_2}{A_{22}A_{11} - A_{12}A_{21}} \quad ; \quad \hat{k}_2 = \frac{A_{21}C_1 - A_{11}C_2}{A_{22}A_{11} - A_{12}A_{21}} \qquad (5.22)$$

From eqns. (5.22) are obtained the estimates shown in table 27.

Table 27: Parameter estimates by SDM for the NO oxidation problem

h	$\hat{k}_1 \times 10^6$	$\hat{k}_2 \times 10^4$
6	4.576	3.062
9	4.596	3.114
7	4.461	2.762
QLLS estimates	4.577	2.797

Clearly, taking h = 7, which splits the domain into two roughly equal parts, yields parameter estimates in good agreement with those obtained by quasilinearisation/least squares. Other values of h near the middle of the domain also yield acceptable estimates.

ii) Confidence Analysis. A method for confidence analysis has been devised which requires rather less algebraic manipulation than the Taylor series method presented earlier. A description will be found in Appendix A2.8.

A comparison of the results with those from QLLS is shown in table 28. Clearly SDM is less efficient than least squares, but the agreement is very good.

Table 28: A comparison of the results from SDM (with h = 7) and QLLS

Method	$\hat{k}_1 \times 10^6$	(95% confidence interval on $\hat{k}_1$) $\times 10^6$	$\hat{k}_2 \times 10^4$	(95% confidence interval on $\hat{k}_2$) $\times 10^4$	$\rho_{\hat{k}_1,\hat{k}_2}$	SOS
SDM	4.461	$\pm$0.625	2.762	$\pm$1.751	0.55	23.49
QLLS	4.577	$\pm$0.356	2.797	$\pm$1.124	0.66	21.87

The confidence interval calculation is explained in Appendix A2.10.

The parameter joint confidence region. It has been established in Appendix A2.8 that $\hat{k}_1$ and $\hat{k}_2$ each have a Normal marginal distribution: it follows that they will have a bi-variate Normal joint frequency distribution described by the probability density function

$$f(\underline{k}) = \frac{1}{2\pi}(|\underline{\underline{C}}|)^{-\frac{1}{2}} \exp\{-\tfrac{1}{2}\{\hat{\underline{k}}-E(\hat{\underline{k}})\}^T \underline{\underline{C}}^{-1}\{\hat{\underline{k}}-E(\hat{\underline{k}})\}\} \qquad (5.23)$$

where $\hat{\underline{k}} = (\hat{k}_1 \quad \hat{k}_2)^T$

Further, the elements of the parameter variance-covariance matrix are known:-

$$\underline{\underline{C}} = \begin{bmatrix} C_{11} & C_{12} \\ C_{21} & C_{22} \end{bmatrix} = \begin{bmatrix} \text{Var}(\hat{k}_1) & \text{Covar}(\hat{k}_1,\hat{k}_2) \\ \text{Covar}(\hat{k}_2,\hat{k}_1) & \text{Var}(\hat{k}_2) \end{bmatrix} \qquad (5.24)$$

Note that $C_{21} = C_{12}$

Consider the quadratic form, extracted from the RHS of eqn (5.23)

$$Q \equiv (\hat{\underline{k}} - E(\hat{\underline{k}}))^T \underline{\underline{C}}^{-1}(\hat{\underline{k}} - E(\hat{\underline{k}})) \qquad (5.25)$$

It may be proved - see Appendix A2.9 - that Q follows a χ^2 distribution with 2 degrees of freedom and that the boundary of the 95% joint confidence region corresponds to

$$Q = 5.991 \qquad (5.26)$$

Combining eqns. (5.26) and (5.24) there results an equation describing the boundary of the 95% joint confidence region in parameter space:-

$$k_1^2\{C_{22}\} + k_1\{-2\hat{k}_1 C_{22} - 2C_{12}(k_2-\hat{k}_2)\} + \{C_{22}\hat{k}_1^2 + C_{12}\hat{k}_1(k_2-\hat{k}_2) + C_{11}(k_2-\hat{k}_2)^2\}$$
$$= 5.991\{C_{11}C_{22} - C_{12}^2\} \qquad (5.27)$$

Eqn. (5.27) is written as a quadratic in k_1. The values of $\hat{k}_1$, $\hat{k}_2$ and the C_{ij}'s are known. Therefore, if a value is chosen for k_2 the corresponding value of k_1 may be calculated by solving eqn.(5.27). Performing this operation repeatedly for different values of k_2 allows one to calculate the boundary of the 95% joint confidence region. That boundary is shown in fig. 5.4 as the broken ellipse.

The <u>efficiency</u> of SDM relative to the maximum likelihood method (implemented here as QLLS) may be computed as

$$\sqrt{\frac{|\underline{\underline{C}}|_{QLLS}}{|\underline{\underline{C}}|_{SDM}}} = 0.39$$

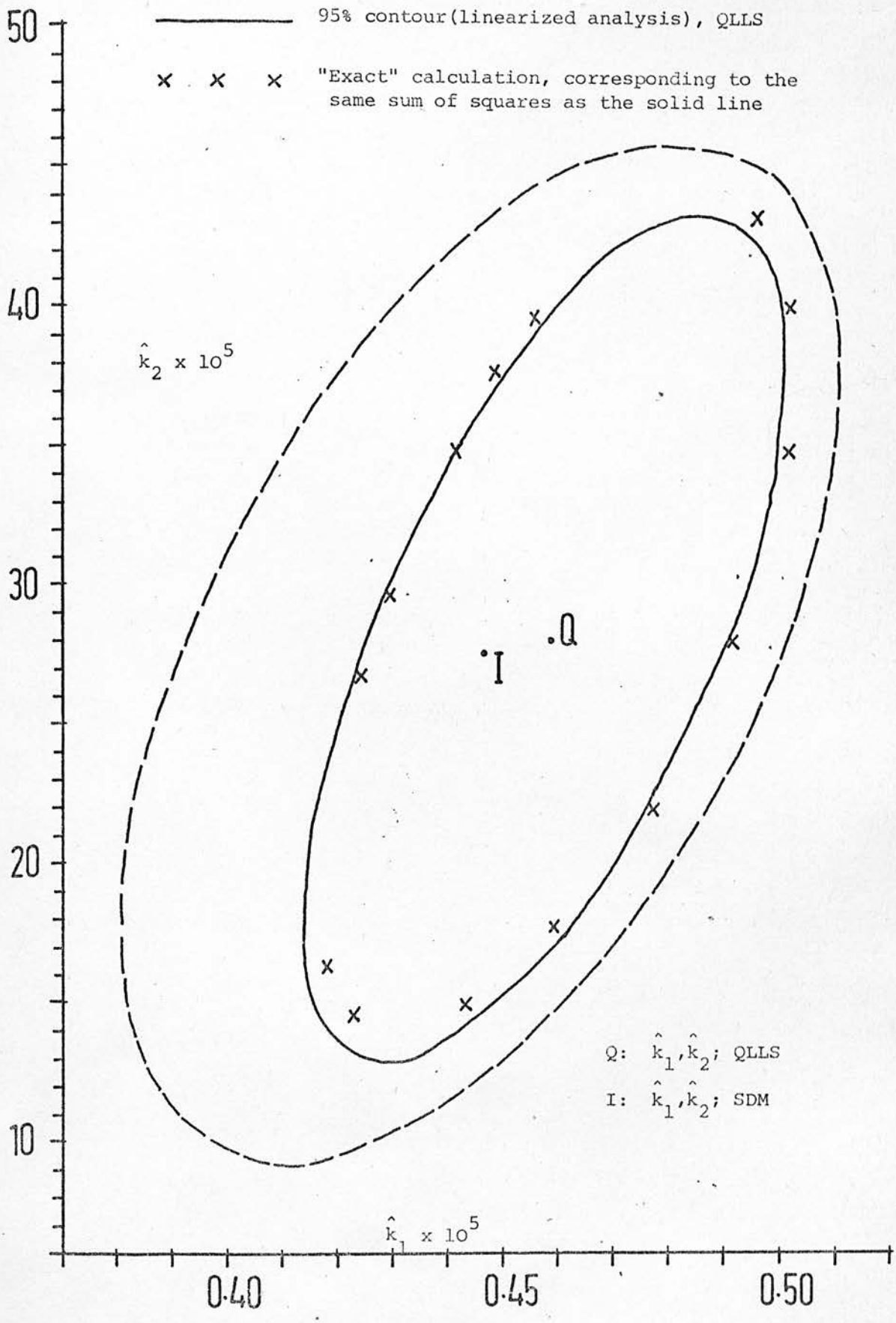

FIGURE 5·4 Confidence Contours In Parameter Space

i.e. for this problem, SDM has an efficiency equal to 39% of that of the maximum likelihood method.

In summary it has proved possible to use SDM to obtain good parameter estimates and to calculate rapidly the parameter joint confidence region.

5.7 Application of LSRM to the NO oxidation problem

Following the spirit of section 4.3 it is easy to reduce eqn.(5.20) to the form

$$k_1 \int_o^{t_m} g_1^2\, dt - k_2 \int_o^{t_m} g_1 g_2 dt = \int_o^{y_m} g_1 dy$$

$$k_1 \int_o^{t_m} g_1 g_2 dt - k_2 \int_o^{t_m} g_2^2 dt = \int_o^{y_m} g_2 dy$$

and the corresponding LSRM equations are

$$\hat{k}_1 \sum_{i=o}^{m-1} \{G_{1,i}^2 + G_{1,i+1}^2\}\{t_{i+1} - t_i\} - \hat{k}_2 \sum_{i=o}^{m-1} \{G_{1,i}G_{2,i} + G_{1,i+1}G_{2,i+1}\}\{t_{i+1} - t_i\}$$

$$= \sum_{i=o}^{m-1} \{G_{1,i} + G_{1,i+1}\}\{Y_{i+1} - Y_i\}$$

$$\hat{k}_1 \sum_{i=o}^{m-1} \{G_{1,i}G_{2,i} + G_{1,i+1}G_{2,i+1}\}\{t_{i+1} - t_i\} - \hat{k}_2 \sum_{i=o}^{m-1} \{G_{2,i}^2 + G_{2,i+1}^2\}\{t_{i+1} - t_i\}$$

$$= \sum_{i=o}^{m-1} \{G_{2,i} + G_{2,i+1}\}\{Y_{i+1} - Y_i\}$$

which may be written in an obvious notation as

$$\begin{aligned} B_{11}\hat{k}_1 - B_{12}\hat{k}_2 &= D_1 \\ B_{21}\hat{k}_1 - B_{22}\hat{k}_2 &= D_2 \end{aligned} \qquad (5.28)$$

where $B_{12} = B_{21}$

Solving eqns. (5.28) yields the LSRM estimator equations:-

$$\hat{k}_1 = \frac{B_{22}D_1 - B_{12}D_2}{B_{22}B_{11} - B_{12}^2} \quad ; \quad \hat{k}_2 = \frac{B_{12}D_1 - B_{11}D_2}{B_{22}B_{11} - B_{12}^2} \qquad (5.29)$$

The estimates so obtained are shown in table 29.

Confidence region analysis. An analysis by Taylor series is performed: the details are presented in Appendix A2.11.

An alternative analysis was performed using a "Monte-Carlo method", as follows:-

a) Use LSRM to obtain $\hat{k}_1$ and $\hat{k}_2$, and then integrate the model eqns. (3.12) and (3.15) to obtain a profile which will approximate to $y(t)$. Estimate σ_E^2 from eqn. (A2.25).

b) Generate 1000 'pseudo' experimental profiles $Y(t_i)$ from the approximate $y(t_i)$ in the usual way, where the pseudo-error has mean zero and standard deviation σ_E.

c) From each profile, use LSRM to calculate values of $\hat{k}_1$ and $\hat{k}_2$ and so obtain the approximate distributions of those parameter estimates.

d) Use a χ^2 goodness-of-fit test to show that the distributions are approximately Normal. Then calculate the variances of the parameter estimates, and compute confidence intervals as described in Appendix A2.10.

5.8 Summary

The weighted residual methods have been extensively tested on a variety of integral kinetic data-sets, experimental and simulated, and have been found to yield estimates of acceptable efficiency and bias.

Table 29: A comparison of the 'interval estimates' of the parameters obtained by different methods.

Method	$\hat{k}_1 \times 10^6$ (with 95% confidence limits)	$\hat{k}_2 \times 10^4$ (with 95% confidence limits)
LSRM (Taylor Series)	4.268 ± 0.411	2.523 ± 1.530
LSRM (Monte-Carlo)	4.268 ± 0.404	2.523 ± 1.493
SDM (with method of Appendix A2.8)	4.461 ± 0.625	2.762 ± 1.751
QLLS (with standard linearisation analysis)	4.577 ± 0.356	2.797 ± 1.124

It will be seen that the two methods used for calculating the parameter variances for LSRM agree very well, and that all three estimation methods provide very similar point estimates. The least squares method is most efficient, followed by LSRM, with SDM being least efficient.

The advantages claimed for them over classical methods are that they make much smaller demands on the user's mathematical and computing knowledge, on his time and on his budget. Further they provide estimates which are suitable for refinement by classical techniques since they would appear always to fall within the convergence region of the classical methods. Moreover, on one (demanding) problem, when applied to model discrimination they yielded the same conclusion as did the classical procedures.

As justification for developing such 'short-cut' procedures, Tukey's statement reported in section 3.3 may be cited, as may another of his remarks in the same paper:-

> "We need to face up to the necessarily approximate nature of useful results in data analysis. Our formal hypotheses and assumptions will never be broad enough to encompass actual situations. Even results that pretend to be precise in derivation will be approximate in application. Consequently we are likely to find that results which are approximate in derivation or calculation will prove no more approximate in application than those that pretend to be precise."

CHAPTER 6: Extension of Weighted Residual Methods to Partial Differential Equations

6.1 Introduction.

6.2 The finite difference technique.

6.3 The Integral technique.

6.4 Further testing on simulated data.

6.5 Application to real experimental data.

6.6 Remarks and summary.

6.1 Introduction

The estimation of parameters in partial differential equations (p.d.e.'s) is a difficult problem for those cases where an analytical solution to the equation(s) is not available. However, for least squares estimation, Seinfeld and Chen (208) have demonstrated that quasilinearisation and steepest descent algorithms may be devised, and King(209) has presented a Newton-like method. An alternative technique involves constructing approximate solutions to the p.d.e.'s - using, for instance, orthogonal collocation (208) or Galerkin's method (210) - and using these directly in the sum-of-squares criterion.

By contrast, the approach developed below involves reducing the p.d.e. to one or more o.d.e.'s, and applying the weighted residual methods to these. This device may well be capable of generalisation for, as Kagiwada (211) has remarked, there are many types of mathematical model which may be converted into sets of initial value o.d.e.'s. She lists p.d.e.'s, integro-differential equations, integral equations, differential-difference equations and boundary-value o.d.e.'s as being the most obvious. Of the model forms listed, p.d.e.'s are undoubtedly of most importance in reaction engineering.

6.2 The finite difference technique

Perhaps the most obvious way to reduce a d-dimensional p.d.e. model to a set of o.d.e.'s is by finite differencing in (d-1) dimensions. Consider, for instance, the linear, parabolic, two-dimensional p.d.e. which describes the steady-state dimensionless temperature distribution in an annular packed bed (this model is derived and discussed in detail in chapters 7 & 8).

$$GC_p \frac{\partial t}{\partial Z} - k_e \left(\frac{\partial^2 t}{\partial r^2} + \frac{1}{r}\frac{\partial t}{\partial r}\right) = 0 \qquad (6.1)$$

where $t(r,Z)$ is the dimensionless temperature in the bed, $t \equiv \frac{T-T_{wa}}{T_{wb}-T_{wa}}$

$T(r,Z)$ is the temperature in the bed

T_{wa}, T_{wb} are the known inner and outer wall temperatures

Z is the axial distance along the bed from the inlet, $Z = 0$

r is the radial distance from the axis

G, C_p are the known mass flux of gas through the bed, and the gas specific heat and k_e is the bed effective thermal conductivity, which is to be estimated from the $Y_{j,i}$'s, the measured values of $t(r,Z)$.

The boundary conditions are

(i) At the inner wall; $r = r_a$, $Z > 0$; $k_e \frac{\partial t}{\partial r} = h_a t$

(6.2)

At the outer wall; $r = r_b$, $Z > 0$, $k_e \frac{\partial t}{\partial r} = h_b(t-1)$

where h_a = effective wall heat transfer coefficient, inner wall

h_b = effective wall heat transfer coefficient, outer wall.

ii) at the bed inlet, $Z = 0$, $r_a \leq r \leq r_b$, $t = t_{in}(r)$ (6.3)

The function $t_{in}(r)$ is a simple function derived by 'fitting' measured values of the inlet temperature profile.

The measured values Y_{ji} are available at various radial positions in the bed $r_j (j = 0,1,\ldots M)$, $r_a < r_j < r_b$, but not at the walls, and at various axial positions Z_i, $i = 0,1,m$.

Using central differences

$$\frac{\partial t}{\partial r} \doteq \frac{1}{2\Delta r}(t_{j+1} - t_{j-1}); \quad \frac{\partial^2 t}{\partial r^2} \doteq \frac{1}{(\Delta r)^2}(t_{j-1} - 2t_j + t_{j+1})$$

and defining $\Delta_j \equiv r_{j+1} - r_j$

$$\Delta\Delta_j \equiv \Delta^2_{j-1}\Delta_j + \Delta_j{}^2\Delta_{j-1}$$

one can reduce eqn. (6.1) to the form

$$GC_p \Delta\Delta_j \frac{dt_j}{dZ} - k_e f(t_{j+1}, t_j, t_{j-1}) = 0; \quad j = 0,1,M \qquad (6.4)$$

where $f(t_{j+1}, t_j, t_{j-1}) \equiv t_{j+1}\{2\Delta_{j-1} + \frac{\Delta^2_{j-1}}{r_j}\} + t_j\{-2(\Delta_j + \Delta_{j-1}) - \frac{\Delta^2_{j-1} - \Delta^2_j}{r_j}\}$

$$+ t_{j-1}\{2\Delta_j - \frac{\Delta^2_j}{r_j}\} \qquad (6.5)$$

S.D.M. Application of this method to eqn. (6.4) yields

$$\hat{k}_e)_j = \frac{GC_p \Delta\Delta_j \{Y_{j,m} - Y_{j,o}\}}{\frac{1}{2}\sum_{i=o}^{m-1}\{f(Y_{j+1,i}, Y_{j,i}, Y_{j-1,i}) + f(Y_{j+1,i+1}, Y_{j,i+1}, Y_{j-1,i+1})\}\{Z_{i+1} - Z_i\}} \qquad (6.6)$$

The form of eqn. (6.6) is such that for each $Y_{j,i}$ used one also needs values for $Y_{j,i-1}$ and $Y_{j,i+1}$. The equation is therefore applied only for $j = 1,2\ldots(M-1)$, and k_e is found by averaging the $\hat{k}_e)_j$.

L.S.R.M. The equation residuals corresponding to eqn. (6.4) are

$$R_j(Z) \equiv GC_p \Delta\Delta_j \frac{dt_j}{dZ} - k_e f(t_{j+1}, t_j, t_{j-1})$$

The LSRM estimate follows from the approximate equivalent of

$$\min_{k_e}\left\{\sum_{j=1}^{M-1}\int_{o}^{Z_m} R_j^2\,(Z)\,dZ\right\}$$

which yields

$$\hat{k}_e = \frac{GC_p\sum_{j=1}^{M-1}\Delta\Delta_j\{\sum_{i=o}^{m-1}\{f(Y_{j+1,i},Y_{j,i},Y_{j-1,i})+f(Y_{j+1,i+1},Y_{j,i+1},Y_{j-1,i+1})\}\{Y_{j,i+1}-Y_{j,i}\}}{\sum_{j=1}^{M-1}\sum_{i=o}^{m-1}\{f^2(Y_{j+1,i},Y_{j,i},Y_{j-1,i})+f^2(Y_{j+1,i+1},Y_{j,i+1},Y_{j-1,i+1})\}\{Z_{i+1}-Z_i\}} \qquad (6.7)$$

Testing the methods. Simulated experimental measurements were generated by adding Normal 'error' of zero mean to the numerical solution of eqns. (6.1) to (6.3). The data used in the simulation are shown below.

Simulation Data

r_a = 6 mm, r_b = 35.3 mm; Z_m = 360 mm, G = 3.744 kg/m^{2}s; d_p = 0.09 m

Pe = 2.0; $Bi_1 = 2.63 = Bi_2$. The undefined symbols are defined and discussed in chapters 7 & 8.

Number of axial increments used = 60; Number of radial increments used = 20.

Inlet profile: defining a dimensionless radial co-ordinate $y = \frac{r-r_a}{r_b-r_a}$

Use was made of $t_{in} = a_o \exp(a_1 y)$

with $a_o = 8.598 \times 10^{-3}$; $a_1 = 4.0604$

This set of data corresponds to a value $k_e = 16.85\ ^{J}/_{m^2}\ (\frac{degK}{m})s$

The measurements were assumed to be equally spaced in each dimension, but it was assumed that no measurements could be made near the wall.

A large number of calculations were performed to assess the effect of the number and location of measurements, of the magnitude of the 'error' imposed and of the true value of k_e. The results showed the method to be of very limited application - see Table 30 for an example.

Table 30: Results of applying SDM to 100 simulated experiments

Radial measurement locations: 9, equally spaced between 16.25 and 29.44mm

Axial measurement locations: 21, equally spaced between 30 and 120 mm

$\sigma_E \equiv$ standard deviation of error on Y

σ_E	$k_e)_{true}$	$\bar{\hat{k}}_e$	$\sigma_{\hat{k}_e}$
10^{-6}	16.85	16.84	1.3×10^{-2}
10^{-4}	16.85	16.89	8×10^{-1}
10^{-3}	16.85	18.09	7×10^{1}
10^{-2}	16.85	10.08	1.5×10^{2}

Clearly the results are useless for $\sigma \gtrsim 10^{-3}$, which corresponds to a standard deviation of measured temperature $\sim 0.1^{o}C$, a measurement accuracy which cannot be achieved in a packed bed. Results obtained using larger (and thus more realistic) distances between axial measurements are no better, and the results obtained by applying the methods to real experimental data were clearly nonsensical. It is concluded that the method is inadequate in the face of a realistic size of experimental error. The inadequacy is doubtless due to the rather crude numerical differentiation corresponding to the finite differencing of the 'experimental data'.

6.3 The Integral Technique

Since the source of inadequacy is adjudged to arise from attempting to differentiate the radial temperature profiles, it is clearly attractive to replace that operation by integration.

Multiply eqn. (6.1) through by F(r), a function to be specified later, and integrate w.r.t. r from r_o to r_M, the innermost and outermost measurement locations:-

$$GC_p \int_{r_o}^{r_M} F(r) \frac{\partial t(r,Z)}{\partial Z} dr - k_e \{ \int_{r_o}^{r_M} F(r) \frac{\partial^2 t(r,z)}{\partial r^2} dr + \int_{r_o}^{r_M} \frac{F(r)}{r} \frac{\partial t(r,Z)}{\partial r} dr \} = 0 \tag{6.8}$$

Now consider this equation term by term:

On reversing the order of the operators, the first term becomes

$$GC_p \frac{\partial}{\partial Z} \{ \int_{r_o}^{r_M} F(r) t(r,Z) dr \}$$

The second and third integrations in eqn. (6.8) are performed "by parts" to yield

$$\int_{r_o}^{r_M} F(r) \frac{\partial^2 t}{\partial r^2} dr = \frac{\partial t}{\partial r} F(r) \Big|_{r_o}^{r_M} - \{ t F'(r) \Big|_{r_o}^{r_M} - \int_{r_o}^{r_M} t F''(r) dr \} \tag{6.9}$$

$$\int_{r_o}^{r_M} \frac{F(r)}{r} \frac{\partial t}{\partial r} dr = t \frac{F(r)}{r} \Big|_{r_o}^{r_M} - \int_{r_o}^{r_M} t \{ - \frac{F(r)}{r^2} + \frac{F'(r)}{r} \} dr \tag{6.10}$$

It is now specified that F(r) be such that

$$F(r_o) = 0 = F(r_M) \tag{6.11}$$

Eqn. (6.8) can then be written as

$$GC_p \frac{d}{dZ} g(Z) - k_e h(Z) = 0 \tag{6.12}$$

where

$$g(Z) \equiv \int_{r_o}^{r_M} F(r) t(r,Z) dr \tag{6.13}$$

$$h(Z) \equiv -\{t(r_M,Z)F'(r_M)-t(R_o,Z)F'(r_o)\}+\int_{r_o}^{r_M} t(r,Z)\{F''(r)+\frac{F(r)}{r^2}-\frac{F'(r)}{r}\}dr \qquad (6.14)$$

Note that the p.d.e. has been reduced to the o.d.e. eqn. (6.12), and that the introduction of F(r) has eliminated all derivatives of t from the problem, leaving only the observed variable, t(r,Z) itself.

The weighted residual methods may now be applied to eqn. (6.12), to yield

S.D.M.

$$\hat{k}_e = \frac{GC_p\{g(Z_m) - g(0)\}}{\frac{1}{2}\sum_{i=o}^{m-1}\{h(Z_i)+h(Z_{i+1})\}\{Z_{i+1}-Z_i\}} \qquad (6.15)$$

L.S.R.M.

$$\hat{k}_e = \frac{GC_p\sum_{i=o}^{m-1}\{h(Z_i)+h(Z_{i+1})\}\{g(Z_{i+1})-g(Z_i)\}}{\sum_{i=o}^{m-1}\{h^2(Z_i)+h^2(Z_{i+1})\}\{Z_{i+1}-Z_i\}} \qquad (6.16)$$

It is to be understood that in using eqns. (6.15) and (6.16), h(Z) and g(Z) are to be evaluated in the usual way i.e. by applying eqns. (6.13) and (6.14) with the integrals evaluated using the trapezoidal rule applied to the observed values of t(r,Z), viz. $Y_{i,j}$.

The methods may thus be used straightforwardly, once the function F(r) is specified.

Choice of the weighting function F(r). So far, the only requirements made of F(r) are that it be twice-differentiable and satisfy eqn. (6.11). Two obvious choices of F(r) are as follows:-

i) The lowest order polynomial in r - a quadratic - satisfying the requirements.

$$F(r) = -r^2 + r(r_o + r_M) - r_o r_M \qquad (6.17)$$

ii) A 'natural'function which ensures that the integral in eqn. (6.14) is unweighted, so that:

$$F''(r) + \frac{F(r)}{r^2} - \frac{F'(r)}{r} = 1 \qquad (6.18)$$

Solving the o.d.e. eqn. (6.18) with the boundary conditions given by eqn. (6.11) yields

$$F(r) = (r_M \ln r_o - r_o \ln r_M)r - (r_M - r_o)r\ln r + (\ln r_M / r_o)r^2 \qquad (6.19)$$

Testing the methods: The methods are tested on the same simulated experimental data as was the finite-difference technique: see table 31.

It can be seen immediately that this 'integration technique' is much more successful than the 'finite difference technique', the former being able to cope with an error standard deviation roughly two orders of magnitude larger than that which can be handled by the latter technique. Both weighting functions seem to be effective, and both weighted residual methods succeed, although the LSRM estimate exhibits a significant bias at a lower level of imposed error than the SDM estimate.

However, the problem examined above has certain shortcomings as a test problem although it is a necessary prelude to the interpretation of real experimental data reported in section 6.5. First, it involves three parameters (k_e, h_a, h_b), only one of which is estimated. Secondly, the measurement zone was restricted to a region far from the walls. Thirdly, because of (i) the restricted measurement zone, (ii) the form of the boundary conditions and (iii) the parameter values used, the range $t(r_o,Z)$ to $t(r_M,Z)$ is rather small ($\sim$0.2), so that the relative importance of the imposed 'error' is much exaggerated.

σ_E	SDM				LSRM				$k_{e,true}$
	'quadratic' F(r)		'natural' F(r)		'quadratic' F(r)		'natural' F(r)		
	$\hat{k}_e$	$\sigma_{\hat{k}_e}$	$\hat{k}_e$	$\sigma_{\hat{k}_e}$	$\hat{k}_e$	$\sigma_{\hat{k}_e}$	$\hat{k}_e$	$\sigma_{\hat{k}_e}$	
0	17.05	-	16.57	-	16.89	-	16.56	-	16.85
10^{-4}	17.06	0.027	16.58	0.026	16.89	0.025	16.57	0.024	16.85
10^{-3}	17.14	0.27	16.66	0.26	16.88	0.25	16.56	0.24	16.85
10^{-2}	18.47	3.32	17.94	3.23	12.10	1.85	12.02	1.79	16.85
5×10^{-2}	21.05	81.66	19.44	56.10	1.11	1.56	1.155	1.54	16.85

Table 31: Weighted residual methods and the integration technique

Clearly it would be useful to test the technique on a problem without these limitations, so that the limits of its applicability might be established more clearly.

6.4 Further testing on simulated data

In order that the 'integration technique' may be compared with least squares estimation, it is convenient to choose a model with an analytical solution. The problem chosen is that of estimating the diffusivity 'k' in the heat equation in rectangular co-ordinates

$$\frac{\partial u}{\partial v} = k \frac{\partial^2 u}{\partial x^2} \tag{6.20}$$

with the boundary conditions $u(v,1) = 0 = u(v,0); \quad 0 \leqslant v \leqslant V$

and the initial condition $u(0,x) = \sin \pi x \quad ; \quad 0 \leqslant x \leqslant 1$

(6.21)

Observations on the state u are made at m times at each of M spatial locations. Simulated data was generated in the usual way, by adding Normal 'error' to the equation solution

$$u(v_i, x_j, k) = (\sin \pi x_j) \exp(-\pi^2 k v_i) \tag{6.22}$$

using the parameter value k = 1.

Proceeding as before there results

$$\frac{d}{dv} \tilde{u}(v) = k u^*(v) \tag{6.23}$$

where

$$\tilde{u}(v) \equiv \int_0^1 F(x) u \, dx$$

$$u^*(v) \equiv \int_0^1 u \, dx \tag{6.24}$$

and F(x) is the 'natural' weighting function

$$F(x) = \tfrac{1}{2} x(x - 1) \tag{6.25}$$

The least squares estimator is

$$\min_{\hat{k}} \left\{ \sum_{i=1}^{m} \sum_{j=1}^{M} \{Y_{ij} - u(v_i, x_j, k)\}^2 \right\} \qquad (6.26)$$

where Y_{ij} is an 'observed value'.

The weighted residual estimators are:

SDM

$$\hat{k} = \frac{\tilde{u}(V) - \tilde{u}(0)}{\frac{1}{2} \sum_{i=0}^{m-1} \{u^*(v_i) + u^*(v_{i+1})\}\{v_{i+1} - v_i\}}$$

LSRM

$$\hat{k} = \frac{\sum_{i=0}^{m-1} \{u^*(v_i) + u^*(v_{i+1})\}\{\tilde{u}(v_{i+1}) - \tilde{u}(v_i)\}}{\sum_{i=0}^{m-1} \{u^{*2}(v_i) + u^{*2}(v_{i+1})\}\{v_{i+1} - v_i\}}$$

where $\tilde{u}$ and u^* are evaluated from eqns. (6.24) using the trapezoidal rule applied to the Y_{ij}.

The new estimators are again found to be promising: a comparison of their bias and efficiency with that of least squares, as a function of the number of spatial points (M), number of points in the time dimension (m) and error variance (σ_E^2), is shown in figs. 6.1 to 6.6.

6.5 Application to real experimental data

When the integration technique is applied to real experimental data (see chapter 8) corresponding to the model of section 6.2 and 6.3, plausible values of $\hat{k}_e$ are obtained:-

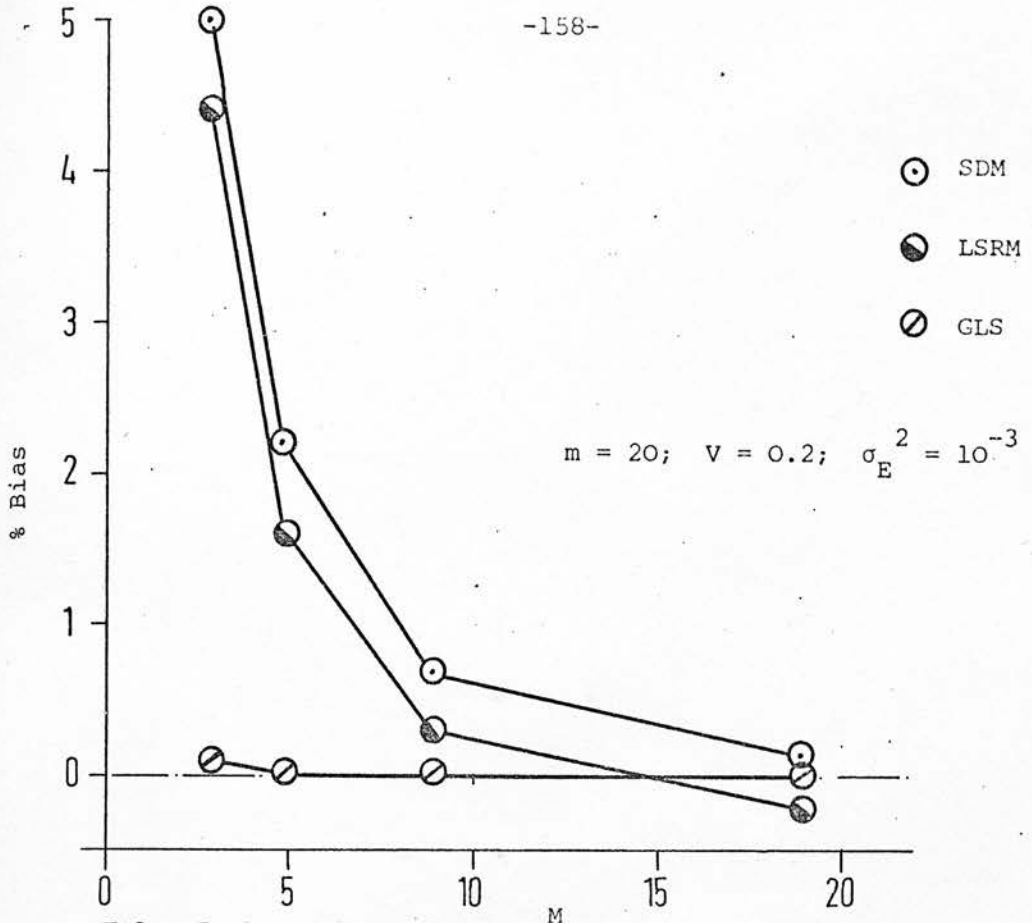

FIGURE 6.1 Bias As A Function Of M

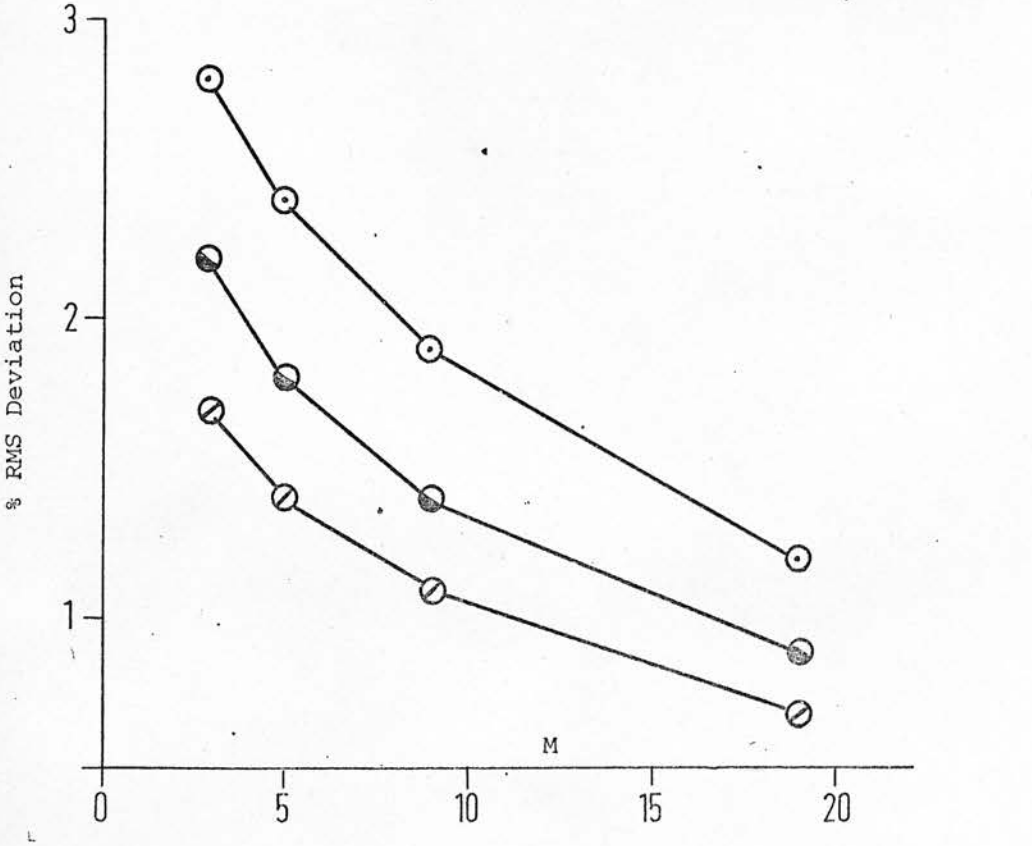

FIGURE 6.2 Efficiency As A Function Of M

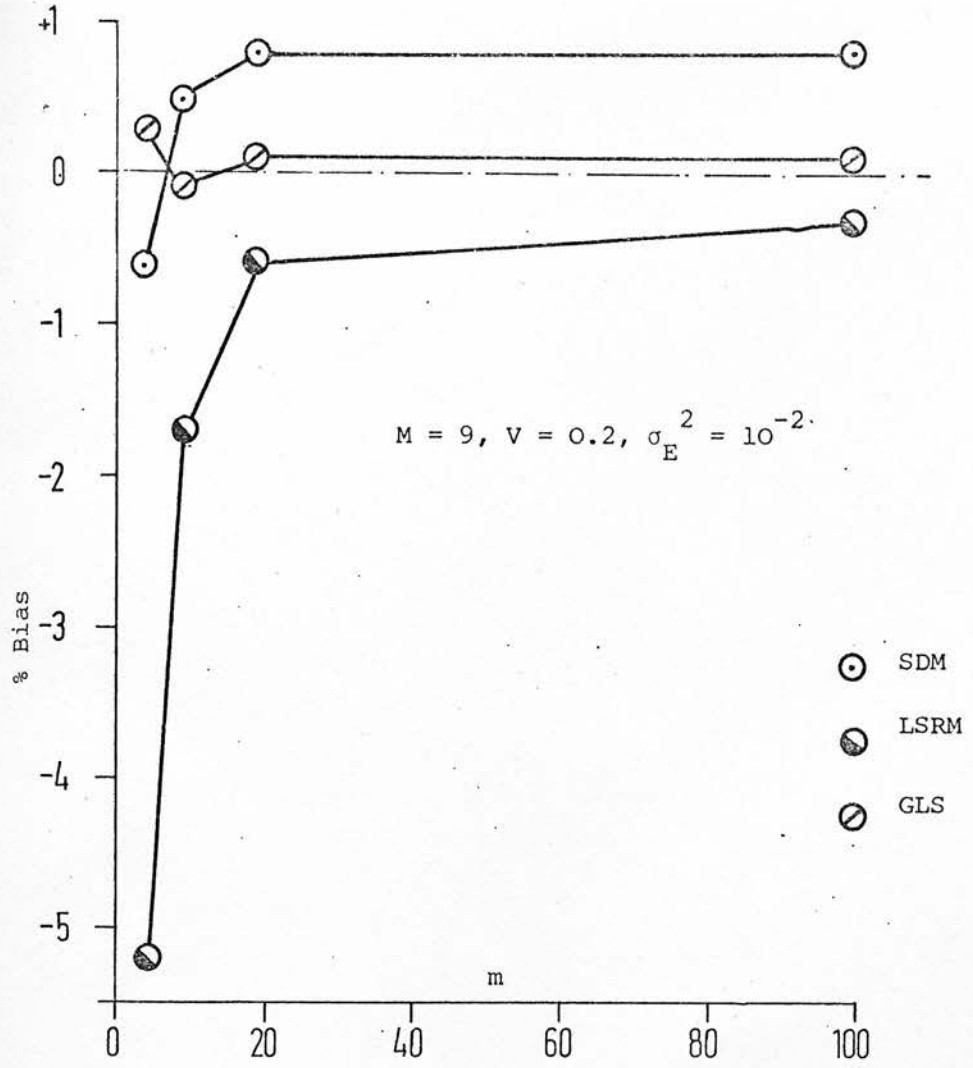

FIGURE 6.3 Bias As A Function Of m

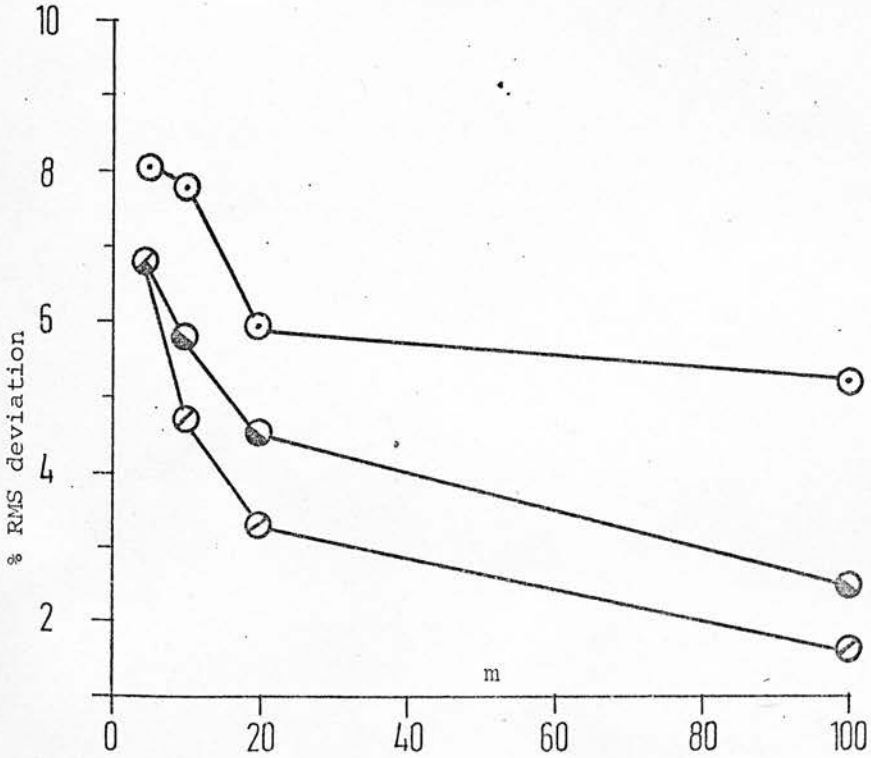

FIGURE 6.4 Efficiency As A Function Of m

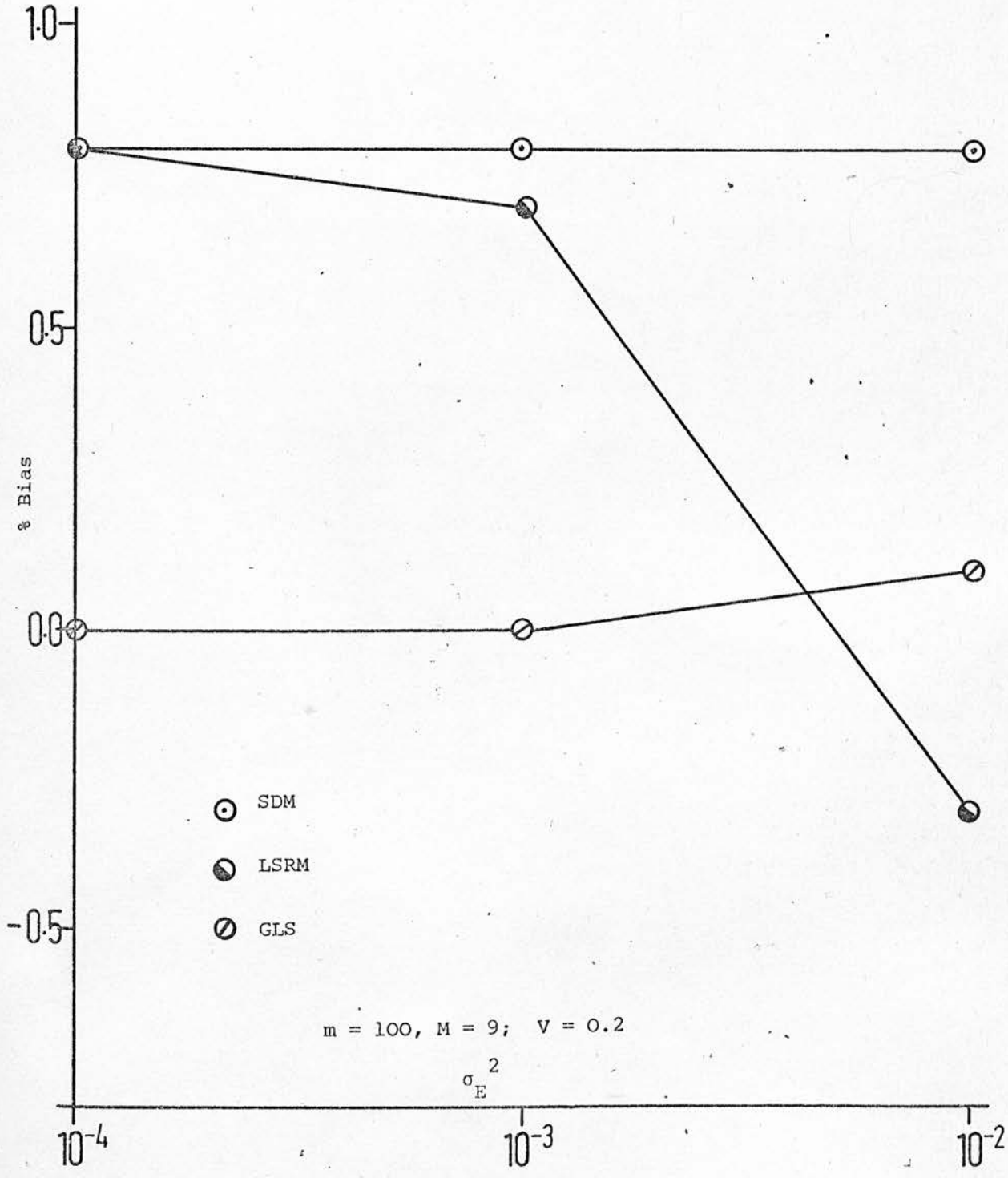

FIGURE 6.5 Bias As A Function Of σ_E^2

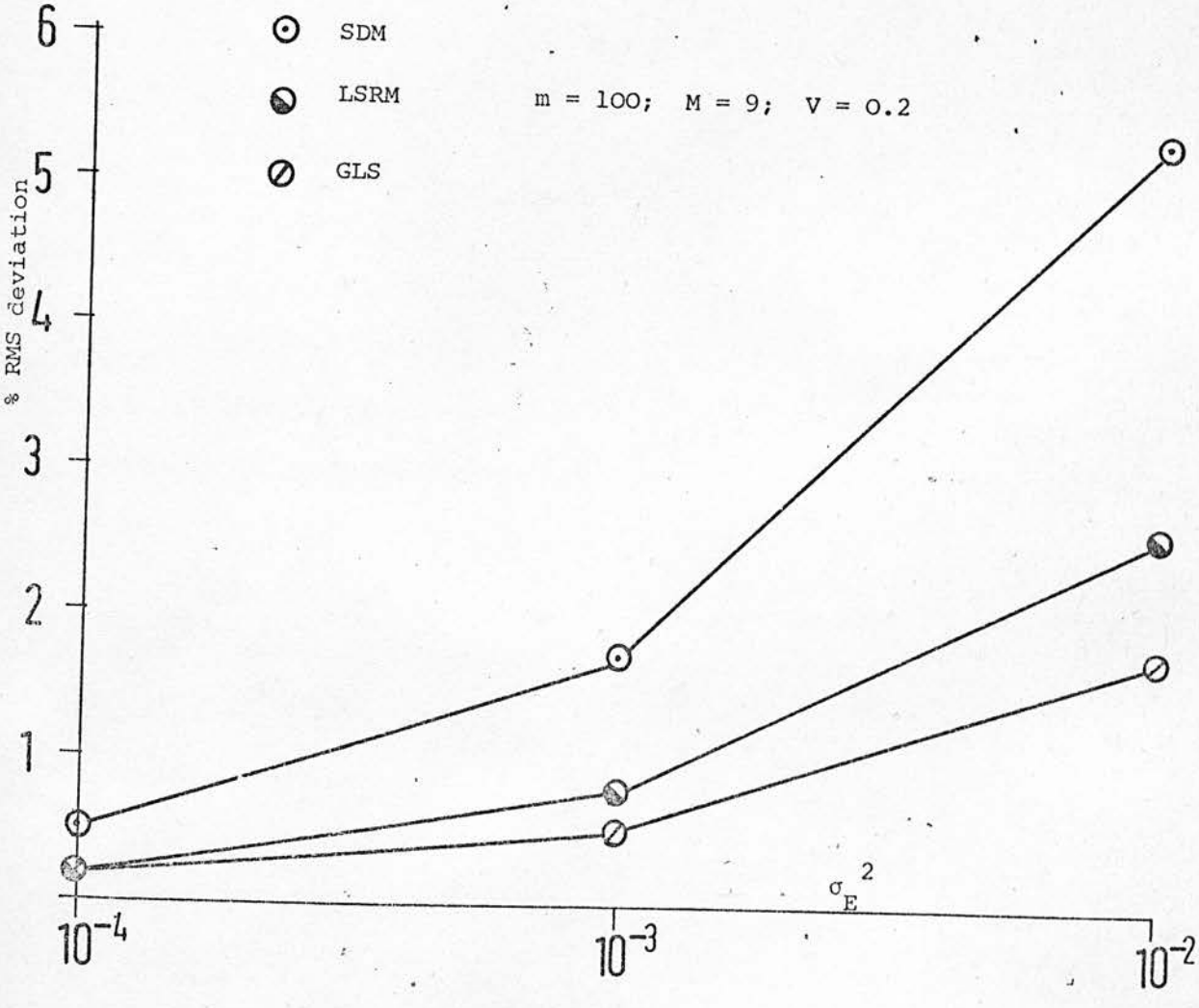

FIGURE 6.6 Efficiency As A Function Of σ_E^2

Table 32. Results of the SDM/integration technique applied to experimental data

Series Number	12	7	11	8	10	9
$\hat{k}$	0.925	2.231	3.489	3.927	4.502	6.604

These results were obtained using the 'natural' weighting function

Moreover, when a least squares procedure is used for parameter estimation in this model (see chapter 8), these values prove to fall within the (not very large) convergence region. However, the estimates of k_e found by the weighted residual methods are larger by about a factor of three than those found by the least squares method. A likely explanation for this discrepancy is as follows: the integration technique is applied to a model wherein the p.d.e. is assumed to hold between r_o and r_M, with parameter k_e. The least squares approach is based on the assumption that the p.d.e. holds between r_a and r_b with parameter k_e, and with additional parameters h_a and h_b to account for the increase in heat transfer resistance near the walls. If the p.d.e. does not represent faithfully the behaviour of the physical system - e.g. if k_e is not independent of r - then the two approaches are based on incompatible assumptions and this might be expected to yield different parameter estimates. The adequacy of the model (eqns.(6.1), (6.2), (6.3)) will be further discussed in chapter 8 .

Shortcoming. A shortcoming of the weighted residual/integration technique is that it has permitted estimation only of the parameter appearing in the p.d.e. and not of the parameters in the boundary conditions.

This deficiency is attributable to the experimental difficulty in measuring $t(r_a)$ and $t(r_b)$. If these temperatures were measurable, then it is easily shown that the integration technique may be applied, omitting the requirement that the weighting function F(r) be zero at its extremities, and that the model reduces to the o.d.e.

$$GC_p \frac{dg(Z)}{dZ} - k_e\{-\frac{h_b}{k_e} + t(r_b)\{\frac{h_b}{k_e} + \frac{F(r_b)}{r_b} - F'(r_b)\} - t(r_a)\{\frac{h_a}{k_e} + \frac{F(r_a)}{r_b} - F'(r_a)\} -$$

$$\int_{r_a}^{r_b} t\{F''(r) + \frac{F(r)}{r^2} - \frac{F'(r)}{r}\}dr = 0$$

from which all three parameters might, in principle, be estimated.

6.6 Remarks and Summary

Extension of the weighted residual methods to p.d.e.'s was effected by devising the 'integral technique'. This permits estimation of parameters appearing within the p.d.e., but it has been shown that experimental difficulties may be such that the procedure will not permit estimation of parameters appearing in the boundary conditions.

If one were interested in parameter estimation in first-order p.d.e.'s, or in second order p.d.e.'s where the first derivative(s) of the dependent variable(s) are observed in addition to the variables themselves, then the weighted residual methods could be applied, following the spirit of the integration technique, but often without the need to introduce the weighting function F(r).

These new methods for p.d.e.'s have the advantage that they may reduce computing times by several orders of magnitude, and make many fewer demands on the experimenter's time and mathematical skills.

LSRM is rather similar to the method of Himmelblau et al (184), whilst SDM is related to a method proposed in the Electrical Engineering literature (212, 213). However, the new methods presented here have been analysed more carefully and extended much further than have the other 'approximate methods' so far presented in the literature (see section 3.6).

Moreover, the methods were here devised by deliberately trying to construct analogues to the Method of Weighted Residuals (M.W.R.) used in solving o.d.e.'s (see section 2.5). This formulation not only serves to demonstrate the relationship between the two methods (LSRM and SDM), but has the advantage of suggesting other weighted residual methods suitable for other parameter estimation problems. For instance, Cresswell (214) has performed parameter estimation in a non-linear two-point boundary value problem by constructing an analogue to the "Method of Moments" (see section 2.5).

The utility of the new methods can be finally judged only when other workers have tried to apply them to their own problems. But, there can be no doubt that some kineticists feel the need for such methods (215).

CHAPTER 7. An Introduction to the Heat Transfer Investigation

7.1 Introductory remarks.

7.2 Experimental apparatus.

7.3 Discussion of the apparatus design, and its operation.

7.4 Sources of experimental error.

7.5 Analysis of angular temperature variations.

7.6 Models of heat transfer through the stagnant bed.

7.7 Parameter estimation in models I and II.

7.8 A study of the voidage structure of the packed bed.

7.9 Testing of model III.

7.10 Summary.

7.1 Introductory remarks

The choice of model to be used in analysing experimental data will be much influenced by the intended application of the results of the analysis. The most important use for models of heat transfer in packed beds is probably in the prediction of the steady-state performance of packed bed gas/solid catalytic reactors:- "The design of fixed-bed tubular reactors can only be attempted with a full knowledge of the heat transfer characteristics of the system. In most industrial reactors, heat transfer considerations largely determine the size of the reactor and the limits of profitable and safe operating conditions" (216). A brief description of some models used for this task was presented in chapter one. A more detailed inspection is now required, based on an examination of the interests of the reactor designer. For the moment, the problem of axial dispersion in the bed will be ignored.

In many packed tubular reactors, particularly those of small diameter, the long-range axial temperature and concentration profiles are the most important features of reactor behaviour. Consequently a 'one-dimensional' model of the reactor has been developed, ascribing a single temperature to the whole of a radial cross-section of the bed. The only heat transfer parameter involved is an 'overall heat transfer coefficient' to account for heat transfer from the bed to the cooled tube wall.

However, there are also situations - particularly with very exothermic reactions or beds of large diameter - where the designer needs to predict long-range radial temperature profiles, perhaps because of selectivity problems or because of the danger of catalyst deterioration at high

temperature. The simplest model suitable to this task is the 'two dimensional homogeneous model', in which a point temperature is ascribed to each radial and axial position in the bed. The heat transfer parameters used are a bed-effective radial conductivity and an effective wall heat-transfer coefficient. A comparison of the predictions of one- and two-dimensional models is presented in Appendix 5.

The next level of complexity normally considered is that of distinguishing between the temperature of the two phases, which can be of great importance since chemical reaction rates are often very sensitive to temperature. The simplest method is to distinguish between the phase temperatures only for the purpose of calculating reaction rates, using an effectiveness factor for a pseudo-pellet, without trying to distinguish between the radial heat fluxes in the two phases. This model, which is used in Appendix 5, is usually referred to as a 'homogeneous model', although 'semi-heterogeneous' might be a better term. A fully heterogeneous model has been devised (63) which does account for these separate fluxes.

The models discussed above have one paradoxical feature in common - all describe the packed bed, with its discrete two-phase nature, either as one continuous quasi-phase, or as two. The experiments reported below reveal one striking feature of the packed bed for which such models do not account, namely the existence of angular temperature variations. To cope with this phenomenon, a model would probably need to incorporate an effective thermal conductivity in the tangential direction, (such as is used in the analysis of heat transfer in timber (217)), and would

presumably need to be stochastic in character. Such a model would involve a proliferation of parameters which would be hard to determine because of measurement difficulties.

The most refined model to find wide application - the two-dimensional homogeneous model - should be seen as being rather a crude representation of a complex system for which more sophisticated models are perhaps not justified, because of the uncertainties likely to be involved in the available design data (see chapter one). So, the models used in the analysis of experimental results might reasonably be expected to be little more complicated than the two-dimensional homogeneous model, which ignores short-range gradients, the two-phase nature of the bed, and angular temperature fluctuations.

Research into heat transfer in packed beds continues (218-221) because current knowledge is inadequate - agreement between the behaviour of experimental reactors and the predictions of models using available heat transfer correlations is generally poor (66, 222-224). Moreover, the industrially important case of low tube to particle diameter ratio (low 'aspect ratio') has received little attention (225-227). Consequently, it was decided that a preliminary investigation of heat transfer in packed beds of low'aspect ratio' would be pursued, with the intention of (i) discovering if the behaviour of such beds exhibited any unusual features or whether, on the contrary, currently available correlations and models apply, and (ii) estimating parameter values to be used in designing a more complete experimental investigation and, perhaps, as a guide in constructing a more detailed model of heat transfer in such packed beds.

7.2 Experimental apparatus.

Having decided on an apparatus to operate in the steady state, the problem arises of imposing a sufficiently large radial temperature gradient across the bed. The solution adopted is the established technique of using an annular bed (59). The outer wall of the annulus is heated electrically, and the inner wall is cooled with water, so that a temperature difference of up to ca. 120 deg. K may be established across the bed.

Figure 7.1 is a diagram of the apparatus, which is conveniently described by considering in turn four sections:-

i) The air flow section. Air is drawn from the laboratory compressed air line through ½" conduit piping [1]. The delivery pressure to the drying region [5] is controlled between 0 and 30 p.s.i.g. by a regulating valve [3]. The air flow-rate is controlled by a ½" gate valve [2b], and measured by a rotameter [6]. Air flow-rates of up to 200 litres/minute at 25°C and 0-2 p.s.i.g. may be obtained. The air stream is then split into two streams which are fed symmetrically into a long calming section [7] packed with ⅜" x ⅜" hollow aluminium cylinders [8]. Air leaving the calming section then passes through a distributor plate and flows upwards through the test section to atmosphere.

ii) The water flow section. Water is pumped rapidly from a constant temperature bath [18] up through a 12 mm O.D. copper pipe [12] which is situated along the vertical axis of the calming section and of the test section itself. To facilitate dismantling of the apparatus, the copper pipe was made up in two lengths which were joined by a brass

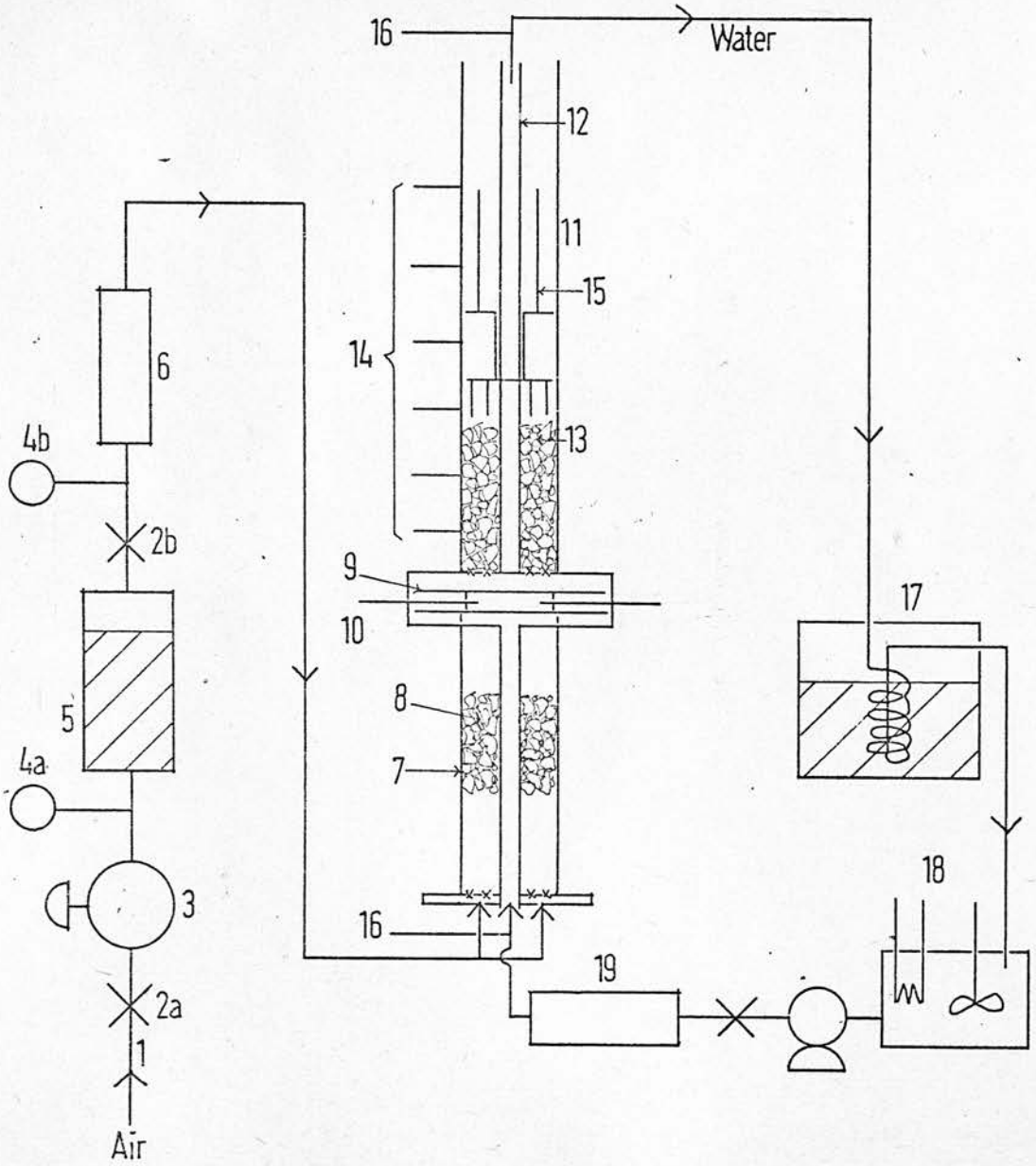

FIGURE 7.1 Schematic Diagram Of Experimental Layout

(1) ½" conduit pipe
(2) ½" gate valve
(3) Pressure regulating valve
(4) Pressure gauges.
(5) Drying section packed with silica gel
(6) Rotameter for air flow measurement
(7) 18" x 3" diameter pyrex calming section
(8) Hollow aluminium cylinders ⅜" x ⅜"
(9) PVC flange
(10) 6 thermocouples inserted through flange
(11) Test section brass cylinder
70.6 mm ID. 76.2 mm OD
(12) 12 mm OD copper pipe carrying water flow
(13) Test section packing
(14) Thermocouples inserted into wall
(15) Supporting cross for radial thermocouples
(16) Inlet and outlet thermocouples on water line
(17) Refrigerator and ice bath
(18) Constant temperature bath
(19) Rotameter for water flow

Not shown are electric heating coils wrapped around the test section.

union nut at the top of the calming section. Since the water system is a closed circuit, it is necessary to use a refrigerator and ice bath [17] to remove from the water the heat which it absorbed on passing through the hot test section.

iii) The test section is constructed of brass and flanged with mild steel at one end to mate up with the calming section. Heat leakage from the flange of the hot test section to the calming section flange is restricted, but not eliminated, by interposing a 9 mm thick PVC gasket and lining all the connecting bolt holes with asbestos.

It was hoped originally that a uniform temperature profile could be obtained in the air stream entering the test section, but the heat leakage from the test section causes an appreciable radial temperature gradient near the outer tube wall. Therefore six thermocouples (T.C.'s) are inserted radially through the PVC gasket to measure the inlet temperature profile: the positions of the tips of these thermocouples are noted in table 33, where r is the radial co-ordinate measured from the central axis of symmetry of the apparatus i.e. from the centre of the copper water-pipe.

Table 33: Position of the inlet thermocouples

T.C. number	1	2	3	4	5	6
r (mm)	12	16	23	28	31	34

Thermocouples are also hard-soldered into the outer wall of test section. The test section column is wrapped tightly with aluminium foil, and then wrapped in four (later six) sections with electric heating cable ("Thermotrace"). The whole is then tightly wrapped with another

layer of aluminium foil, and surrounded with glass fibre thermal insulation ("Cosy-wrap"). The heat input to each section is controlled with a variac.

Two different test sections were used in the experiments: details are presented in table 34.

Table 34: Details of the two test sections used

	1	2
Length (mm)	439	1223
I.D. (mm)	70.6	70.6
O.D. (mm)	76.2	76.2
Number of T.C.'s inserted into wall)	6	10
Spacing of T.C.'s	80 mm apart starting 24 mm from inlet	Bottom six were 102 mm apart starting at 57 mm from inlet; upper four spaced at 127 mm

The inlet and outlet water temperatures are also measured with thermocouples. The various thermocouples are connected to 'Comark' electronic thermometers, with an ice/water cold junction.

iv) The thermocouple cross. The radial temperature profile is measured using thermocouples mounted on a brass cross which is suspended above the bed - see figure 7.2. The assembly can be locked in position using nuts on the screwed rod supports [7]. Two crosses were constructed containing four and six arms respectively. The former cross was used initially to obtain radial temperature profiles in beds of small diameter

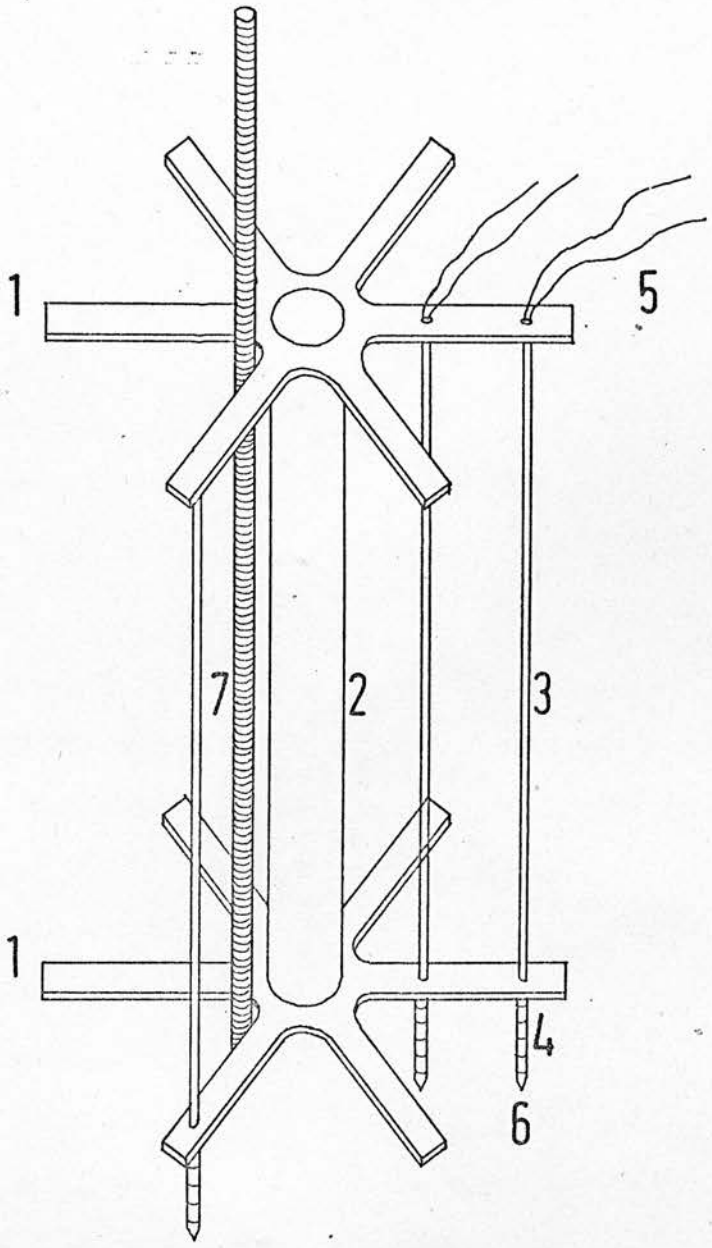

(1) Six membered cross 70.6 mm. diameter
(2) Hollow Brass tube 102 mm x 12 mm I.D.
(3) Stainless steel capillary tubing
(4) Interlocking guide beads
(5) Insulated thermocouple wires
(6) 1 mm. Cr/Al thermocouples
(7) ¼" screwed rod support (one of three)

FIGURE 7.2 Brass Cross For Holding Radial Thermocouples

particles (< ¼"), whilst the latter was used in beds of larger diameter particles. The location of the thermocouples on the crosses is shown in figure 7.3. The six-armed cross was modified during the course of the work, by adding on an extra thermocouple at 9 mm and at 34 mm, on the arm at lower right of the diagram.

7.3 Discussion of the apparatus design, and its operation

i) Operation of the apparatus. The temperature of the outer wall of the test section is held uniform by adjustment of the variacs controlling the potential difference across the heating cables. The inner wall temperature is nearly uniform due to the high flow-rate of the cooling water. In the experiments which involve the flow of air through the test section, the radial temperature profile at a series of bed depths was measured as follows:-

First, a shallow bed was formed by trickling pellets into the test section. The six-armed cross was then lowered into position. The apparatus was allowed to reach steady-state, and the temperatures noted. The cross was then rotated through five successive angles of 60°, and the indicated temperatures again recorded. The cross was removed, more pellets added, and the process repeated. Each bed-depth was measured using a dip-stick.

In experiments performed in the absence of air flow through the bed, there is no axial temperature profile and so the bed depth used was of little importance: for convenience the top of the bed was about half-way up test section number one. Since,in these experiments, the cross thermocouples were immersed in the bed, rotation of the cross was not possible.

Four-Armed Cross

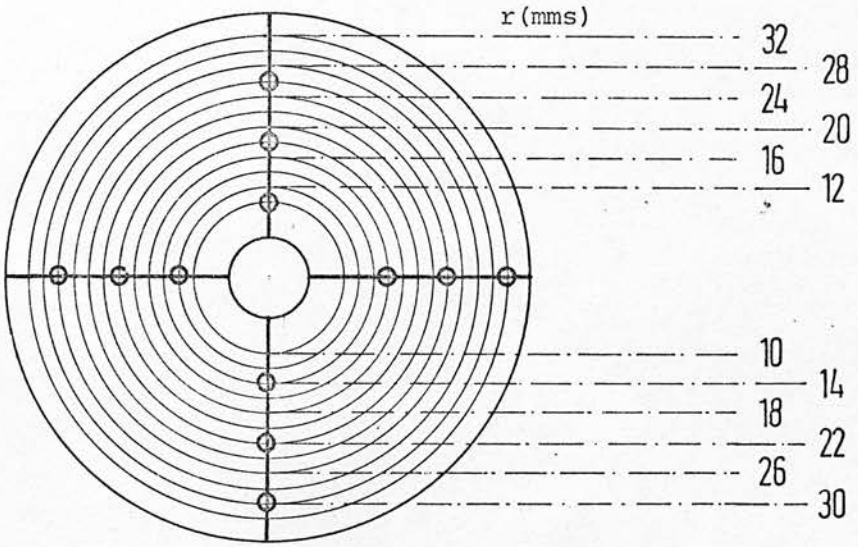

Six-Armed Cross

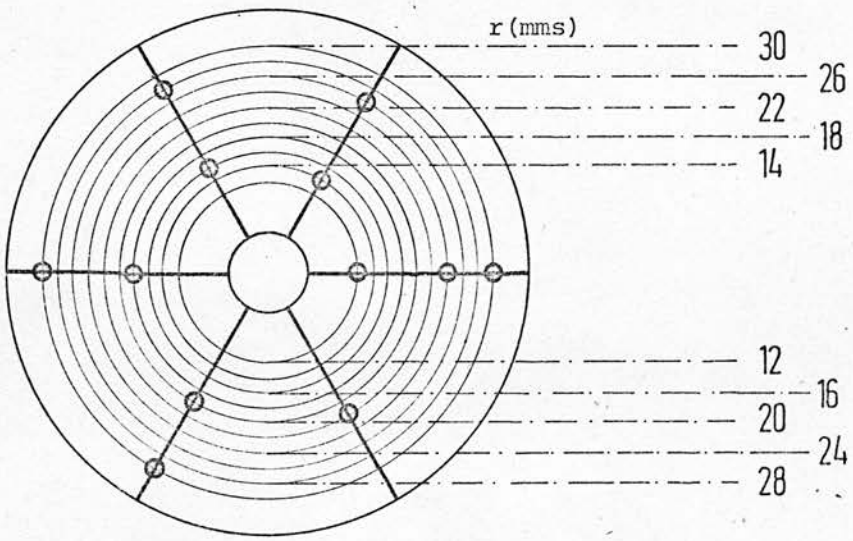

FIGURE 7.3 Location Of Radial Thermocouples

ii) Heat conduction along the thermocouple wires. The thermocouples attached to the brass cross are situated in a non-uniform temperature field, and it is possible that heat will be conducted to or from the thermocouple junction, thereby yielding a biased reading. An attempt was made to restrict this effect by using thin-wired leads and low-conductivity ceramic guide beads (fig. 7.2, [4]), and to gauge its magnitude by a simple experiment:- the thermocouples and beads were immersed in a constant temperature bath of hot water, while the metal cross was placed in a stream of cold air. The temperature difference so created between the thermocouple junction and the main body of the cross had no observable effect on the indicated temperature of the hot water, and so it was concluded that the effect is negligible.

iii) Rejection of one test section design. It was intended to have a series of thermocouples, at different axial locations, projecting through the test section wall and 13 mm into the packed bed, and test section 2 was originally appropriately constructed - see figure 7.4. However, it was decided to check whether these 'axial' thermocouples produced a biased reading due to heat leakage from the hot test section wall and guide tube. Consequently, the apparatus was operated with the bed packed to a height level with a chosen 'axial' thermocouple, and the cross was positioned so that the tip of one of its thermocouples was very close to the tip of the 'axial' thermocouple. It was found that the axial thermocouples were indicating temperatures much higher (by ca 20 deg K) than those attached to the cross, and were thus clearly substantially in error. Three different methods were then devised for supporting the axial thermocouples, with the hope of eliminating this error.

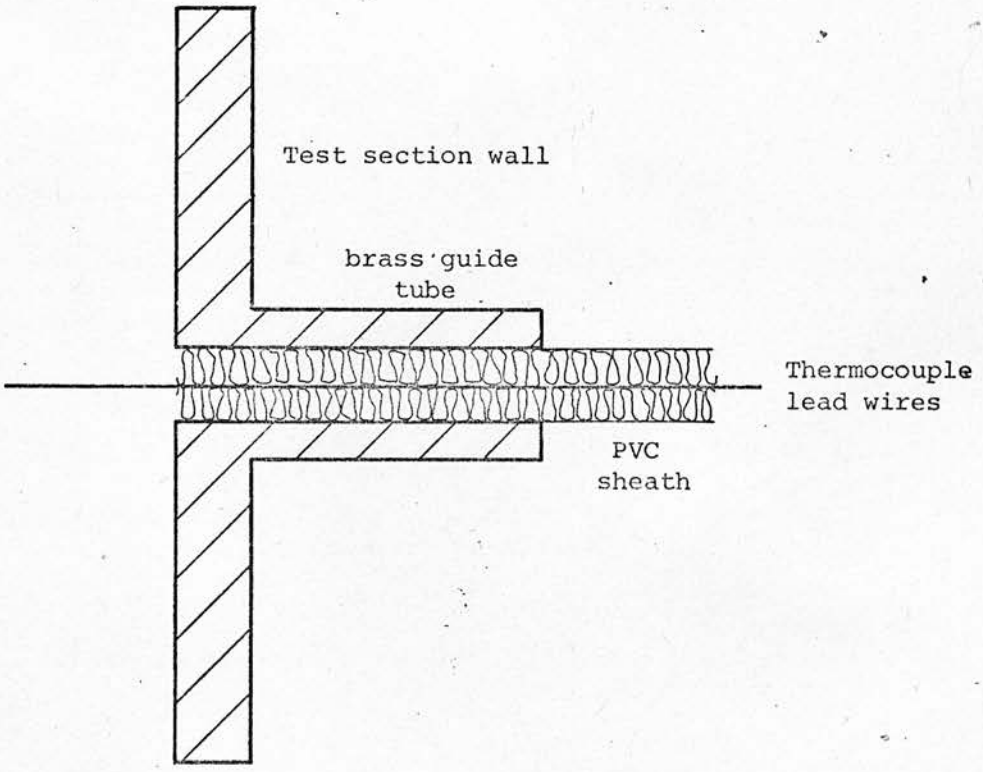

FIGURE 7.4 Early Design Of The Test Section

First, the PVC sheath shown in figure 7.4 was replaced by a brass sheath, with an air gap between it and the brass guide tube. There was a brass/brass 'line contact' at the outer end of the guide tube. This design fared no better, and nor did a second design using an asbestos sheath. Lastly, a fine thermocouple was used, having only a very thin glass fibre covering, and held in position at the inner end of the guide tube by a small asbestos ring, and at the outer end by a rubber O-ring clamped tight by a bevelled nut. The thermocouple was thus surrounded largely by air and had no direct contact with the brass. This design did not remedy the problem either. It was then decided to operate without these thermocouples, and the guide tubes were plugged.

By inserting a thermocouple down the empty test section and through the distributor plate, it was possible to show that the thermocouples measuring the temperature of the inlet air show little bias (< 2 deg K), presumably because the flange through which they are inserted is cooler than the test section wall.

iv) Use of the thermocouples. Before using the thermocouples attached to the cross, two decisions are required.

First, should the thermocouples be immersed in the bed, or located just above the surface of the bed? The advantage of the latter choice is that it is possible to rotate the cross and so obtain temperature readings for different angular positions at the same radial positions. However, it is not clear a priori that any temperatures so measured are representative of temperatures in the bed. The issue was settled by a simple experiment whereby the thermocouples were located just above the bed, and then buried with successive layers of pellets poured from above.

When there was appreciable gas flow through the bed, it was found that the submersion of the thermocouples had no significant effect, but in the case of no air flow - a stagnant bed - it was found that the temperature profile changed markedly with the addition of layers of pellets, stabilising when about five layers had been added: see figure 7.5. Consequently, in the experiments on the stagnant bed the thermocouples were immersed, whilst in the flow experiments they were located just above the surface of the bed.

Secondly, should the practice of imbedding the thermocouples within pellets be adopted? A simple experiment showed that the measured temperature profile differed according to whether the thermocouples were buried - figure 7.6 - but there is no compelling reason to choose one or other profile as being more representative. It was decided to refrain from imbedding the thermocouples on pragmatic grounds:-

a) an imbedded thermocouple cannot be located nearer than one half pellet diameter from the walls of the annulus, which is a severe restriction, as will be seen below.

b) experiments in a transparent perspex model of the test section revealed that the imbedded thermocouples distorted the packing pattern of the pellets in the layers above the thermocouples much more than did the alternative arrangement, thus introducing a possible source of error into the experiments.

v) Packings used: Two different types of catalyst support material were used as packings:-

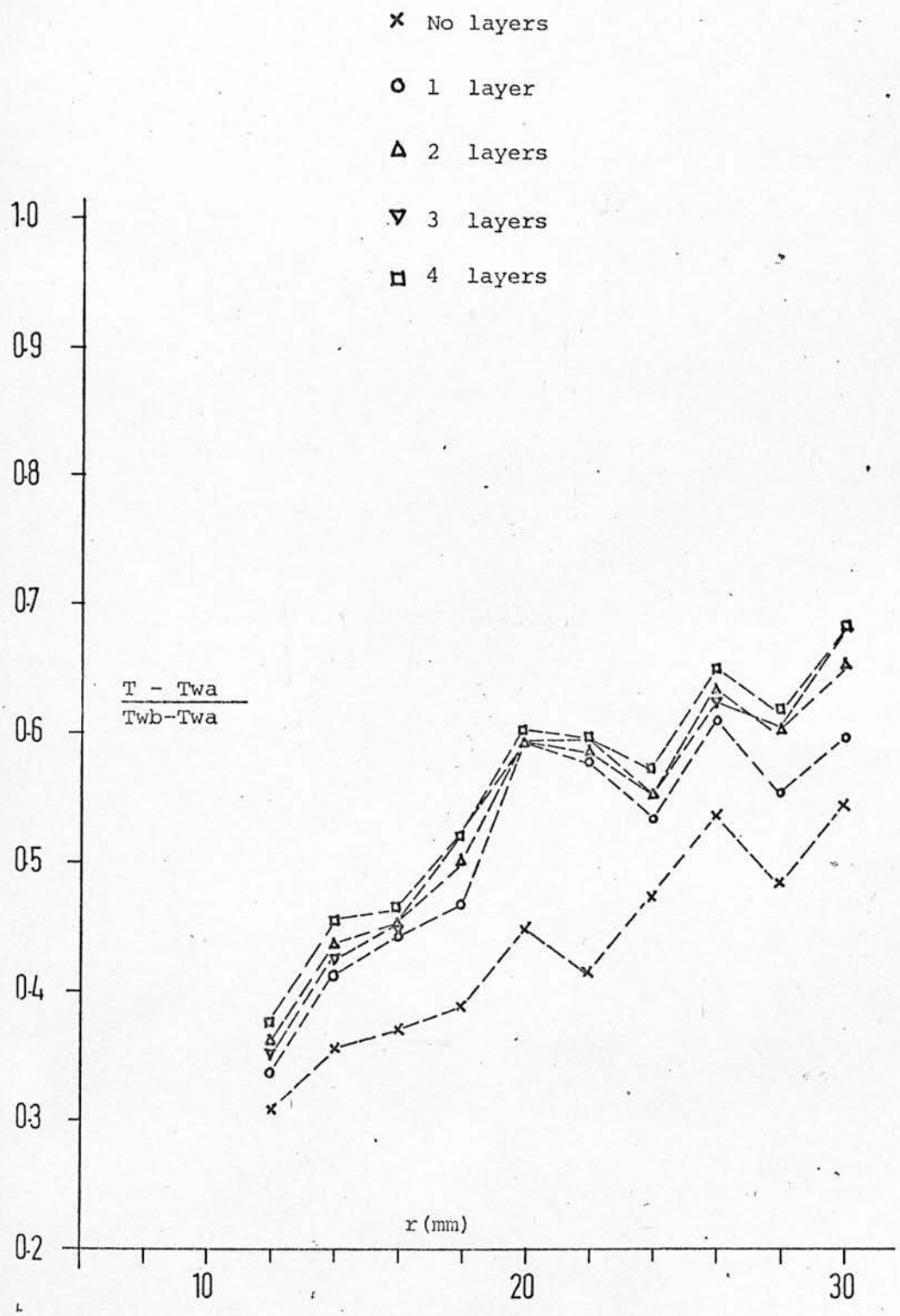

FIGURE 7.5 The Effect Of Adding Layers Of Packing

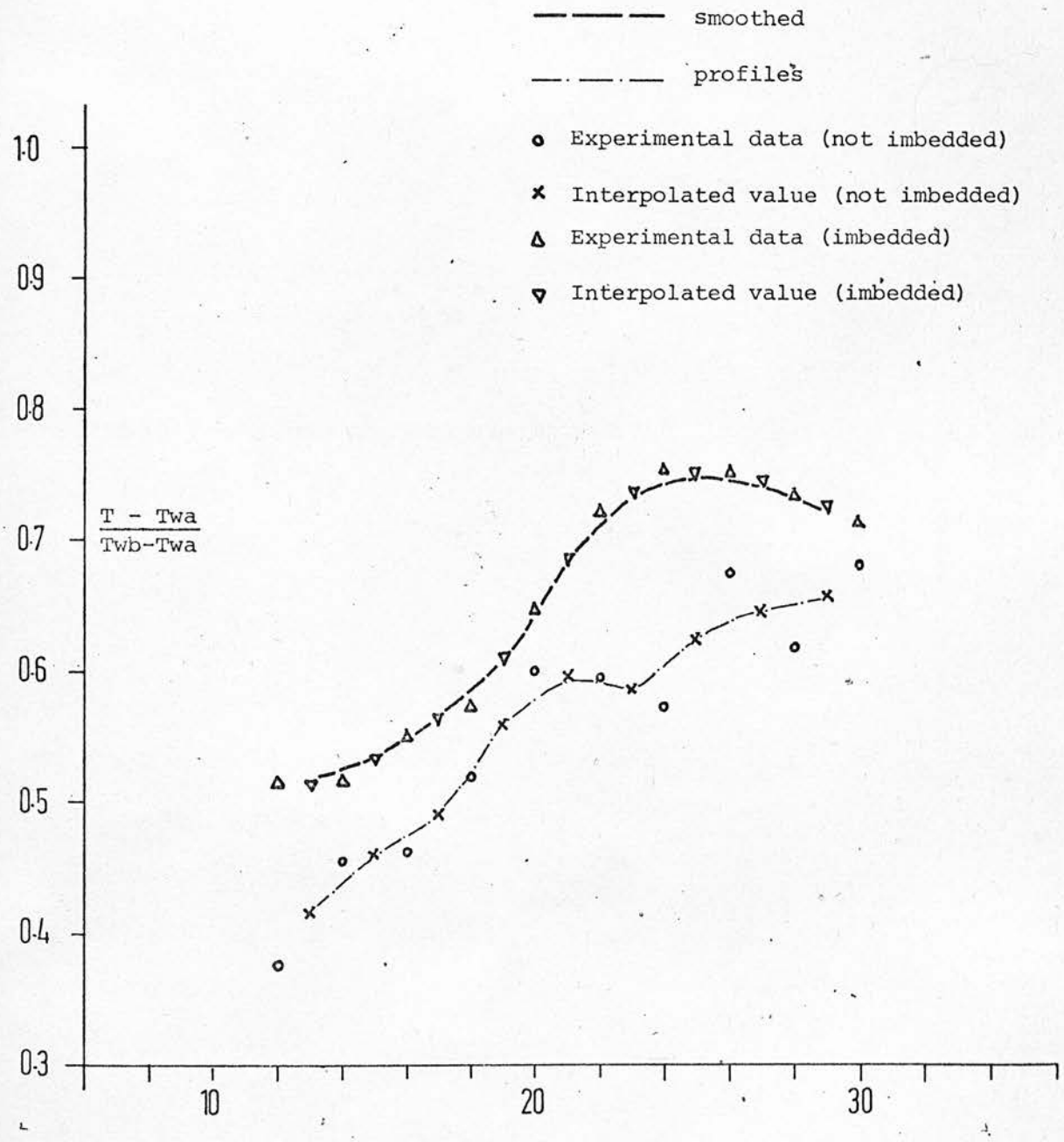

FIGURE 7.6 The Effect Of Embedding The Thermocouples

Table 35: Packings used

	"Small pellets"	"Large pellets"
Type	Alundum "Macroport' Catalyst Carrier Type SA5205 (spheres)	Inert Ceramic spheres (manufacturer: Norton Co.)
Apparent Porosity	55-61%	non-porous
Density	2.25 g/ml	2.12 g/ml
Diameter	6.3 ± 0.3 mm	10.1 ± 0.18 mm
Mean Bed Voidage	∿0.41	∿ 0.38

7.4 Sources of experimental error

As was discussed in chapter 3, it is important to determine the characteristics of the experimental error before proceeding to parameter estimation. Various sources of experimental error suggest themselves:-

i) Location errors. Other workers (229) have suggested that the major source of error in temperature measurement in packed beds lies in the uncertainty in the radial position of the thermocouples - in this case, the thermocouples attached to the cross. In the experiments reported below, temperature gradients of ca 7 deg K/mm were observed near the walls of the bed, and of ca 2 deg K/mm far from the walls. Since the thermocouples used are ca 1 mm in diameter, and are probably located within ± 1 mm of their nominal settings, then errors of ± 10°C and ± 3°C might arise, in the different regions of the bed, due to 'location errors'. These error magnitudes are consistent with the

three replicate measurements (ca $\pm$ 5°C) performed at r = 30 mm, with the six-armed cross. However, other explanations of the errors in replicate readings are plausible, as discussed below.

In an attempt to reduce location error, the fit of the sliding cross on the inner tube of the annulus was made tight, and the thermocouples were held rigid with interlocking guide beads fixed with 'Araldite' epoxy resin , as shown in figure 7.2. The positions of the thermocouple tips were also re-measured from time to time, and the thermocouples re-aligned if necessary.

ii) Errors in the measurement of temperature. The thermocouples and measuring instruments were calibrated against a 0.1°C standard reference mercury thermometer, in a specially designed thermostatic bath, over the range 25-100°C. Part of the results is shown in table 36.

Table 36: Calibration of thermocouples and measuring instrument

Mercury Thermometer	Thermocouples											
	1	2	3	4	5	6	7	8	9	10	11	12
50.9	50.9	50.9	51.0	51.2	51.4	51.3	51.2	51.1	51.0	51.0	51.0	51.0
94.9	95.4	95.4	95.4	95.5	95.5	95.5	95.3	95.3	95.3	95.2	95.1	95.2

The results show that the thermocouples agree reasonably well with the mercury thermometer, and, even more important, agree well with each other. Replicate experiments performed by immersing the thermocouples in boiling water showed that the thermocouples provide perfectly reproducible results to the reading accuracy of the 'electronic thermometer', viz. ca. 0.01°C.

The reproducibility of 'point' temperature measurements was checked by carrying out replicate runs, by bringing the bed to steady-state, recording the temperature measurements and then shutting off the wall heaters for 25 minutes, so that the bed cooled to room temperature. The heaters were then switched on and the bed brought to a new steady-state, and the temperature measurements again recorded. The old and new steady state radial temperature profiles are compared in Table 37.

Table 37: Comparison of near-replicate radial temperature profiles

	Temperature at different radial positions											
Run 1: T°C	50.2	54.0	53.6	60.0	64.0	63.5	67.7	71.8	76.1	75.4	75.0	81.3
Run 2: T°C	50.8	54.2	54.6	60.1	64.2	63.7	68.0	71.9	75.6	75.0	74.7	80.7
r(mm)	10	12	14	16	18	20	22	24	26	28	30	32

Note that the table is headed 'near-replicate' because the wall temperatures did not return to precisely the same steady-state values (Run 1; 23.5, 91.3°C: Run 2; 24.3, 90.4°C). Nevertheless the agreement is excellent, suggesting a small error variance (ca 0.1 $(^{o}C)^{2}$) in temperature measurement.

iii) Miscellaneous sources of error

(a) The 35.XP air rotameter used (figure 7.1 6) was calibrated against a dry gas meter, which was then calibrated against a water displacement bell. The calibration chart so obtained agreed with the manufacturer's to within a few per cent.

(b) There is some uncertainty associated with defining the whereabouts of the ends of a packed bed. The inlet of the bed was taken to be the plate which supported the bed. To define the position of the top of the bed, six different measurements were made with a dip-stick: agreement was always within a quarter-particle diameter of the mean, which was the value used in subsequent calculations.

iv) Temperature fluctuations due to non-homogeneity of the bed.

The radial temperature profiles presented in figures 7.5 and 7.6 are far from smooth, suggesting that there might be considerable error in the temperature measurements. Therefore replicate experiments were performed to examine the apparent measurement error of the thermocouples when used above the packed bed. An eight-armed cross was used yielding temperature measurements at eight radial locations across the top of the bed. The experiment was then repeated after re-packing the bed. Figure 7.7 summarises the results. It will be seen that there is a considerable, apparently random, scatter. In similar experiments above a stagnant bed, the form of the results is the same, although the amount of scatter is less.

Since the scatter, in each case, much exceeds the error in temperature measurement per se (see (ii) above), its cause is attributed to the non-homogeneity of the packed bed. There are two obvious sources of non-homogeneity. First, it may be that the two phases - gas and solid - are at different temperatures, and thus that the readings from the thermocouples depend on how close they are to a solid pellet - i.e. whether they are immediately above a void or a pellet. Secondly, the interstices of

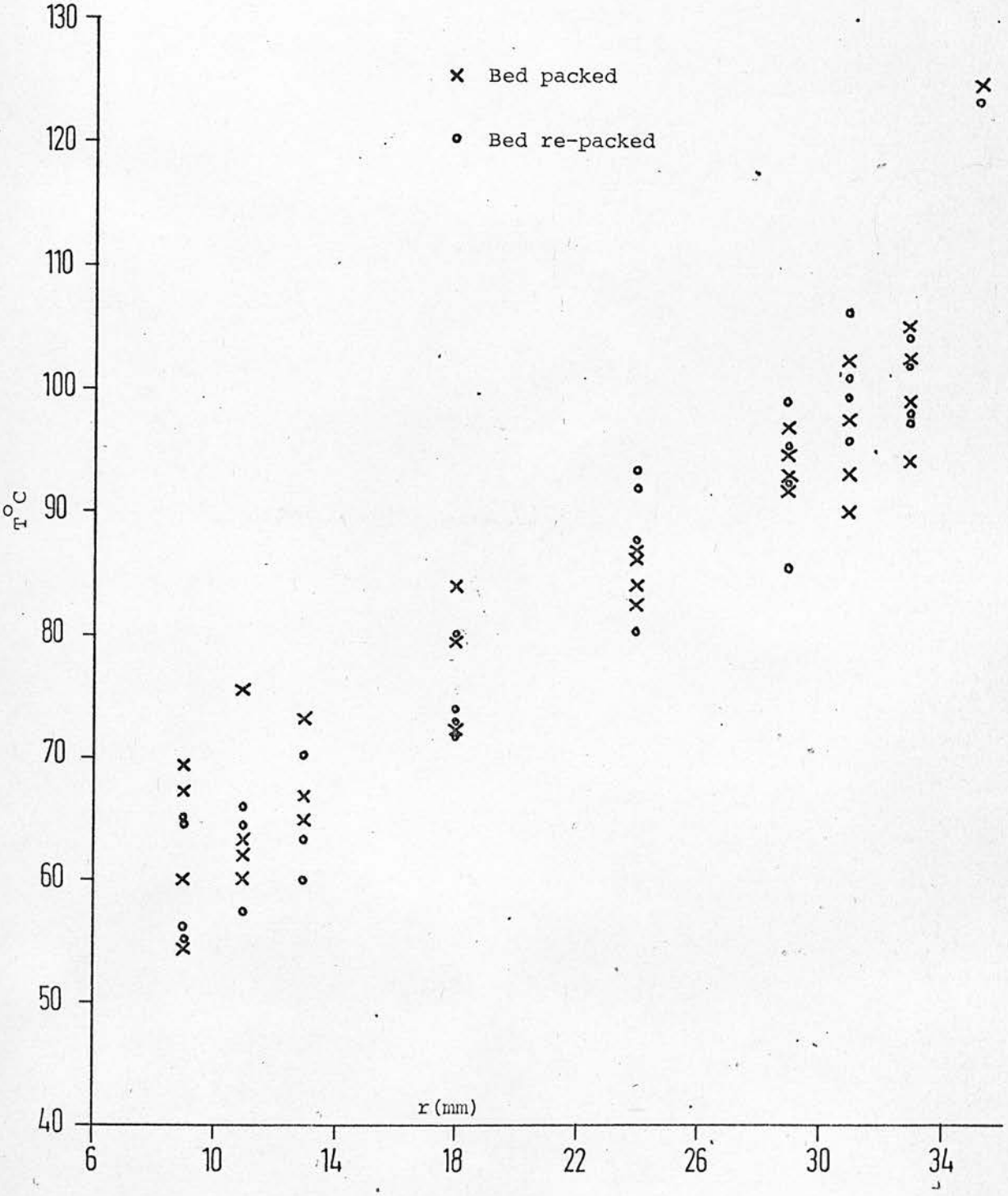

FIGURE 7.7 Angular Temperature Fluctuations

the bed have a chaotic character such that a thermocouple may be exposed to air coming (by flow or natural convection) from a hot region near the outer wall or from a colder region near the inner wall. The air streams affecting the thermocouple depend not only on its radial position, but also on its angular position.

The traditional models used for the description of heat transfer in packed beds (see sections 7.1 and 7.5) take no account of these fluctuations or their cause, and to that extent may be deemed inadequate. The usual advice of the writer on statistics is that an inadequate model should be rejected or modified. Whilst it may be necessary eventually to consider rejecting the models and constructing more complex models, it might be preferable to consider first whether use of the traditional models may be defended by arguments other than the powerful argument of expediency.

Since engineers and scientists doubtless use models which they know to be, in some sense, inadequate, it is reasonable to enquire as to the statistical (rather than practical) reasons for avoiding inadequate models. Part of the reason is that 'errors' which arise from model inadequacy - such as, for instance, assuming a reaction to be first order when it is actually second order - are likely to show distinctly different features from measurement errors. The 'inadequacy errors' are unlikely (a) to have zero mean (b) to be independent (c) to have a common form of distribution, let alone be Normally distributed, or (d) to have known variances and co-variances. That is, they are unlikely to exhibit the properties listed in table 8. These features make it difficult to provide theoretical justification for the use of any statistical parameter

estimation technique, because the assumptions on which the technique is based will not approximate physical reality.

For the packed bed problem, however, use of such estimation methods as least squares may be justified as follows. The models of heat transfer in the bed have, as dependent variable, temperature, and as one of their independent variables, radial position. One might choose to look upon that temperature as corresponding to the angular- mean temperature. The temperatures measured at different angular positions may be regarded as error-influenced measurements of this angular-mean value. If it can be shown that the apparent measurement errors - i.e. differences between the mean and individual values - behave like true measurement errors, then the use of standard estimation methods would be warranted. The experimental data are analysed accordingly.

7.5 Analysis of angular temperature variations

Consider first the independence of the apparent errors. If the conclusion that the errors are due to bed inhomogeneity is correct, then any degree of order in the bed might impose some regular type of 'error' such that the thermocouples do not yield readings which can be treated as independent. For instance, it might be that adjacent thermocouples on the same arm of the cross might yield correlated results. This possibility is investigated by calculating correlation coefficients for such adjacent thermocouple pairs. Table 38 shows some results obtained for 'Series 7' (flow case), when the temperatures were measured using the six-armed cross of figure 7.3 (modified to include an extra thermocouple at 9 and 34 mm on the arm shown on the lower right of the diagram). There are 14 different thermocouples, and the cross was rotated through angles of 60°, providing 6 readings per thermocouple.

Table 38: Thermocouple correlation coefficients

Thermocouple pair	Bed depth no.2	Bed depth no.3
1,7	-0.564	-0.684
7.14	0.164	0.032
4,10	0.394	0.286
3,9	0.414	0.859
2,8	-0.161	0.140
8,13	0.653	-0.057
5,11	-0.301	0.964
6,12	-0.011	0.142

Only two pairs (3,9) and (5,11) on depth no. 3 have particularly high correlation coefficients, but high coefficients will occasionally arise by chance, of course. There is no consistency of correlation coefficient from one bed depth to another, except, perhaps, for the pair (1,7), and that pattern does not carry over to other bed depths. It therefore appears reasonable to treat the 'errors' as if they are independent.

Next, constancy of variance may be examined. Table 39 shows how the estimated standard deviations of the dimensionless temperature (defined by eqn. (7.8)) depends on radial position, for the same two data sets.

Table 39: Estimated 'error' standard deviation (dimensionless temperature)

r	9	12	14	16	18	20	22	24	26	28	30	30	30	34
Bed depth no.2	.022	.024	.036	.025	.030	.049	.038	.039	.045	.051	.066	.052	.035	.049
Bed depth no.3	.033	.023	.020	.023	.045	.022	.039	.029	.037	.046	.027	.021	.071	.036

It will be seen that the standard deviation appears to vary more or less randomly with r, and does not appear to change significantly with bed depth. Constancy of variance may therefore be reasonably assumed.

The frequency distribution of the 'errors' is next examined. Figure 7.8 shows a typical plot of the 'errors' on Normal probability paper. The data are well represented by a straight line, implying that the 'errors' are approximately Normally distributed.

It is thus reasonable to assume that the 'errors' in the flow experiments are independent and Normally distributed with mean zero and constant variance. The same conclusion was reached for the experiments in the stagnant bed where, of course, the cross had to be positioned just above the bed to permit examination of the 'errors'. It is presumed that the conclusions hold when the cross is buried. In the stagnant experiments the 'error' standard deviation is much smaller than in the flow experiments.

One further observation was made regarding the 'errors'. As shown in figure 7.9, for four different angular positions of the four-armed cross, the apparent error appears to be regularly scattered above and below the zero line, with a peak-to-peak spacing of roughly one particle diameter. This pattern lends support to the supposition that the 'error' is attributable to the non-homogeneity of the bed. Note that the location of the peaks is different for each angular position, which explains why the errors can still appear to be independent and Normally distributed in the tests performed above.

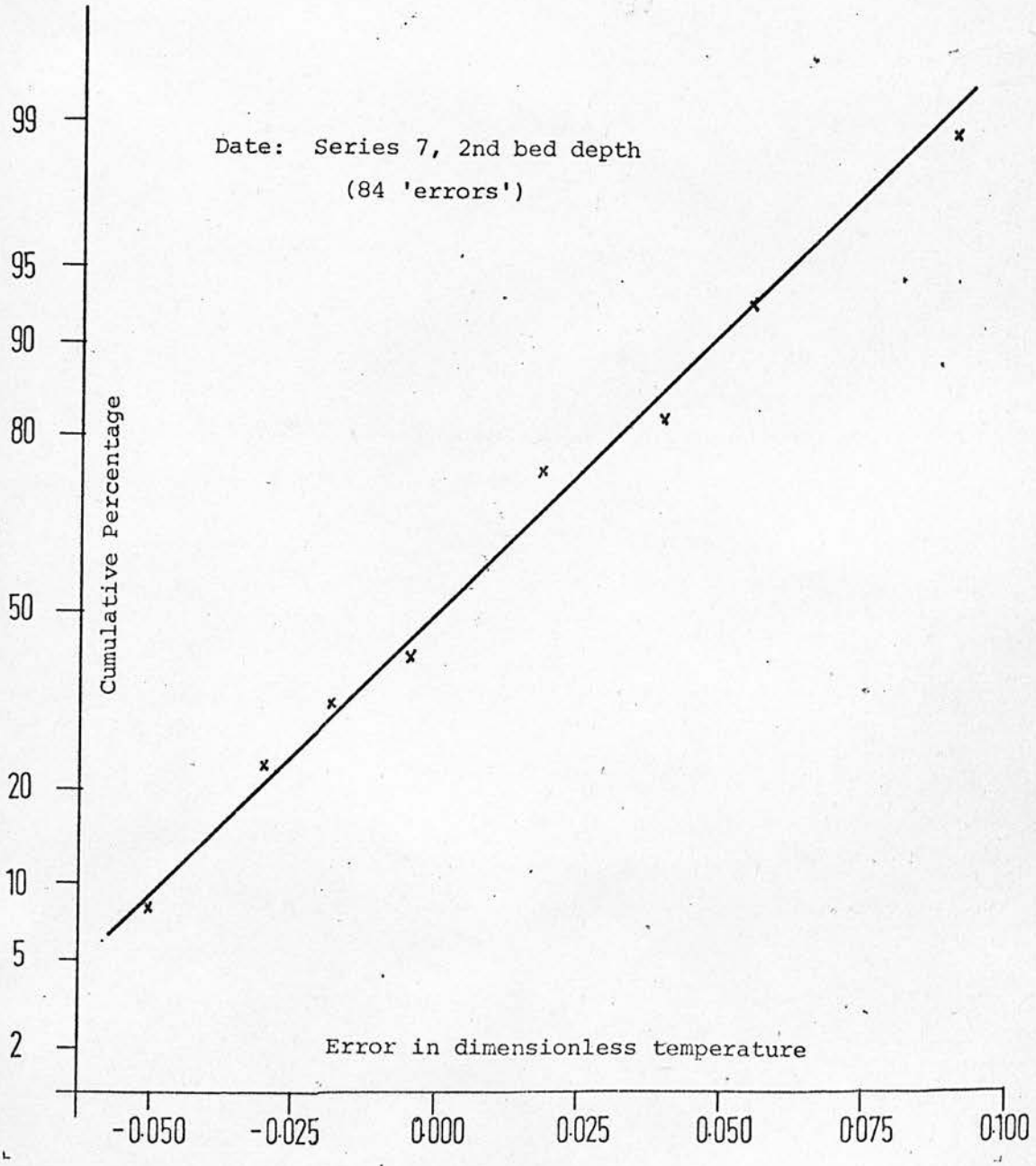

FIGURE 7·8 Test For The Normality Of The 'Error' Distribution

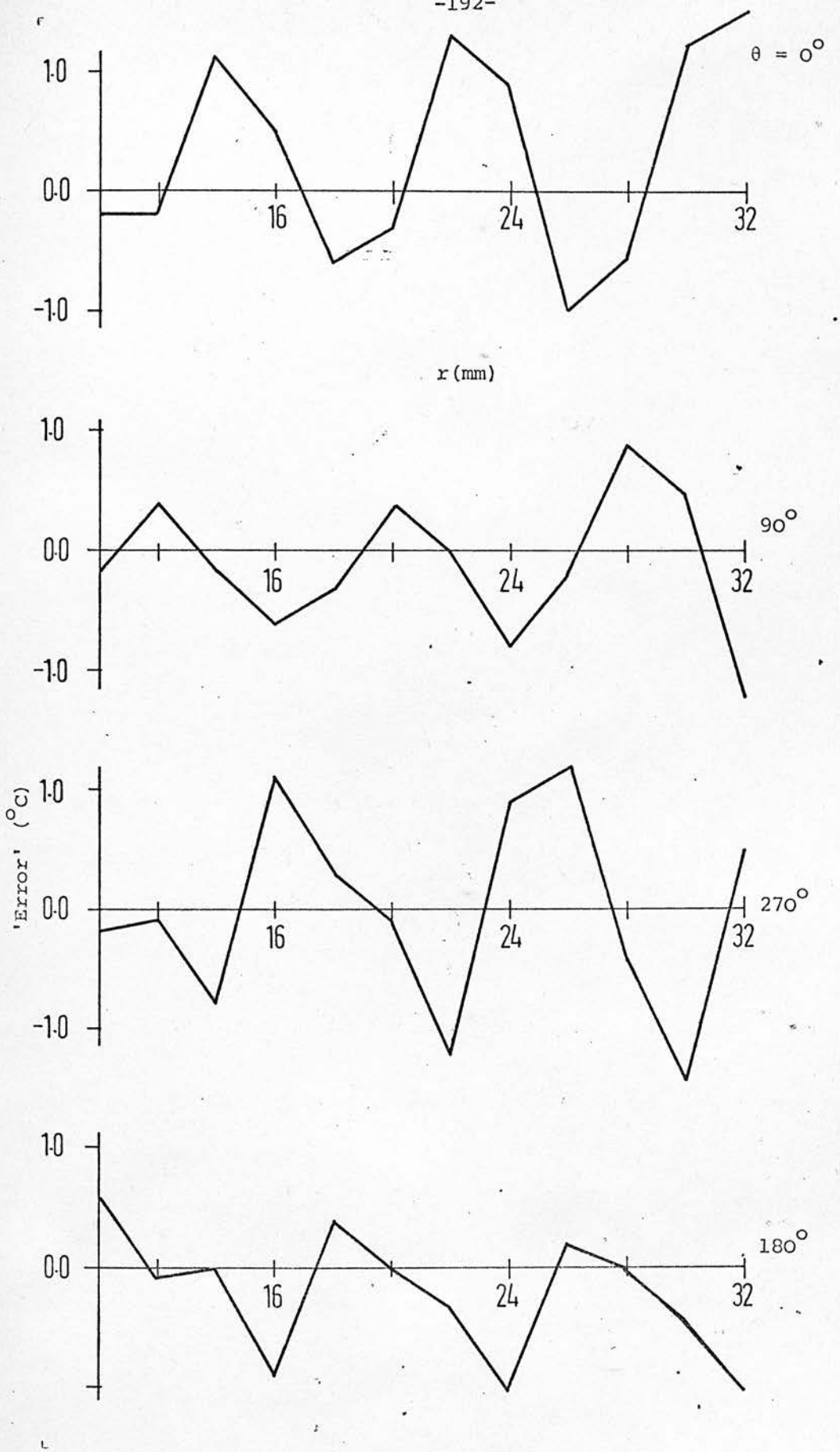

FIGURE 7·9 Deviations Of Point Temperatures From The Mean At Various Angular Positions [d_p =6·3mm]

In summary, the evidence suggests that the source of 'apparent error' in the measurements is the non-homogeneity of the bed, but that the properties of this 'apparent error' are such as to justify use of standard parameter estimation methods such as "least squares". It will be possible to check this conclusion by an examination of residuals after parameter estimation has been performed.

7.6 Models of heat transfer through a stagnant bed

Before examining heat transfer through a packed bed with gas flow, the case of heat transfer through a stagnant bed is considered: partly because the case is interesting in its own right, partly to test the experimental apparatus and partly because, as will be explained in chapter eight, the parameter estimation problem in stagnant beds corresponds mathematically to the problem of estimation from the 'asymptotic profiles' developed in beds with flow.

An inspection of figures 7.5 and 7.6 reveals that the stagnant bed, like the bed with flow, exhibits a high heat transfer resistance near the walls, and this feature must be accounted for in the development of suitable models. Four models for consideration are shown in table 40. Each model describes heat transfer in the radial direction only, since there is no long-range axial temperature profile in the stagnant case. The models are therefore limiting cases or reduced forms of the general models discussed in section 7.1.

Model I - the conventional quasi-homogeneous model - accounts for heat transfer in the bed by an effective thermal conductivity k_e, and the resistance near the walls is idealised into a resistance at the walls, accounted for by effective wall heat transfer coefficients h_a and h_b.

Table 40: Models considered for the description of heat transfer in a stagnant packed bed

Number	Model equations	Solution
I	$\frac{d^2T}{dr^2} + \frac{1}{r}\frac{dT}{dr} = 0$ $r = r_a;\ k_e \frac{dT}{dr} = h_a(T - Twa)$ $r = r_b;\ k_e \frac{dT}{dr} = h_b(Twb - T)$	$\boxed{T = A \log r + B}$ (7.1) $A \equiv \frac{Twb - Twa}{\frac{1}{Bi_a} + \frac{1}{Bi_b} + \log {}^{r_b}/_{r_a}}$; $B \equiv Twa + A(\frac{1}{Bi_a} - \log r_a)$ (7.2) $Bi_a \equiv \frac{r_a h_a}{k_e}$; $Bi_b \equiv \frac{r_b h_b}{k_e}$ (7.3)
II	$\frac{d^2T_j}{dr^2} + \frac{1}{r}\frac{dT_j}{dr} = 0;\ j = a,m,b$ $r = r_a;\ T_a = Twa$ $r = s_1;\ T_a = T_m,\ k_a \frac{dT_a}{dr} = k_m \frac{dT_m}{dr}$ $r = s_2;\ T_m = T_b,\ k_m \frac{dT_m}{dr} = k_b \frac{dT_b}{dr}$ $r = r_b;\ T_b = Twb$	$\boxed{T_j = A_j \log r + B_j\ ;\ j = a,m,b}$ (7.4) $A_m \equiv \frac{Twb - Twa}{k_1 \log {}^{s_1}/_{r_a} - k_2 \log {}^{s_2}/_{r_b} + \log {}^{s_2}/_{s_1}}$ $B_m \equiv Twa + A_m(k_1 \log {}^{s_1}/_{r_a} - \log s_1)$ (7.5) $B_a \equiv Twa - A_m k_1 \log r_a$; $B_b \equiv Twb - A_m k_2 \log r_b$ $A_a \equiv k_1 A_m$; $A_b \equiv k_2 A_m$ $k_1 \equiv {}^{k_m}/_{k_a}$; $k_2 \equiv {}^{k_m}/_{k_b}$ (7.6)

Table 40 (contd.):

Number	Model equations	Solution
III	$\frac{1}{r}\frac{d}{dr}\left(r\, k_r \frac{dT}{dr}\right) = 0$ $r = r_a;\quad T = Twa$ $r = r_b;\quad T = Twb$	$\frac{T - Twa}{Twb - Twa} = \frac{\int_a^r \frac{dr}{r\, k_r}}{\int_a^b \frac{dr}{r\, k_r}}$ (7.7)
IV	$\frac{d^2T_s}{dr^2} + \frac{1}{r}\frac{dT_s}{dr} = \frac{h_e A_e}{k_{es}(1-\bar{\varepsilon})}(T_s - T_f)$ $\frac{d^2T_f}{dr^2} + \frac{1}{r}\frac{dT_f}{dr} = \frac{h_e A_e}{k_{ef}(1-\bar{\varepsilon})}(T_f - T_s)$	Solution of this model and of various sets of boudary conditions appropriate to these o.d.e.'s is presented in Appendix A3.1

This model is therefore a limiting case of the 'two dimensional homogeneous model' of section 7.1. In model I, T(r) represents the temperature of the quasi-phase, no distinction being made between the gas and solid. T(r) might therefore be looked upon as some average of the temperatures of the gas and the solid.

Model II, the composite continuum model, uses an effective conductivity in the bulk of the bed, k_m, and the resistance in the neighbourhood of the walls is represented by defining zones of reduced conductivity, k_a in $r_a \leqslant r \leqslant s_1$ and k_b in $s_2 \leqslant r \leqslant r_b$. (Where r_a and r_b are the radial co-ordinates of the inner and outer wall, and s_1 and s_2 the co-ordinates of the boundaries of the zones of reduced conductivity). The model treats the bed as a composite material made up from layers of three different quasi-phases:- the low conductivity quasi-phase near the inner wall the high conductivity quasi-phase in the core of the bed, and another low conductivity quasi-phase near the outer wall.

The third model, the non-uniform continuum model, views the bed as a quasi-phase of non-uniform properties: the effective thermal conductivity, k_r, is taken to be a continuous function of radial position. The purpose of this model is to see whether k_r can be related to the voidage distribution in the bed, $\varepsilon(r)$. Since the voidage tends to unity at the walls, it should, in principle, be possible so to account for the high heat transfer resistance at the walls.

The fourth model is a heterogeneous model, wherein the temperatures of the solid and fluid, T_s and T_f, are distinguished. The heat transfer in the bed is described using separate phase effective conductivities, k_{es} and k_{ef}, whilst the resistance near the walls may be represented in a number of ways. This model suffers from the great disadvantage of incorporating many parameters, and further consideration of it is confined to Appendix A3.1.

Note that none of these models attempts to incorporate the angular dependence of temperature.

As shown in table 40, models I and II may be solved to yield closed form solutions - eqns. (7.1) and (7.4) - each involving two dimensionless parameters; Biot numbers, Bi_a and Bi_b, in model I, and conductivity ratios, k_1 and k_2, in model II. Model III is soluble in terms of quadratures. The parameters in this model are implicit in the use of k_r in eqn. (7.7), for the relationship between k_r and $\varepsilon(r)$ will involve unknown parameters (see Section 7.9).

A simple test of models I, II and III is easily performed - it can be shown that for all of them, the dimensionless temperature

$$t \equiv \frac{T - Twa}{Twb - Twa} \qquad (7.8)$$

is a function only of radial position, irrespective of the actual values of wall temperature (Twa and Twb) used. Simple experiments showed this to be the case for Twa $\sim 25^{o}C$, and Twb in the range 80-140^{o}C.

7.7 Parameter Estimation in Models I and II

There are no great difficulties involved in performing parameter estimation in models I and II. The conclusion of section 7.4 - that the errors are in T rather than r, and that they are independent, Normally distributed and of constant variance - suggests that unweighted least squares estimation is appropriate, and the existence of analytical model solutions - eqns. (7.1) and (7.4) - renders the task straightforward. In model II, the values of s_1 and s_2 chosen were $s_1 = r_a + 0.5\ d_p$; $s_2 = r_b - 0.5\ d_p$.

However, to examine the effect of the error assumptions, additional calculations were performed on the basis that the errors were in r rather than T.

Since eqns. (7.1) is of the form

$$T = A(Bi_a, Bi_b)\log r + B(Bi_a, Bi_b) \qquad (7.9)$$

the problem is one of non-linear estimation, performed by Simplex search. The objective functions are respectively:-

$$\text{Error in T: } \min_{Bi_a, Bi_b} \left\{ \sum_{i=1}^{12} \{T_{OBS,i} - A(Bi_a, Bi_b)\log r_i - B(Bi_a, Bi_b)\}^2 \right\} \qquad (7.10)$$

$$\text{Error in r: } \min_{Bi_a, Bi_b} \left\{ \sum_{i=1}^{12} \{ r_{SET,i} - \exp\left(\frac{T_i - B(Bi_a, Bi_b)}{A}\right)\}^2 \right\} \qquad (7.11)$$

No convergence difficulties occurred because good starting values were obtained by performing a linear regression of T on log r to find values of A and B from which values of Bi_a and Bi_b were readily found. Note, too, that equations of the form of eqn. (7.10) and (7.11) apply for model II since all the observed values of T happen to be within the range $s_1 < r < s_2$.

Conventional linearisation analyses were performed to obtain approximate values for parameter marginal standard deviations and parameter cross-correlation coefficients - details are presented in Appendix 3.2. A precis of the results is shown in tables 41 and 42, and the fit of the models, with the error assumed to be in T, is shown in figures 7.10 and 7.11.

Table 41: Estimation results for model I

	Data Set No.1: d_p = 6.3 mm (see Appendix A3.2)		Data Set No.2: d_p = 10.1 mm (see Appendix A3.2)	
	Error assumed to be in T	Error assumed to be in r	Error assumed to be in T	Error assumed to be in r
$\hat{Bi}_a$	2.42	4.24	1.98	3.23
$\sigma(\hat{Bi}_a)$	0.57	2.06	0.56	1.88
$\hat{Bi}_b$	2.70	3.57	1.28	1.53
$\sigma(\hat{Bi}_b)$	0.44	0.62	0.17	0.25
$\rho(\hat{Bi}_a, \hat{Bi}_b)$	0.84	0.84	0.92	0.94

The temperature profiles predicted using the two different error assumptions are plotted in figure 7.12, for data set number 1.

Table 42: Estimation results for model II

	Data Set No.1: d_p = 6.3 mm		Data Set No.2: d_p = 10.1 mm	
	Error assumed to be in T	Error assumed to be in r	Error assumed to be in T	Error assumed to be in r
$\hat{k}_1$	1.98	1.56	1.90	1.55
$\sigma(\hat{k}_1)$	0.23	0.27	0.26	0.32
$\hat{k}_2$	4.96	3.99	6.73	5.78
$\sigma(\hat{k}_2)$	0.65	0.52	0.76	0.78
ρ	0.84	0.84	0.92	0.94

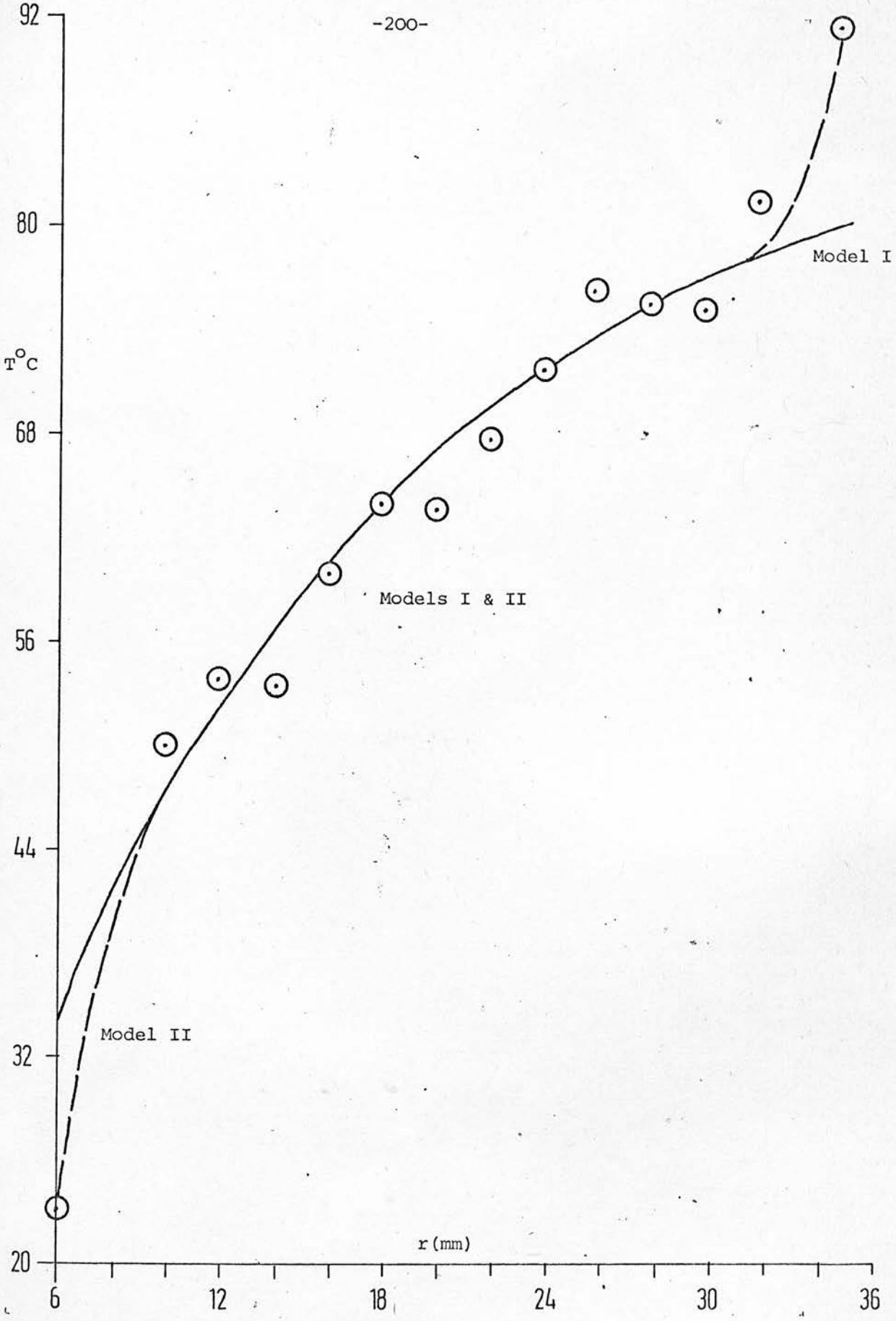

FIGURE 7.10 Least Square Fits Of Models I & II To Data Set No. 1

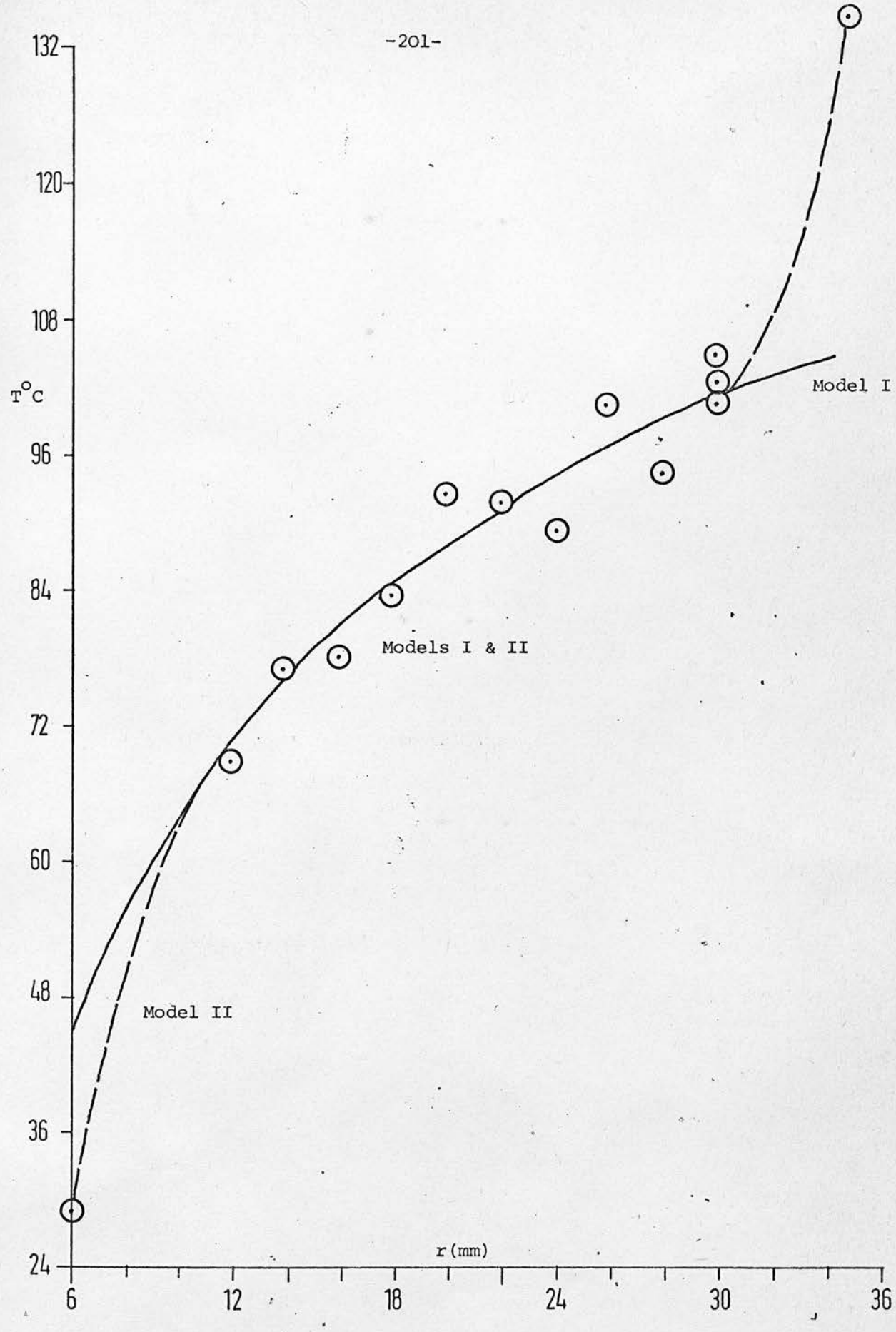

FIGURE 7.11 Least Square Fits Of Models I & II To Data Set No. 2

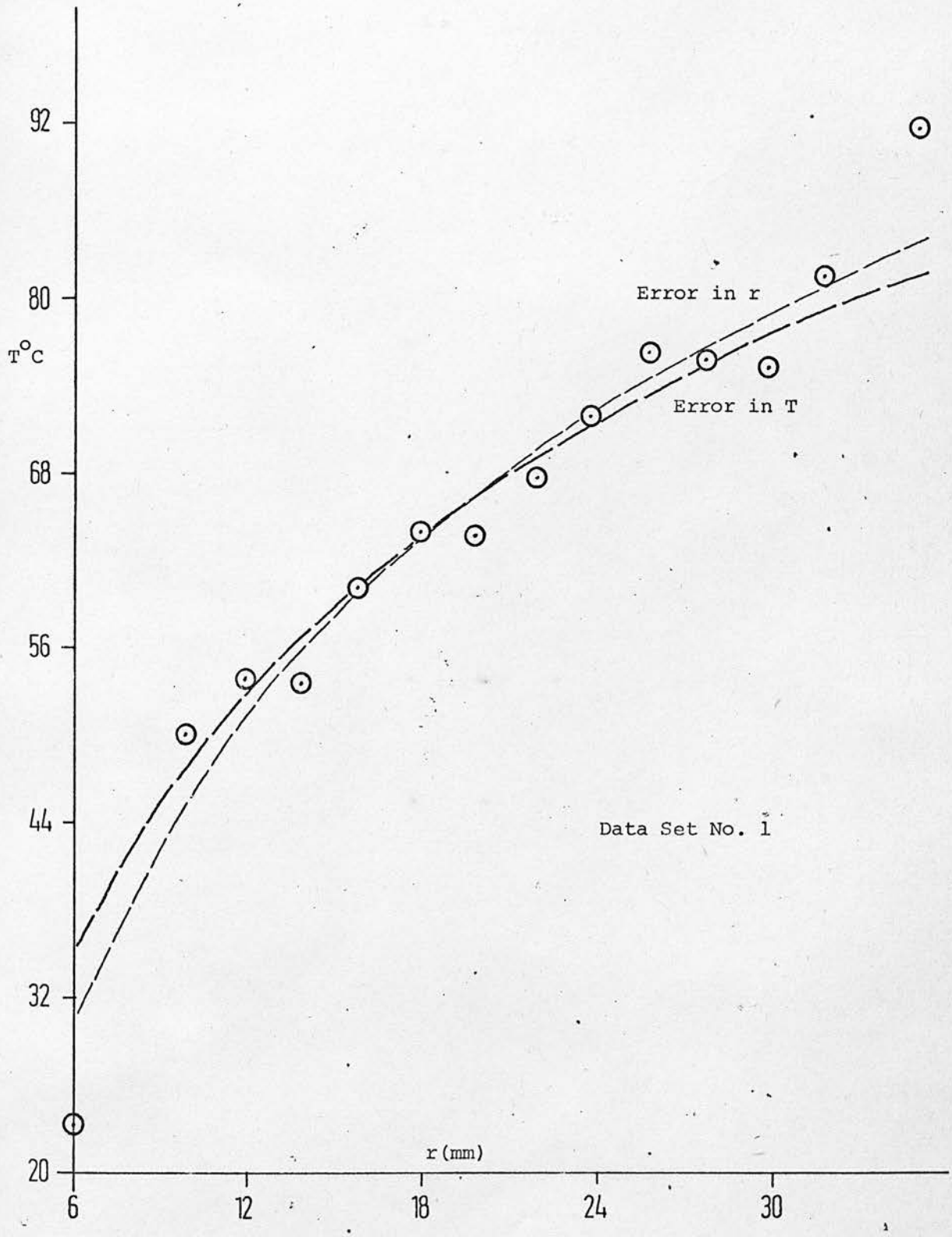

FIGURE 7.12 Fitting Of Model I To Data Set No. 1 Using Different Error Assumptions

The adequacy of the models is tested, first by residual plotting - figure 7.13 is an example - and secondly by an analysis of variance (Table 41) exploiting the replicate thermocouples at r = 30 mm. It should, however, be recalled that the technique used - the F-test - is notoriously sensitive to departures from error Normality, and applies rigorously only to problems which are linear in the parameters.

Table 43: ANOVA for model I (error assumed to be in T: data set no.2)

Source	df	SS	MS	F-ratio
Residual	10	96.1	$9.6 = S_r^2$	
Lack of fit	8	89.3	$11.2 = MS_L$	3.28
Pure error	2	6.8	$3.4 = S_1^2$	(not significant at 5% level)

The F-test provides no evidence on which to reject the model. In figure 7.13 the residuals are plotted against radial position r. The scatter of points appears to be random, and the points appear to lie within a horizontal 'band', indicating that the variance is approximately constant. Similar plots ensue when the residuals are plotted against T.

Comparison of models I and II. Reference to figures 7.10 and 7.11 reveals that Models I and II predict exactly the same result in the central zone of the bed; discrimination between the models demands that temperature measurements be made within a half particle diameter of the wall - a difficult

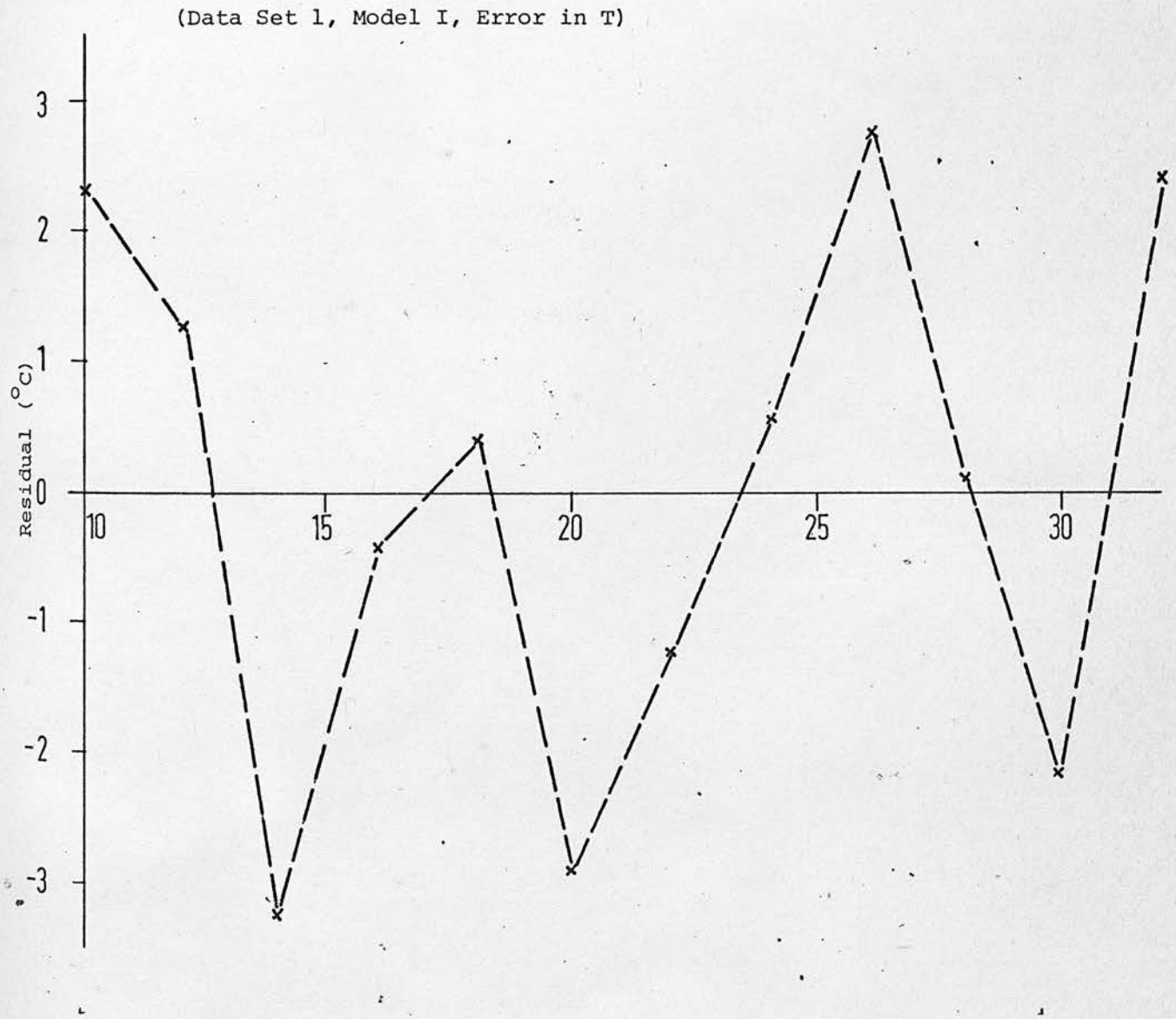

FIGURE 7.13 Residual Versus Radial Position

task in small diameter beds. Thus, on the data to hand, models I and II appear equally acceptable.

However, tables 41 and 42 show that the parameter estimate standard deviations for model II are proportionately smaller than those for model I - good estimates of the Biot numbers are inherently difficult to obtain since they correspond to good estimates of the temperature gradients at the two walls, and no measurements can be made very near the walls. The tables further show that the parameter estimates for model I are more sensitive to the error assumption made than those of model II. These two observations imply that model II is perhaps worthy of greater consideration than it has received in the literature heretofore.

Both models exhibit high parameter cross-correlation coefficients. This finding may indicate a model inadequacy or it may result from the (apparently inevitable) errors of observation. It is not easy to see how to resolve the ambiguity.

N.B. The term 'residual' is used here in the standard statistical sense, of the difference between the observed and predicted values of the variables.

7.8 A study of the voidage structure of the packed bed.

It might reasonably be expected that the variation in voidage (void fraction) with radial position should have considerable influence on point heat transfer rates - indeed, model III of table 40 takes explicit account of this effect. It was therefore decided to measure that voidage variation. The method adopted is to make a physical model of the annular bed, but using steel ball-bearings in place of ceramic spheres. The central tube is perforated at its base, and hot araldite epoxy resin is poured down it, so that the resin level in the bed rises gradually,

displacing all the air from the voids. The resin is then cured in an oven. By removing the solid mass so formed from the mould, and turning off successive layers on a lathe, it should be possible to determine the voidage structure of the bed, as described by Benenati and Brosilow (230).

After considerable effort had been expended, this method was abandoned because of a practical difficulty which arose. When the bed is turned down to below the equator of the outermost layer of balls, there is then a tendency for a ball to leave the matrix in which it is imbedded rather than be turned down further. This means that it is difficult to measure the voidage to a radial position much deeper than $\frac{1}{2}d_p$ from the outer wall of the bed. In an attempt to overcome this difficulty, the balls were softened in a vacuum oven and cleaned ultrasonically, before use, to decrease the resistance of the balls to turning and to improve the steel-resin bond, but to no avail.

An alternative experimental method was then devised. A physical model of the bed is again made, this time using expanded polystyrene spheres and PVC cylinders. The void space in the bed is filled with dyed candle-wax, and, after solidification, the bed is sawn into slices in the radial plane. A photograph is then taken of the surface of each 'cross-section 'slice', and from that photograph it is possible to measure the voidage at different radial positions. The technique contrived for this task is to superimpose on the photograph of the slice a transparency of polar graph paper, so that at any radial position it is easy to measure the fraction of the circumference occupied by void - see figure 7.14.

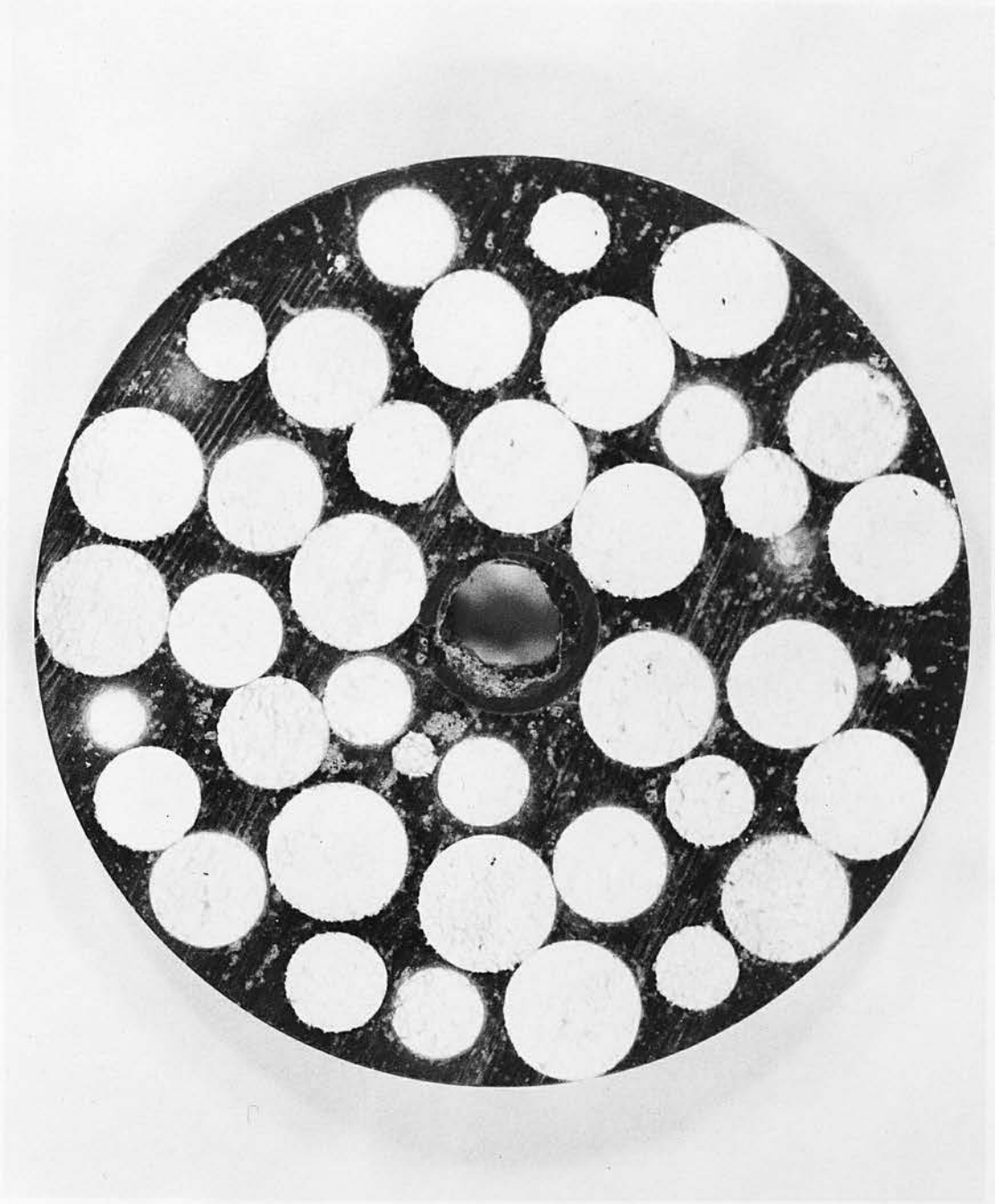

FIGURE 7.14

It should be noted that the voidage measured here is the 'line voidage' (231), whereas other workers have measured 'area voidage' (231) or 'volume voidage' (230). However, it is normal to ignore the differences in these quantities (232).

Experimental details. The model was constructed from materials ready to hand, so that the proportions are approximately, rather than accurately, those of the heat transfer test section packed with the large pellets of table 35. The inner and outer diameters of the annulus are 3.2 and 16.5 cm respectively, and the sphere diameter is 2.5 cm. The bed height is 15 cm, and the photographed slice faces are located 6 and 9.7 cm from the base.

The voidage (or rather, the fraction of solid = 1-voidage) is measured at 23 radial positions equally-spaced across the annular gap, in each of six equal sectors of the slice. The sectors are aligned relative to a reference line marked on the side of the wax model as shown in the diagram below.

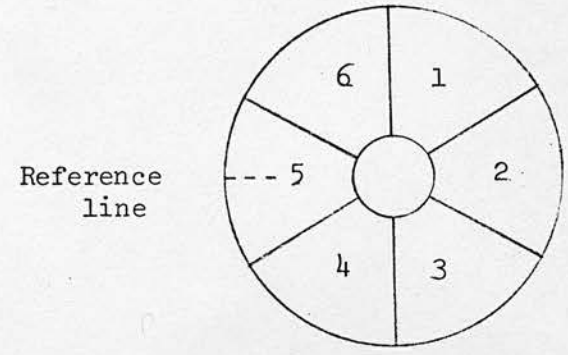

The data reported in tables 44 and 45 show how much the solid fraction can vary with angular position, and the method is also capable of revealing axial variation. Integration of the data shows the faces

Radial Position \ Sector no.	1	2	3	4	5	6	Mean
1	0.332	0.122	0.423	0.000	0.269	0.414	0.260
2	0.596	0.530	0.622	0.153	0.420	0.557	0.480
3	0.786	0.707	0.830	0.358	0.603	0.647	0.655
4	0.883	0.804	0.910	0.418	0.667	0.736	0.736
5	0.900	0.813	0.921	0.452	0.682	0.722	0.748
6	0.848	0.743	0.803	0.387	0.653	0.658	0.682
7	0.667	0. 525	0.642	0.442	0.505	0.683	0.577
8	0.450	0.473	0.333	0.498	0.427	0.654	0.472
9	0.217	0.560	0.267	0.628	0.364	0.476	0.419
10	0.560	0.667	0.612	0.758	0.718	0.555	0.645
11	0.798	0.805	0.793	0.797	0.858	0.606	0.776
12	0.911	0.907	0.889	0.802	0.911	0.607	0.838
13	0.942	0.907	0.900	0.728	0.871	0.549	0.816
14	0.874	0.850	0.867	0.525	0.683	0.347	0.633
15	0.683	0.727	0.720	0.522	0.393	0.117	0.508
16	0.462	0.394	0.575	0.532	0.733	0.367	0.510
17	0.233	0.278	0.600	0.683	0.736	0.543	0.512
18	0.400	0.533	0.789	0.820	0.862	0.663	0.678
19	0.500	0.872	0.887	0.853	0.942	0.742	0.799
20	0.538	0.923	0.933	0.790	0.987	0.778	0.825
21	0.506	0.712	0.950	0.511	0.993	0.772	0.741
22	0.392	0.478	0.875	0.487	0.947	0.694	0.646
23	0.242	0.000	0.660	0.375	0.825	0.542	0.441

Table 44: Solid fraction as a function of radial position

(Slice 7, face located 9.7 cm from the model base)

N.B.: Radial position no. 1 is nearest to the outer wall.

Radial Position \ Sector No.	1	2	3	4	5	6	Mean
1	0.067	0.367	0.286	0.222	0.180	0.380	0.250
2	0.372	0.511	0.433	0.350	0.592	0.589	0.474
3	0.642	0.717	0.619	0.502	0.781	0.838	0.683
4	0.761	0.811	0.683	0.571	0.847	0.928	0.767
5	0.772	0.817	0.653	0.715	0.847	0.950	0.792
6	0.700	0.783	0.767	0.621	0.754	0.887	0.752
7	0.318	0.632	0.769	0.572	0.457	0.683	0.572
8	0.279	0.394	0.584	0.602	0.458	0.375	0.449
9	0.636	0.280	0.667	0.453	0.433	0.000	0.412
10	0.710	0.517	0.684	0.693	0.500	0.387	0.582
11	0.862	0.672	0.622	0.760	0.500	0.596	0.669
12	0.898	0.706	0.465	0.751	0.522	0.675	0.670
13	0.885	0.650	0.340	0.658	0.451	0.716	0.617
14	0.740	0.553	0.567	0.367	0.400	0.665	0.589
15	0.523	0.340	0.770	0.275	0.573	0.483	0.494
16	0.398	0.671	0.940	0.233	0.350	0.583	0.529
17	0.358	0.611	0.895	0.633	0.400	0.550	0.574
18	0.494	0.733	0.722	0.849	0.433	0.617	0.641
19	0.628	0.813	0.583	0.918	0.533	0.667	0.690
20	0.700	0.822	0.567	0.967	0.628	0.683	0.728
21	0.678	0.789	0.450	0.950	0.417	0.700	0.664
22	0.567	0.740	0.000	0.767	0.333	0.673	0.513
23	0.050	0.600	0.000	0.350	0.000	0.608	0.268

Table 45: Solid fraction as a function of radial position (Slice 4, face located 6 cm from the model base).

of slices 4 and 7 to have mean voidages of 0.386 and 0.444 respectively, which tallies tolerably well with the measurement reported in table 35.

The solid fractions of the different sectors and slices are averaged, and shown in figure 7.15, as is the curve which has been fitted to the average values as described in Appendix A3.3. The curve is cyclic, with a peak-to-peak spacing ca d_p.

Clearly this very simple experimental method is capable of revealing much more detail of the structure of the bed than are conventional methods (230, 231, 233).

With the voidage now measured as a function of radial position, and a suitable empirical mathematical representation of the dependence established, it is possible next to examine model III of table 40.

7.9. Testing of Model III

A very simple model to relate k_r to $\varepsilon(r)$ is derived by viewing the point effective thermal conductivity k_r as depending upon the parallel conduction of heat through the solid phase (of effective conductivity k_{es}) and the fluid phase (of effective conductivity k_{ef}). Consequently

$$k_r = k_{ef}\,\varepsilon(r) + k_{es}(1-\varepsilon(r)) \qquad (7.12)$$

Eqn. (7.7) then reduces to

$$T = Twa + (Twb - Twa)\ \frac{\theta(r)}{\theta(r_b)} \qquad (7.13)$$

where

$$\theta(r) \equiv \int_{r_a}^{r} \frac{dr}{r\{(\alpha-1)\varepsilon(r) + 1\}} \qquad (7.14)$$

and

$$\alpha \equiv k_{ef} / k_{es} \qquad (7.15)$$

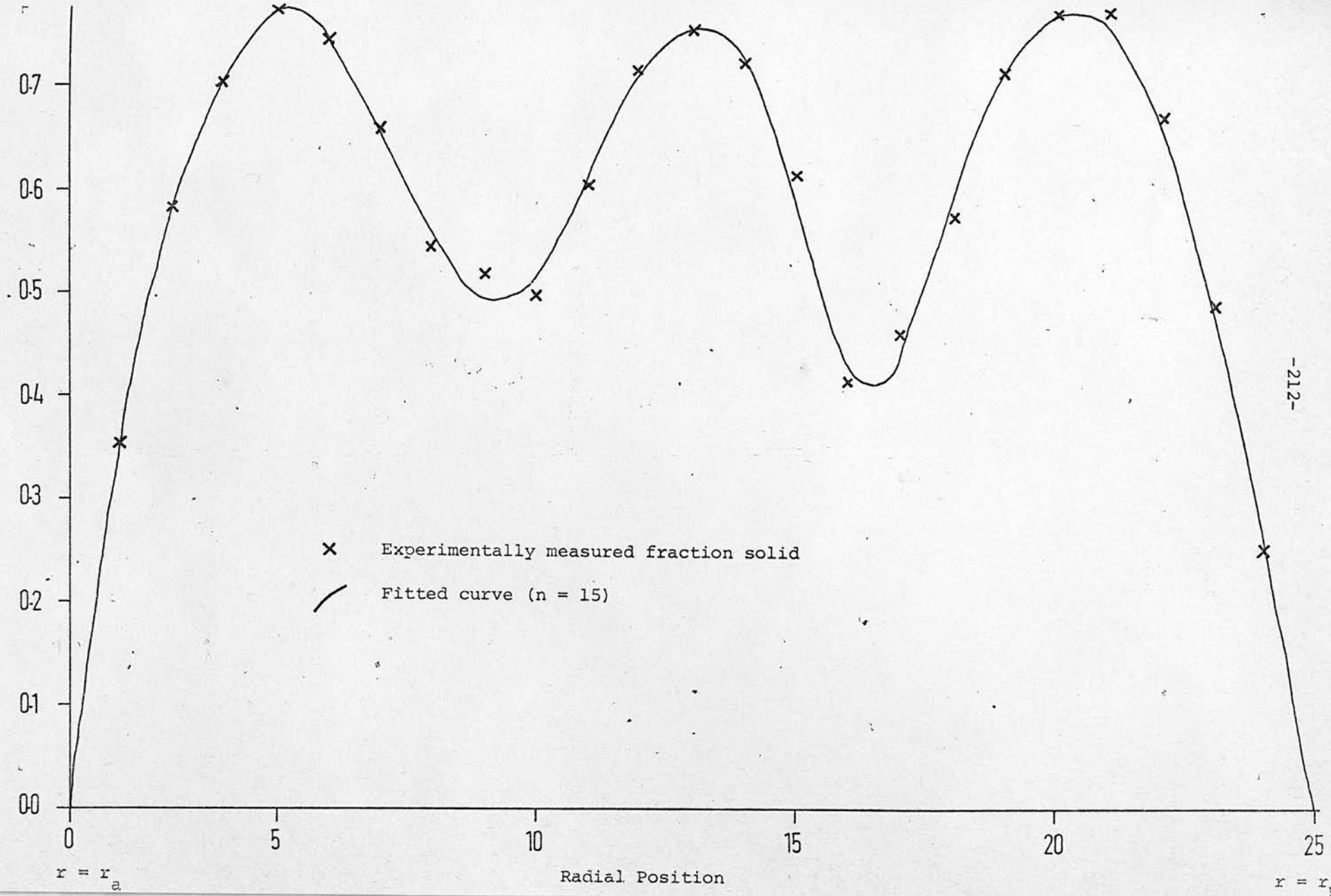

FIGURE 7·15 Solid Fraction As A Function Of Radial Position

Thus the temperature profile depends on only one parameter, α, which may be estimated using a conventional least-squares method, with measurement errors assumed to lie in T rather than r, and with $\varepsilon(r)$ in eqn.(7.14) represented as a trigonometric series in r. The variance of $\hat{\alpha}$ may be calculated as explained in Appendix A3.5.

As remarked earlier, this model is intended to 'explain' the high thermal resistance near the wall as being due to the high voidage there. The model was applied to data set no. 2 (Appendix A3.2), but no physically reasonable value of $\hat{\alpha}$, $0 < \hat{\alpha} < 1$, could be found. Investigation revealed the cause of this failure to be the inability of the model to account for the magnitude of the resistance near the outer wall. Predicted profiles for three different values of α are shown in figure 7.16. A series resistance model fared no better.

It may therefore be inferred that the resistance near the wall cannot be accounted for in such a simple way.

7.10 Summary

Experimentation revealed several features of heat transfer in packed beds studies which appear to have been inadequately considered by previous workers - the importance of measuring the inlet temperature profile, the magnitude of the angular variations of temperature (especially in the flow case), the statistical nature of the apparent experimental errors, and the relationship between the voidage distribution and temperature profile in the bed.

A method has been devised for measuring the voidage distribution, and an empirical mathematical representation for it found. Consequently it has been possible to propose and test a simple model for heat transfer through

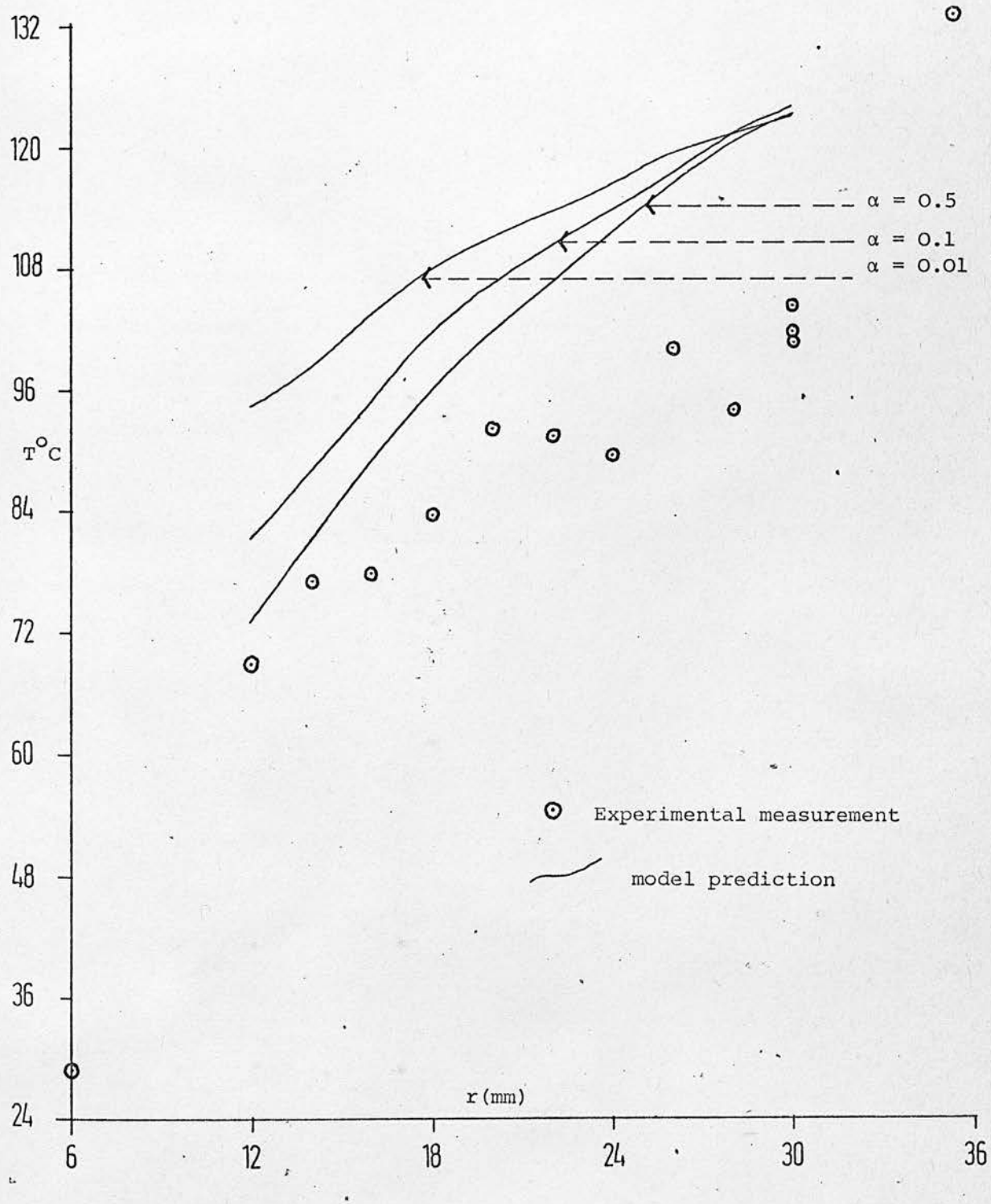

FIGURE 7.16 The Inadequacy Of The Parallel Resistance Model

the stagnant bed. The new model is found wanting. Conventional models (with two, rather than one, adjustable parameters) were found to be adequate, although suffering from the twin disadvantages of (i) exhibiting high parameter cross-correlation and (ii) using parameters with no obvious basis in the physical situation.

The new non-uniform continuum model clearly fails to account adequately for the magnitude of the heat transfer resistance near or at the wall. An obvious adaption of the model which would doubtless improve the 'fit' would be the introduction of wall heat transfer coefficients into the boundary conditions. This, however, would lead to a proliferation of parameters, unless those coefficients could be estimated independently. If they are interpreted as being true film coefficients for heat transfer at the wall, then their values may be established by separate mass transfer experiments using transfer to, or from, a suitably-coated wall in a (physical) model of the heat transfer test section. The heat transfer resistance in the neighbourhood of the wall would then be represented as the combination of two physical effects - the decrease in the bed effective thermal conductivity near the wall due to the increase in voidage, and the true gas/wall heat transfer resistance described by a film coefficient.

The construction of such a model in a step-wise fashion, with independent parameter estimation wherever possible, appears more likely to lead to progress in understanding heat transfer through the bed than does an exercise in estimating many parameters simultaneously.

CHAPTER 8:- Heat Transfer in Beds of Low 'Aspect Ratio'

8.1 Introductory remarks

8.2 The mathematical model

8.3 Experimental work

8.4 Parameter estimation

8.5 Some results

8.6 Tests of model adequacy

8.7 A discussion of the results

8.8 Recommendations for further work.

8.1 Introductory remarks

This chapter reports the results of an experimental investigation of heat transfer in packed beds with gas flow. The purpose of the work is not to establish yet more correlations for the heat transfer parameters, but rather to investigate the adequacy of the conventional mathematical model used to describe the system viz. the two-dimensional quasi-homogeneous model. Thus, it is hoped to establish whether the complex processes of heat transfer in a packed bed of low tube to particle diameter ratio can be adequately represented using "effective" parameters in this 'smooth' continuous quasi-homogeneous model.

It had originally been intended to attempt to discriminate between this model and a composite continuum model (II), but the unexpected amount of scatter on the experimental results suggested that the attempt was unlikely to succeed, and it was consequently abandoned.

8.2 The mathematical model.

Consider gas flowing through a cylindrical or annular packed bed. A quasi-homogeneous model may be derived by using T to represent the temperature of the 'quasi-phase'. Let G(r) be the mass flux in the axial direction at radial position r, C_p be the gas specific heat (assumed to be constant), $k_e(r)$ be the bed-effective radial thermal conductivity, Z be the axial co-ordinate and k_{ea} be the bed-effective axial thermal conductivity.

Then a heat balance yields

$$G(r)C_p \frac{\partial T}{\partial Z} - k_{ea} \frac{\partial^2 T}{\partial Z^2} - \frac{1}{r} \frac{\partial}{\partial r} \{ r\, k_e(r) \frac{\partial T}{\partial r} \} = 0 \qquad (8.1)$$

If axial dispersion is ignored, the equation reduces to

$$G(r)C_p \frac{\partial T}{\partial Z} - \frac{1}{r}\frac{\partial}{\partial r}\{rk_e(r)\frac{\partial T}{\partial r}\} = 0 \qquad (8.2)$$

If $k_e(r)$ is assumed to be independent of r, there follows

$$G(r)C_p \frac{\partial T}{\partial Z} - k_e(\frac{\partial^2 T}{\partial r^2} + \frac{1}{r}\frac{\partial T}{\partial r}) = 0 \qquad (8.3)$$

If plug-flow is assumed, then G(r) is independent of r, and

$$GC_p \frac{\partial T}{\partial Z} - k_e(\frac{\partial^2 T}{\partial r^2} + \frac{1}{r}\frac{\partial T}{\partial r}) = 0 \qquad (8.4)$$

or

$$\frac{\partial T}{\partial Z} - \frac{1}{\beta}(\frac{\partial^2 T}{\partial r^2} + \frac{1}{r}\frac{\partial T}{\partial r}) = 0 \qquad (8.5)$$

where

$$\beta \equiv \frac{GC_p}{k_e} \qquad (8.6)$$

The representation of the heat transfer resistance near the walls is discussed in section 7.6: the boundary conditions used here are -

$$r = r_a; \quad k_e \frac{\partial T}{\partial r} = h_a(T-Twa) \qquad (8.7)$$

$Z > 0;$

$$r = r_b; \quad k_e \frac{\partial T}{\partial r} = h_b(Twb-T) \qquad (8.8)$$

The initial condition used is

$$Z = 0; \quad r_a < r < r_b; \quad T(r) = T_{IN}(r) \qquad (8.9)$$

where $T_{IN}(r)$ is a function of r which is presumed to be known from experimental measurement, as discussed in section 8.2 below.

Equations (8.7) and (8.8) may be written as

$$r = r_a; \quad \frac{\partial T}{\partial r} = \alpha_1(T-Twa) \qquad (8.10)$$

$$r = r_b; \quad \frac{\partial T}{\partial r} = \alpha_2(Twb-T) \tag{8.11}$$

where

$$\alpha_1 \equiv \frac{h_a}{k_e}; \quad \alpha_2 \equiv \frac{h_b}{k_e} \tag{8.12}$$

Dimensionless groups. The dimensional groups β, α_1, α_2 in the above equations bear simple relations to useful dimensionless groups. Thus, the Peclet number may be defined as

$$Pe \equiv \frac{GC_p d_p}{k_e} = \beta d_p \tag{8.13}$$

and Biot numbers may be defined as (see eqn(7.3))

$$Bi_a \equiv \alpha_1 r_a; \quad Bi_b \equiv \alpha_2 r_b \tag{8.14}$$

Note that the definition of Peclet number corresponds to the definition usual for packed beds, whereas the Biot numbers differ somewhat from the usual definition (i.e. hd_p/k_e).

Solution of the model equations. Following Carslaw and Jaeger (228), it is possible to derive a solution to eqns(8.5) and (8.9)-(8.11). It may be written as (see Appendix A3.3)

$$T(r,Z) = T_\infty(r) + \sum_{n=1}^{\infty} A_n R_n \exp\left(-\frac{\lambda_n^2 d_p Z}{Pe}\right) \tag{8.15}$$

It consists of two components: an infinite series which decays with increasing Z, and an 'asymptotic solution' - $T_\infty(r)$ - which holds as $Z \to \infty$. This asymptotic solution is identical to eqns.(7.1)-(7.3), and involves only Bi_a and Bi_b, and not Pe.

8.3 Experimental work

The apparatus and procedures used are described in chapter 7. The data analysed below were obtained using the 'large pellets' of table 35, the six-armed cross of figure 7.3 and test section number 1 of table 34. Table 46, shows the bed depths and mass fluxes used,

and the corresponding values of Reynold's number, $Re_p \equiv {}^{Gd_p}/_{\mu}$, where μ is the viscosity of air. The value of μ used for the calculation of Re_p is that appropriate to air at 120°C i.e. ∿Twb:

$\mu = 22.84 \times 10^{-6}$ kg/ms (234).

Table 46. Experimental conditions

Series Number	G(kg/m^{2}s)	Re_p	Bed depths used: Z(mm)
12	0.2644	117	52.5
7	0.4231	187	85
11	0.5183	229	118
8	0.6664	295	188.5
10	0.8197	362	295
9	1.0054	445	

The experimental temperature measurements are listed in the tables of Appendix A4. The form of a typical temperature profile and the scatter due to angular temperature fluctuations are shown in figure 8.7.

8.4 Parameter Estimation.

As reported in chapter 7, 'unweighted least squares' is a reasonable choice of estimation method. Its implementation will now be described.

a) A method has to be devised to deal with the variation of wall temperature from run to run (i.e. bed depth to bed depth) in the same series (i.e. for the same Re_p). The solution adopted is to calculate the sum-of-squares objective function in terms of dimensionless temperature (eqn. 7.8).

b) A way must be found to represent the inlet temperature profile. The procedure used is to take all the inlet temperature profiles for a given series, reduce them to dimensionless form, and 'fit' a low-order polynomial through them. The algorithm used is described in Appendix A3.4. As shown in figure A3.6.1, the 'fit' obtained is rather approximate, but is perhaps adequate for its purpose. It should be noted that many other workers have made no attempt to measure their inlet temperature profile, but appear merely to have assumed it to be uniform.

c) Before an iterative search procedure can be used to locate the minimum of the sum-of-squares function, the model equations must be solved to provide 'predicted values'. The analytical solution reported above was not used, in part because of the disadvantages described in Appendix A3.3. To overcome these difficulties, a numerical method is used, which has the additional advantage that it can treat the case of G and k_e being functions of r. The Crank-Nicolson finite difference scheme was chosen - see Appendix A3.5. The nodes of the scheme do not, in general, coincide with the observation locations, and so a two-dimensional linear interpolation is performed to obtain the 'predicted values'. The sum of squares function is an unweighted sum taken over all axial, radial and angular positions.

d) An iterative search method requires starting values. Starting values for Bi_a and Bi_b are obtained by analysing the radial temperature profiles measured at the greatest bed depths, on the assumption that this corresponds approximately to the asymptotic profile, $T_\infty(r)$.

The method used in this analysis is described in chapter 7. Starting values for k_e are obtained using the weighted residual method developed in chapter 6.

e) The search method chosen is that of Powell (160), as implemented in ERCC library routine 18.420.504. This method was chosen because it was expected to converge faster than the simplex method used hitherto (ERCC library routine 18.420.505), from the hopefully accurate starting values. In fact, the starting values were not particularly close approximations to the estimates eventually obtained, but nevertheless fell within the convergence region of the algorithm.

f) An approximate linearised analysis is performed on the experimental data to provide confidence intervals for the parameter estimates (Appendix A3.6). This step has been omitted by previous workers.

8.5 Some results.

The data for each series were examined. Each analysis involved 420 measurements (5 depths, 6 angular orientations and 14 radial locations, of which three are replicates), and three adjustable parameters (h_a,h_b,k_e). The predictions are compared with the observations in figures 8.1 to 8.6 - for clarity, only the angular-mean dimensionless temperature is plotted for each radial position and bed depth. On a gross scale, there is clearly a fair measure of agreement between the observed and predicted values.

A more detailed inspection suggests certain model inadequacies. On figure 8.1, for instance, the predicted values lie fairly systematically below the measured values for the first bed depth, above for the second

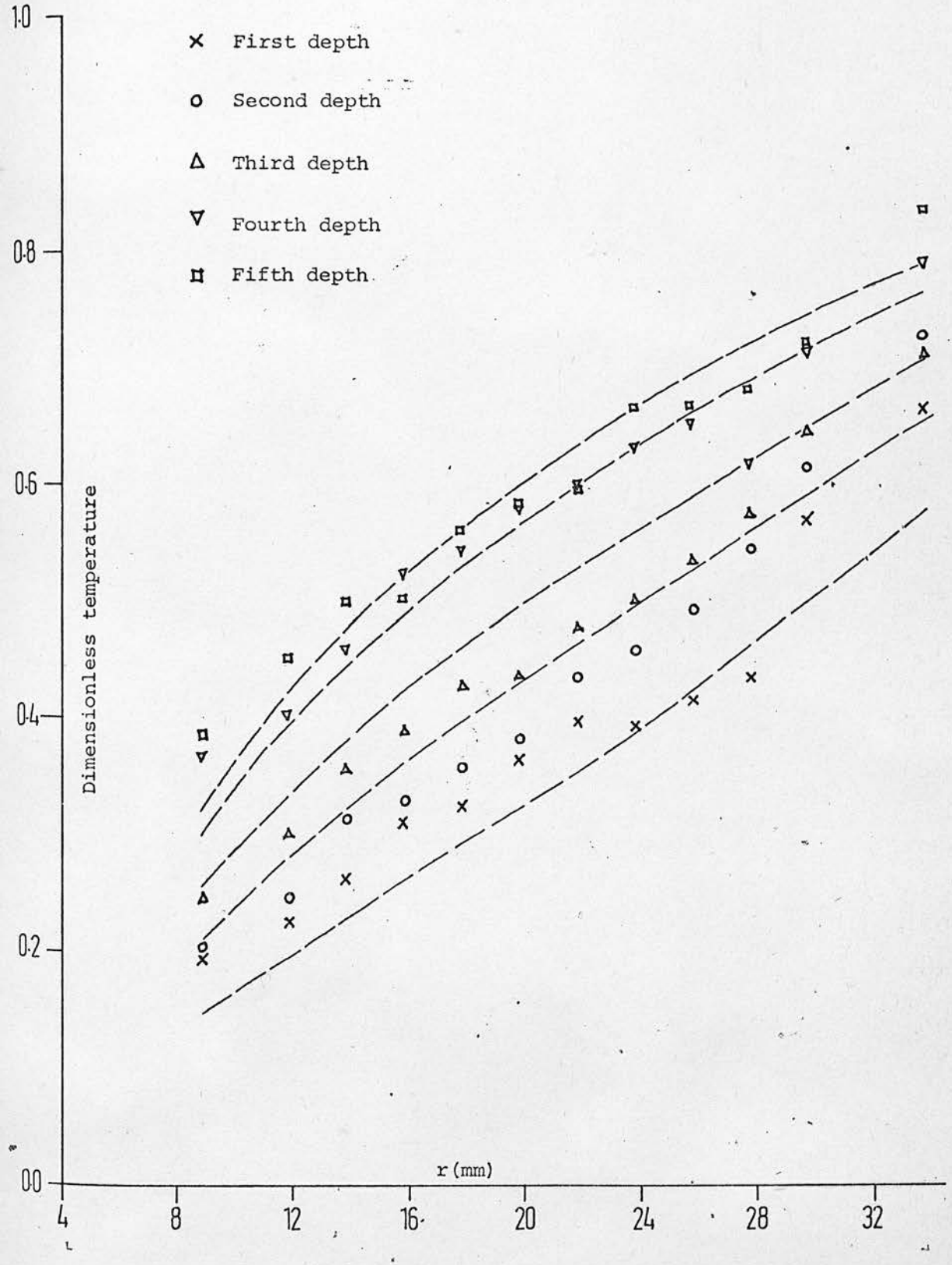

FIGURE 8·1 Fit To All The Data From Series 7

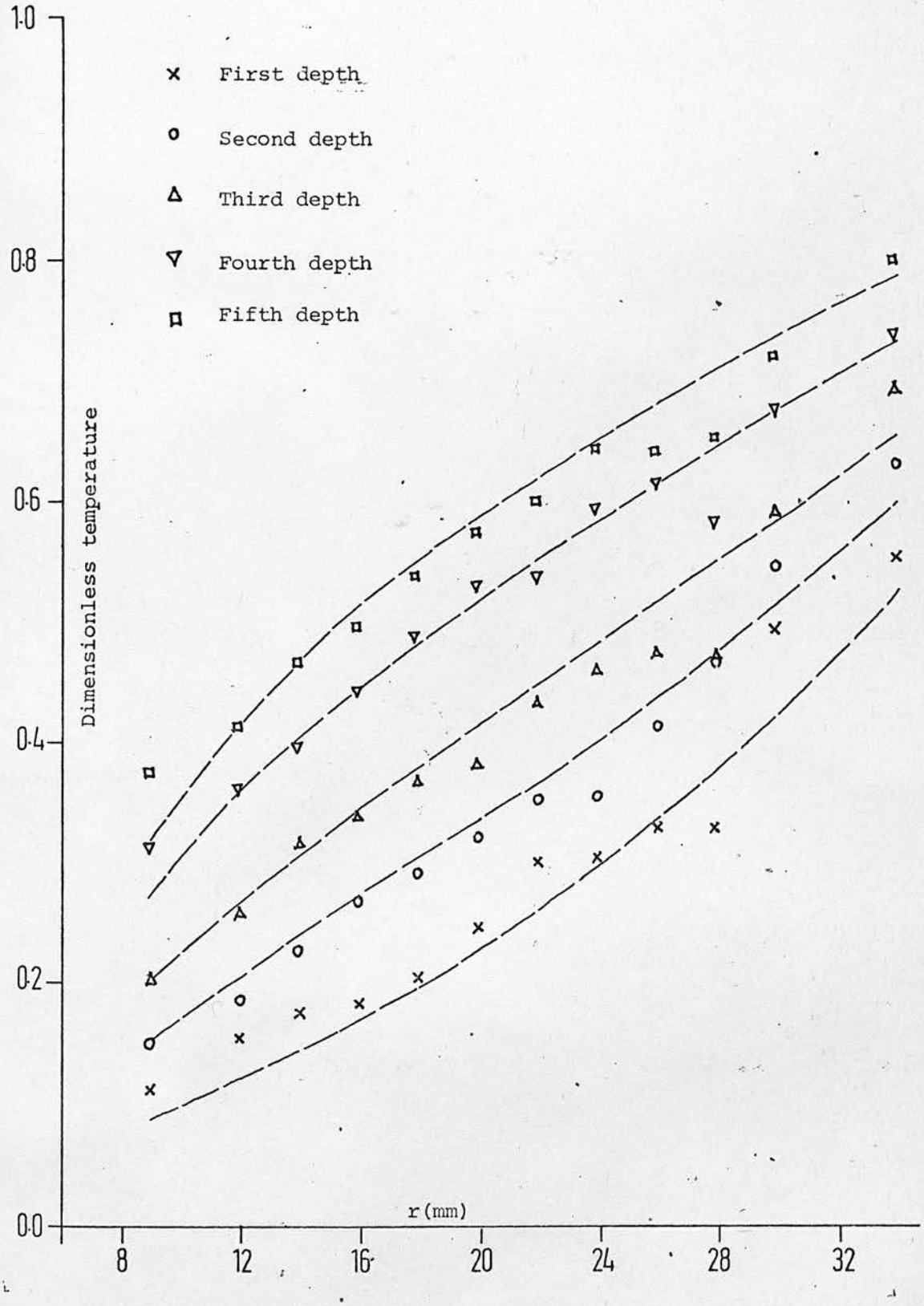

FIGURE 8·2 Fit To All The Data From Series 8

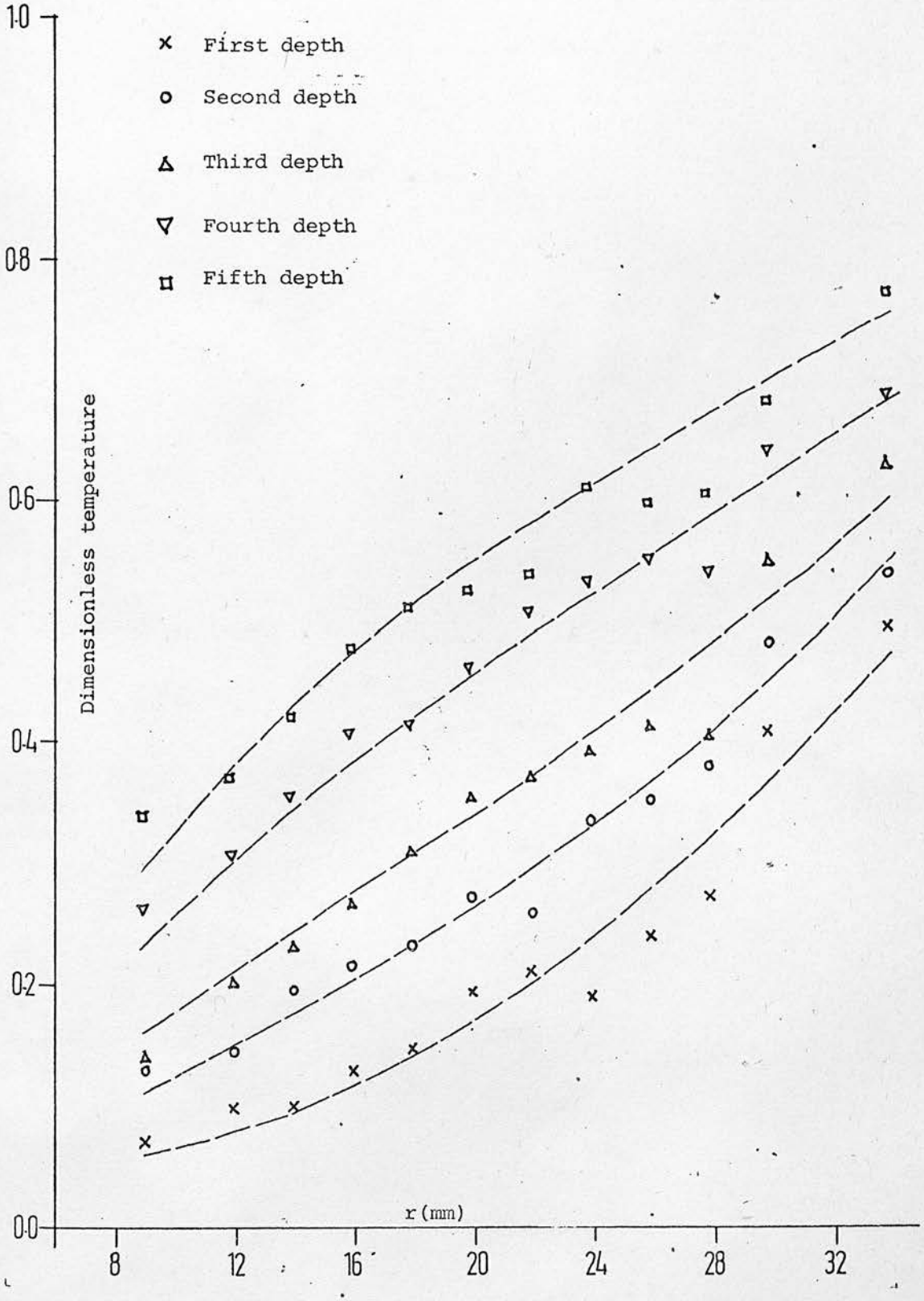

FIGURE 8·3 Fit To All The Data From Series 9

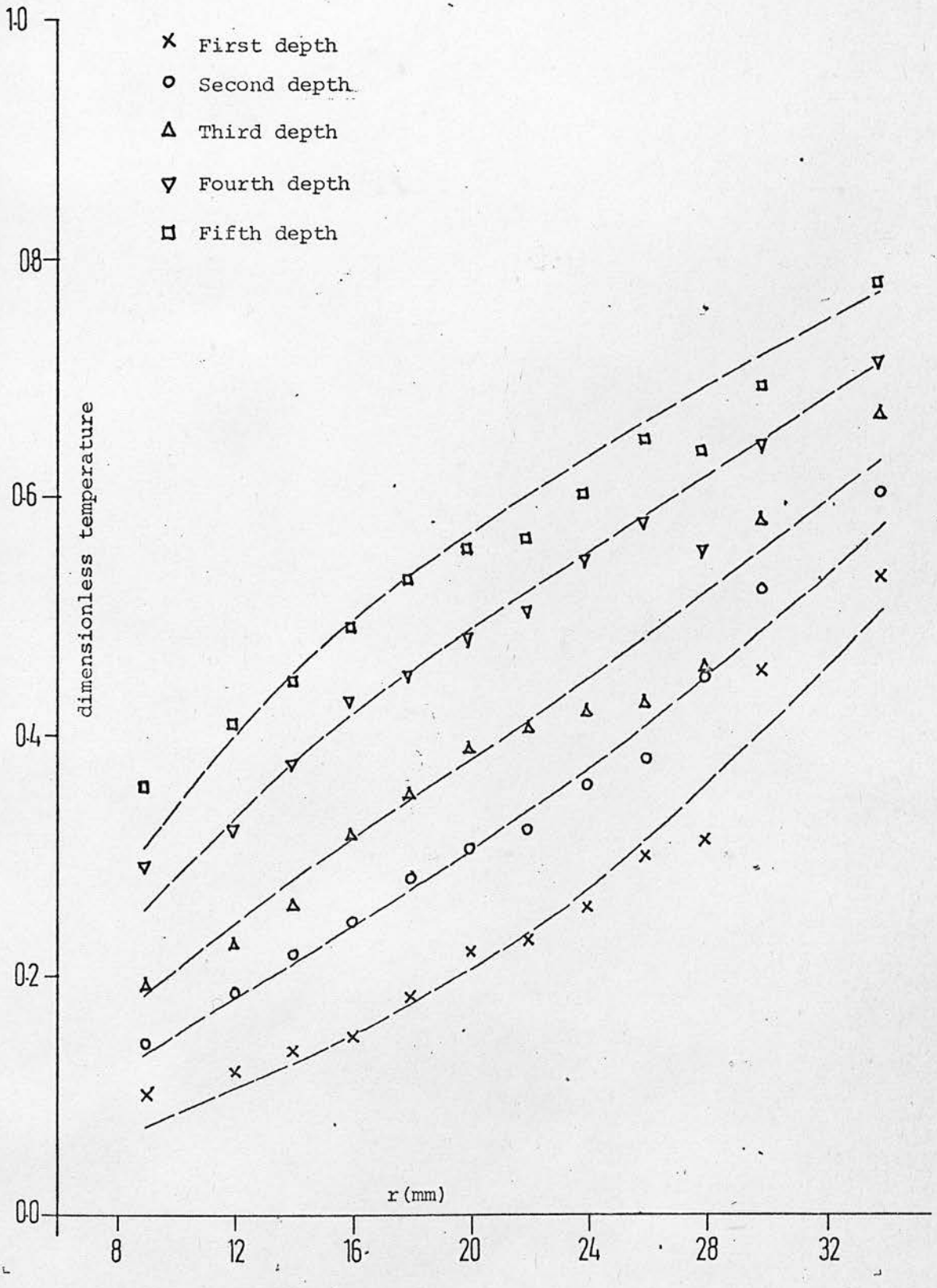

FIGURE 8·4 Fit To All The Data From Series 10

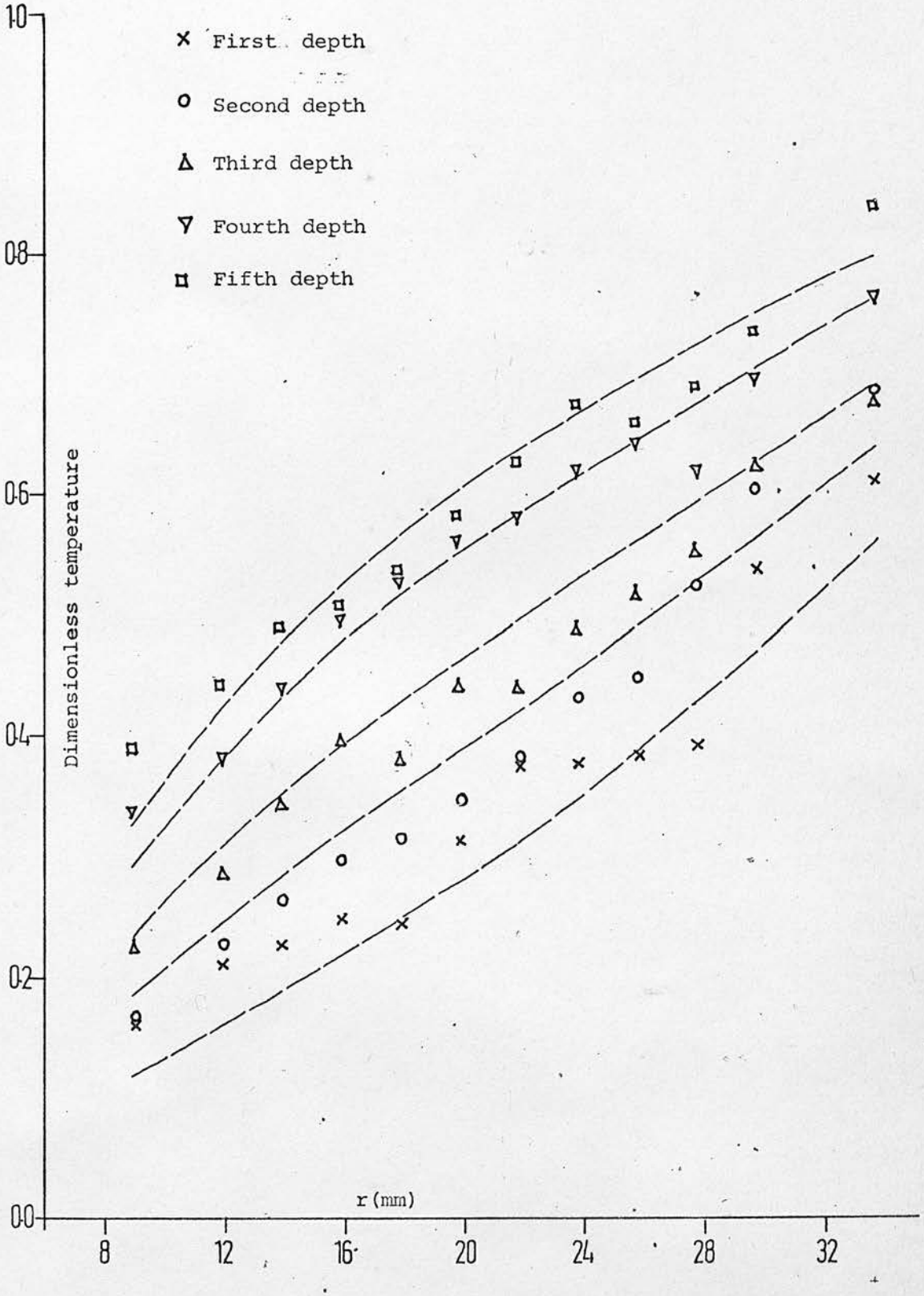

FIGURE 8.5 Fit To All The Data From Series 11

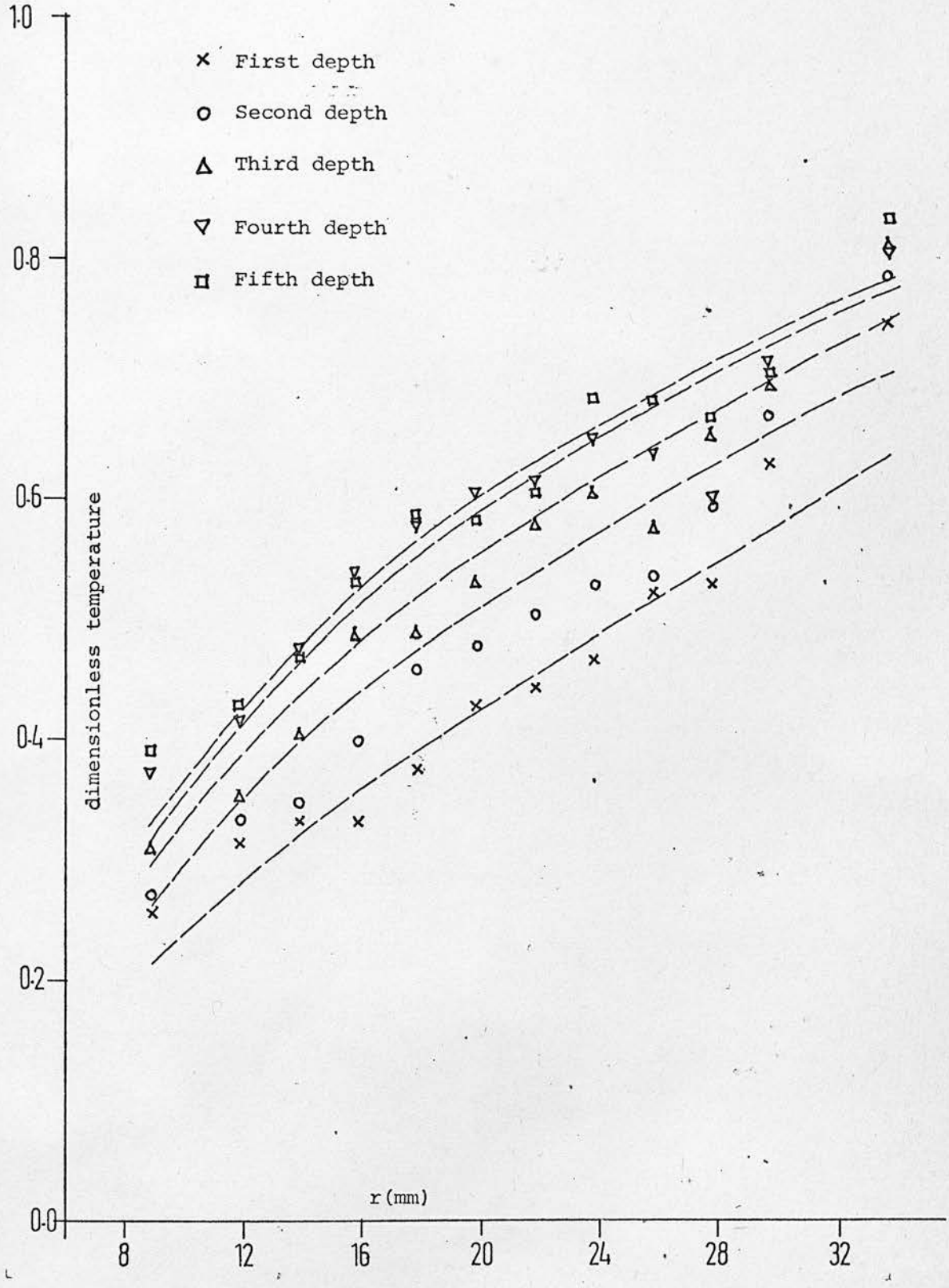

FIGURE 8·6 Fit To All The Data From Series 12

and third, and below for the fourth. At the fifth bed depth there is no such consistent pattern. Perhaps one might discount the imperfect fit at the first bed depth, since the fit there will be most affected by the uncertainty in the inlet temperature profile, but the imperfections at the other bed depths merit attention. On figures 8.2 to 8.5 the inadequacies are much less marked, but for series 12 (figure 8.6) the predictions usually lie above the observations for depths two and three, and below for depth five. In summary, there is some evidence of model inadequacy for the two series (7 and 12) with the lowest gas flow-rates.

Consider next the radial distribution of discrepancies. There is a consistent indication that the predictions are unable to reproduce a 'hump' or 'kink' in the observed profile in the neighbourhood of the outer wall. There is also some suggestion of a 'hump' near the inner wall - see the sketch below.

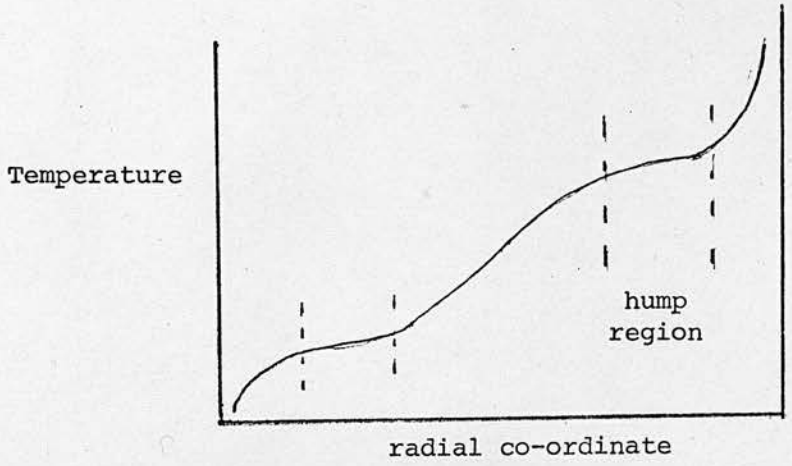

A similar hump (near the outer wall of a cylindrical bed) has been reported by Marivoet (220) and by De Wasch and Froment (218).

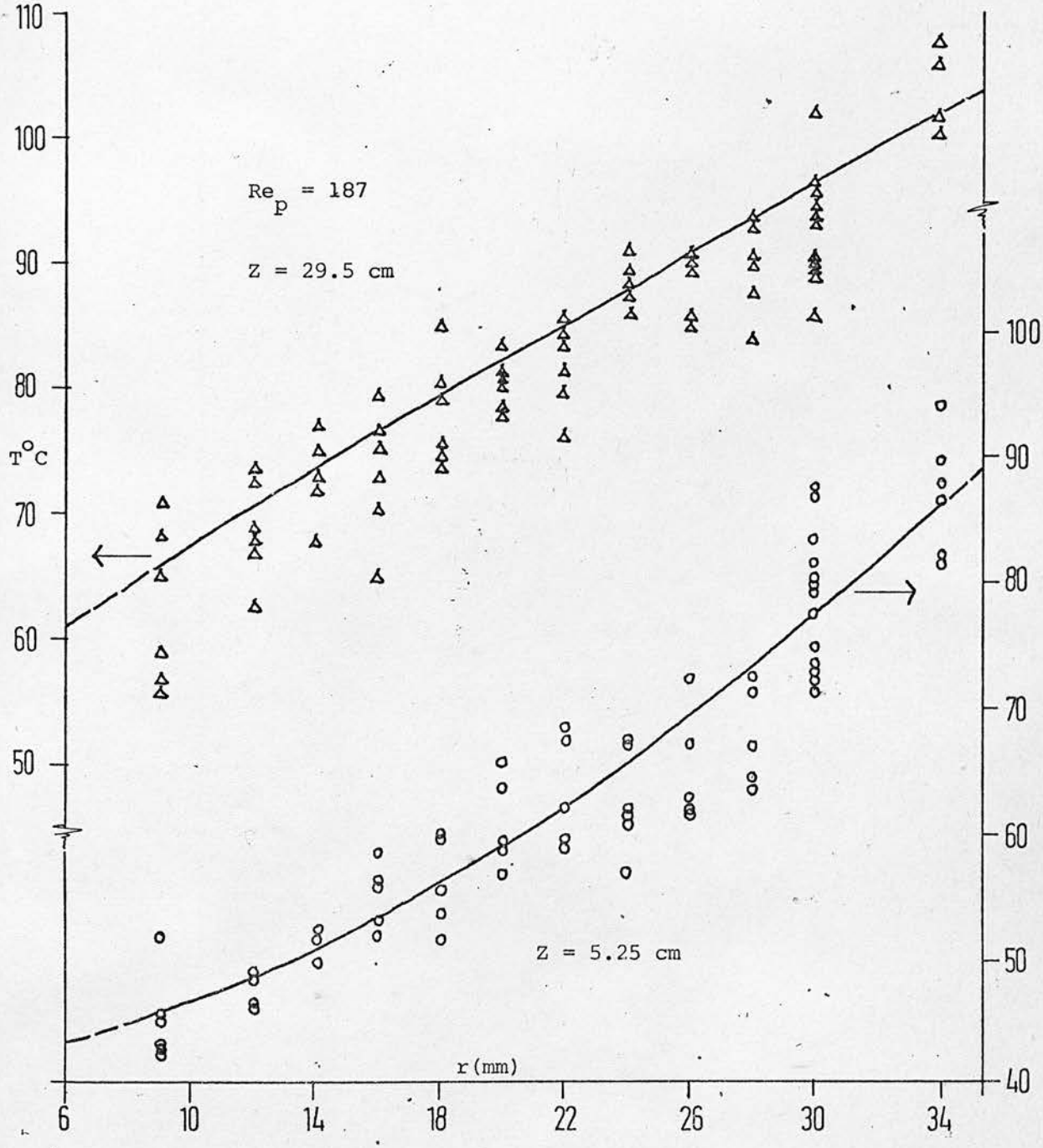

FIGURE 8.7 Comparison Of Angular Temperature Measurements With The 'Best Fit' Predictions

Table 47: Parameter estimates obtained by least squares

Series	12	7	11	8	10	9
Re_p	117	187	229	295	362	445
G	0.2644	0.4231	0.5183	0.6664	0.8197	1.0054
$\hat{Bi}_a$	1.830	1.866	1.815	1.759	1.730	1.689
$\hat{Bi}_b$	1.581	1.778	1.968	1.967	1.946	1.957
$\hat{Pe}$	1.674	2.721	3.385	4.096	4.670	5.388
$\hat{h}_a$	486	488	468	482	511	531
$\hat{h}_b$	71.4	79.1	86.2	91.6	97.7	104.5
$\hat{k}_e$	1.59	1.57	1.55	1.64	1.77	1.88
$\sigma(\hat{h}_a)$	89.2	100	102	109	131	163
$\sigma(\hat{h}_b)$	5.18	4.54	4.64	4.28	4.58	5.07
$\sigma(\hat{k}_e)$	0.201	0.175	0.161	0.151	0.166	0.182
$\sigma(\hat{h}_a)/\hat{h}_a$	0.183	0.205	0.219	0.226	0.256	0.308
$\sigma(\hat{h}_b)/\hat{h}_b$	0.072	0.057	0.054	0.047	0.047	0.048
$\sigma(\hat{k}_e)/\hat{k}_e$	0.126	0.112	0.104	0.092	0.093	0.097
$\rho(\hat{h}_a, \hat{k}_e)$	0.356	0.347	0.382	0.413	0.458	0.476
$\rho(\hat{h}_a, \hat{h}_b)$	0.791	0.685	0.592	0.530	0.510	0.456
$\rho(\hat{k}_e, \hat{h}_b)$	0.449	0.161	0.003	-0.063	-0.055	-0.101

The parameter estimates are shown in table 47. The marginal standard deviations reported show that the inner wall heat transfer coefficient is poorly determined, that the effective conductivity is established rather better, and the outer wall coefficient better yet. The likely cause of the outer wall coefficient being better determined than the inner is that a greater number of measurements are concentrated near the outer wall than near the inner.

The parameter cross correlation coefficients are most consistently high for $(\hat{h}_a, \hat{h}_b)$ and appear to be smallest for $(\hat{k}_e, \hat{h}_b)$.

8.6 Tests of model adequacy

Some comments on model adequacy were made in section 8.5. This topic is now explored more fully. First, a formal "goodness-of-fit" analysis may be performed. The F-test is used, subject to the qualifications expressed in section 7.7. The test leads to rejection of the model as inadequate for all the series - a typical calculation is shown in table 48.

Table 48: ANOVA for SERIES 9

Source	d.f.	ss	MS	F ratio
Residual	417	0.992		
Pure Error	350	0.667	1.91×10^{-3}	Ratio = $\frac{4.85}{1.91} = 2.545$
Lack-of-fit	67	0.325	4.85×10^{-3}	$F(67,350,0.95) \doteq F(60,\infty,0.95) = 1.32 < 2.545$ $\therefore$ The model is inadequate at the significance level $\alpha = 0.05$

Correlation of parameters with bed depth. The model may be further tested by performing a 'depth-by-depth' analysis i.e. by estimating parameter values using the inlet temperature profile and the bed temperatures at only one chosen bed depth. If the model were adequate then the estimates so obtained would be substantially independent of the bed depth used or, at least, their variation would be random. Figures 8.8, 8.9 and 8.10 and table 49 display the results of such calculations. It will be seen that $\hat{h}_b$ and $\hat{k}_e$ generally decrease systematically with bed depth. De Wasch and Froment (218) observed similar trends.

This analysis implies that the model is inadequate, a conclusion which has been confirmed with a 'layer-by-layer' analysis, using the inlet profile and pairs of adjacent bed depths.

Table 49: Parameter estimates from a depth-by-depth analysis of the measurements of SERIES 7

Depth number	1	2	3	4	5
$\hat{k}_e$	1.302	0.849	0.869	1.028	0.503
$\sigma(\hat{k}_e)$	0.301	0.172	0.204	0.516	0.178
$\hat{h}_a$	59.6	80.0	124.7	140.7	41.93
$\sigma(\hat{h}_a)$	209.6	148.4	130.3	148.3	46.31
$\hat{h}_b$	99.4	84.2	66.67	61.84	43.01
$\sigma(\hat{h}_b)$	12.2	10.4	5.86	7.38	5.37
$\rho(\hat{h}_a,\hat{k}_e)$	0.835	0.833	0.879	0.948	0.923
$\rho(\hat{h}_a,\hat{h}_b)$	-0.128	-0.227	-0.059	0.682	-0.157
$\rho(\hat{k}_e,\hat{h}_b)$	-0.410	-0.532	-0.368	0.491	-0.447

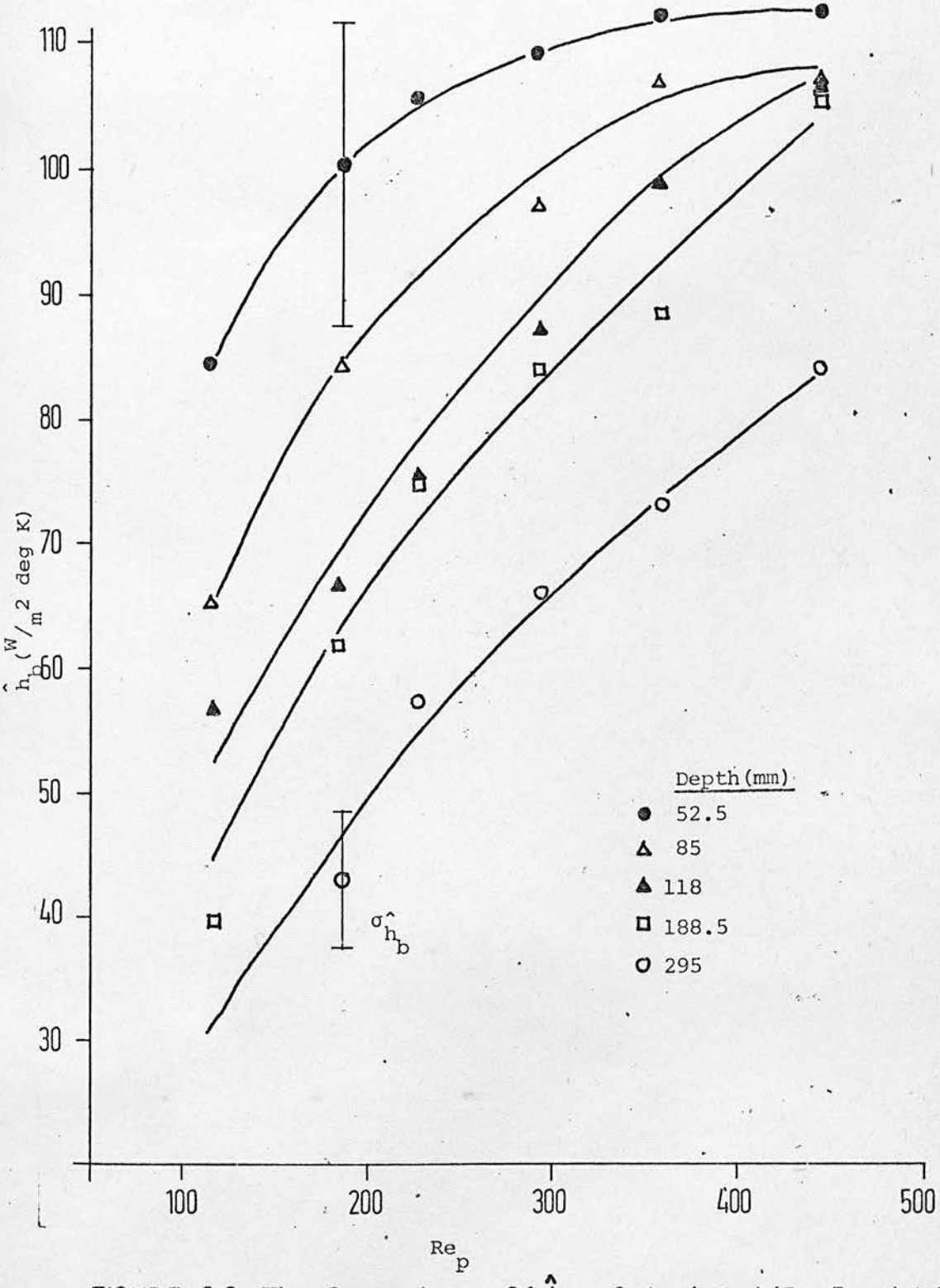

FIGURE 8.8 The Dependence Of $\hat{h}_b$, Calculated 'By Depth', On Re_p

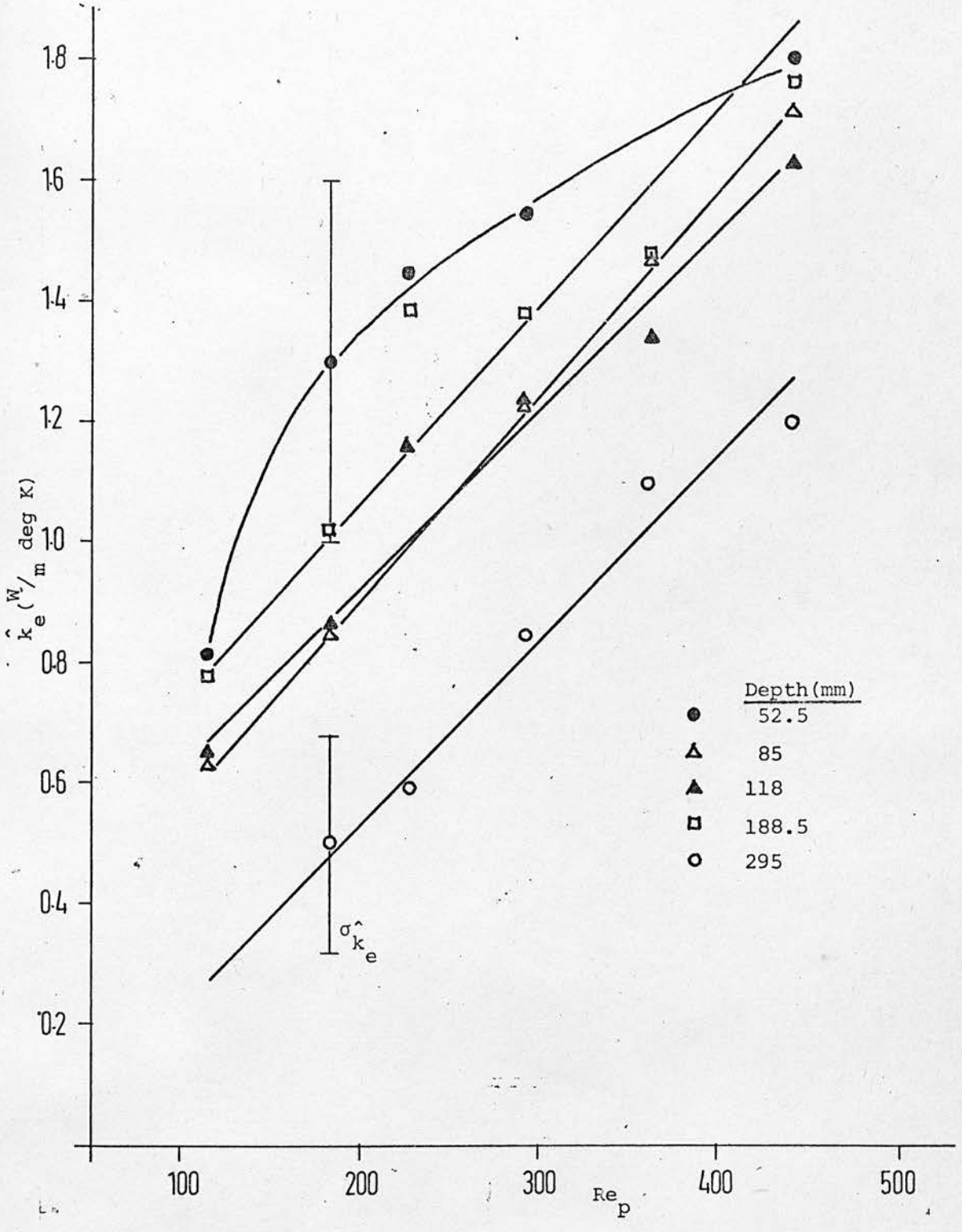

FIGURE 8·9 The Dependence Of $\hat{k}_e$, Calculated 'By Depth', On Re_p

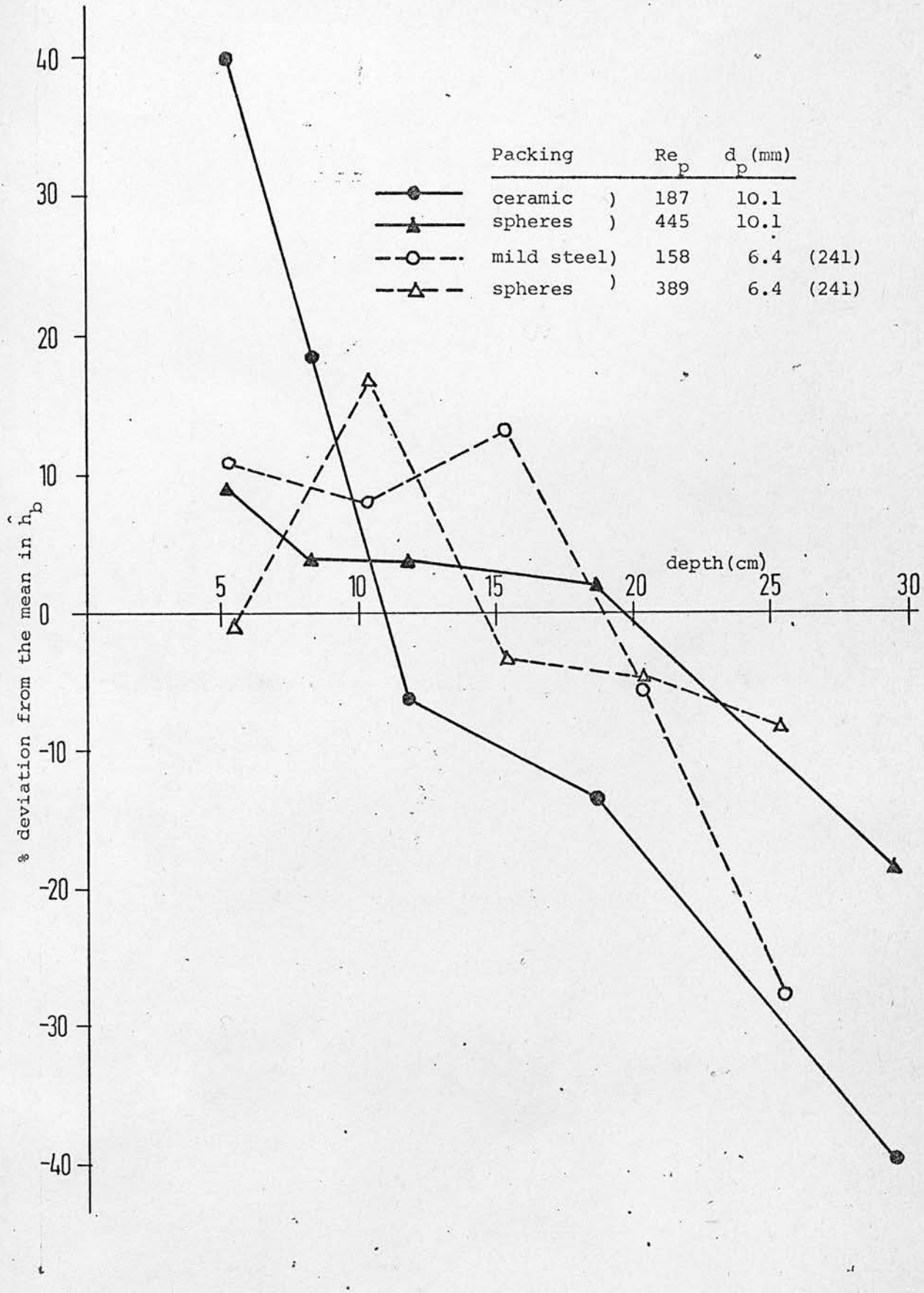

FIGURE 8.10 Variation Of $\hat{h}_b$ From A 'Depth By Depth' Analysis With Bed Depth

Table 50: Parameter estimates obtained by treating separately the measurements for each angular orientation

Series	12	7	11	8	10	9
Re_p	117	187	229	295	362	445
G	0.2644	0.4231	0.5183	0.6664	0.8197	1.0054
$\bar{\hat{h}}_a$	491	497	501	502	513	662
$\bar{\hat{h}}_b$	71.7	79.4	86.6	91.8	98.0	105
$\bar{\hat{k}}_e$	1.61	1.58	1.55	1.65	1.77	1.91
$\sigma(\hat{h}_a)$	61.6	93.5	175	153	115	449
$\sigma(\hat{h}_b)$	4.19	5.37	8.23	6.09	7.87	12.0
$\sigma(\hat{k}_e)$	0.235	0.248	0.132	0.139	0.133	0.240
$\rho(\hat{h}_a,\hat{k}_e)$	-0.008	-0.026	-0.480	0.599	0.797	0.943
$\rho(\hat{h}_a,\hat{h}_b)$	0.628	0.522	0.618	-0.194	0.173	0.200
$\rho(\hat{h}_b,\hat{k}_e)$	0.102	0.346	0.155	-0.025	0.620	0.377

One further test of the model has been performed. Sets of parameter estimates may be obtained by treating separately the data from each angular orientation, and, from these sets, parameter estimates, their marginal standard deviations and cross-correlation coefficients can be calculated. If the linear confidence analysis is valid and if the errors all follow the same Normal distribution, then the estimates so derived-shown in Table 50 - should agree with those presented in Table 47. The agreement is acceptable, suggesting again that the error assumptions are adequate and thus that the lack of fit may be attributed to model inadequacy.

8.7 A discussion of the results

Although the model has been shown to be inadequate, it is worthwhile discussing the results and comparing them with those of other workers.

i) Angular temperature variations. Many workers have commented on the existence of angular temperature variations, but none appear to have reported their magnitudes, nor to have incorporated them into a parameter confidence analysis. They have instead presented angle-averaged temperatures as a function of radial position. The averaging, of course, 'smooths' the readings considerably - transforming figure 7.7 to figure 8.11.

Analysis of the data of this work using angle-averaged temperatures produces parameter point estimates, and cross-correlation coefficients, little different from those obtained by the full analysis reported above, but the calculated parameter marginal standard deviations are markedly smaller, as shown in Table 51.

Table 51: Parameter marginal standard deviations using angle-averaged temperatures

Re_p	117	187	229	295	362	445
$\sigma(\hat{h}_a)$	63.7	74.2	72.2	71.2	79.3	93.8
$\sigma(\hat{h}_b)$	3.70	3.32	2.93	2.80	2.78	2.91
$\sigma(\hat{k}_e)$	0.143	0.128	0.113	0.098	0.100	0.105

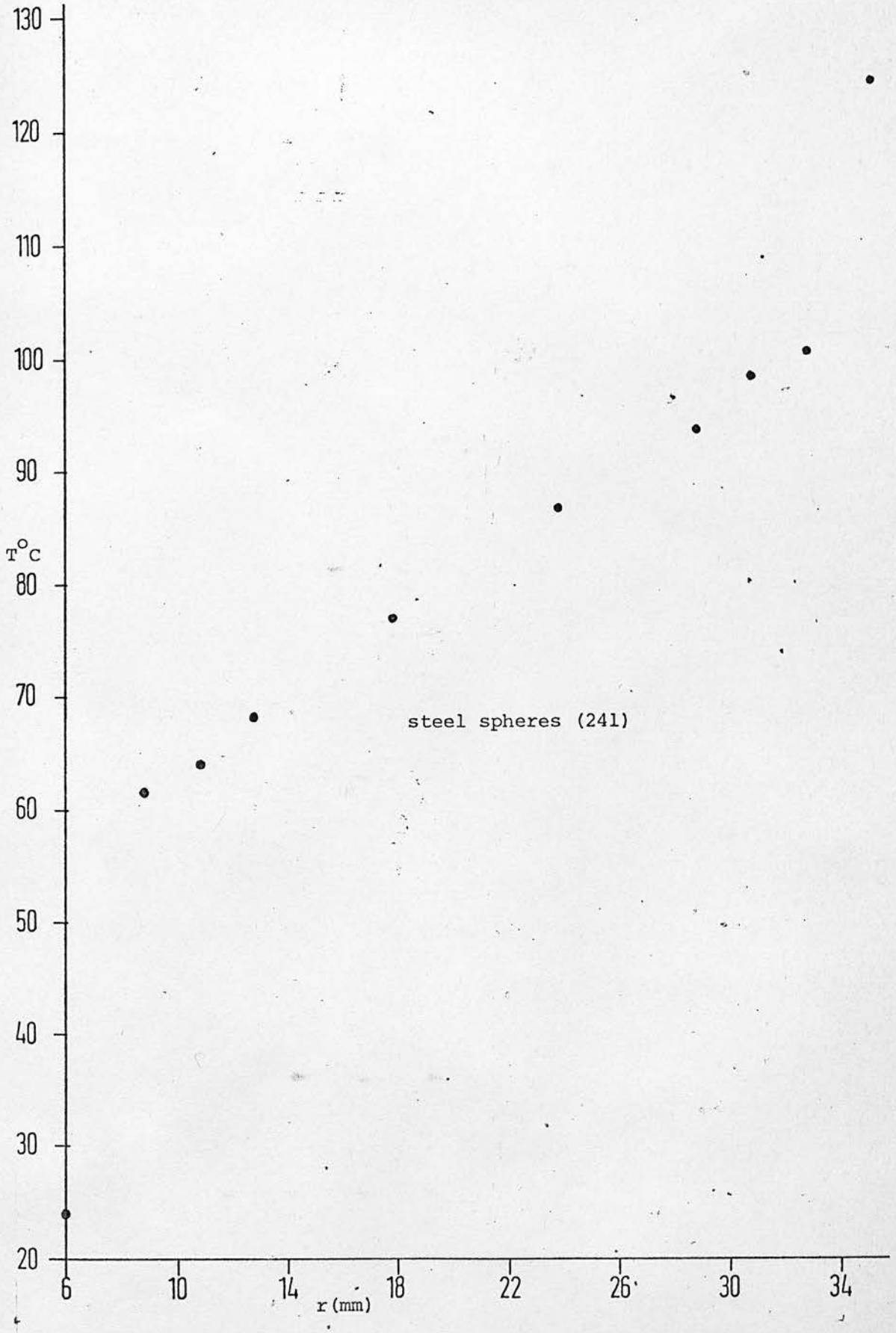

FIGURE 8·11 Mean Radial Temperature As A Function Of r

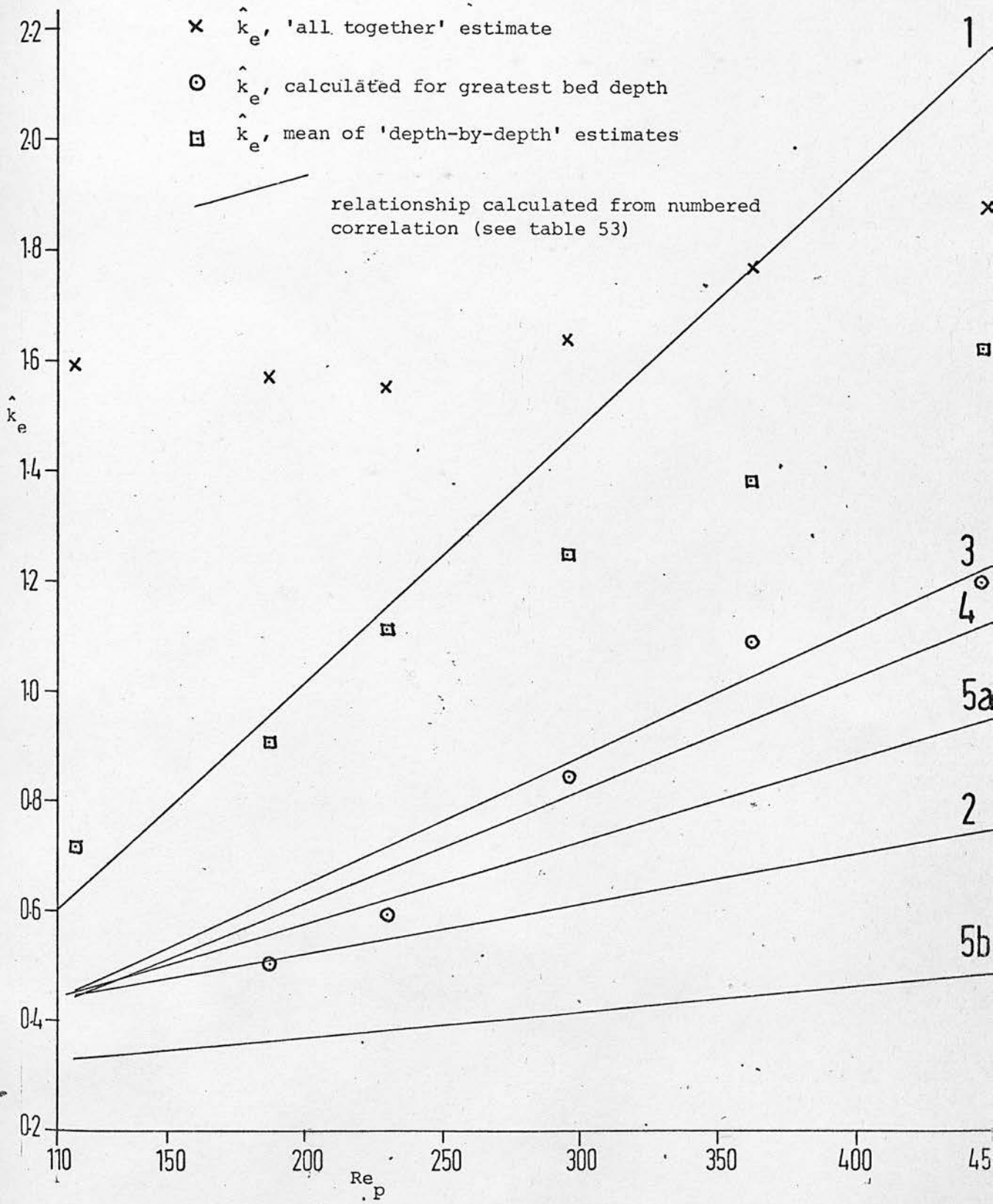

FIGURE 8·12 Comparison Of $\hat{k}_e$ With Available Correlations

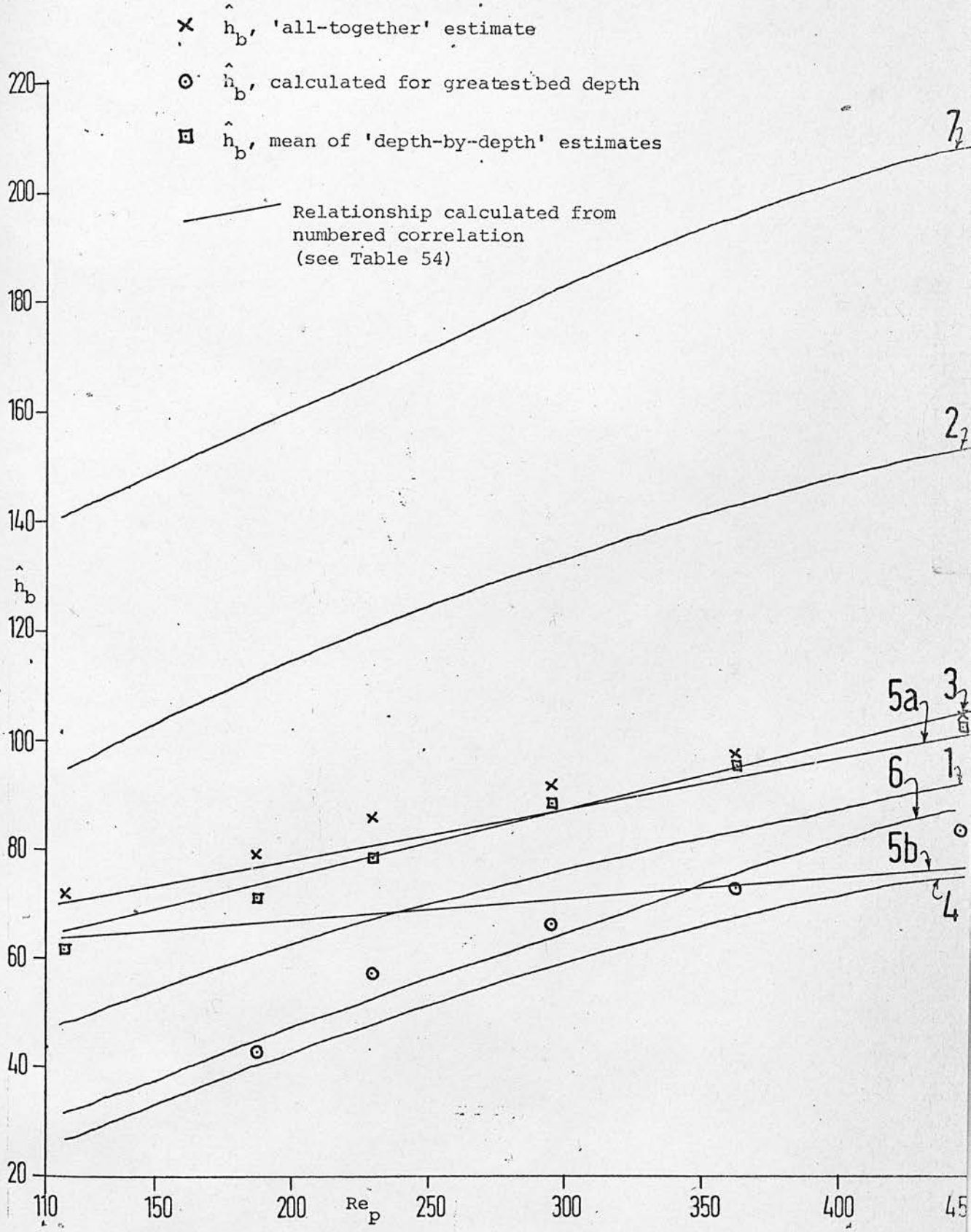

FIGURE 8·13 Comparison Of $\hat{h}_b$ With Available Correlations

Thus, the use of angle-averaged temperatures should be avoided since it leads to underestimation of the uncertainty in the parameter estimates.

Some indication of the possible magnitude of the angular variation of bed properties comes from the voidage data of chapter 7, from the velocity measurements of Marivoet et al (220), and from the mass dispersion studies of Fahien and Smith (235).

ii) Different approaches to parameter estimation. Comparison of the results of different workers is made more difficult because of the different data analysis techniques used. Early workers used graphical methods, with their inherent difficulties, while recently, 'least squares' has been used. But 'least squares' has been applied to different sorts of data: Potter et al (219,225) had available only axial temperature profiles for one radial position, whilst De Wasch and Froment (218) restricted themselves to a 'depth-by-depth' analysis using angle-averaged temperatures. Figures 8.12 and 8.13 show how different estimation methods can lead to different estimates.

iii) Importance of the inlet temperature profile. Another difficulty which arises is that not all workers have accounted for the inlet temperature profile - Olbrich and Potter (219) did so, whilst De Wasch and Froment (218) appear to have assumed that their inlet profile was uniform. Different estimates result if a non-uniform profile is assumed uniform - Table 52.

Table 52: Parameter estimates for SERIES 7 on different inlet assumptions

Inlet profile used	$\hat{Pe}$	$\hat{Bi}_a$	$\hat{Bi}_b$
$T_o(r) = T_{IN}(r)$	2.721	1.866	1.778
$T_o(r) = Twa$	2.001	2.099	1.638
$T_o(r) = \frac{1}{2}\{Twa + T_{IN}(r_b)\}$	3.618	1.665	1.981

iv) Comparison with other workers' results. Other difficulties arise in trying to effect comparisons. Only Potter and his colleagues (219, 225) have examined beds of low d_t/d_p, and they used cylindrical, rather than annular, beds. Whilst Yagi and Kunii (236) are confident that results from the two sorts of beds may reasonably be compared, Marivoet et al (220) have expressed doubts.

Figures 8.12 and 8.13 compare the various estimates of k_e and h_b with predictions from the correlations listed in Tables 53 and 54.

The physical properties used in the calculations were those of air at 120°C, viz. $k = 3.365 \times 10^{-2}$ J/ms deg K, and Pr = 0.689 (239).

Clearly the 'all together' estimates for h_b fall within the (very wide) range of predictions, whilst the 'all together' estimates of k_e are generally rather higher than the predictions. This may be associated with the 'humps' - regions of high conductivity - which occupy a large proportion of the radius of an annular bed of low aspect ratio, and perhaps on an 'entrance effect' since the 'all together' estimates, unlike those of De Wasch and Froment for instance, are not based on neglect of the measured profiles near the bed entrance.

Table 53: Correlations used for k_e

	Author	Correlation	Comments
1	Agnew and Potter (225)	$\frac{k_e}{k_f} = \frac{k_e^o}{k_f} + \frac{Re_p\, Pr}{C}$	Take C = 5, from their Figure 6 $k_e^o/k_f = 2.65$, after Kunii and Smith (237)
2	Calderbank and Pogorski (216)	$k_e = 0.2 + 0.00052\, Re_p$ (Btu/ft. hr. ^oF)	Their original equation is here re-written in terms of Re_p
3	Yagi and Kunii (236)	$\frac{k_e}{k_f} = \frac{k_e^o}{k_f} + (\alpha\beta) Re_p Pr$	Take $k_e^o/k_f = 5.5$, $(\alpha\beta) = 0.10$ from their Table 1
4	Yagi and Wakao (238)	$\frac{k_e}{k_f} = \frac{k_e^o}{k_f} + (\alpha\beta) Re_p Pr$	Take $k_e^o/k_f = 6$, $(\alpha\beta) = 0.09$ from their equation (5).
5	De Wasch and Froment (218)	$k_e = k_e^o + \frac{0.0025}{1 + 46(\frac{d_p}{d_t})^2} Re$ (kcal/m. hr. ^oC)	Take $k_e^o = 0.240$, from their table 2. a) Take $d_p/d_t = \frac{10.1}{2 \times 35.3} = 0.143$ b) Take $d_p/d_t = \frac{10.1}{\text{annular gap}} = \frac{10.1}{29.3} = 0.345$

Table 54: Correlations used for h_b

	Author	Correlation	Comments
1	Agnew and Potter (225)	$\frac{h_b d_p}{k_f} = 2.58\ Re_p^{0.33} Pr^{0.33} + 0.094 Re_p^{0.8} Pr^{0.4}$	Suggested by Beek(6) as suitable for cylindrical pellets.
2	Calderbank and Pogorski (216)	$\frac{h_b d_p}{k_f} = 3.6 Re_p^{0.365} \varepsilon^{-0.365}$	Take $\varepsilon = 0.41$, the mean volume fraction calculated from the data of tables 44 and 45
3	Yagi and Kunii (236)	$\frac{h_b d_p}{k_f} = \alpha^o + 0.054 Re_p Pr$	From their table 3, $12 < \alpha^o < 19$, say $\alpha^o = 15$
4	Yagi and Wakao (238)	$\frac{h_b d_p}{k_f} = 0.18 Re_p^{0.8}$	
5	De Wasch and Froment (218)	$h_b = h_b^o + 0.01152 \frac{d_t}{d_p} Re_p$ (kcal/m^{2}hr.^{o}C)	Take $h_b^o = 51.0$, from their Table 2. a) $d_t/d_p = 6.990$ b) use $\frac{\text{annular gap}}{d_p} = 2.901$
6	Beek (6)	$\frac{h_b d_p}{k_f} = 0.203 Re_p^{0.33} Pr^{0.33} + 0.220 Re_p^{0.8} Pr^{0.4}$	Suggested by Beek as suitable for spherical pellets
7	Olbrich and Potter (219)	$\frac{h_b d_p}{k_f} = 8.9 Re_p^{0.34} Pr^{0.33}$	Intended to yield a lower bound on h_b

Certainly the values of $\hat{Pe}$ reported in Table 47 are rather lower (and therefore $\hat{k}_e$ is rather higher) than would have been expected from measurements on beds of high aspect ratio. Potter and co-workers (225, 240) showed theoretically and experimentally that k_e should increase, and Pe decrease, with decrease in d_t/d_p, but have more recently doubted their own conclusion (219). The matter is not resolved, but the results of this chapter do suggest that in tubes of low aspect ratio {in this work $^{(\text{annular gap})}/d_p = 2.9$} the value of k_e is higher than most available correlations predict.

In view of the model inadequacy already demonstrated, and the size of the parameter marginal standard deviations and cross-correlation coefficients, it would perhaps be rash to claim that the dependence of k_e and h_b on Re_p, as shown in figures 8.12 and 8.13, is sufficiently well-established to permit any general conclusion to be drawn.

v) The neglect of axial dispersion. At Reynold's numbers of the magnitude used here, it is usual to ignore the effect of axial dispersion (218). Recently, however, Gunn and Khalid (221) suggested that this neglect may have introduced errors into the correlations currently available, but did not prove their point directly from their data.

Young and Finlayson (62) have presented an equation (their equation 15) permitting evaluation of the error introduced into predicted temperature as an effect of ignoring axial dispersion. Consider using that equation here: clearly an upper bound on the error would be that occurring at the outer wall if the inlet temperature profile were uniform at the temperature of the inner wall. Then,

using the parameter estimates of Table 47, the maximum error in temperature due to neglect of axial dispersion is = 2.5°C at the shallowest bed depth and the error decreases rapidly with depth. This pessimistic estimate is not large compared with the angular temperature variation, or even compared with the error involved in representing the inlet temperature profile. It is therefore inferred that the neglect of axial dispersion probably is justified.

8.7 Recommendations for further work.

i) Adaptions to the apparatus. The electrical heating used on the outer wall needs rather time-consuming adjustment to ensure a uniform wall temperature. It should be replaced by the use of condensing steam. Further attempts should be made to obtain an inlet profile which is flatter and, even more important perhaps, more reproducible.

ii) Measurement of solid and gas temperatures. Further work should seek to elucidate (a) the source of the 'entrance effect', (b) the origin of the angular variation in temperature and (c) the cause of the model inadequacy. A possible explanation is that, in beds of such low aspect ratio, the solid and gas phases are not at equal temperatures at given radial position. This hypothesis might explain the 'humps' on the radial temperature profile and thus account for part of (c). It might also account for (a), and thus for a portion of (c), since the effect of unequal phase temperatures might be greatest near the bed entrance, where axial temperature gradients are most severe.

Lastly, it might account for (b), since different angular positions might simply correspond to a thermocouple touching a pellet (or perhaps being immersed in a stagnant fillet of fluid adjacent to the pellet), or being in free-flowing gas.

The hypothesis has the merit that it can be tested experimentally by using thermocouples carefully located in solid and gas. To make accurate location possible without disrupting the structure of the bed, use could be made of ordered, rather than random, beds. If the hypothesis were proved, it would then be necessary to construct a two-phase model which would doubtless exploit the voidage data reported in chapter 7.

iii) Measurement of velocity profiles. It is well known (e.g. 220) that there exists a radial velocity profile in packed beds. It is likely that, for beds of low aspect ratio, this will significantly affect their performance as reactors, and it may well affect their heat transfer characteristics in the absence of reaction - for example, a developing velocity profile may account for part of the 'entrance effect'. It would be useful to measure velocity profiles and to correlate them with bed voidage. Conventional anemometric methods (220) are rather unsatisfactory because they are sensitive to turbulent intensity as well as to velocity in the axial direction. Further, it is very difficult to use such anemometers inside, rather than above, a packed bed.

By constructing a bed with transparent walls, it might be possible to use a laser doppler anemometer (242) to measure gas velocities within the bed. Again, the use of an ordered bed might be attractive - it

would probably have a velocity profile somewhat different from that of a random bed, but it would probably make measurement within the bed much simpler.

iv) Effect of the entrance region on reactor performance.

It would be of some interest to perform simulations to measure the sensitivity of reactor behaviour to the 'entrance effect'. The high values of effective conductivity and wall heat transfer coefficient near the entrance should decrease predicted hot-spot temperatures, and improve stability.

CHAPTER 9:- Concluding Remarks

9.1 Recent publications.

9.2 Reflections.

9.1 Recent publications

Some publications which have appeared since the bulk of this thesis was completed must be mentioned.

Priestley and Agnew (243) have evaluated the relative importance of different parameters in reactor modelling. In accord with the conclusions of chapter 1, they find that the interphase transfer coefficients are not an important source of uncertainty, whilst the kinetic parameters and the bed heat transfer parameters are the major sources of uncertainty (they did not consider intrapellet resistances).

Aris (244) has published a two-volume text which contains a huge literature review of relevance to chapter 2. Marek and Stuchl (245) and Ha and Hanna (246) have devised new approximate methods for calculating effectiveness factors, whilst Carey and Finlayson (247) have presented an extension of the method developed in chapter 2. Hite and Jackson (248) have reported that "our former suggestion on the range of validity of {the conventional ordinary differential equation formulation of reaction and diffusion} was unnecessarily pessimistic .... . These equations are correct for steady states in catalyst pellets of arbitrary shape, provided only that the total molar concentration and composition are the same at all points of the surface."

Hsiang and Reilly (249) have explored some difficulties in using a modern Bayesian model discrimination technique in catalytic kinetics, while Pritchard and Bacon (250) have described deficiencies in 'traditional' methods.

9.2 Reflections

Although it ill becomes the author to say so, it is his opinion that the mathematical problems of reaction with diffusion have attracted disproportionate attention. More experimental work to investigate model adequacy is required.

The parameter estimation methods presented in chapters 4,5 and 6 need further development. Their robustness in the face of non-Normal errors needs testing, their capabilities in multi-response problems should be further investigated and the technique proposed for 'bias compensation' must be more fully evaluated. Extension to permit estimation of parameters appearing in boundary conditions would be most useful. The performance of these methods, and of classical methods, when dealing with the serially-correlated errors which probably arise in most integral kinetic studies, should be explored.

The heat transfer study presented an attempt to study the measurement errors in some depth, to justify use of a statistical measure of model adequacy. Although the model was adjudged inadequate, the parameter estimates are still likely to be of some use, particularly the observation that rather high values of $\hat{k}_e$ were obtained.

One stimulus to the work of this thesis was the difficulty which Caldwell (66) and Ellis (223) found in accounting for the thermal stability of their o-xylene oxidation reactor. In Appendix A5 the contribution which physical resistances might make to reactor stability is investigated. Another explanation of reactor stability comes from some work of the present writer (251), confirmed by Calderbank (252), which revealed that at a temperature of $\sim 440^{\circ}C$ there is a sudden decline in the activation energy of the oxidation reaction. Now, perhaps, a third (partial) explanation may be offered - the effective thermal conductivity of the bed may well have been higher than was originally anticipated.

It may be asked whether attempts to refine models of heat transfer in packed beds are worthwhile in view of the likely deficiencies of the kinetic data available for reactor design. One answer is that it will be easier to investigate inadequacies in the kinetics if only heat transfer were better understood! The engineer who awaits a profound undertsanding of industrial catalysis may wait for rather a long time.

A second answer is that it now appears possible that packed beds may be used in nuclear reactors (253), where the kinetics of heat release are rather well established. This provides a powerful incentive to improve the current models.

The achievement of a substantial improvement, however, may well be a "gey sair fecht".

APPENDIX 1

Matters relating to effectiveness factor calculations

A1.1 The use of cubic splines.

A1.2 Integral Equation Method.

A1.3 Algorithm for the construction of η versus Φ plots: interface case.

A1.4 Other remarks.

A1.1 The use of cubic splines

A cubic spline approximation consists of a piecewise continuous cubic with a continuous first derivative and continuous second derivative. There will normally be a jump discontinuity in the 3rd derivative at the junction points.

The equation to be treated is the heat balance equation for the zeroth reaction (no-interface) case. From equations(2.2),(2.3) and (2.5)

$$\frac{d^2t}{dy^2} = -\frac{a}{y}\frac{dt}{dy} - \beta Q^2 \exp\{\gamma(1-1/t)\} \qquad (A1.1)$$

$$\text{with} \quad \frac{dt}{dy} = 0 \quad \text{at } y = 0 \qquad (A1.2)$$

$$t = 1 - \frac{1}{Nu}\frac{dt}{dy} \quad \text{at} \quad y = 1 \qquad (A1.3)$$

and, using L'Hôpital's rule (A1.1) at y = 0 becomes

$$(a+1)\ \frac{d^2t}{dy^2} = -\beta Q^2 \exp\{\gamma(1-1/t)\} \qquad (A1.4)$$

Now, we partition the interval (0,1) into N subintervals by the mesh points y_n, $0 = y_1 < y_2 < \ldots < y_{N+1} = 1$

The partition defines the mesh spacings $h_n \equiv y_{n+1} - y_n$ (A1.5)

Our approximate sol^n to(A1.1) and (A1.4), $\tau(y)$ is a cubic spline function: in each subinterval (y_n, y_{n+1}), $\tau(y)$ is a cubic polynomial $Z_n(y)$. The Z_n's are chosen so that τ is continuous, and has continuous second derivatives. It follows from this that we may represent τ by

$$\tau(y) = Z_n(y),\ y_n < y < y_{n+1} \quad n = 1,2 \ldots N$$

$$Z_n(y) = \tau_n y_+ + \tau_{n+1} y_- - \left(\frac{h_n^2}{6}\right)\{\tau''_n(y_+ - y_+^3) + \tau''_{n+1}(y_- - y_-^3)\} \quad \text{(A1.6)}$$

where $y_+ \equiv \dfrac{y_{n+1} - y}{h_n}$; $y_- \equiv \dfrac{y - y_n}{h_n}$ (A1.7)

are the normalised distances to the adjacent mesh points. τ_n and τ''_n are the values of $\tau(y_n)$ and $\tau''(y_n)$ which are to be determined.

The continuity conditions to be satisfied are

$$Z_n^{(j)}(y_n) = Z_{n-1}^{(j)}(y_n) \qquad \begin{matrix} j = 0,1,2 \\ n = 2,3 \ldots N \end{matrix} \quad) \quad \text{(A1.8)}$$

As written in A1.6, the Z_n's satisfy the conditions on continuity of value and 2nd derivative. Matching 1st derivatives yields

$$h_n\tau_{n-1} - (h_n + h_{n-1})\tau_n + h_{n-1}\tau_{n+1} =$$

$$\frac{h_n h_{n-1}}{6}\{h_{n-1}\tau''_{n-1} + 2(h_n + h_{n-1})\tau''_n + h_n\tau''_{n+1}\} \quad \text{(A1.9)}$$

$$n = 2,3 \ldots N$$

Requiring that $\tau(y)$ satisfies the differential eqn yields

$$\tau''_n = -\frac{a}{y_n}\tau'_n - \beta Q^2 \exp\{\gamma(1 - \frac{1}{\tau_n})\} \quad \text{(A1.10)}$$

$$n = 2,3 \ldots N+1$$

and from (A1.4),

$$\tau''_1 = -\frac{\beta Q^2}{a+1} \exp\{\gamma(1 - \frac{1}{\tau_1})\} \quad \text{(A1.11)}$$

The first derivative τ'_n may be given, using one of the cubics, by

$$\tau'_n = Z'_n(x_n) = \frac{\tau_{n+1} - \tau_n}{h_n} - \frac{h_n}{6}(2\tau''_n + \tau''_{n+1}) \quad \text{(A1.12)}$$

$$n = 1,2 \ldots N$$

or, using the other cubic, by

$$\tau'_n = Z'_{n-1}(x_n) = \frac{\tau_n - \tau_{n-1}}{h_{n-1}} + \frac{h_{n-1}}{6}(2\tau''_n + \tau''_{n-1}) \quad \text{(A1.13)}$$

In addition, we have the boundary conditions, eqns. (A1.2) and (A1.3)

$$\left.\begin{aligned} \tau'_1 &= 0 \\ \tau_{N+1} &= 1 - \frac{1}{Nu}\tau'_{N+1} \end{aligned}\right\} \qquad \text{(A1.14)}$$

The eqns. (A1.4) to (A1.14) may be worked to yield (2N+2) non-linear relations among the (2N+2) unknowns τ_n, τ''_n, n=1 ... N+1. The eqns. will be solved by some iterative procedure.

We consider one possible iterative scheme:-

From eqns. (A1.10) and (A1.13)

$$\tau''_n = \frac{1}{1+\frac{a}{y_n}\frac{h_{n-1}}{3}}\left\{-\frac{a}{y_n}\left(\frac{\tau_n-\tau_{n-1}}{h_{n-1}} + \frac{h_{n-1}}{6}\tau''_{n-1}\right) - \beta Q^2 \exp\left\{\gamma\left(1-\frac{1}{\tau_n}\right)\right\}\right\} \qquad \text{(A1.15)}$$

$$n = 2,3 \ldots N+1$$

From Eqns. (A1.12) and (A1.14) we obtain

$$-\tau_1 + \tau_2 = \frac{h_1^2}{6}(2\tau''_1 + \tau''_2) \qquad \text{(A1.16)}$$

and from Eqns. (A1.11) and (A1.13)

$$-\frac{1}{Nuh_N}\tau_N + \left(1 + \frac{1}{Nuh_N}\right)\tau_{N+1} = 1 - \frac{h_N}{6Nu}(2\tau''_{N+1} + \tau''_N) \qquad \text{(A1.17)}$$

So, if we define

$$R_1 \equiv \frac{h_1^2}{6}(2\tau''_1 + \tau''_2) \qquad \text{(A1.18)}$$

$$R_n \equiv \frac{h_n h_{n-1}}{6}\{h_{n-1}\tau''_{n-1} + 2(h_n + h_{n-1})\tau''_n + h_n\tau''_{n+1}\} \qquad \text{(A1.19)}$$

$$R_{N+1} \equiv 1 - \frac{h_N}{6Nu}(2\tau''_{N+1} + \tau''_N) \qquad \text{(A1.20)}$$

then we may write eqns. (A1.16), (A1.9) and (A1.17) as :-

$$\begin{aligned} -\tau_1 + \tau_2 &= R_1 \\ h_2\tau_1 - (h_2 + h_1)\tau_2 + h_1\tau_3 &= R_2 \\ h_3\tau_2 - (h_3 + h_2)\tau_3 + h_2\tau_4 &= R_2 \end{aligned} \qquad \text{(A1.21)}$$

$$h_N\tau_{N-1} - (h_N + h_{N-1})\tau_N + h_{N-1}\tau_{N+1} = R_N$$

$$-\frac{1}{Nuh_N}\tau_N + (1 + \frac{1}{Nuh_N})\tau_{N+1} = R_{N+1}$$

The algorithm is then:-

1) Guess values for τ_n, n = 1 ... (N+1).

2) Use equation (A1.11) to calculate τ''_1 and (A1.15) to calculate τ''_n, n = 2 ... (N+1).

3) Using the definitions of R_n in equations (A1.18) to (A1.20), solve the tridiagonal set of linear equations (A1.21) by the method of Thomas, to obtain a new iterate for τ_n, n = 1 ... (N+1).

4) Repeat until convergence is obtained.

No difficulties were found in implementing the method.

References:-

Ahlberg, J.H., Nilson, E.N. and Walsh, J.L., "The Theory of Splines and Their Applications", Academic Press, N.Y. 1967.

Greville, T.N.E., "Theory and Application of Spline Functions", Academic Press, N.Y., 1969.

Blue, J.L., C.A.C.M. 12,6,327 (1969).

A1.2 Integral Equation Method

Consider the material balance equation for nth order reaction

$$\frac{d^2C}{dy^2} + \frac{a}{y}\frac{dC}{dy} = \varphi^2 \exp\{\gamma(1 - \frac{1}{t})\}C^n \qquad (A1.22)$$

By use of an enthalpy balance at the pellet surface, and Prater's relation,

$$t(y) = (1 + \beta\frac{Sh}{Nu}) + \beta(1 - \frac{Sh}{Nu})C(1) - \beta C(y) \qquad (A1.23)$$

This relation may be substituted into equation (A1.22), whereupon equation (A1.22) becomes an equation in only one variable, C(y), with boundary conditions

$$C = 1 - \frac{1}{Sh}\frac{dC}{dy} \quad \text{at} \quad y = 1 \qquad (A1.24)$$

$$\frac{dC}{dy} = 0 \qquad \text{at } y = 0 \qquad (A1.25)$$

Equation (A1.22) may be written in Sturm-Liouville form

$$\frac{d}{dy}\{y^a \frac{d}{dy}\}C = y^a\, g(C(y)) \qquad (A1.26)$$

where g(C(y)) represents the R.H.S. of the substituted version of eqn. (A1.22).

Conversion into a Fredholm Integral Equation

For a sphere (a = 2), (A1.26) can be written as

$$\frac{d}{dy}(y^2\frac{dC}{dy}) = y^2 g(C(y)) = \mu_2(y,C) \qquad (A1.27)$$

We write

$$C(y) = \frac{1}{y^2\{u(y)v'(y) - u'(y)v(y)\}} \int_0^1 G(y,\lambda)\mu_2(\lambda,C)d\lambda \qquad (A1.28)$$

where the Green's function

$$G(y,\lambda) = \begin{cases} u(\lambda)c(y) & 0 \leq \lambda \leq y \\ u(y)v(\lambda) & y \leq \lambda \leq 1 \end{cases}$$

u(y) and v(y) are readily determined, and it is found that (A1.28) becomes

$$C(y) = \{\frac{Sh + (1-Sh)C(1)}{Sh(1-C(1))} - \frac{1}{y}\} \int_0^y \lambda^2 g(C(\lambda),C(1))d\lambda$$

$$+ \int_y^1 \{ \frac{Sh + (1-Sh)C(1)}{Sh(1-C(1))} - \frac{1}{\lambda} \} \lambda^2 g(C(\lambda),C(1))d\lambda \qquad (A1.29)$$

where, in full,

$$g(C(\lambda),C(1)) = \varphi^2 \exp\{\gamma(1 - \frac{1}{(1+\frac{Sh}{Nu}\beta) + \beta(1-\frac{Sh}{Nu})C(1) - \beta C(\lambda)}) C^n(\lambda)$$

(A1.30)

The solution procedure used was to guess a profile C(y) - which of course includes C(1) - and substitute this profile into the R.H.S. of eqn. (A1.29). The integrals were evaluated by recursive use of the trapezoidal rule, and thus the L.H.S. yields a new approximation of C(y). The method converged only from good starting guesses.

Reference: Kesten, A.S., A.I.Ch.E.Jl 15,128 (1969).

A1.3 Algorithms for the construction of η versus Q plots: interface case

We deal first with Slab Geometry (a = 0), and consider the zeroth order reaction.

Consideration of the fluxes of mass and heat at the pellet surface yields

$$t_s = 1 + \frac{Sh}{Nu}\beta(1 - C_s) \tag{A1.31}$$

Prater's relation is written as

$$t(y) = t_s - \beta(C(y) - C_s) \tag{A1.32}$$

At the interface $y = y_I$, $C(y_I) = 0$, so that eqn. (A1.31) and A(1.32) may be combined to yield

$$t(y_I) = t_s(1 - \frac{Nu}{Sh}) + (\beta + \frac{Nu}{Sh}) \tag{A1.33}$$

We define a new independent variable $\lambda \equiv Q(y - y_I)$ (A1.34)

Note that, at $y = y_I$, $\lambda = 0$ (A1.35)

Thus $t(\lambda = 0) = t_s(1 - \frac{Nu}{Sh}) + (\beta + \frac{Nu}{Sh})$ (A1.36)

Further, the central boundary condition may be written as

$$\left(\frac{dt}{d\lambda}\right)_{\lambda=0} = 0 \tag{A1.37}$$

The surface boundary condition is transformed to

$$t_s = 1 - \frac{1}{Nu} Q \left.\frac{dt}{d\lambda}\right|_{\lambda=\lambda_s}$$

or

$$\Phi = \frac{-Nu(t_s - 1)}{1} \quad \frac{1}{\left.\frac{dt}{d\lambda}\right|_{\lambda=\lambda_s}} \tag{A1.38}$$

For calculation of the effectiveness factor we use the relation

$$\eta = Nu \frac{(t_s - 1)}{\beta Q^2} (a + 1) \tag{A1.39}$$

For SLAB, a = 0, the energy balance becomes

$$\frac{d^2t}{d\lambda^2} = -\beta \exp\{\gamma(1-\frac{1}{t})\}.C^o \qquad \text{(A1.40)}$$

where the C^o serves to remind us that the R.H.S. is zero at $\lambda = 0$ and equal to $-\beta \exp\{\gamma(1 - \frac{1}{t})\}$ elsewhere.

Principle of method

1. Choose some value of t_s.
2. Calculate $t(\lambda = 0)$ using eqn. (A1.36).
3. With $t(\lambda = 0)$ and eqn. (A1.37) as initial conditions, we integrate eqn. (A1.40) until $t = t_s$.
4. We evaluate Q using eqn. (A1.38) and thereafter η using eqn. (A1.39).

Detail of method

Let us define $\psi \equiv \frac{dt}{d\lambda}$ (A1.41)

Hence we manipulate eqn. (A1.40) in to the form

$\lambda > 0$;

$$\begin{cases} \frac{dt}{d\lambda} = \psi \\ \\ \frac{d\psi}{d\lambda} = -\beta \exp\{\gamma(1 - \frac{1}{t})\} \end{cases} \qquad \text{(A1.42)}$$

$\lambda = 0$;

$$\begin{cases} \frac{dt}{d\lambda} = \psi \\ \\ \frac{d\psi}{d\lambda} = 0 \end{cases} \qquad \text{(A1.43)}$$

We integrate eqns. (A1.41) and (A1.42) until, hopefully, $t = t_s$.

In general, we would expect that our outward integration would 'overshoot' the chosen t_s i.e. that we would not arrive exactly at t_s, but at some value $t_s^* < t_s$.

Let us denote that value of λ at which $t = t_s^*$ by λ^*

Let us denote that value of $\frac{dt}{d\lambda}$ at which $t = t_s^*$ by ψ^*

Wheeler's algorithm

Define $$\Lambda \equiv \frac{d^2t}{d\lambda^2} \tag{A1.44}$$

Hence $$\frac{d\psi}{dt} = \frac{\Lambda}{\psi} \tag{A1.45}$$

Further, from eqn. (A1.40), for $\lambda > 0$

$$\Lambda = -\beta \exp\{\gamma(1 - \frac{1}{t})\} \tag{A1.46}$$

Thus we may write eqns. (A1.45) and (A1.42) as

$$\begin{aligned} \frac{d\psi}{dt} &= -\frac{\beta}{\psi} \exp\{\gamma(1 - \frac{1}{t})\} \\ \frac{d\lambda}{dt} &= \frac{1}{\psi} \end{aligned} \tag{A1.47}$$

So, we integrate the set of eqns. (A1.47) from initial values

$$\begin{aligned} t &= t_s^* \quad ; \quad \lambda = \lambda^* \\ \psi &= \psi^* \end{aligned} \tag{A1.18}$$

to $t = t_s$. There we evaluate $\psi(t = t_s) = \left.\frac{dt}{d\lambda}\right|_{\lambda = \lambda_s}$

We calculate Q using eqn. (A1.38), and thereafter η using eqn. (A1.39). Note that we cannot use Wheeler's algorithm in place of the complete procedure, since we cannot conveniently use the condition

$$\left(\frac{d\lambda}{dt}\right)_{\lambda=0} = \infty \tag{A1.19}$$

For the case of spherical geometry, the presence of the first derivative invalidates the procedure above. The McGinnis (113) iteration procedure was used, with t_I as the guessed "missing initial condition".

References

Weisz, P.B. and Hicks, J.S., Chem.Eng.Sci. 17, 265 (1962).

Wheeler, D.J., Computer Jl. 2,23 (1959).

A1.4 Other remarks

An attempt was made to devise an approximate method from a variational approach.

Defining $\theta \equiv \frac{t-1}{\beta^{Sh}/Nu}$, it can be shown that the solution to eqn. (A1.1) is that $\theta(y)$ which extremises I, given by

a = 0,2

$$I = \int_0^1 \{y^a (\frac{d\theta}{dy})^2 + 2y^a \frac{Nu}{Sh} Q^2 \int_0^\theta \exp(\frac{\gamma\beta Sh\lambda}{\beta Sh\lambda+Nu}) d\lambda\} dy + Nu\, \theta^2(1)$$

a = 1

$$I = \int_0^1 \{e^y (\frac{d\theta}{dy})^2 + 2e^y \frac{Nu}{Sh} Q^2 \int_0^\theta \exp(\frac{\gamma\beta Sh\lambda}{\beta Sh\lambda+Nu}) d\lambda\} dy + e\, Nu\, \theta^2(1)$$

The analysis was carried no further since it appeared to offer no route to a rapid approximate method better than that already devised.

Similarily abandoned were attempts to devise a 'nearly isothermal pellet' method, and an attempt to base an M.W.R. technique on the use of a "Richardson profile".

References

Schechter, R.S., "The Variational Method in Engineering", McGraw-Hill, N.Y., 1967.

Pakes, H.W. and Storey, C., Chem.Engr. (London), May 1967, 208, CE 96.

Richardson, P.D., Int.Jl.Heat and Mass Transfer 8, 557 (1965)

A.I.A.A. Jl. 1, 2659 (1963).

APPENDIX 2:- Matters relating to parameter estimation

A2.1 Confidence region calculations: NO oxidation.

A2.2 The generation of a normalised Normally-distributed variable.

A2.3 The generation of numbers from a multi-variate Normal distribution.

A2.4 Bias analysis by expansion in Taylor series.

A2.5 A note on the transformation of parameters.

A2.6 Application of QLLS to the adiabatic reactor problem.

A2.7 Confidence analysis for weighted residual methods applied to o.d.e.'s non-linear in the parameters.

A2.8 Variance-covariance analysis for SDM applied to NO oxidation.

A2.9 The approximations used in appendix A2.8.

A2.10 Confidence region calculations.

A2.11 Variance-covariance analysis for LSRM applied to the NO problem.

A2.12 Remarks pertaining to the comparison of the GLS and Box-Draper results.

A2.1: Confidence region calculations: NO oxidation

For non-linear problems, it is not possible to calculate a confidence region exactly. One must either calculate; (i) an approximate region corresponding to a known confidence level (e.g. 95%), or (ii) an exact region corresponding to a degree of confidence which is not known exactly. Method (i) is computationally the simplest and very much the fastest. The theory is developed in Chapter 10 of Draper and Smith (148), and its implementation for o.d.e.'s is presented as eqn.s (53) to (62) in Chapter 8 of Rosenbrock and Storey (68). The error properties assumed are discussed in section 3.7. The 95% confidence intervals and the parameter cross-correlation coefficient are presented in Chapter 4, table 16, and the approximate 95% confidence ellipse is shown as the solid line in figure 4.1. The boundary of this approximate region corresponds to the contour

$$S = S_{min}\{1 + \frac{n_p}{m - n_p} F(n_p, m-n_p, 0.95)\}$$

$$= 36$$

where S: the sum of squares corresponding to the 95% approximate contour

S_{min}: the minimum sum of squares (= 21.87) corresponding to the parameter estimates

n_p : the number of parameters (= 2)

m : the number of observations (= 14)

and F is the familiar F-statistic (here, F(2,12,0.95) = 3.88). Calculation of points on the contour requiresonly the integration of two o.d.e.'s, followed by repetitive solution of a quadratic equation.

The alternative (ii) is to calculate, by iterative search and repetitive integration of the model o.d.e., those combinations (k_1, k_2) which give rise to a value of S = 36. The contour so found is

indicated by the crosses on figure 4.1. The closeness of these points to the solid ellipse shows that the approximations inherent in the linearised confidence analysis (i) are justified in this case. Examples of situations where the linearised analysis is misleading have been reported by:-

Pfeiffer L. and Lichtenwalner C.P., Rev. Sci. Instrum. 45, 803(1974).

Emig. G. and Hosten L.H., Chem.Eng.Sci. 29, 475 (1974).

A2.2 The generation of a normalised Normally-distributed variable

The ERCC sub-routine RANDOM (i,n) generates a rectangularly-distributed pseudo-random variable x_j if n is set equal to 1, and i to an odd integer, preferably > 50,001. If n > 1, the sum of n such variables is obtained. The procedure is an implementation of a standard IBM sub-routine. Hamming (p34 and p389) shows that an approximately Normally distributed random variable N can be calculated from

$$N = \sum_{j=1}^{12} x_n - 6$$

and that to obtain a Normally distributed variable N_S with specified mean AM and standard deviation S, one need only employ

$$N_S = N * S + AM$$

In the IMP programming language the procedure is then effected by

```
% realfn GAUSS (% integername I, % real S,AM)
% result  =  (RANDOM (I,12) - 6) * S + AM
% end
```

In using this sub-routine it is important that, after a first value ("seed") has been assigned to I, the value of I must be allowed to change as dictated by the sub-routine RANDOM.

Although this generation method is well-known, it was felt to be prudent to perform some few tests on the hypothesis that the numbers so generated do follow a normalised Normal distribution of specified mean and standard deviation. The tests used are described in the table below, and were performed on a sample of 1000 values.

	Property	Method	Source
1	Standard deviation	$\chi^2/_{df}$ test	Dixon and Massey, p.86
2	Mean	Z test	ibid, p.94
3	Goodness-of-fit	χ^2 test	Davies and Goldsmith
4	Skewness	Third moment test	Pearson and Hartley Table 34B
5	Kurtosis	Fourth moment test	ibid. Table 34C

The only difficulty encountered was that an extension to the $\chi^2/_{df}$ table in Dixon and Massey had to be calculated, to cope with a sample of 1000 values.

The results were satisfactory at the 5% level i.e. the hypothesis was not disproved, and so the sub-routine was deemed adequate.

The "seeds" used were 65549 and 65539.

References:-

Hamming R.W., "Numerical Methods for Scientists and Engineers", McGraw-Hill, N.Y., 1962.

Dixon W.J. and Massey F.J., "Introduction to Statistical Analysis", McGraw-Hill, N.Y., 1951.

Pearson E.S. and Hartley H.O., "Biometrika Tables for Statisticians'" C.U.P., Vol 1, 3rd Edn., 1966.

Davies O.L. and Goldsmith P.L. "Statistical Methods in Research and Production", Oliver and Boyd, Edinburgh, 1972.

A2.3 The generation of numbers from a multi-variate Normal distribution

A technique described by Naylor et al is used. Where $\underline{x}$ is a Normal N-vector with mean $\underline{\mu}$ and variance-covariance matrix $\underline{\underline{U}}$, the p.d.f. is

$$f(\underline{x}) = (2\pi)^{-\frac{1}{2}N}(|\underline{\underline{U}}|)^{-\frac{1}{2}} \exp\{-\tfrac{1}{2}(\underline{x} - \underline{\mu})^T \underline{\underline{U}}^{-1}(\underline{x} - \underline{\mu})\}$$

The generation of vectors $\underline{x}$ exploits a theorem (see Anderson) which states that if $\underline{Z}$ is a standard Normal vector, i.e. it contains independent Normal variable components with zero mean and unit variance, there exists a unique lower triangular matrix $\underline{\underline{B}}$ such that

$$\underline{x} = \underline{\underline{B}}\,\underline{Z} + \underline{\mu} \qquad \text{(A2.1)}$$

The elements of $\underline{\underline{B}}$ can be calculated recursively from the elements of $\underline{\underline{U}}$ as follows:-

$$b_{il} = \frac{U_{il}}{\sqrt{U_{ll}}} \quad ; \quad 1 \leq i \leq N$$

$$b_{ii} = \{ U_{ii} - \sum_{k=1}^{i-1} b_{ik}^2 \}^{\frac{1}{2}} \quad ; \quad 1 < i \leq N$$

$$b_{ij} = \{ U_{ij} - \sum_{k=1}^{j-1} b_{ik} b_{jk} \}/U_{jj} \quad ; \quad 1 < j < i \leq N \qquad \text{(A2.2)}$$

$$b_{ij} = 0 \quad ; \quad j > i$$

So, one generates the matrix $\underline{\underline{B}}$ from eqns.(A2.2), one computes vectors $\underline{Z}$ using the method of appendix A2.2, and finally calculates vectors $\underline{x}$ from eqn. (A2.1).

For the particular case of a bi-variate Normal distribution, the result is

$$\begin{bmatrix} x_1 \\ x_2 \end{bmatrix} = \begin{bmatrix} \sigma_1 Z_1 \\ \sigma_2\{Z_1\rho_E + Z_2\sqrt{(1-\rho_E^2)}\} \end{bmatrix} + \begin{bmatrix} \mu_1 \\ \mu_2 \end{bmatrix} \qquad \text{(A2.3)}$$

and, in the case of interest here, $\mu_1=0=\mu_2$, and so eqn. (A2.3) yields the simple 'rule' for calculating the variates.

References:-

Anderson T.W., "An Introduction to Multivariate Statistical Analysis", Wiley, N.Y., 1958.

Naylor T.H., Balintfy J.L., Burdick J.S. and Chu K, "Computer Simulation Techniques", Wiley, N.Y., 1966.

A2.4 Bias analysis by expansion in Taylor series

For simplicity, the single first order reaction is studied, and the treatment is modified from that of section 4.8 to minimise the amount of numerical calculation. The model is eqn. (4.16) and the RLSM estimator from eqn. (4.19) is written as

$$\hat{k} = \frac{Y_o^2 - Y_m^2}{2\int_o^{t_m} Y^2 dt} \qquad \text{(A2.4)}$$

Writing $Y = y + e$, the denominator is seen to be

$$\left(\int_o^{t_m} y^2 dt\right)\left\{1 + \frac{\int_o^{t_m}(e^2 + 2ey)dt}{\int_o^{t_m} y^2 dt}\right\}$$

and so, if the second term in the square bracket is less than unity, expansion in Taylor series yields

$$\hat{k} \simeq \frac{y_o^2 - y_m^2}{2\int_o^{t_m} y^2 dt} \left(1 - \frac{\int_o^{t_m} (e^2 + 2ey)dt}{\int y^2 dt}\right) \qquad \text{(A2.5)}$$

which yields, on taking $Y_o = y_o$ and $Y_m = y_m + e_m$,

$$\hat{k}_1 \simeq \frac{y_o^2 - y_m^2}{\int_o^{t_m} y^2 dt} + \frac{1}{I}\left\{\frac{y_o^2 - y_m^2}{2I}\int_o^{t_m}(e^2+2ey)dt - e_m y_m - \tfrac{1}{2}e_m^2 + \frac{y_m e_m}{I}\int_o^{t_m}(e^2+2ey)dt + \frac{e_m^2}{2I}\int_o^{t_m}(e^2+2ey)dt\right\} \qquad \text{(A2.6)}$$

where $I \equiv \int_o^{t_m} y^2 dt$ (A2.7)

The first term on the RHS of eqn. (A2.6) will be recognised as k_{true}: the remainder of the RHS is an approximation to the bias in the estimator.

Before eqn. (A2.6) can be used, certain expected values must be established: $E(\int_o^{t_m} eydt) = 0$; $E(e_m \int_o^{t_m} e^2 dt) = 0$; $E(e_m^2 \int_o^{t_m} eydt) = 0$

$E(\int_o^{t_m} e^2 dt) = \sigma_E^2 t_m$; $E(e_m \int_o^{t_m} eydt) = \sigma_E^2 \int_o^{t_m} ydt$; $E(e_m^2 \int_o^{t_m} e^2 dt) = 3\sigma_E^4 t_m$

Then, taking expectations in eqn. (A2.6)

$$\hat{k} \simeq k_{true} - \frac{\sigma_E^2}{2I^2}\{t_m(y_o^2 - y_m^2) + \int_o^{t_m} y^2 dt - 4y_m \int_o^{t_m} ydt\} + \frac{3t_m\sigma_E^4}{2I^2} \qquad \text{(A2.8)}$$

With the values $k_{true} = 1$, $\sigma_E^2 = 10^{-3}$, $t_m = 2.5$, and with the integrals conveniently evaluated using the analytical solution eqn. (4.18), eqn. (A2.8) yields

$$\hat{k} \doteq 0.9946$$

$$\text{i.e. } k_{bias} \doteq 0.0054$$

This bias pertains to the case where there are an infinite number of measurements available, since the analytical solution was used with the integrals evaluated analytically rather than by trapezoidal rule.

It has thus been shown that it is possible to estimate the degree of bias in a weighted residual estimator. However, this example is atypical in that the 'true value' of k and of y(t) is known. In a typical problem, an approximation to y(t) would be generated using $\hat{k}$, and so eqn. (A2.8) or its equivalent would be used iteratively. It should be remarked that this topic of 'bias compensation' has not yet been fully investigated.

A2.5 A note on the transformation of parameters

From eqn. (5.12) $$A = RT_b A_1 \qquad \text{(A2.9)}$$

and so $$E(A) = RT_b E(A_1) \qquad \text{(A2.10)}$$

Thus the calculation of the expected value of A from that of A_1 is straightforward, and requires only direct use of eqn. (A2.9). However, the calculation of the expected value of k_o from that of k_1 is not so straightforward.

Writing eqn. (5.11) as $$k_o = k_1 \exp(A_1) \qquad \text{(A2.11)}$$

and proceeding with a (by now familiar) Taylor series analysis results in

$$E(k_o) \doteq E(k_1).\exp(E(A_1)) + \exp(E(A_1)).\{E(k_1)\tfrac{1}{2}\text{var}(A_1)+\text{covar}(k_1,A_1)\} \qquad \text{(A2.12)}$$

and so the estimate of k_o ought not to come from direct substitution of $E(k_1)$ and $E(A_1)$ into eqn.(A2.11). However, for simplicity that imperfect procedure is used in drawing up the tables in chapter 5: the magnitude of the terms in eqn. (A2.12) suggest that the error thus introduced will not be large.

A2.6 Application of QLLS to the adiabatic reactor problem

Eqn.(5.13) is written as

$$\frac{dy_1}{dt} = a y_2 (b-y_1)^n \exp\left(\frac{y_3 y_1}{1 + y_1}\right) \qquad \text{(A2.13)}$$

and has adjoined to it

$$\frac{dy_2}{dt} = 0 = \frac{dy_3}{dt} \qquad \text{(A2.14)}$$

where $y_1 \equiv \theta$; $y_2 \equiv k_1$; $y_3 \equiv A_1$

$a \equiv (J/T_b)^{1-n}$; $b \equiv \theta_m$

For convenience, the uncertainty in a and b is ignored, but it is assumed that $\theta(0)$ is known no more exactly than any of the subsequent $\theta(t_i)$. The initial conditions for eqn.s(A2.13) and (A2.14) therefore are.

$$y_i(0) = y_{io} \ , \quad i = 1,2,3 \ ; \quad \text{where all the } y_{io} \text{ are unknown}$$

Writing the set as $$\frac{d\underline{y}}{dt} = \underline{f}(\underline{y},t) \qquad \text{(A2.15)}$$

$$\underline{y}(0) = \underline{y}_o \qquad \text{(A2.16)}$$

quasilinearisation yields

$$\frac{d\underline{y}^{(1)}}{dt} \doteq \underline{f}^{(0)} + \underline{\underline{J}}^{(0)} (\underline{y}^{(1)} - \underline{y}^{(0)}) \qquad \text{(A2.17)}$$

where $$\underline{\underline{J}} \equiv \frac{\partial \underline{f}}{\partial \underline{y}}$$

The elements of $\underline{\underline{J}}$ are found to be

$$\frac{\partial f_1}{\partial y_1} = \exp\left(\frac{y_3 y_1}{1+y_1}\right) a y_2 (b-y_1)^n \left\{ \frac{y_3}{(1+y_1)^2} - \frac{n}{b-y_1} \right\} \qquad \text{(A2.18)}$$

$$\frac{\partial f_1}{\partial y_2} = \exp\left(\frac{y_3 y_1}{1+y_1}\right) a y_2 (b-y_1)^n \left\{\frac{1}{y_2}\right\} \; ; \; \frac{\partial f_1}{\partial y_3} = \exp\left(\frac{y_3 y_1}{1+y_1}\right) a y_2 (b-y_1)^n \left\{\frac{y_1}{1+y_1}\right\}$$

$$\frac{\partial f_2}{\partial y_1} = 0 = \frac{\partial f_2}{\partial y_2} = \frac{\partial f_2}{\partial y_3} = \frac{\partial f_3}{\partial y_1} = \frac{\partial f_3}{\partial y_2} = \frac{\partial f_3}{\partial y_3}$$

With eqns.(A2.18) and the i.e.'s eqn.(A2.16), the linear o.d.e. eqn.(A2.17) may be solved using the superposition principle

$$\underline{y}^{(1)}(t) = \underline{p}^{(1)}(t) + \sum_{j=1}^{3} c_j^{(1)} h_j^{(1)}(t) \qquad \text{(A2.19)}$$

Note that there are 3 homogeneous solutions corresponding to the 3 unknown i.c.'s.

The particular solution can be generated from eqn. (A2.17)

$$\frac{d}{dt}\underline{p}^{(1)} = \underline{\underline{J}}^{(0)} \underline{p}^{(1)} + \underline{f}^{(0)} - \underline{\underline{J}}^{(0)} \underline{y}^{(0)}$$

with $\underline{p}^{(1)}(0) = \underline{0}$

Note that two of the elements of $\underline{p}$ follow immediately as:

$$p_2^{(1)}(t) = 0 = p_3^{(1)}(t).$$

The homogeneous solutions come from

$$\frac{d}{dt} h_j^{(1)} = \underline{\underline{J}}^{(0)} h_j^{(1)}$$

$$h_{jk}^{(1)}(0) = \delta_{jk} = \begin{cases} 0 & j \neq k \\ 1 & \text{otherwise.} \end{cases}$$

Some of the components follow immediately:

$$h_{12}^{(1)}(t) = 0 = h_{13}^{(1)}(t); \quad h_{23}^{(1)}(t) = 0; \quad h_{22}^{(1)}(t) = 1;$$
$$h_{32}^{(1)}(t) = 0; \quad h_{33}^{(1)}(t) = 1.$$

Minimisation of an unweighted sum of squares criterion:

$$\Phi = \sum_{i=o}^{n} (Y_i - y_1^{(1)}(t_i))^2$$

leads to a set of three linear algebraic equations in three unknowns - the C_j's. The parameter values found are reported in chapter 5. It should be noted that the 'best' value of y_{1O} corresponds to a value of T_O which never differed from the measured value of T_O by more than $\sim 0.2^oC$. Fig. 5.3 shows the convergence region for the method, where the first guess at $\theta(O)$ corresponds to the measured value of T_O.

Confidence analysis. Use was made of eqns.(68-76) of chapter 8 of the text by Rosenbrock and Storey (68), but their eqn.(69) was corrected to read (in their notation)

$\underline{\underline{X}} = \underline{\underline{A}}(t)\underline{\underline{X}}$; $\underline{\underline{X}}(O) = \underline{\underline{I}}$, where $\underline{\underline{I}}$ is the identity matrix.

A2.7 Confidence analysis for weighted residual methods applied to o.d.e.'s non-linear in the parameters

The weighted residual methods lead to estimator equations of the form

$$G(\hat{A}, Y_o, Y_1 \ldots Y_m) = O$$

where A is the parameter, and $Y_o \ldots Y_m$ are the observations, each having the same error variance σ_E^2.

A Taylor series analysis leads to

$$\hat{\sigma_A^2} = \sigma_Y^2 \sum_{i=o}^{m} \left(\frac{\partial G}{\partial Y_i}\right)^2 / \left(\frac{\partial G}{\partial A}\right)^2$$

The method has been applied to the adiabatic reactor problem, but the necessary algebra is lengthy. To test the technique, a simple problem

is worked: estimate the parameter A, given the observation Y_1, from the model

$$Y_1 - \exp\left(\frac{AY_1}{1+Y_1}\right) = 0$$

The result is

σ_{Y_1}	$\sigma_{\hat{A}}$(simulation)	$\sigma_{\hat{A}}$(Taylor Series)
0.1	8.561×10^{-3}	8.563×10^{-3}
1.0	8.65×10^{-2}	8.62×10^{-2}

and clearly the agreement is good.

A2.8: Variance-Covariance analysis for SDM applied to NO oxidation

If in eqns.(5.22) one substitutes $Y_i = y_i + e_i$ and invokes the assumptions listed in appendix A2.9, the estimator equations yield

$$\hat{k}_1 = \frac{A_{22}(y_h-y_o) - A_{12}(y_m-y_h)}{A_{22}A_{11} - A_{12}A_{21}} + \frac{A_{22}e_h-A_{22}e_o-A_{12}e_m+A_{12}e_h}{A_{22}A_{11} - A_{12}A_{21}}$$

$$\hat{k}_2 = \frac{A_{21}(y_h-y_o) - A_{11}(y_m-y_h)}{A_{22}A_{11} - A_{12}A_{21}} + \frac{A_{21}e_h-A_{21}e_o-A_{11}e_m+A_{11}e_h}{A_{22}A_{11} - A_{12}A_{21}} \quad \text{(A2.20)}$$

From these equations it may be shown that SDM is (approximately) unbiased. However, the purpose here is to perform a variance-covariance analysis.

Eqn. (A2.20) may be written as

$$\hat{k}_1 = k_{1)_{true}} + (A_1e_h + B_1e_o + C_1e_m)$$

$$\hat{k}_2 = k_{2)_{true}} + (A_2e_h + B_2e_o + C_2e_m) \quad \text{(A2.21)}$$

where $D \equiv A_{22}A_{11} - A_{12}A_{21}$

and $A_1 \equiv \frac{A_{22} + A_{12}}{D}$; $B_1 = -\frac{A_{22}}{D}$; $C_1 \equiv -\frac{A_{12}}{D}$

$A_2 \equiv \frac{A_{21} + A_{11}}{D}$; $B_2 = -\frac{A_{21}}{D}$; $C_2 \equiv -\frac{A_{11}}{D}$

The error assumptions made are those of section 3.7: the error variance will be denoted by σ_E^2. Since the bias term in eqn.(A2.21) is a weighted sum of errors from the same Normal distribution, it follows that each k has a <u>marginal distribution</u> which is Normal, with mean $k)_{true}$.

Further, assuming that $e_o = 0$ for this particular problem (as was assumed in section 3.7), then the parameter variances follow immediately from eqn.(A2.21):-

$$\begin{aligned} \text{Var}(\hat{k}_1) &= (A_1^2 + C_1^2)\,\sigma_E^2 \\ \text{Var}(\hat{k}_2) &= (A_2^2 + C_2^2)\,\sigma_E^2 \end{aligned} \qquad \text{(A2.22)}$$

as does the covariance

$$\begin{aligned} \text{Covar}(\hat{k}_1,\hat{k}_2) &\equiv E\{(\hat{k}_1 - E(\hat{k}_1)).(\hat{k}_2 - E(\hat{k}_2))\} \\ &= (A_1A_2 + C_1C_2 + A_2C_1 + A_1C_2)\,\sigma_E^2 \end{aligned} \qquad \text{(A2.23)}$$

The parameter cross-correlation coefficient follows immediately from

$$\rho(\hat{k}_1,\hat{k}_2) \equiv \frac{\text{Covar}(\hat{k}_1,\hat{k}_2)}{\text{Var}(\hat{k}_1).\text{Var}(\hat{k}_2)} \qquad \text{(A2.24)}$$

The parameter variances and cross-correlation may thus be calculated (immediately) from eqns.(A2.22),(A2.23) and (A2.24). The only hindrance is that there is no value of σ_E^2 available from replicate data, and so it must be estimated from

$$\sigma_E^2 = \frac{SOS}{m - n_p} \qquad \text{(A2.25)}$$

where m ≡ number of observations (= 14)

n_p = number of parameters (= 2)

and SOS is the sum of squared discrepancies corresponding to the parameter estimates i.e.

$$SOS = \sum_{i=1}^{m} (y(t_i) - Y_i)^2 \Big|_{\underline{k}=\hat{\underline{k}}} \qquad (A2.26)$$

which can be calculated from a single numerical integration of the o.d.e. eqn.(3.12). That integration would anyway be performed so that $y(t_i)$ and Y_i might be compared!

For the problem in hand, using h = 7,

$$SOS = 23.49$$

and so it follows that $Var(\hat{k}_1) = 2.755 \times 10^{-7}$

$$Var(\hat{k}_2) = 7.720 \times 10^{-5}$$

$$\text{and } \rho(\hat{k}_1, \hat{k}_2) = 0.55.$$

A2.9 The approximations used in Appendix A2.8

a. Assuming the errors to be symmetrically distributed with mean zero

$$E(e) = 0, \quad \text{where E is the expectation operator}$$

$$\text{and } E(e^{2n+1}) = 0, \; n = 0,1,2\ldots$$

b. Since the errors are random, they will therefore be both positive and negative, and so tend to cancel when integrated. A reasonable approximation is therefore $\int \underline{e(t)dt = 0}$

This may be derived alternatively by arguing that since E(e(t)) = 0, then $E(\int_D e(t)dt) = 0$, and so $\int_D e(t)dt \doteq 0$ is plausible.

c. A term of the form $\int (y^2+e^2)dt$ may be written as $\int y^2(1 + e^2/y^2)dt$, and so, since $\frac{e}{y} << 1$ for data which are reasonably accurate, $\underline{\int (y^2+e^2)dt \doteq \int y^2 dt}$

d. The approximation $\int \underline{ye\ dt} \simeq 0$ may be shown to be valid by defining $Z \equiv \int e(t)dt$ so that

$$\int ye\ dt = \int y \frac{dZ}{dt} dt = \int y\ dZ$$

$$= yZ - \int Z\ dy = yZ - \int Z \frac{dy}{dt} dt$$

and so, since $Z = 0$ by (b) above and dy/dt is finite, then the result follows.

Alternatively, $E(\int ye\ dt) = \int E(ye)dt$

$= \int y\ E(e)dt$, if e is independent of y

$= 0$

and so the result is plausible.

Using these approximations it can be shown that $\int G_1 dt = \int g_1 dt$ and $\int G_2 dt = \int g_2 dt$ and so the values calculated for A_{11}, A_{12}, A_{21} and A_{22} are (approximately) unbiased.

A2.10 Confidence Region Calculations

a) The $100(1-\alpha)\%$ confidence interval for the parameter k_i $(i=1,2)$ is given by (193)

$$\hat{k}_i - t_{1-\frac{\alpha}{2}} \sqrt{Var(\hat{k}_i)} \leq k_i \leq \hat{k}_i + t_{1-\frac{\alpha}{2}} \sqrt{Var(\hat{k}_i)}$$

where $t_{1-\frac{\alpha}{2}}$ is the t-variate with the appropriate number of degrees of freedom. In the NO oxidation example, there were 14 data points and 2 parameters, so the number of degrees of freedom = 12. Thus, from table C-3 of reference (193), the appropriate value of t is 2.179. The 95% confidence intervals for the SDM method were calculated accordingly.

b) That Q of Eqn.(4.42) follows a χ^2 distribution with 2 degrees of freedom can be proved as shown in equations 10-36 to 10-41 of Deutsch (149). It follows that the 100γ % confidence interval

$$\text{Prob}\{0 < Q < Q_*\} = \gamma$$

can be computed with the aid of the probability density function.

$$p(\chi^2) = \begin{cases} \dfrac{1}{2^{\nu/2}\Gamma(\frac{\nu}{2})} (\chi^2)^{(\frac{\nu}{2} - 1)} \exp(-\chi^2/2) & ; \quad \chi^2 > 0 \\ 0 & ; \quad \chi^2 \leq 0 \end{cases}$$

where ν = number of degrees of freedom.

Combining these equations, and recalling that Q is distributed as χ^2

$$\text{Prob}\{0 < Q < Q_*\} = \text{Prob}\{\chi^2 \leq \chi^2_*\} .$$

$$= \frac{1}{2^{\nu/2}\Gamma(\frac{\nu}{2})} \int_0^{\chi^2_*} (\chi^2)^{(\frac{\nu}{2} - 1)} \exp(-\frac{\chi^2}{2}) \, d\chi^2 = \gamma \quad \text{(A2.27)}$$

Now ν is known - $\nu = 2$ - and for a 95% confidence region, $\gamma = 0.95$. Eqn.(A2.27) is now an equation in one unknown χ^2_*. The root of the equation is tabulated as a function of ν and γ, for instance in table C-2 of Himmelblau (193).

For $\nu = 2$ and $\gamma = 0.95$, one may read $\chi^2_* = 5.991$, whence $Q_* = 5.991$.

So the 95% joint confidence region for k_1 and k_2 corresponds to

$$\text{Prob}\{Q < 5.991\} = 0.95$$

and the boundary of the region is given by eqn.(5.27).

A2.11. Variance-Covariance analysis for LSRM applied to the NO problem

The analysis is performed using a Taylor series approach as outlined in section 4.8, and invoking the error assumptions of section 3.7.

The estimator equations are written in the form

$$\hat{k}_j = \Phi_j(\underline{e}) \quad ; \quad j = 1,2$$

Expanding in Taylor series about $\underline{e} = \underline{0}$ yields

$$\hat{k}_j = \Phi_j(\underline{o}) + \sum_{i=1}^{m} \left(\frac{\partial \Phi_j}{\partial e_i}\Big|_{\underline{e}=\underline{o}}\right) e_j + \tfrac{1}{2} \sum_{i=1}^{m} \left(\frac{\partial^2 \Phi_j}{\partial e_i^2}\Big|_{\underline{e}=\underline{o}}\right) e_j^2 + \ldots . \quad \text{(A2.28)}$$

Truncating eqn.(A2.28) after the second term on the RHS, and taking variances -

$$\text{Var}(\hat{k}_j) \doteq \sigma_E^2 \sum_{i=1}^{m} \left(\frac{\partial \Phi_j}{\partial e_i}\Big|_{\underline{e}=\underline{o}}\right)^2 \quad \text{(A2.29)}$$

Truncating eqn.(A2.28) after the second term and taking the covariance -

$$\text{Covar}(\hat{k}_1, \hat{k}_2) \doteq \sigma_E^2 \sum_{i=1}^{m} \left\{\left(\frac{\partial \Phi_1}{\partial e_i}\right)_{\underline{e}=\underline{o}} \cdot \left(\frac{\partial \Phi_2}{\partial e_i}\Big|_{\underline{e}=\underline{o}}\right)\right. \quad \text{(A2.30)}$$

Truncating eqn.(A2.28) after the third term and taking expectations

$$E(\hat{k}_i) \doteq \Phi(\underline{o}) + \tfrac{1}{2} \sigma_E^2 \sum_{j=1}^{m} \left(\frac{\partial^2 \Phi_i}{\partial e_j^2}\Big|_{\underline{e}=\underline{o}}\right) \quad \text{(A2.31)}$$

Eqn(A2.31) in principle allows one to attempt a 'bias compensation' calculation, while eqns.(A2.30) and (A2.31) permit the approximate calculation of the parameter marginal variances and covariance: see below.

Details of the Calculation

First, the trapezoidal rule - eqn.(4.6) - is written in the form

$$\int_o^{t_m} G \, dt \doteq \tfrac{1}{2}\{G_m(t_m - t_{m-1}) + G_o(t_1 - t_o) + \sum_{i=1}^{m-1} G_i(t_{i+1} - t_{i-1})\} \quad \text{(A2.32)}$$

and eqn.(3.12) as

$$dy/dt = k_1(a-y)(b-y)^2 - k_2 y^2$$

so that $(a,b) = (126.2, 91.9)$

Then, recalling that $e_o = 0$, substituting $(y_i + e_i)$ for Y_i, and using the notation of eqn.(5.29)

$$D_1 = ab^2(y_m+e_m) - \tfrac{1}{2}b(b+2a)(y_m+e_m)^2 + \tfrac{1}{3}(a+2b)(y_m+e_m)^3 - \tfrac{1}{4}(y_m+e_m)^4$$

(A2.33)

$$D_2 = \frac{1}{3}(y_m+e_m)^3; \quad B_{22} = \tfrac{1}{2}\{(y_m+e_m)^4(t_m-t_{m-1}) + y_o^4(t_1-t_o) + \sum_{i=1}^{m-1}(y_i+e_i)^4 \cdot (t_{i+1}-t_{i-1})\}$$

B_{11} approximates: $\int_o^{t_m} \{(ab^2)^2 - 2(ab^2)(2ab+b^2)Y + \{(2ab+b^2)^2 + 2ab^2(a+2b)\}Y^2$

$$+\{-2ab^2 - 2(2ab+b^2)(a+2b)\}Y^3 + \{(a+2b)^2 + 2(2ab+b^2)\}Y^4$$

$$- \{2(a+2b)\}Y^5 + Y^6\}\, dt$$

$$= \int_o^{t_m} (\alpha_o + \alpha_1 Y + \alpha_2 Y^2 + \alpha_3 Y^3 + \alpha_4 Y^4 + \alpha_5 Y^5 + \alpha_6 Y^6)\, dt \qquad \text{(A2.34)}$$

in an obvious notation

whence, using (A2.32)

$$B_{11} = \tfrac{1}{2}\{\{\alpha_o + \alpha_1(y_m+e_m) + \alpha_2(y_m+e_m)^2 + \alpha_3(y_m+e_m)^3 + \alpha_4(y_m+e_m)^4 + \alpha_5(y_m+e_m)^5 + \alpha_6(y_m+e_m)^6\}$$

$$\times (t_m - t_{m-1}) + \{\alpha_o + \alpha_1 y_o + \alpha_2 y_o^2 + \alpha_3 y_o^3 + \alpha_4 y_o^3 + \alpha_4 y_o^4 + \alpha_5 y_o^5 + \alpha_6 y_o^6\} \times (t_1 - t_o)$$

$$+ \sum_{i=1}^{m-1} \{\alpha_o + \alpha_1(y_i+e_i) + \alpha_2(y_i+e_i)^2 + \alpha_3(y_i+e_i)^3 + \alpha_4(y_i+e_i)^4 + \alpha_5(y_i+e_i)^5 + \alpha_6(y_i+e_i)^6\}$$

$$\times (t_{i+1} - t_{i-1})\} \qquad \text{(A2.35)}$$

and similarily

$$B_{12} = \tfrac{1}{2}\{\{\beta_2(y_m+e_m)^2 + \beta_3(y_m+e_m)^3 + \beta_4(y_m+e_m)^4 + \beta_5(y_m+e_m)^5\} \times (t_m - t_{m-1})$$

$$+\{\beta_2 y_o^2 + \beta_3 y_o^2 + \beta_4 y_o^4 + \beta_5 y_o^5\} \times (t_1 - t_o)$$

$$+ \sum_{i=1}^{m-1} \{\beta_2(y_i+e_i)^2 + \beta_3(y_i+e_i)^3 + \beta_4(y_i+e_i)^4 + \beta_5(y_i+e_i)^5\} \times (t_{i+1} - t_{i-1})\}$$

(A2.36)

where $\beta_2 = ab^2$; $\beta_3 = -(2ab+b^2)$; $\beta_4 = (a+2b)$; $\beta_5 = -1$

Next, eqns.(5.29) are written as

$$\hat{k}_1 = \frac{B_{22}D_1 - B_{12}D_2}{B_{22}B_{11} - B_{12}^2} = \Phi_1(e_1, e_2 \cdots e_m) \qquad (A2.37)$$

$$\hat{k}_2 = \frac{B_{12}D_1 - B_{11}D_2}{B_{22}B_{11} - B_{12}^2} = \Phi_2(e_1, e_2 \cdots e_m)$$

and from these must be found $\frac{\partial \Phi_1}{\partial e_i}$ and $\frac{\partial \Phi_2}{\partial e_i}$

Clearly, $\frac{\partial \Phi_1}{\partial e_i} = \frac{\partial \Phi_1}{\partial B_{22}} \frac{\partial B_{22}}{\partial e_i} + \frac{\partial \Phi_1}{\partial D_1} \cdot \frac{\partial D_1}{\partial e_i} + \cdots\cdots$ (A2.38)

The terms $\frac{\partial B_{22}}{\partial e_i}$ etc. can be found readily from eqns.(A2.33) to (A2.36), and $\frac{\partial \Phi_1}{\partial B_{22}}$ etc. from eqn. (A2.37). After some manipulation one obtains

$$\left.\frac{\partial \Phi_1}{\partial e_i}\right|_{\underline{e}=\underline{o}} = \frac{1}{2D^2}\{4y_i^3(t_{i+1}-t_{i-1})(d_1D-b_{11}N_1)+(2\beta_2 y_i+3\beta_3 y_i^2+4\beta_4 y_i^3+5\beta_5 y_i^4)\cdot$$

$$(t_{i+1}-t_{i-1})(2b_{21}N_1-d_2D) + (\alpha_1+2\alpha_2 y_i+3\alpha_3 y_i^2+4\alpha_4 y_i^3+5\alpha_5 y_i^4+6\alpha_6 y_i^5)\cdot$$

$$(t_{i+1}-t_{i-1})(-b_{22}N_1)\} \quad ; \quad i \neq m \qquad (A2.39)$$

$$\left.\frac{\partial \Phi_1}{\partial e_m}\right|_{\underline{e}=\underline{o}} = \frac{1}{D^2}\{2y_m^3(t_m-t_{m-1})(d_1D-b_{11}N_1)+\tfrac{1}{2}(t_m-t_{m-1})(2\beta_2 y_m+3\beta_3 y_m^2+4\beta_4 y_m^3+5\beta_5 y_m^4)\cdot$$

$$(2b_{21}N_1-d_2D) + \tfrac{1}{2}(t_m-t_{m-1})(\alpha_1+2\alpha_2 y_m+3\alpha_3 y_m+4\alpha_4 y_m^3+5\alpha_5 y_m^4+6\alpha_6 y_m^5)\cdot$$

$$(-b_{22}N_1)+(ab^2-b(b+2a)y_m+(a+2b)y_m^2 - y_m^3)(b_{22}D)+y_m^2(-b_{12}D)\} \qquad (A2.40)$$

$$\frac{\partial \Phi_2}{\partial e_i}\Big|_{\underline{e=o}} = \frac{1}{2D^2}\{4y_i^3(t_{i+1}-t_{i-1})(-b_{11}N_2)+(d_1D+2b_{12}N_2)(2\beta_2 y_i+3\beta_3 y_i^2+4\beta_4 y_i^3$$

$$+ 5\beta_5 y_i^4)(t_{i+1}-t_{i-1})+(-d_2D-b_{22}N_2)(\alpha_1+2\alpha_2 y_i+3\alpha_3 y_i^2+4\alpha_4 y_i^3$$

$$+ 5\alpha_5 y_i^4+6\alpha_6 y_i^5)(t_{i+1}-t_{i-1})\}; \; i \neq m \qquad \text{(A2.41)}$$

$$\frac{\partial \Phi_2}{\partial e_m}\Big|_{\underline{e=o}} = \frac{1}{D^2}\{2y_m^3(t_m-t_{m-1})(-b_{11}N_2)+\tfrac{1}{2}(d_1D+2b_{12}N_2)(t_m-t_{m-1})(2\beta_2 y_m+3\beta_3 y_m^2$$

$$+ 4\beta_4 y_m^3+5\beta_5 y_m^4) + \tfrac{1}{2}(t_m-t_{m-1})(2\alpha_2 y_m+3\alpha_3 y_m^2+4\alpha_4 y_m^3$$

$$+ 5\alpha_5 y_m^4+6\alpha_6 y_m^5)(-d_2D-b_{22}N_2)+(b_{12}D)(ab^2-b(b+2a)y_m$$

$$+(a+2b)y_m^2-y_m^3) - b_{11}D\, y_m^2\} \qquad \text{(A2.42)}$$

where $b_{11} = \int(\alpha_o+\alpha_1 y+\alpha_2 y^2+\alpha_3 y^3+\alpha_4 y^4+\alpha_5 y^5+\alpha_6 y^6)\,dt$

$b_{21} = \int(\beta_2 y^2+\beta_3 y^3+\beta_4 y^4+\beta_5 y^5)\,dt$; $b_{22} = \int y^4 dt$

$d_1 = ab^2 y_m - \tfrac{1}{2}b(b+2a)y_m^2 + \frac{1}{3}(a+2b)y_m^3 - \tfrac{1}{4}y_m^4$; $D = b_{22}b_{11}-b_{21}^2$

$d_2 = \frac{1}{3}y_m^3$; $N_1 = b_{22}d_1-b_{12}d_2$; $N_2 = b_{21}d_1 - b_{11}d_2$

(The integrals of y may be calculated from the profile y(t) calculated using $\hat{k}_1, \hat{k}_2$)

Thus eqns.(A2.39) to (A2.42) permit use of eqns.(A2.29) and (A2.30). The second derivatives

$$\frac{\partial^2 \Phi_j}{\partial e_i^2}$$

may be obtained in a similar way, although the manipulations would be lengthy.

A2.12 Remarks pertaining to the comparison of the GLS and Box-Draper results

Inspection of table 20 reveals that the parameter variances found for the Box-Draper (B-D) method are smaller than for GLS. Since, as explained in section 4.7, the former may be looked upon as an approximation to the latter, this result requires explanation. Investigation has not been pursued far enough to permit a final judgement, but a tentative explanation can be offered, as follows.

Although the procedure for generating Normally distributed variates (Appendix A2.2) is satisfactory, the combination of two variates to yield a bi-variate Normal distribution is sometimes less successful. Eqn.(A2.3) is used to generate variates x_1 and x_2 using 65549 and 65539 as 'seeds', and various values of σ_1^2, σ_2^2 and ρ_E. From the generated distributions of x_1 and x_2, the actual marginal variances and correlation may be calculated - $Var(x_1)$, $Var(x_2)$ and $\rho(x_1,x_2)$ - using samples of 1000 values of each variate. The table below shows that the 'imposed' and 'actual' values agree well on some but not on all occasions.

Imposed ρ_E	$\sigma_1^2 = \sigma_2^2$	$Var(x_1)$	$Var(x_2)$	$\rho(x_1,x_2)$
0.9	10^{-4}	0.969×10^{-4}	0.941×10^{-4}	0.897
0.1	10^{-4}	0.969×10^{-4}	0.965×10^{-4}	0.063

So, in the parameter estimation problem, the error marginal variances and covariance used in GLS may be inappropriate, and so render that method less accurate than B-D.

Of course, this deficiency in the generation of correlated Normally distributed 'errors' does not invalidate the comparisons of LSRM with WLS and B-D, which are, in practice, the important comparisons. But, it does imply that the values of ρ_E reported in tables 19 and 20 should be treated as only approximate values.

Appendix 3. Matters pertaining to the heat transfer investigation

3.1 A two-phase model for heat transfer.

3.2 Confidence analysis and related topics for the stagnant bed.

3.3 Fitting a trigonometric series to voidage data.

3.4 Confidence analysis for model III.

3.5 The analytical solution to the two-dimensional quasi-homogeneous model.

3.6 Fitting of the inlet temperature profile.

3.7 Finite difference solution to the model equations (flow case).

3.8 Confidence region analysis for the flow case.

A3.1 The two-phase model for heat transfer

Define h_e = effective interphase heat transfer coefficient

A_e = effective area for inter-phase heat transfer per unit volume of bed

$\bar{\varepsilon}$ = void fraction of any cylindrical surface in the bed, concentric with the bed ($\bar{\varepsilon}$ is assumed to be independent of r).

Then a heat balance on an annular element of bed results in

$$\frac{d^2T_s}{dr^2} + \frac{1}{r}\frac{dT_s}{dr} = \frac{h_e A_e}{k_{es}(1-\bar{\varepsilon})}(T_s - T_f) \qquad (A3.1)$$

$$\frac{d^2T_f}{dr^2} + \frac{1}{r}\frac{dT_f}{dr} = \frac{h_e A_e}{k_{ef}\bar{\varepsilon}}(T_f - T_s) \qquad (A3.2)$$

where T_s = solid temperature; T_f = fluid temperature

k_{es} = solid effective thermal conductivity; k_{ef} = fluid effective conductivity.

Solution of the o.d.e.'s

Eqns.(A3.1) and (A3.2) are written, in an obvious notation, as

$$\frac{d^2T_s}{dr^2} + \frac{1}{r}\frac{dT_s}{dr} = A_s(T_s - T_f) \qquad (A3.3)$$

$$\frac{d^2T_f}{dr^2} + \frac{1}{r}\frac{dT_f}{dr} = -A_f(T_s - T_f) \qquad (A3.4)$$

Subtracting eqn. (A3.4) from (A3.3) yields

$$\frac{d^2u}{dr^2} + \frac{1}{r}\frac{du}{dr} - M^2u = 0 \qquad (A3.5)$$

where $u \equiv T_s - T_f$

$$M^2 \equiv A_s + A_f \qquad (A3.7)$$

Eqn.(A3.5) is recognised to be a Modified Bessel Equation, and is thus easily solved to yield

$$u(r) = B_1 I_o(Mr) + B_2 K_o(Mr) \qquad (A3.8)$$

where B_1 and B_2 are constants to be determined from the boundary conditions, and

I_o = modified Bessel function of the first kind, of order zero

K_o = modified Bessel function of the second kind, of order zero.

Further, defining $v \equiv k_{es}(1 - \bar{\varepsilon})T_s + k_{ef}\bar{\varepsilon}\,T_f \qquad (A3.9)$

then eqns.(A3.1) and (A3.2) are readily manipulated to yield

$$\frac{d}{dr}\{rv(r)\} = 0 \qquad (A3.10)$$

whence

$$v(r) = B_3 \log r + B_4 \qquad (A3.11)$$

where B_3 and B_4 are determined from the boundary conditions.

Thus, solutions have been obtained for u(r) and v(r) - eqns.(A3.8) and (A3.11) - from which solutions for $T_f(r)$ and $T_s(r)$ are easily obtained from the linear relationships (A3.6) and (A3.9). The only task remaining is to establish the values of B_1 to B_4 from the boundary conditions.

Boundary Conditions

No one set suggests itself as obviously correct. The simplest set would involve equating the phase temperatures at the walls to the wall temperatures, whilst a general set might involve the imposition of an effective wall heat transfer coefficient for each phase, at each wall. Perhaps the most attractive set would equate the solid temperature to the wall temperature, at each wall, but impose a fluid phase effective wall heat transfer at each wall.

Once a set of boundary conditions has been chosen, the complete solution to the problem is obtained as outlined above. The algebra is lengthy, straightforward but of no great interest,and is consequently omitted.

A3.2 Confidence Analysis and related topics for the stagnant bed

The results presented in section 7.5 are obtained from the data sets below:-

	Data Set No.1			Data Set No.2			
Pellet size	6.3 ± 0.3mn			10.1 ± 0.18mm			
Twa	23.3 ± 1.4°C			28.8 ± 0.7°C			
Twb	91.3 ± 1.3°C			134 ± 2.4°C			
	Cross number 1			Cross number 2			
r(mm)	T_{obs}	T_{pred}	ΔT	r(mm)	T_{obs}	T_{pred}	ΔT
10	50.2	47.9	2.3	12	68.7	70.0	-1.3
12	54.0	52.8	1.2	14	77.1	75.3	1.8
14	53.6	56.9	-3.3	16	77.9	79.9	-2.0
16	60.0	60.4	-0.4	18	83.7	84.0	-0.3
18	64.0	63.5	0.5	20	92.3	87.6	4.7
20	63.5	66.4	-2.9	22	91.7	90.9	0.8
22	67.7	68.9	-1.2	24	89.4	93.9	-4.5
24	71.8	71.2	0.6	26	100.1	96.6	3.5
26	76.1	73.3	2.8	28	94.1	99.2	-5.1
28	75.4	75.3	0.1	30	100.8	101.5	-0.7
30	75.0	77.1	-2.1	30	104.4	101.5	2.9
32	81.3	78.9	2.4	30	101.9	101.5	0.4

The confidence analysis is the usual linearisation procedure described by Draper and Smith (148). The error standard deviation is estimated from the "residual sum of squares" (eqn.(A2.25)). The analysis is straightforward once certain derivatives are calculated:-

a) Homogeneous model: error in T

Equation (7.1) is written as

$$T_i = A \log r_i + B = f_i(Bi_a, Bi_b)$$

and the necessary derivatives are

$$\frac{\partial f_i}{\partial Bi_a} = \frac{(Twb-Twa)\beta_a^2}{(\beta_a+\beta_b+\log r_{b/r_a})^2}\{\log r_i + \beta_a - \log r_a\} - A\beta_a^2$$

$$\frac{\partial f}{\partial Bi_b} = \frac{(Twb-Twa)\beta_b^2}{(\beta_a+\beta_b+\log r_{b/r_a})^2}\{\log r_i + \beta_a - \log r_a\}$$

where $\beta_a \equiv \frac{1}{Bi_a}$; $\beta_b \equiv \frac{1}{Bi_b}$

b) Homogeneous model: error in r

Equation (7.1) is re-written as

$$r_i = \exp\left(\frac{T_i-B}{A}\right) = g_i(Bi_a, Bi_b)$$

whence the derivatives are obtained:-

$$\frac{\partial g_i}{\partial Bi_a} = \left\{-\frac{1}{A}\exp\left(\frac{T_i-B}{A}\right)\frac{Twa-Twb}{(\beta_a+\beta_b+\log r_{b/r_a})^2}\left\{\frac{T_i-B}{A} + \beta_a - \log r_a\right\} - \exp\left(\frac{T_i-B}{A}\right)\right\}.$$

$$\{-\beta_a^2\}$$

$$\frac{\partial g_i}{Bi_b} = \left\{-\frac{1}{A}\exp\left(\frac{T_i-B}{A}\right)\frac{Twa-Twb}{(\beta_a+\beta_b+\log r_{b/r_a})^2}\left\{\frac{T_i-B}{A} + \beta_a - \log r_a\right\}\{-\beta_b^2\}\right.$$

c) Composite continuum model: error in T

The measurements are all in the central zone of the bed, so there applies just one of the three eqns.(7.4) viz.

$$T_{m,i} = A_m \log r_i + B_m = F(k_1, k_2)$$

There follow:-

$$\frac{\partial F}{\partial k_1} = A_m \log \frac{s_1}{r_a} + \frac{(-1)(Twb-Twa)\log {}^{s_1}/_{r_a}\{\log r_i + k_1 \log {}^{s_1}/_{r_a} - \log s_1\}}{(k_1 \log {}^{s_1}/_{r_a} - k_2 \log {}^{s_2}/_{r_b} + \log {}^{s_2}/_{s_1})^2}$$

$$\frac{\partial F}{\partial k_2} = \frac{(Twb-Twa)\log({}^{s_2}/_{r_b})\{\log r_i + k_1 \log {}^{s_1}/_{r_a} - \log s_1\}}{(k_1 \log {}^{s_1}/_{r_a} - k_2 \log {}^{s_2}/_{r_b} + \log {}^{s_2}/_{s_1})^2}$$

d) Composite continuum model: error in r

The relevant equation is

$$r_i = \exp\left(\frac{T_{m,i} - B_m}{A_m}\right) = G(k_1, k_2)$$

so that

$$\frac{\partial G}{\partial k_1} = -\frac{1}{A_m} \exp\left(\frac{T_{m,i} - B_m}{A_m}\right)\left\{\frac{(-1)(Twb-Twa)\log({}^{s_1}/_{r_a})}{(k_1 \log {}^{s_1}/_{r_a} - k_2 \log {}^{s_2}/_{r_b} + \log {}^{s_2}/_{s_1})^2}\right.$$

$$\left.\left\{\frac{T_{m,i} - B_m}{A_m} + k_1 \log {}^{s_1}/_{r_a} - \log s_1\right\} + A_m \log {}^{s_1}/_{r_a}\right\}$$

$$\frac{\partial G}{\partial k_2} = -\frac{1}{A_m} \exp\left(\frac{T_{m,i} - B_m}{A_m}\right)\left\{\frac{(Twb-Twa)\log {}^{s_2}/_{r_b}}{(k_1 \log {}^{s_1}/_{r_a} - k_2 \log {}^{s_2}/_{r_b} + \log {}^{s_2}/_{s_1})^2}\right.$$

$$\left.\left\{\frac{T_{m,i} - B_m}{A_m} + k_1 \log {}^{s_1}/_{r_a} - \log s_1\right\}\right\}$$

A3.3 Fitting a trigonometric series to voidage data

It is well known (v Karman and Biot) that a trigonometric series

$$S_n(Z) = \sum_{m=1}^{n} a_m \sin mZ + \sum_{m=o}^{n} b_m \cos mZ \qquad \text{(A3.12)}$$

may be used to represent some function f(Z) over the range $0 < Z < 2\pi$, and that the coefficients a_m and b_m which yield a 'best fit' in the least-squares sense are given by

$$b_o = \frac{1}{2\pi} \int_o^{2\pi} f(Z)\,dZ$$

$$b_m = \frac{1}{\pi} \int_o^{2\pi} f(Z) \cos mZ\, dZ \qquad m > 0 \qquad \text{(A3.13)}$$

$$a_m = \frac{1}{\pi} \int_o^{2\pi} f(Z) \sin mZ\, dZ$$

Values for voidage as a function of radial position were obtained as described in section 7.8, and an attempt was made to 'fit' this data using the procedure described above, having 'normalised' the radial co-ordinate to the range $0-2\pi$. The trigonmetric (or Fourier) series was chosen because of the cyclic variation of ε (the voidage) with r (the radial co-ordinate).

Integration. Since the experimental data are discrete rather than continuous, a suitable approximate method must be used to calculate the integrals in (A3.13). Tranter has reported a procedure due to Filon which is particularly well suited to this task. After some manipulation, there results

$$b_o \doteq \frac{1}{2\pi}\,\frac{h}{3}\{f(o) + 2\sum_{k=1}^{p-1} f(2kh) + 4\sum_{k=1}^{p} f((2k-1)h) + f(2ph)\}$$

$$b_m \doteq \frac{1}{\pi}\, h\,\{\beta C + \gamma D\} \qquad m > 0$$

$$a_m \doteq \frac{1}{\pi}\, h\,\{\beta S + \gamma T\}$$

where the range $0\text{-}2\pi$ has been divided into $2p$ equal sub-intervals of width h, and

$$C \equiv 2\sum_{k=1}^{p} f(2kh)\cos(m\,2kh); \quad D \equiv \sum_{k=1}^{p} f((2k-1)h)\cos(m(2k-1)h)$$

$$S \equiv 2\sum_{k=1}^{p} f(2kh)\sin(m2kh); \quad T \equiv \sum_{k=1}^{p} f((2k-1)h)\sin(m(2k-1)h)$$

$$\beta \equiv \frac{1+\cos^2\theta}{\theta^2} - \frac{2\sin\theta\cos\theta}{\theta^3} \;; \quad \gamma \equiv \frac{4}{\theta^3}(\sin\theta - \theta\cos\theta); \quad \theta \equiv mh.$$

The reduction to this form involves the assumption that $f(O) = f(2\pi)$, which holds for the experimental data since the voidage at each wall is identically 1.

Results. The results of using the technique reported in the above paragraphs are unsatisfactory. Although the data are well fitted far from the wall, the fit is much poorer nearer the wall, which is the region of most interest. Further, the procedure cannot produce a 'fit' consistent with the voidage being 1 at the walls.

Improved procedure. A much better 'fit' is achieved as follows. Instead of 'fitting' ε an attempt is made to 'fit' $(1-\varepsilon)$, the solid fraction, and this is normalised over the range $0-\pi$, instead of $0-2\pi$. The reflection of $(1-\varepsilon)$ about the Z-axis is constructed on the range $\pi-2\pi$, and adjoined to the function $(1-\varepsilon)$ in $0-\pi$. This new composite function on $0-2\pi$ is then'fitted' with a trigonometric series.

It is simple to show that the terms in cos mZ vanish i.e. that $b_o = 0 = b_1 = ...b_m$, leaving

$$1 - \varepsilon(Z) = \sum_{m=1}^{n} a_m \sin mZ.$$

from which it follows, as required, that

$$1 - \varepsilon(Z) = 0 \text{ at } Z = 0 \text{ and } Z = \pi$$

This procedure results in a much more satisfactory 'fit': the coefficients a_m derived for the average values from tables 44 and 45 are tabulated below, along with the sum-of-squared discrepancies (SOS), and the maximum discrepancy (MAX).

M	SOS	MAX	A
1	1.3492@ 0	4.01@ -1	7.87072590@ -1
2	1.3480@ 0	3.94@ -1	-9.4897000@ -3
3	4.5403@ -1	2.40@ -1	2.7329648@ -1
4	4.5372@ -1	2.40@ -1	-3.8627222@ -3
5	6.6431@ -2	1.34@ -1	1.8119825@ -1
6	5.6429@ -2	1.14@ -1	-2.9404648@ -2
7	1.7837@ -2	6.05@ -2	-5.7491488@ -2
8	1.4188@ -2	6.05@ -2	-1.6513794@ -2
9	7.9199@ -3	4.84@ -2	2.3983159@ -2
10	7.2918@ -3	4.54@ -2	6.0926901@ -3
11	6.6943@ -3	3.94@ -2	6.2261988@ -3
12	4.5096@ -3	3.94@ -2	-1.3932663@ -2
13	4.3725@ -3	3.69@ -2	-2.5268376@ -3
14	3.9681@ -3	3.46@ -2	-4.6502840@ -3
15	2.9098@ -3	2.32@ -2	9.0188338@ -3
16	2.8189@ -3	2.67@ -2	1.7609843@ -3
17	2.4024@ -3	2.52@ -2	-5.8857097@ -3
18	2.3156@ -3	2.28@ -2	-2.3899750@ -3
19	1.6692@ -3	2.45@ -2	6.5840201@ -3
20	1.4353@ -3	2.20@ -2	2.9131761@ -3
21	1.4097@ -3	2.10@ -2	1.3764082@ -3
22	1.3986@ -3	2.13@ -2	5.5763818@ -4
23	6.6473@ -4	1.72@ -2	-4.2158968@ -3

References.

V. Karman T. and Biot M.A., "Mathematical Methods in Engineering", McGraw-Hill, N.Y., 1940.

Tranter C.J., "Integral Transforms in Mathematical Physics", Methuen, London, 1951.

3.4 Confidence analysis for model III

The model equation is eqn. (7.13), and θ may be written, in general, as a function of $\underline{\alpha}$, an n_p-vector of parameters

$$\theta(r) \equiv \int_{r_a}^{r} \frac{dr}{r\Phi(r,\underline{\alpha})} \qquad \text{(A3.14)}$$

The analysis requires determination of

$$\hat{\underline{\underline{X}}} \equiv \begin{bmatrix} \hat{x}_{11} & \cdots\cdots & \hat{x}_{1,n_p} \\ & & \\ \hat{x}_{m,1} & \cdots\cdots & \hat{x}_{m,n_p} \end{bmatrix}$$

where $\hat{x}_{ij} \equiv \left.\frac{\partial T}{\partial \alpha_j}\right|_{r_i,\hat{\underline{\alpha}}}$

It follows from eqns. (A3.14) and (7.13) that

$$\hat{x}_{ij} = -\frac{(Twb-Twa)}{\theta^2(r_b)}\left\{\theta(r_b)\int_{r_a}^{r_i}\frac{\Psi_j dr}{r\Phi^2(r,\underline{\alpha})} - \theta(r_i)\int_{r_a}^{r_b}\frac{\Psi_j dr}{r\Phi^2(r,\underline{\alpha})}\right\}$$

$$\text{where } \Psi_j \equiv \frac{\partial\Phi}{\partial\alpha_j}$$

For the particular case of the parallel resistances model, there is only one parameter as shown in eqns.(7.14) and (7.15), and the above equation specialises to

$$\hat{x}_i = -\frac{Twb-Twa}{\theta^2(r_b)} \{\theta(r_b)\ \Omega\ (r_i) - \theta(r_i)\ \Omega\ (r_b)\}$$

where $\Omega\ (r_i) \equiv \int_{r_a}^{r_i} \frac{\varepsilon(r)dr}{r\{(\alpha-1)\varepsilon(r) + 1\}^2}$

The variance of $\hat{\alpha}$ is given by

$$\sigma^2(\hat{\alpha}) = \frac{\sigma^2_E}{\sum_{i=1}^{m} (\hat{x}_i)^2}, \quad \text{with } \sigma^2_E \text{ calculated from eqn.(A2.25).}$$

A3.5 The analytical solution to the two-dimensional quasi-homogeneous model

Equation (8.15) is, in full

$$T(r,Z) = T_\infty(r) + \sum_{n=1}^{\infty} A_n \exp\left(-\frac{\lambda_n^2 d_p Z}{Pe}\right)\left\{J_o(\lambda_n r) - \frac{\beta_{1n}}{\beta_{2n}} Y_o(\lambda_n r)\right\}$$

where $\beta_{1n} \equiv Bi_a J_o(\lambda_n r_a) + \lambda_n r_a J_1(\lambda_n r_a)$

$\beta_{2n} \equiv Bi_a Y_o(\lambda_n r_a) + \lambda_n r_a Y_1(\lambda_n r_a)$

$\beta_{3n} \equiv Bi_b Y_o(\lambda_n r_b) - \lambda_n r_b Y_1(\lambda_n r_b)$

$\beta_{4n} \equiv Bi_b J_o(\lambda_n r_b) - \lambda_n r_b J_1(\lambda_n r_b)$

The infinite set of real, distinct eigenvalues, λ_n, is determined from the roots of the transcendental equation:

$$\beta_{1n}\beta_{3n} - \beta_{2n}\beta_{4n} = 0.$$

The constants A_n need to be calculated from the initial condition $T_{IN}(r)$. Except for the case $T_{IN}(r)$ = constant, a calculation must be performed based on the assumption that $\{T_{IN}(r) - T_\infty(r)\}$ can be expanded in a uniformly convergent Bessel series on the interval (r_a, r_b). A computational problem arises for large n since the eigenfunctions R_n of eqn.(8.15) are not orthogonal on that interval.

A second problem which arises in the use of the analytical solution (eqn.(8.15)) is that, for small bed depths, a large number of terms in the infinite series must be evaluated.

A3.6 Fitting of the inlet temperature profile

Both the measured temperatures and the radial co-ordinate are first transformed to dimensionless form:-

$$t_i \equiv \frac{T_i - Twa}{Twb - Twa} \quad ; \quad y_i \equiv \frac{r_i - r_a}{r_b - r_a}$$

Next, t is written as a trinomial in y

$$t = a_1 y^j + a_2 y^k + a_3 y^l$$

and the values of a_1, a_2 and a_3 established by unweighted least squares:-

$$\text{Min}\{\Phi = \sum (t_i - a_1 y_i^j - a_2 y_i^k - a_3 y_i^l)$$

The 'normal equations' are

$$a_1 \sum y_i^{j+j} + a_2 \sum y_i^{k+j} + a_3 \sum y_i^{l+j} = \sum t_i y_i^j$$

$$a_1 \sum y_i^{j+k} + a_2 \sum y_i^{k+k} + a_3 \sum y_i^{l+k} = \sum t_i y_i^k$$

$$a_1 \sum y_i^{j+l} + a_2 \sum y_i^{k+l} + a_3 \sum y_i^{l+l} = \sum t_i y_i^l$$

and solution of this set of linear equations establishes the values of a_1, a_2 and a_3.

Various combinations of values for (j,k,l) were tried, and the set (0,2,3) was found to be satisfactory. A sample plot of fitted and measured values is shown in figure A3.6.1. The coefficients determined for each series are shown below.

Series	a_1	a_2	a_3
7	-1.412192×10^{-2}	7.692138×10^{-5}	4.132036×10^{-1}
8	-3.175861×10^{-2}	-7.975334×10^{-2}	4.598648×10^{-1}
9	-2.418147×10^{-2}	-1.619457×10^{-1}	5.048273×10^{-1}
10	-1.956348×10^{-2}	-1.105705×10^{-1}	4.703279×10^{-1}
11	-2.195369×10^{-2}	-3.843628×10^{-2}	4.341843×10^{-1}
12	9.412518×10^{-3}	6.667680×10^{-2}	3.605513×10^{-1}

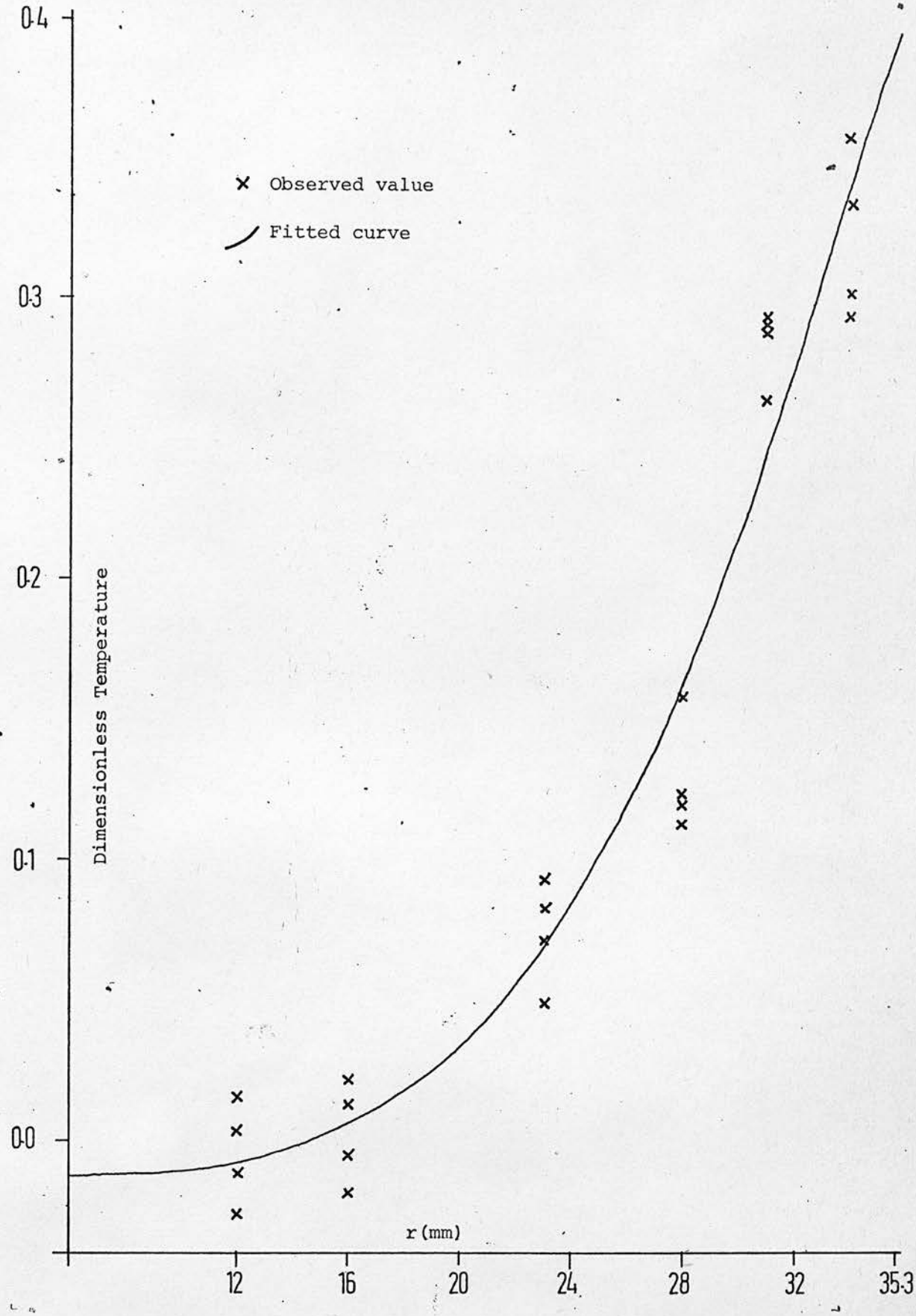

FIGURE A3·6·1 Fitting Of Inlet Profile [Series 7]

A3.7 Finite difference solution to the model equations (flow case)

The derivatives are replaced by finite-difference analogues (Carnahan et al):-

$$\left.\frac{\partial^2 T}{\partial r^2}\right|_{i,j+\frac{1}{2}} \simeq \theta \frac{T_{i-1,j+1} - 2T_{i,j+1} + T_{i+1,j+1}}{(\Delta r)^2} + (1-\theta)\frac{T_{i-1,j} - 2T_{i,j} + T_{i+1,j}}{(\Delta r)^2}$$

$$\left.\frac{\partial T}{\partial r}\right|_{i,j+\frac{1}{2}} \simeq \frac{1}{2\Delta r}\{\theta(T_{i+1,j+1} - T_{i-1,j+1}) + (1-\theta)(T_{i+1,j} - T_{i-1,j})$$

$$\left.T\right|_{i,j+\frac{1}{2}} \simeq \theta\, T_{i,j+1} + (1-\theta)T_{i,j}$$

$$\left.\frac{\partial T}{\partial Z}\right|_{i,j+\frac{1}{2}} \simeq \frac{1}{\Delta Z}(T_{i,j+1} - T_{i,j})$$

where the mesh spacing is shown below.

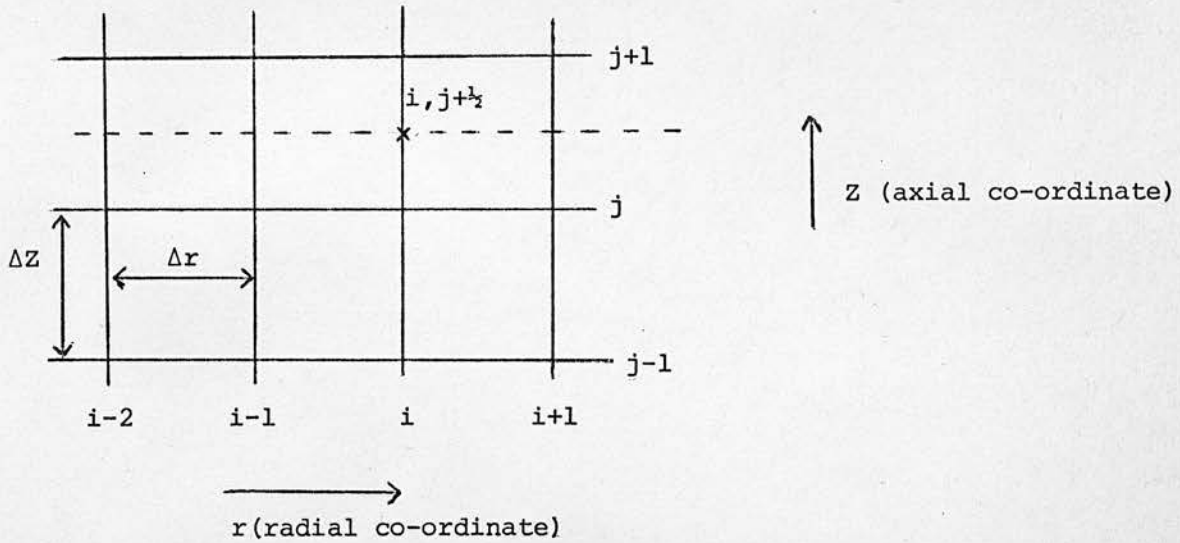

Setting $\theta = \frac{1}{2}$ conforms to the Crank-Nicolson scheme, which is unconditionally stable, of high accuracy and of fair computational simplicity.

These finite difference approximations are then substituted into eqn.(8.5), and manipulated to yield

$$T_{i-1,j+1}\left\{-\frac{\theta}{\beta(\Delta r)^2}+\frac{\theta}{2\beta(\Delta r)r_i}\right\}+T_{i,j+1}\left\{\frac{1}{\Delta Z}+\frac{2\theta}{\beta(\Delta r)^2}\right\}+T_{i+1,j+1}\left\{-\frac{\theta}{\beta(\Delta r)^2}-\frac{\theta}{2\beta(\Delta r)r_i}\right\}$$

$$=T_{i-1,j}\left\{\frac{(1-\theta)}{\beta(\Delta r)^2}-\frac{(1-\theta)}{2\beta(\Delta r)r_i}\right\}+T_{i,j}\left\{\frac{1}{\Delta Z}-\frac{2(1-\theta)}{\beta(\Delta r)^2}\right\}+T_{i+1,j}\left\{\frac{(1-\theta)}{\beta(\Delta r)^2}+\frac{(1-\theta)}{2\beta(\Delta r)r_i}\right\} \qquad \text{(A3.15)}$$

At the bed inlet, where $j = 0$, all the terms on the RHS of this equation are known from the initial condition, eqn.(8.9) and the equation therefore involves only three unknowns, all on the LHS, namely $T_{i-1,1}$, $T_{i,1}$ and $T_{i+1,1}$. Now, eqn.(A3.15) is one of a set of equations, and the set may be solved for all the $T_{i,1}$'s. Those values are then used in the RHS of eqn.(A3.15) when it is applied at the first step into the bed, $j = 1$. The calculation proceeds in this fashion, 'marching' along the bed. It remains only to explain how the equation set is solved at each value of j.

Let the nodes run in the radial direction from $i = 0$ at $r = r_a$, to $i = N$ at $r = r_b$. Consider applying the finite difference approximations to the boundary condition, eqn.(8.10). After some manipulation, there follows

$$T_{-1,j+1}\left(-\frac{\theta}{2\Delta r}\right)=T_{1,j+1}\left(-\frac{\theta}{2\Delta r}\right)+T_{o,j+1}(\alpha_1\theta)+T_{1,j}\left(-\frac{1-\theta}{2\Delta r}\right)+T_{o,j}\{\alpha_1(1-\theta)\}$$

$$-\alpha_1 Twa+T_{-1,j}\left(\frac{1-\theta}{2\Delta r}\right) \qquad \text{(A3.16)}$$

where $T_{-1,j+1}$ is the temperature corresponding to an 'imaginary' point outside the packed bed. Combination of this equation with eqn.(A3.15) applied at i = 0 yields

$$T_{o,j+1}\{\frac{1}{\Delta Z}+\frac{2\theta}{\beta(\Delta r)^2}-(-\frac{\theta}{2\beta(\Delta r)^2}+\frac{\theta}{2\beta(\Delta r)r_o})(\frac{2\Delta r}{\theta})(\alpha_1\theta)\} + T_{1,j+1}\{-\frac{2\theta}{\beta(\Delta r)^2}\}$$

$$= T_{-1,j}\{-\frac{(1-\theta)}{\beta(\Delta r)^2}-\frac{(1-\theta)}{2\beta(\Delta r)r_o}\}+T_{i,j}\{\frac{1}{\Delta Z}-\frac{2(1-\theta)}{\beta(\Delta r)^2}\}+T_{i+1,j}\{\frac{(1-\theta)}{\beta(\Delta r)^2}+\frac{(1-\theta)}{2\beta(\Delta r)r_o}\}$$

$$+\{-\frac{\theta}{\beta(\Delta r)^2}+\frac{\theta}{2\beta(\Delta r)r_o}\}\{\frac{2\Delta r}{\theta}\}\{T_{1,j}(-\frac{1-\theta}{2\Delta r})+T_{o,j}\{\alpha_1(1-\theta)\}-\alpha_1 Twa$$

$$+T_{-1,j}(\frac{1-\theta}{2\Delta r})\} \qquad \text{(A3.17)}$$

Eqn.(A3.17) relates unknown temperatures at the 'new' step, (j+1), to known temperatures at the 'old' step, j. A similar treatment of the other boundary condition, eqn.(8.11), results in

$$T_{N-1,j+1}\{-\frac{2\theta}{\beta(\Delta r)^2}\}+T_{N,j+1}\{\frac{1}{\Delta Z}+\frac{2\theta}{\beta(\Delta r)^2}+(-\frac{\theta}{\beta(\Delta r)^2}-\frac{\theta}{2\beta(\Delta r)y_N}$$

$$(\frac{2\Delta r}{\theta})(-\theta\alpha_2)\}$$

$$= T_{N-1,j}\{\frac{(1-\theta)}{\beta(\Delta r)^2}-\frac{(1-\theta)}{2\beta(\Delta r)r_N}\}+T_{N,j}\{\frac{1}{\Delta Z}-\frac{2(1-\theta)}{\beta(\Delta r)^2}\}+T_{N+1,j}\{\frac{(1-\theta)}{\beta(\Delta r)^2}$$

$$+\frac{(1-\theta)}{2\beta(\Delta r)r_N}\}-\{-\frac{\theta}{\beta(\Delta r)^2}-\frac{\theta}{2\beta(\Delta r)r_N}\}\{\frac{2\Delta r}{\theta}\}\{T_{N-1,j}(\frac{1-\theta}{2\Delta r})$$

$$+T_{N,j}\{-(1-\theta)\alpha_2\}+T_{N+1,j}(-\frac{1-\theta}{2\Delta r})+\alpha_2 Twb\} \qquad \text{(A3.18)}$$

Now, eqns.(A3.15), (A3.16) and (A3.17) may be written, in an obvious, notation, as:-

$$\begin{aligned} b_o T_o + C_o T_1 &= d_o \\ a_i T_{i-1} + b_i T_i + C_i T_{i+1} &= d_i \qquad i = 1(1)N-1 \qquad (A3.19) \\ b_N T_{N-1} + C_N T_N &= d_N \end{aligned}$$

It will be seen that there are (N+1) equations in the (N+1) unknowns T_i, i = O(1)N. These equations are easily solved (as explained below). It should be pointed out that the terms d_o and d_N contain the 'imaginary' variables $T_{-1,j}$ and $T_{N+1,j}$. The values of these are established from eqn. (A3.16) applied at the previous step, and from the corresponding equation at the other boundary. The only difficulty arises on trying to establish values for $T_{-1,O}$ and $T_{N+1,O}$, due to the discontinuity at $r = r_a$, r_b when Z = O. Two different approaches were tried:- i) Set $T_{-1,O}$ = Twa, $T_{N+1,O}$ = Twb and ii) calculate values of $T_{-1,O}$ and $T_{N+1,O}$ from extrapolation of the function $T_{IN}(r)$. Each approach gives the same results after a very few steps along the bed, since the effect of the discontinuity dies away very quickly.

The Thomas Algorithm (Ames) is used to solve the set of equations (A3.19). Since a_i, b_i and C_i are all independent of j, then, before the 'marching' process is begun, one computes

$$bb_i = {}^1/b_i \qquad i = O(1)N$$

$$cc_o = c_o bb_o \; ; \qquad c_N = O$$

$$\left.\begin{aligned} ee_i &= {}^1/(b_i - a_i cc_{i-1}) \\ cc_i &= c_i ee_i \end{aligned}\right\} \qquad i = 1(1)N$$

Now, the d_i are functions of j, so at each step one computes

$$dd_o = d_o bb_o$$

$$dd_i = (d_i - a_i dd_{i-1}) ee_i \qquad i = 1(1)N$$

$$T_N = dd_N$$

$$T_i = dd_i - cc_i T_{i+1} \qquad i = N-1(-1)0$$

and so the values of the T_i's ($T_{i,j+1}$'s) are found.

References:-

Carnahan A., Luther H.A. and Wilkes J.O., "Applied Numerical Methods", Wiley, N.Y., 1969.

Ames W.F., "Numerical Methods for Partial Differential Equations", Nelson, London, 1969.

A3.8 Confidence analysis for the heat equation

A linearised confidence analysis is presented. The uncertainty involved in the measurement of the wall and inlet temperatures is neglected in this analysis because -

i) The analysis is thus simplified.

ii) The major source of uncertainty in the experimental data appears to lie in the measurement of bed temperatures rather than wall or inlet temperatures.

iii) In principle, the measurement of the wall and inlet temperatures could be refined until the error involved is very small, whereas the 'apparent error' in the bed temperatures is believed to be unavoidable. Hence the analysis corresponds to the important limiting case of the smallest joint confidence region which can be achieved using the experimental arrangements adopted here.

The heat equation is written as

$$\frac{\partial T}{\partial Z} - \frac{k_e}{GC_p}\left(\frac{\partial^2 T}{\partial r^2} + \frac{1}{r}\frac{\partial T}{\partial r}\right) = 0 \qquad \text{(A3.20)}$$

with boundary conditions

$$Z > 0, \quad r = r_a; \quad \frac{\partial T}{\partial r} = \frac{h_a}{k_e}(T-Twa) \qquad \text{(A3.21 a)}$$

$$Z > 0, \quad r = r_b; \quad \frac{\partial T}{\partial r} = \frac{h_b}{k_e}(Twb-T) \qquad \text{(A3.21 b)}$$

and initial condition

$$Z = 0; \quad r_a \leq r \leq r_b \; ; \quad T(r) = T_{in}(r) \qquad \text{(A3.21 c)}$$

where, as explained above, Twa, Twb and $T_{in}(r)$ are assumed to be known with negligible uncertainty.

To perform the confidence analysis it is necessary to obtain the 'parameter influence coefficients' i.e. the partial derivatives of the dependent variable, T, with respect to the parameters, k_e, h_a and h_b:

$$\lambda_1 \equiv \frac{\partial T}{\partial k_e} \; ; \quad \lambda_2 \equiv \frac{\partial T}{\partial h_a} \; ; \quad \lambda_3 \equiv \frac{\partial T}{\partial h_b} \qquad \text{(A3.22)}$$

Differentiating eqn.(A3.22) w.r.t. k_e yields

$$\frac{\partial}{\partial k_e}\left\{\frac{\partial T}{\partial Z}\right\} - \frac{\partial}{\partial k_e}\left\{\frac{k_e}{GC_p}\left(\frac{\partial^2 T}{\partial r^2} + \frac{1}{r}\frac{\partial T}{\partial r}\right)\right\} = 0$$

$$\therefore \quad \frac{\partial}{\partial k_e}\left\{\frac{\partial T}{\partial Z}\right\} - \frac{k_e}{GC_p}\left(\frac{\partial}{\partial k_e}\left\{\frac{\partial^2 T}{\partial r^2}\right\} + \frac{\partial}{\partial k_e}\left\{\frac{1}{r}\frac{\partial T}{\partial r}\right\}\right)$$

$$- \left(\frac{\partial^2 T}{\partial r^2} + \frac{1}{r}\frac{\partial T}{\partial r}\right)\frac{1}{GC_p} = 0$$

and reversing the order of differentiation yields

$$\frac{\partial \lambda_1}{\partial Z} - \frac{k_e}{GC_p}\left(\frac{\partial^2 \lambda_1}{\partial r^2} + \frac{1}{r}\frac{\partial \lambda_1}{\partial r}\right) - \frac{1}{GC_p}\left(\frac{\partial^2 T}{\partial r^2} + \frac{1}{r}\frac{\partial T}{\partial r}\right) = 0 \qquad \text{(A3.23)}$$

Similarily, differentiating the boundary conditions, eqns.(A3.21a) and (A3.21b), followed by reversing the order of differentiation yields:

$$r = r_a \; ; \qquad \frac{\partial \lambda_1}{\partial r} = \frac{h_a}{k_e} \lambda_1 - \frac{h_a}{k_e} (T-Twa) \frac{1}{k_e}$$

$$r = r_b \; ; \qquad \frac{\partial \lambda_1}{\partial r} = -\frac{h_b}{k_e} \lambda_1 - \frac{h_b}{k_e} (Twb-T) \frac{1}{k_e} \qquad \text{(A3.24)}$$

Proceeding similarily, there are found

$$\frac{\partial \lambda_2}{\partial Z} - \frac{k_e}{GC_p} \{ \frac{\partial^2 \lambda_2}{\partial r^2} + \frac{1}{r} \frac{\partial \lambda_2}{\partial r} \} = 0$$

$$\frac{\partial \lambda_3}{\partial Z} - \frac{k_e}{GC_p} \{ \frac{\partial^2 \lambda_3}{\partial r^2} + \frac{1}{r} \frac{\partial \lambda_3}{\partial r} \} = 0 \qquad \text{(A3.25)}$$

$$r = r_a ; \; \frac{\partial \lambda_2}{\partial r} = \frac{h_a}{k_e} \lambda_2 + \frac{T-Twa}{k_e} \; ; \; \frac{\partial \lambda_3}{\partial r} = \frac{h_a}{k_e} \lambda_3$$

$$r = r_b ; \; \frac{\partial \lambda_2}{\partial r} = -\frac{h_b}{k_e} \lambda_2 \; ; \; \frac{\partial \lambda_3}{\partial r} = -\frac{h_b}{k_e} \lambda_3 + \frac{Twb-T}{k_e} \qquad \text{(A3.26)}$$

and finally, from the initial condition eqn.(A3.21c), there follows

$$Z = 0, \quad r_a \leq r \leq r_b \; ; \quad \lambda_1 = 0 = \lambda_2 = \lambda_3 \qquad \text{(A3.27)}$$

So, there is now established a set of three p.d.e.'s - eqns. (A3.23) and (A3.25) - with boundary conditions and initial values given by eqns.(A3.24), (A3.26) and (A3.27). The three p.d.e.'s are not coupled together, but are coupled to the original eqn.(A3.20).

The three equations are then solved, numerically, simultaneously with eqn.(A3.20), using the estimated values of the parameters. Then, writing λ_{ij} for the derivative of T w.r.t. the j^{th} parameter at the i^{th}

observation point, the linearised analysis can proceed in the usual way (148), namely by calculating the parameter variance-covariance matrix $\underline{\underline{C}}$ from

$$\underline{\underline{C}} = \sigma_E^2 \, (\hat{\underline{\underline{X}}}^T \hat{\underline{\underline{X}}})^{-1}$$

where

$$\hat{\underline{\underline{X}}} \equiv \begin{bmatrix} \hat{\lambda}_{11} & \hat{\lambda}_{12} & \hat{\lambda}_{13} \\ \hat{\lambda}_{21} & \hat{\lambda}_{22} & \hat{\lambda}_{23} \\ \hat{\lambda}_{m1} & \hat{\lambda}_{m2} & \hat{\lambda}_{m3} \end{bmatrix}$$

, m = total number of observations

and σ_E^2 is calculated as follows:-

a) Var(t) is calculated from eqn. (A2.25).

Thus, for series 7, the residual sum of squares is 1.131, based on 14 x 6 x 5 = 420 data points, and 3 parameters

$$\therefore \text{Var}(t) = \frac{1.131}{417}$$

b) Now

$$t = \frac{T-Twa}{Twb-Twa}$$

$$\therefore \text{Var}(T) = (Twb-Twa)^2 \, \text{Var}(t)$$

Mean values of Twb and Twa are about 120 and 30°C

Thus

$$\text{Var}(T) \doteq 90^2 \, \frac{1.131}{147} = 21.97$$

$$\underline{\text{i.e. } \sigma_E^2 \doteq 21.97^\circ\text{C.}}$$

The values of σ_E^2 used are tabulated below:-

Run No.	Re_p	σ_E^2
7	187	21.97
8	295	17.35
9	445	19.27
10	362	17.43
11	229	21.31
12	117	22.36

Appendix 4: Experimental measurements for the flow case, arranged by angle

(The reported temperatures are in degrees centigrade.)

Series 7: Depth 1 $\bar{T}wb = 117.63$; $\sigma(Twb) = 0.36$

$\bar{T}wa = 27.65$; $\sigma(Twa) = 0.39$

A	B	C	D	E	F
51.7	44.9	42.6	45.4	42.9	43.1
48.3	48.4	45.9	46.3	48.4	49.0
52.3	52.1	51.6	49.7	49.4	51.6
56.2	56.2	55.8	53.0	52.0	58.5
55.5	59.4	53.6	51.6	59.6	59.8
65.7	63.7	56.7	57.0	59.5	58.6
62.2	59.5	67.3	61.9	58.8	68.5
67.0	62.0	61.4	57.1	60.6	68.2
72.3	61.7	61.6	62.9	61.7	67.2
64.6	67.1	71.2	63.6	64.7	67.2
73.3	86.5	74.7	77.4	77.5	81.4
83.3	79.5	71.2	72.7	72.2	77.7
87.5	87.4	77.3	74.8	79.1	80.3
81.8	86.5	94.2	89.5	87.9	81.4

Depth 2 $\bar{T}wb = 117.34$; $\sigma(Twb) = 0.26$

$\bar{T}wa = 31.53$; $\sigma(Twa) = 0.18$

A	B	C	D	E	F
52.5	48.9	48.6	47.5	47.4	48.8
55.5	53.5	49.8	52.3	53.6	51.0
60.3	53.9	55.9	59.1	57.9	62.5
59.1	55.6	59.5	59.0	60.1	62.1
62.2	59.9	58.2	64.6	64.8	62.2
60.0	60.2	64.7	64.4	63.4	71.6
64.9	65.8	69.2	66.6	72.8	71.9
67.2	68.8	69.2	68.1	75.8	73.1
73.5	67.5	74.6	71.1	78.9	74.7
81.8	75.0	78.6	70.9	82.7	78.7
86.1	76.0	89.2	82.9	78.8	75.2
81.8	78.4	90.6	79.9	82.2	79.2
89.1	87.9	88.6	82.8	91.7	89.8
94.2	91.9	96.8	90.6	98.8	87.2

Depth 3

$\overline{T}wb = 116.32$; $\sigma(Twb) = 0.42$

$\overline{T}wa = 34.21$; $\sigma(Twa) = 0.17$

A	B	C	D	E	F
51.4	58.4	52.5	54.9	52.9	56.6
57.2	60.0	61.3	57.6	56.6	60.3
64.2	65.5	61.1	61.5	62.7	63.7
64.1	69.2	64.1	66.1	65.9	66.2
69.4	65.4	70.8	65.2	68.2	75.0
71.8	67.7	71.3	67.6	70.5	69.8
78.2	70.4	71.4	70.5	76.2	72.7
76.8	76.4	74.3	70.6	75.6	76.5
78.8	82.4	74.8	74.6	79.2	76.2
78.6	84.7	84.2	84.1	76.6	77.6
87.4	84.7	89.3	86.1	87.3	91.0
88.1	84.3	86.8	88.7	84.8	87.0
83.2	96.8	83.9	87.3	85.0	79.9
90.9	95.0	94.3	88.1	94.6	89.5

Depth 4

$\overline{T}wb = 118.20$; $\sigma(Twb) = 0.48$

$\overline{T}wa = 26.91$; $\sigma(Twa) = 0.29$

A	B	C	D	E	F
57.4	63.5	56.6	58.6	62.6	63.2
59.1	66.5	61.4	60.0	66.4	66.7
64.2	73.4	68.7	66.5	68.0	71.1
72.4	76.6	75.9	71.7	71.6	78.0
75.6	81.1	79.0	70.7	72.6	78.0
81.4	82.6	80.2	74.1	75.6	82.8
83.8	82.6	82.8	80.3	75.5	81.8
86.4	84.9	84.6	81.0	79.9	88.4
89.8	87.9	85.3	82.6	82.7	88.0
89.0	81.5	82.8	78.5	80.7	84.7
95.8	90.8	88.8	90.3	85.3	89.1
93.2	94.2	94.4	90.8	90.9	88.4
97.5	92.0	93.9	92.6	89.3	92.1
99.4	97.5	100.7	98.7	92.7	98.9

Depth 5 $\bar{T}wb = 119.25$; $\sigma(Twb) = 0.69$

$\bar{T}wa = 27.25$; $\sigma(Twa) = 0.44$

A	B	C	D	E	F
65.3	59.0	56.7	55.7	70.9	68.2
66.8	72.6	73.1	62.6	68.7	67.9
74.8	73.3	71.8	77.0	73.0	67.7
76.5	70.3	64.8	79.2	75.1	72.8
80.5	84.8	75.3	74.0	81.0	74.9
80.0	81.0	80.6	77.8	83.3	78.2
84.0	75.9	79.6	83.4	85.6	81.3
87.5	90.8	88.4	85.7	89.0	87.2
90.5	84.7	90.3	89.0	85.5	88.8
87.3	89.6	83.8	93.5	92.5	90.2
90.2	94.3	93.8	88.6	89.2	95.5
93.0	93.5	92.3	85.6	89.9	92.5
96.0	101.8	94.9	95.5	95.4	93.1
105.3	105.2	101.5	107.3	101.1	100.1

Series 8: Depth 1 $\bar{T}wb = 121.45$; $\sigma(Twb) = 1.27$

$\bar{T}wa = 29.98$; $\sigma(Twa) = 0.67$

A	B	C	D	E	F
42.4	41.2	38.5	38.0	40.0	41.9
44.7	42.8	44.3	43.9	43.4	45.2
47.5	46.9	49.0	44.9	44.6	43.6
44.1	49.7	47.9	47.8	46.2	44.6
46.4	46.1	54.7	49.2	47.8	47.0
54.5	53.6	52.6	53.9	51.4	49.2
54.6	53.7	60.1	60.0	59.0	56.4
61.5	57.3	57.1	55.0	54.6	59.8
59.0	62.8	60.0	59.4	59.1	59.8
56.9	63.4	58.5	64.4	59.0	57.4
70.2	69.9	76.4	70.4	74.4	73.9
74.0	78.8	78.4	76.4	69.2	73.0
80.8	75.8	75.2	72.1	71.5	85.4
82.7	82.6	77.6	78.0	85.7	74.4

Depth 2

$\overline{T}wb = 116.64$; $\sigma(Twb) = 0.64$

$\overline{T}wa = 31.60$; $\sigma(Twa) = 0.22$

A	B	C	D	E	F
43.2	44.6	44.9	46.5	44.0	43.6
46.7	46.4	47.9	46.3	47.2	48.7
54.3	48.0	50.5	51.6	50.6	50.8
54.7	56.1	52.4	54.6	53.7	54.7
58.2	52.9	55.0	57.9	56.1	58.2
56.2	56.4	59.5	59.0	59.3	62.4
58.0	60.0	61.4	60.2	64.7	64.3
60.8	60.0	60.3	62.5	60.4	66.1
71.5	61.1	65.2	65.0	67.7	69.0
76.8	70.3	67.7	67.4	71.7	72.2
82.7	71.9	72.3	72.0	80.8	75.6
76.8	77.8	82.3	80.1	79.3	77.1
77.8	78.3	75.8	78.2	78.6	82.0
87.6	80.5	92.4	80.5	88.3	80.8

Depth 3

$\overline{T}wb = 120.61$; $\sigma(Twb) = 0.90$

$\overline{T}wa = 33.60$ $\sigma(Twa) = 0.22$

A	B	C	D	E	F
48.9	54.0	49.8	52.3	52.7	49.6
57.0	55.1	53.2	60.0	57.2	53.2
62.5	60.9	58.5	64.0	61.1	59.5
66.2	62.8	60.0	61.7	63.4	63.5
65.3	64.6	61.3	69.3	63.1	68.7
66.7	62.6	63.1	69.9	69.6	68.1
74.8	66.2	66.0	72.4	69.7	77.6
70.5	72.1	67.2	76.6	72.1	82.0
73.4	72.7	69.2	78.4	72.2	81.4
77.2	73.8	70.7	69.6	72.7	82.3
81.6	86.6	81.0	84.8	81.9	93.6
82.2	83.1	81.3	86.0	78.4	88.8
81.4	82.3	87.1	88.6	85.9	86.3
95.9	93.2	92.9	91.6	87.3	99.4

Depth 4

$\overline{T}wb = 121.34$; $\sigma(Twb) = 0.44$

$\overline{T}wb = 25.82$; $\sigma(Twb) = 0.42$

A	B	C	D	E	F
53.4	58.0	52.0	54.0	57.9	57.6
59.5	61.3	57.6	59.4	60.0	63.8
64.9	65.9	61.9	62.5	56.9	69.8
71.5	73.3	64.2	66.4	61.5	69.6
74.8	77.9	74.5	67.5	63.9	74.5
79.5	78.4	78.0	71.9	71.0	77.8
79.4	80.1	77.0	72.9	73.2	79.3
87.1	82.9	80.7	76.0	78.9	88.5
90.0	88.1	82.8	78.2	77.5	88.1
88.4	86.1	81.0	77.0	74.9	78.5
94.2	93.2	90.9	89.3	85.0	85.1
92.6	90.5	91.7	90.1	87.2	88.6
96.7	91.2	82.5	86.2	91.8	93.6
96.0	95.8	101.1	97.6	92.8	91.2

Depth 5

$\overline{T}wb = 121.01$; $\sigma(Twb) = 0.59$

$\overline{T}wa = 29.70$; $\sigma(Twa) = 0.41$

A	B	C	D	E	F
63.6	68.2	59.6	61.1	63.2	67.7
72.7	65.5	61.1	65.1	67.8	71.1
67.2	72.4	73.3	71.8	73.1	75.0
70.4	71.3	74.1	74.3	77.2	80.8
79.6	74.6	74.1	78.7	83.1	81.9
78.9	78.1	80.4	85.1	79.7	87.4
80.8	80.0	83.5	81.3	89.6	89.7
94.1	89.6	83.8	85.1	86.2	90.2
78.0	93.1	87.4	88.3	87.8	92.3
87.7	90.2	82.6	89.1	89.6	94.0
90.5	95.2	93.3	90.7	94.8	97.8
90.7	90.7	91.2	92.8	92.2	95.5
102.3	100.7	99.2	95.6	98.6	96.1
102.0	98.7	97.8	100.6	106.2	108.4

Series 9: Depth 1

$\overline{T}wb = 120.28$; $\sigma(Twb) = 0.34$

$\overline{T}wa = 30.39$; $\sigma(Twa) = 0.46$

A	B	C	D	E	F
38.9	36.2	35.6	37.9	34.6	37.0
40.4	39.9	39.1	37.8	38.9	38.8
40.3	39.4	39.9	39.7	38.1	38.7
41.8	41.1	44.8	42.9	40.0	40.8
43.3	44.1	44.6	43.7	43.0	40.6
46.1	48.5	51.2	44.3	47.2	49.5
52.9	49.5	47.8	50.0	42.4	53.6
48.1	46.6	47.5	45.4	50.1	46.2
55.3	53.0	54.0	51.7	46.6	50.4
59.3	56.2	56.5	51.1	52.3	53.2
68.0	69.3	67.3	66.9	61.6	61.9
69.5	66.9	66.9	65.0	71.6	68.2
71.3	67.3	62.1	68.8	64.6	66.4
72.4	80.9	78.8	83.2	56.1	76.4

Depth 2

$\overline{T}wb = 117.66$; $\sigma(Twb) = 1.28$

$\overline{T}wa = 28.50$; $\sigma(Twa) = 0.48$

A	B	C	D	E	F
38.4	38.6	46.4	36.6	39.3	41.5
42.4	41.8	42.4	40.3	39.5	43.0
53.7	47.2	45.3	42.8	42.2	44.1
47.8	46.2	48.7	49.7	45.8	47.4
53.3	48.2	45.2	51.1	46.1	51.3
51.7	50.4	54.3	60.2	48.3	51.4
53.7	48.7	51.3	48.4	52.7	54.1
64.8	57.3	54.5	60.8	52.2	59.6
62.8	58.2	60.0	59.4	58.4	59.1
66.6	58.2	65.5	62.9	58.1	63.0
75.4	69.9	67.1	65.7	68.6	70.7
69.6	75.7	66.9	72.9	66.5	66.3
78.2	75.8	68.3	80.1	67.6	76.3
83.8	73.5	81.8	74.9	70.4	73.8

Depth 3

$\overline{T}wb = 121.03$; $\sigma(Twb) = 0.63$

$\overline{T}wa = 27.25$; $\sigma(Twa) = 0.40$

A	B	C	D	E	F
38.9	41.4	39.1	37.6	43.8	40.6
47.1	46.2	47.1	45.1	44.1	46.5
51.8	49.8	50.9	47.1	48.3	45.3
51.0	51.6	53.2	50.8	55.7	50.8
57.9	56.5	54.9	57.3	56.1	53.6
64.8	60.3	62.6	59.1	57.4	57.3
61.6	70.0	63.1	58.6	52.3	65.8
60.3	72.8	65.9	65.0	58.6	61.9
69.6	63.3	68.1	63.3	67.3	61.8
65.7	64.4	65.2	62.0	67.6	64.8
75.1	81.4	77.8	76.9	73.2	79.6
83.8	80.7	77.4	77.9	76.8	79.8
74.0	82.2	75.7	84.5	76.6	78.4
78.6	92.4	86.4	88.5	77.6	91.1

Depth 4

$\overline{T}wb = 119.75$; $\sigma(Twb) = 0.50$

$\overline{T}wa = 27.03$; $\sigma(Twa) = 0.24$

A	B	C	D	E	F
52.9	54.3	47.1	50.4	51.3	51.1
59.7	57.9	52.5	54.2	53.9	54.2
63.9	61.2	56.4	59.3	58.6	59.3
70.0	66.5	65.2	60.0	60.8	64.6
71.4	70.8	66.6	61.2	60.8	60.5
74.8	73.6	71.7	67.0	65.2	64.6
79.2	77.7	76.8	67.8	71.2	70.0
83.8	78.6	75.2	71.8	75.0	71.9
82.7	81.7	76.8	74.5	79.9	71.2
88.0	80.8	73.9	70.5	73.0	75.2
91.2	89.1	90.1	81.6	82.1	84.3
86.2	89.5	90.1	85.2	83.2	83.0
92.8	89.1	91.8	80.1	77.5	82.7
94.7	91.8	92.9	84.3	87.2	90.7

Depth 5 $\bar{T}wb = 123.53$; $\sigma(Twb) = 0.61$

$\bar{T}wa = 30.54$; $\sigma(Twa) = 0.36$

A	B	C	D	E	F
62.7	61.5	59.2	55.3	58.2	75.0
63.1	65.5	64.0	61.6	64.2	70.0
73.4	76.4	63.8	65.6	67.4	70.3
74.2	68.8	67.0	79.5	78.9	79.0
76.7	72.7	75.4	83.4	82.3	76.1
85.3	74.7	73.0	73.6	86.2	81.2
83.4	79.8	73.5	74.8	86.3	83.7
90.3	86.9	85.7	80.5	86.6	90.0
90.3	87.6	81.6	80.3	84.9	88.9
85.0	86.5	79.7	85.0	92.8	89.0
95.1	94.2	85.6	95.0	96.5	92.5
96.3	88.0	84.7	87.4	90.0	94.6
101.2	100.1	96.7	91.4	100.0	90.7
107.6	105.2	94.5	91.8	106.3	103.9

Series 10: Depth 1 $\bar{T}wb = 121.63$; $\sigma(Twb) = 1.08$

$\bar{T}wa = 30.84$; $\sigma(Twa) = 0.64$

A	B	C	D	E	F
43.8	39.1	39.2	40.0	38.6	39.7
41.7	42.2	41.1	42.9	42.0	41.0
41.8	44.6	45.3	42.4	43.5	42.2
45.2	44.9	46.4	44.0	43.5	41.9
51.4	47.7	45.0	43.3	49.2	48.3
56.7	53.1	55.0	48.1	44.4	47.3
53.3	52.4	50.4	53.6	49.9	50.9
51.9	57.8	56.0	50.0	54.2	54.5
55.8	60.8	58.9	61.4	56.0	53.9
62.7	57.8	60.0	60.1	58.2	55.2
74.4	73.3	73.9	71.1	69.3	78.4
71.8	79.0	71.6	66.5	71.1	65.5
68.6	82.3	71.0	65.4	68.1	72.5
73.8	80.8	77.1	86.1	78.8	77.3

Depth 2 $\overline{T}wb = 125.13$; $\sigma(Twb) = 0.52$

$\overline{T}wa = 27.64$; $\sigma(Twa) = 0.46$

A	B	C	D	E	F
45.5	44.4	38.0	42.9	41.3	38.9
47.8	47.8	41.9	47.0	44.5	45.9
51.2	51.1	45.2	49.3	48.4	47.7
51.9	53.8	49.4	52.4	49.8	52.5
55.8	53.6	53.5	53.7	55.0	58.3
53.6	55.7	57.8	57.2	59.9	60.0
58.6	58.9	54.9	57.6	63.0	61.0
70.6	61.1	56.8	58.9	63.6	63.9
70.7	63.6	66.1	61.6	60.1	64.8
75.9	70.6	78.8	65.3	67.5	70.6
78.1	75.1	72.8	70.1	78.8	76.2
71.2	75.5	86.7	81.7	74.5	78.2
88.9	84.0	76.2	75.4	85.2	85.2
89.6	81.8	87.3	78.6	89.7	89.6

Depth 3 $\overline{T}wb = 125.03$; $\sigma(Twb) = 0.40$

$\overline{T}wa = 28.16$; $\sigma(Twa) = 0.25$

A	B	C	D	E	F
44.7	51.6	46.6	41.9	52.3	44.3
52.2	45.6	47.5	50.5	53.1	51.7
57.8	55.2	51.1	48.4	57.1	47.9
59.3	60.0	59.0	58.8	60.1	54.5
62.4	61.7	61.6	62.7	60.0	64.1
60.2	65.2	63.7	68.0	62.1	75.0
63.8	69.5	66.3	66.5	67.4	70.4
65.8	71.3	63.2	71.4	71.0	69.5
70.7	69.4	70.1	69.7	72.1	64.7
69.4	74.5	71.0	73.0	71.6	73.2
86.9	87.3	79.0	82.0	86.6	70.2
82.2	87.3	77.7	84.6	83.0	90.9
79.9	92.0	80.0	85.2	91.1	86.4
90.1	90.0	90.2	94.0	94.5	96.9

Depth 4 $\bar{T}wb = 123.97$; $\sigma(Twb) = 0.29$

$\bar{T}wa = 28.49$; $\sigma(Twa) = 0.37$

A	B	C	D	E	F
55.8	59.5	55.0	57.4	53.0	55.8
62.7	60.0	57.1	59.0	56.3	60.0
73.2	64.3	61.7	63.6	60.6	62.8
78.0	72.7	69.2	65.2	66.0	64.7
78.3	77.3	73.7	67.1	66.9	66.1
79.9	78.2	76.1	70.0	70.9	71.3
81.1	83.5	75.4	73.4	71.4	73.4
87.4	83.2	80.1	76.2	75.7	79.5
93.5	85.3	82.0	80.1	78.2	80.4
90.7	87.1	78.9	76.5	76.4	77.9
94.9	94.0	87.0	87.0	84.1	89.8
90.8	91.6	90.8	89.9	87.8	89.7
96.6	95.1	87.6	83.7	85.8	88.0
98.8	96.3	99.4	94.0	92.4	96.6

Series 11: Depth 1 $\bar{T}wb = 121.34$; $\sigma(Twb) = 0.68$

$\bar{T}wa = 28.80$; $\sigma(Twa) = 0.58$

A	B	C	D	E	F
46.8	50.7	41.8	40.0	41.4	42.7
47.3	48.3	46.1	43.1	46.3	52.9
52.0	50.8	51.9	48.9	48.3	46.8
47.9	54.7	55.8	52.8	47.5	51.9
51.4	48.2	51.5	50.1	51.6	56.3
58.3	59.9	57.3	59.4	55.6	55.4
64.5	64.3	59.4	65.4	62.8	66.4
64.7	61.8	62.6	63.7	58.7	69.6
72.1	60.4	65.7	63.2	59.0	63.2
60.4	72.7	69.9	62.3	60.0	64.6
83.1	73.9	76.1	77.6	73.5	82.0
82.5	73.8	83.6	76.7	70.2	75.8
89.3	82.6	73.3	80.5	75.0	80.6
80.2	88.0	85.5	82.3	91.3	82.7

Depth 2

$\overline{T}wb = 120.98$; $\sigma(Twb) = 0.43$

$\overline{T}wa = 32.27$; $\sigma(Twa) = 0.20$

A	B	C	D	E	F
46.0	48.3	47.9	47.1	46.3	45.6
52.7	50.6	51.5	51.2	52.3	56.4
56.5	51.9	53.7	55.4	56.0	60.8
58.2	55.6	57.4	59.9	58.8	61.9
60.0	59.0	57.3	62.0	60.0	62.8
62.4	60.1	62.9	63.2	62.5	66.8
62.1	61.2	67.8	64.8	71.0	68.4
68.4	65.4	72.1	67.1	75.8	73.6
75.6	65.9	70.3	66.6	78.0	74.1
82.1	76.1	82.9	72.9	80.4	77.1
86.4	80.0	86.9	79.9	85.1	82.6
87.9	78.9	90.9	83.3	84.9	81.6
88.9	84.7	93.2	82.3	93.0	88.5
93.9	89.0	96.9	90.0	95.7	90.2

Depth 3

$\overline{T}wb = 120.19$; $\sigma(Twb) = 0.47$

$\overline{T}wa = 34.64$; $\sigma(Twa) = 0.16$

A	B	C	D	E	F
57.1	56.4	49.8	52.3	54.7	53.7
59.2	59.8	56.9	59.7	60.7	57.5
66.3	63.9	59.1	70.2	63.1	61.0
69.8	65.4	64.6	74.3	66.9	69.7
67.2	68.9	65.3	66.2	67.1	68.6
72.0	71.8	69.3	73.8	69.7	77.2
71.2	68.0	74.4	66.5	73.5	78.8
79.5	75.3	73.0	75.6	70.2	83.5
77.6	80.6	74.4	83.8	81.3	73.5
83.5	77.1	75.3	86.4	79.4	87.5
82.1	81.7	83.5	87.3	86.9	95.1
85.3	81.5	87.6	89.4	88.5	93.9
89.8	87.3	87.8	87.6	91.5	91.7
86.9	85.6	98.5	88.8	90.8	102.4

Depth 4 $\bar{T}wb = 118.90$; $\sigma(Twb) = 0.72$

$\bar{T}wa = 27.29$; $\sigma(Twa) = 0.24$

A	B	C	D	E	F
58.1	63.9	53.2	55.0	59.0	60.0
59.2	65.1	59.5	60.3	62.5	66.9
66.1	69.7	67.4	63.7	65.7	72.1
71.5	74.8	72.6	69.6	69.9	77.4
73.7	79.7	76.2	70.8	71.0	80.8
79.5	81.3	79.0	74.2	72.9	83.7
83.6	83.6	79.5	75.2	75.1	84.6
87.2	84.2	83.1	80.0	80.4	88.1
91.4	87.8	85.5	81.5	80.2	88.8
88.5	86.8	83.4	80.7	77.5	84.8
93.2	93.2	90.3	88.8	86.1	89.4
94.0	90.7	90.5	89.6	83.7	90.3
96.2	92.7	94.7	84.4	92.1	92.4
99.4	98.1	102.3	98.2	92.2	91.7

Depth 5 $\bar{T}wb = 121.50$; $\sigma(Twb) = 0.63$

$\bar{T}wa = 27.22$; $\sigma(Twa) = 0.48$

A	B	C	D	E	F
64.5	73.8	57.4	54.5	67.9	65.4
68.3	71.5	60.6	70.5	73.1	69.0
71.4	68.4	71.0	71.9	73.9	82.4
75.0	70.6	73.4	77.1	78.9	74.2
80.7	77.6	73.1	73.9	82.4	77.7
80.7	82.9	84.4	80.7	85.2	78.4
84.9	87.0	83.6	88.0	84.2	88.2
90.6	90.7	91.0	94.8	85.5	89.6
87.1	80.7	90.4	91.3	88.8	95.3
91.6	91.8	94.3	91.9	93.6	88.3
101.7	93.6	94.8	94.2	91.5	92.8
94.2	92.6	93.2	90.8	93.0	93.7
99.1	101.7	101.4	104.6	94.2	98.8
105.7	106.4	103.5	105.9	105.4	107.9

Series 12: Depth 1

$\overline{T}wb = 125.90$; $\sigma(Twb) = 0.51$

$\overline{T}wa = 30.32$; $\sigma(Twa) = 0.93$

A	B	C	D	E	F
55.2	47.2	56.3	60.0	55.3	54.1
57.1	61.5	62.5	64.0	57.9	58.2
67.1	62.4	61.8	60.0	58.7	61.3
62.7	63.7	61.2	63.0	60.0	61.1
65.1	73.9	62.6	67.6	66.8	60.0
66.8	71.1	76.1	69.7	69.1	73.5
75.4	68.6	69.6	74.4	71.5	75.5
75.8	74.0	75.8	74.8	76.2	71.5
85.4	77.4	81.7	79.0	80.9	75.0
79.1	82.1	80.4	81.0	79.3	81.4
90.9	90.5	84.4	93.5	89.6	82.8
94.7	95.1	92.5	81.2	87.8	89.9
91.3	91.1	89.9	92.3	98.0	84.8
102.7	105.7	93.2	98.8	99.4	106.1

Depth 2

$\overline{T}wb = 125.50$; $\sigma(Twb) = 0.49$

$\overline{T}wa = 32.45$; $\sigma(Twa) = 0.20$

A	B	C	D	E	F
60.0	62.4	51.6	56.7	54.8	60.5
62.9	65.0	60.5	62.9	67.0	61.7
67.7	61.7	62.2	60.0	68.1	68.4
66.5	68.2	66.1	69.7	72.0	73.7
76.5	69.3	73.4	76.4	73.7	79.4
75.5	74.9	80.7	73.8	77.9	76.3
82.1	81.9	80.7	74.6	77.6	76.9
75.1	75.6	84.5	79.0	86.7	85.9
88.2	80.1	81.9	77.2	83.4	79.7
88.8	89.7	82.0	83.3	93.0	86.9
97.4	90.2	99.0	91.6	88.1	95.2
94.0	91.5	99.1	90.8	92.9	90.0
91.4	93.5	100.4	94.0	100.0	98.2
110.0	110.3	105.7	95.9	107.9	98.8

Depth 3 $\bar{T}wb = 119.66$; $\sigma(Twb) = 1.01$

$\bar{T}wa = 33.88$; $\sigma(Twa) = 0.20$

A	B	C	D	E	F
65.9	60.4	58.2	56.6	63.5	57.4
59.3	67.2	70.2	67.9	61.7	56.7
71.5	66.0	70.5	69.2	68.3	64.5
80.0	74.9	73.8	74.6	75.7	73.5
76.2	70.9	75.2	77.1	78.2	76.0
77.6	81.8	84.0	73.1	79.5	78.1
83.6	87.0	83.4	79.6	80.4	85.6
87.2	88.2	82.8	84.3	87.6	81.8
84.2	85.9	83.8	76.6	83.1	84.0
88.1	89.5	86.1	91.0	90.2	92.2
94.2	96.7	92.7	92.4	93.3	93.0
89.9	99.0	92.8	92.8	89.3	89.3
90.6	90.4	94.1	97.4	95.4	91.9
99.1	105.8	102.4	101.6	102.5	106.9

Depth 4 $\bar{T}wb = 120.92$; $\sigma(Twb) = 0.46$

$\bar{T}wa = 28.79$; $\sigma(Twa) = 0.45$

A	B	C	D	E	F
56.6	68.3	55.2	58.8	73.7	65.9
62.7	70.5	64.3	62.8	74.4	67.2
66.9	76.6	75.8	67.8	75.4	69.8
73.2	82.1	81.6	75.1	80.2	76.5
79.7	89.1	86.3	79.3	79.3	77.9
87.6	87.3	86.7	82.3	80.1	81.3
89.3	89.7	87.9	82.3	81.9	78.7
93.3	89.6	89.3	86.7	84.0	88.3
84.4	92.4	89.5	87.6	82.5	87.4
86.6	86.6	85.0	82.2	75.6	84.6
99.3	99.1	90.6	92.5	86.5	93.9
98.6	97.8	94.6	93.7	87.8	90.8
96.9	93.5	93.1	95.3	90.4	96.4
104.3	105.5	103.6	103.2	102.5	97.6

Depth 5 $\overline{T}wb = 121.91$; $\sigma(Twb) = 0.81$

$\overline{T}wa = 28.74$; $\sigma(Twa) = 0.32$

A	B	C	D	E	F
65.7	68.0	56.9	60.4	67.8	70.5
65.5	65.4	71.8	67.1	67.6	73.8
70.4	69.0	73.3	77.5	73.9	70.5
77.0	72.1	80.3	77.8	81.7	79.4
82.5	85.7	83.4	83.5	82.2	82.8
82.5	80.9	78.3	77.1	85.6	90.7
84.8	81.4	79.1	89.3	90.5	83.6
94.7	89.6	92.3	92.9	91.6	92.5
90.5	93.5	91.4	90.1	89.6	95.9
93.9	87.5	90.5	92.3	87.9	90.9
90.1	95.9	93.2	95.4	94.8	96.1
93.0	93.7	86.8	87.3	92.3	92.6
103.4	98.0	101.0	100.6	83.4	89.0
105.8	104.5	108.0	106.5	100.6	107.9

Series 10: Depth 5 $\overline{T}wb = 124.81$; $\sigma(Twb) = 0.46$

$\overline{T}wa = 28.22$; $\sigma(Twa) = 0.49$

A	B	C	D	E	F
55.4	61.4	64.3	62.1	60.0	73.0
66.8	72.0	66.3	62.8	65.5	72.1
76.1	64.5	66.5	68.5	78.3	73.7
74.2	70.2	77.4	75.7	81.8	74.8
83.6	81.3	76.4	75.1	81.1	78.4
81.8	84.3	79.5	76.6	81.5	87.5
83.5	81.2	83.8	78.9	89.2	78.8
83.6	85.1	82.6	84.2	87.7	92.9
93.1	92.1	89.3	86.5	92.7	89.1
87.9	87.5	89.1	91.3	91.2	90.0
101.0	95.7	87.2	95.9	92.3	93.0
92.8	94.0	87.0	89.6	95.6	98.1
94.0	100.5	97.4	100.0	97.9	94.4
108.5	104.6	101.5	96.3	109.2	98.0

Appendix 5: "Mathematical modelling of the exothermic packed bed reactor: application to O-xylene partial oxidation"

by D.L. Cresswell and W.R. Paterson

which appeared in,

Chemical Engineering Science, 25, 1405-1414 (1970).

Chemical Engineering Science, 1970, Vol. 25, pp. 1405–1414. Pergamon Press. Printed in Great Britain.

Mathematical modelling of the exothermic packed bed reactor: application to *o*-xylene partial oxidation

D. L. CRESSWELL and W. R. PATERSON
University of Edinburgh, Edinburgh, Scotland

(*First received* 2 *March* 1970; *in revised form* 13 *April* 1970)

Abstract—The influences of "in-pore" diffusion and film heat and mass transfer on catalyst effectiveness and selectivity are examined for a system of highly exothermic parallel and consecutive reactions, typified, for example, by the partial oxidation of *o*-oxylene to phthalic anhydride. Parametric sensitivity tests reveal a marked dependence of both effectiveness factor and selectivity on the "in-pore" diffusion coefficient, stressing the need for a more accurate estimate of this parameter.

The effect of restricted "in-pore" diffusion rates on temperature "run-away" in a highly exothermic packed-bed reactor is also explored, and it is shown that the yield of desired product may be considerably improved by inviting an appreciable intraparticle diffusion effect, though at the expense of reduced selectivity.

INTRODUCTION

WITH THE increasing importance of gas–solid catalytic reactions in industry, more attention is being given to the development of mathematical models to supplement experiments. The need for such models becomes apparent when one considers the large number of variables that influence reactor performance. In an actual reactor, conversion of reactants and yield of desired product are influenced by the complex interactions of heat transfer, mass transfer and chemical reaction distributed in the gaseous phase, the solid phase and the boundary region between the two phases. Because of the highly exothermic nature of many of these reactions, heat exchange with the surroundings will also be occurring. A rigorous evaluation of reactor behaviour must in principle account for all of these distributed effects.

The highly non-linear nature of the physicochemical system demands that realistic mathematical models be solved by computer. Invariably, the model must be idealised to provide a compromise between excessive complexity and over simplification. In other words, an acceptable balance must be reached between the accuracy of the model and the costs of development and operation of the computer program. The increasing capacity and speed of computers is enabling the scope of mathematical modelling to be greatly extended. Whereas prior analyses have required gross simplifications in the derivation of the descriptive equations and approximate methods of solution (such as linearisation), it is now feasible to solve exactly even the most complex problems. The work of McGuire and Lapidus [1] on the dynamic behaviour of packed tubular reactors provides an example.

This paper is concerned with the derivation and solution of a relatively complicated mathematical model of a highly exothermic gas–solid reaction system viz. the partial oxidation of *o*-xylene to phthalic anhydride over a V_2O_5 catalyst. We shall illustrate some aspects of the interactions of the chemical and physical transport phenomena by comparing solutions with those of the simpler models available in the literature [2].

KINETICS OF *O*-XYLENE OXIDATION

Froment [2] presents kinetic data which are representative of a practical catalyst. The reaction scheme is viewed to be of the following simplified form

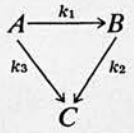

in which A = o-xylene, B = phthalic anhydride, $C = CO_2$ and H_2O.

Owing to the large excess of oxygen, the rate equations are considered to be pseudo first order, so that at atmospheric pressure:

$$\begin{aligned} r_A &= (k_1 + k_3)p_A p_{O_2} \\ r_B &= k_1 p_A p_{O_2} - k_2 p_B p_{O_2} \\ r_C &= k_2 p_B p_{O_2} + k_3 p_A p_{O_2} \end{aligned} \quad (1)$$

with

$$\begin{aligned} k_1 &= \exp(-27{,}000/R_g T_p + 19{\cdot}837) \\ k_2 &= \exp(-31{,}400/R_g T_p + 20{\cdot}86) \\ k_3 &= \exp(-28{,}600/R_g T_p + 18{\cdot}98) \end{aligned}$$

where k_1, k_2 and k_3 are expressed in moles per gm catalyst per atm.²/hr.

Each reaction step is highly exothermic with

$$\begin{aligned} -\Delta H_1 &= 307 \text{ k cal/mole} \\ -\Delta H_3 &= 1090 \text{ k cal/mole.} \end{aligned}$$

We shall suppose that the reaction can be carried out on porous particles in which the catalyst is uniformly distributed, the area per unit mass being comparable with that of an industrial catalyst.

MATHEMATICAL MODEL OF THE CATALYST PELLET

In principle, the kinetic and transport data for the catalyst can be assembled in the form of continuity equations, the solutions of which are usually expressed in the form of an effectiveness factor. However, a proper balance must be achieved between the accuracy of the model and the need to avoid excessive computation, since the set of descriptive equations must be solved repeatedly for each catalyst pellet in the reactor simulation.

THE ISOTHERMAL PELLET MODEL

As a simplifying assumption we shall take the catalyst pellet to be isothermal with the thermal resistance concentrated in the external film. Supporting evidence for this assumption is provided by analysis similar to that of Prater [3] and Butt [4], who calculated the maximum temperature rise permitted between the inside and the boundary of the particle for both simple and complex reactions respectively. Under conditions of complete combustion to byproducts C, we find

$$\Delta T_{max} = \frac{D}{K_p}\{(-\Delta H_2)p_{B0} + (-\Delta H_3)p_{A0}\} \quad (2)$$

where D is the "effective" diffusivity of both o-xylene and phthalic anhydride (assumed equal) within the catalyst, K_p is the "effective" thermal conductivity, and p_{A0}, p_{B0} are the bulk phase partial pressures of o-xylene and phthalic anhydride. Taking $D = 10^{-6}$ g. moles/cm atm sec and $K_p = 7{\cdot}5 \times 10^{-3}$ cal cm sec as being reasonable values for the catalyst support, then for a gas stream containing 1 per cent mole fraction of o-xylene and phthalic anhydride, we obtain from Eq. (2) a maximum temperature rise of 2°C. This value is insufficient to justify a more detailed analysis accounting for an intraparticle temperature profile.

The steady state material balances for diffusion-reaction within a spherical quasihomogeneous catalyst pellet are given by the equations

$$\frac{1}{y^2} \cdot \frac{D\mathrm{d}}{\mathrm{d}y}(y^2 p_A) - \rho r_A = 0 \quad (3)$$

$$\frac{1}{y^2} \cdot \frac{D\mathrm{d}}{\mathrm{d}y}(y^2 p_B) + \rho r_B = 0 \quad (4)$$

where r_A and r_B are given by Eq. (1). Boundary conditions on Eqs. (3) and (4) are given by

$$\frac{\mathrm{d}p_A}{\mathrm{d}y} = \frac{\mathrm{d}p_B}{\mathrm{d}y} = 0; \quad y = 0 \quad (5)$$

and

$$\frac{D\mathrm{d}p_A}{\mathrm{d}y} = k(p_{A0} - p_A) \quad (6)$$

$$; \quad y = R$$

$$\frac{D\mathrm{d}p_B}{\mathrm{d}y} = k(p_{B0} - p_B). \quad (7)$$

Equations (6) and (7) account for mass transfer at the external surface of the pellet in terms of the gas film mass transfer coefficient, k.

The energy balance equation for an isothermal catalyst pellet is written as

$$h(T_0-T_p)+\frac{\rho}{R^2}\left\{(-\Delta H_1)\int_0^R r_B y^2\,dy + (-\Delta H_3)\int_0^R r_C y^2\,dy\right\}=0 \quad (8)$$

where T_0 and T_p signify gas stream and pellet temperatures, and h is the gas film heat transfer coefficient. The model invoked therefore accounts for intraparticle diffusion limitation and interphase heat and mass transfer.

Solution of the equations

The solution of Eqs. (3)–(8) is relatively straightforward. Analytical integration of Eqs. (3) and (4) gives

$$p_A=\frac{3}{s}\cdot g_1\cdot p_{A0}\{\sinh(\sqrt{\alpha_1+\alpha_3})s/\sinh(3\sqrt{\alpha_1+\alpha_3})\} \quad (9)$$

$$p_B=\frac{3}{s}\cdot g_2\cdot\{p_{B0}+\alpha_1 p_{A0}/(\alpha_1+\alpha_3-\alpha_2)\}\sinh(\sqrt{\alpha_2})s/\sinh(3\sqrt{\alpha_2})-\alpha_1 p_A/(\alpha_1+\alpha_3-\alpha_2) \quad (10)$$

where

$$s=3y/R$$

$$\alpha_i=\frac{R^2}{9}\frac{\rho p_{O_2}}{D}\cdot k_i \quad (i=1,2,3)$$

$$g_1=\frac{1}{1+1/Sh\{(\sqrt{\alpha_1+\alpha_3})\coth(3\sqrt{\alpha_1+\alpha_3})-\frac{1}{3}\}}$$

$$g_2=\frac{1}{1+1/Sh\{\sqrt{\alpha_2}\,.\coth(3\sqrt{\alpha_2})-\frac{1}{3}\}}$$

$$Sh=Rk/3D.$$

Substituting Eqs. (9) and (10) in Eq. (8) and carrying out the necessary integrations, we finally obtain an algebraic equation in terms of the pellet temperature, T_p:

$$T_p-T_0=Q\,.\,B\{\alpha_1/Q-\alpha_1\alpha_2/(\alpha_1+\alpha_3-\alpha_2)\}\{Sh(1-g_1)/(\alpha_1+\alpha_3)\}+Q\,.\,B\{\alpha_2\,.\,C+\alpha_1\alpha_2/(\alpha_1+\alpha_3-\alpha_2)\}\,.\,Sh(1-g_2)/\alpha_2 \quad (11)$$

when

$$Q=\frac{(-\Delta H_3)}{(-\Delta H_1)}-1$$

$$B=\frac{3D}{hR}(-\Delta H_1)p_{A0}$$

$$C=p_{B0}/p_{A0}.$$

The right hand side of Eq. (11) is a complicated non-linear function of T_p and is proportional to the rate at which heat is generated within the catalyst pellet by chemical reaction. Intersection with the left hand side of (11), which is proportional to the rate of heat removal, gives the steady state temperature of the pellet, T_p. The root is obtained by iteration, and the result is used to calculate the catalyst effectiveness and selectivity factors. Effectiveness, defined as the ratio of the actual rate of disappearance of *o*-xylene to the rate of disappearance at gas stream conditions of temperature and partial pressure, is given by

$$\eta=\frac{g_1}{(\alpha_1+\alpha_3)_0}\{(\sqrt{\alpha_1+\alpha_3})\coth(3\sqrt{\alpha_1+\alpha_3})-\tfrac{1}{3}\} \quad (12)$$

where subscript $_0$ refers to gas stream conditions. Selectivity, defined as the ratio of the rate of production of phthalic anhydride to the rate of depletion of *o*-xylene, follows from

$$S=\left.\frac{(-dp_B/dy)}{(dp_A/dy)}\right|_{y=R}=\frac{\alpha_1}{(\alpha_1+\alpha_3-\alpha_2)}-\frac{(1-g_2)}{(1-g_1)}\cdot\left(C+\frac{\alpha_1}{\alpha_1+\alpha_3-\alpha_2}\right). \quad (13)$$

SCOPE OF THE INVESTIGATION

Given the kinetic data the factors affecting rates of reaction are of a physical nature—i.e. diffusion rates within the porous catalyst and heat

and mass transfer rates at the external surface of the pellet. The relative importance of these transport processes and the manner in which they influence catalyst effectiveness and selectivity will be explored over the practical range. Parametric sensitivity tests on the solution will indicate the precision required in the determination of these parameters.

With problems involving interaction between heat transfer, mass transfer and chemical reactions, we can expect to find several steady state solutions for certain combinations of parameters. Since questions of uniqueness and stability of the steady state are closely related, it is important to establish whether or not multiple solutions can arise within the practical range.

(i) *Internal diffusion*

The available pore size distribution data indicate a regime of molecular internal diffusion. The "effective" diffusion coefficient of *o*-xylene or phthalic anhydride (assumed equal) is given in terms of the binary diffusion coefficient in air (D_M) by the equation

$$D = \frac{\epsilon}{\tau} \cdot D_M \qquad (14)$$

where ϵ is the internal void fraction and τ is the tortuosity factor. Experimental data for various catalysts (5) are widely scattered and provide little guidance as to what value of τ is to be employed. Consequently, we shall carry out calculations over a range of ϵ/τ values. Aris [6] suggests this range will extend from 0·05 to 0·95. The molecular diffusion coefficient of *o*-xylene in air and its temperature dependence are available in the literature [7].

Figures 1 and 2 summarise the results of effectiveness factor and selectivity calculations over a range of gas stream temperatures for a particular catalyst size, gas stream composition and flow rate. Only at relatively low temperatures (< 325°C) do reaction kinetics control the overall rate process. At higher temperatures, within the practical range, physical transport processes appreciably influence catalyst behaviour, and

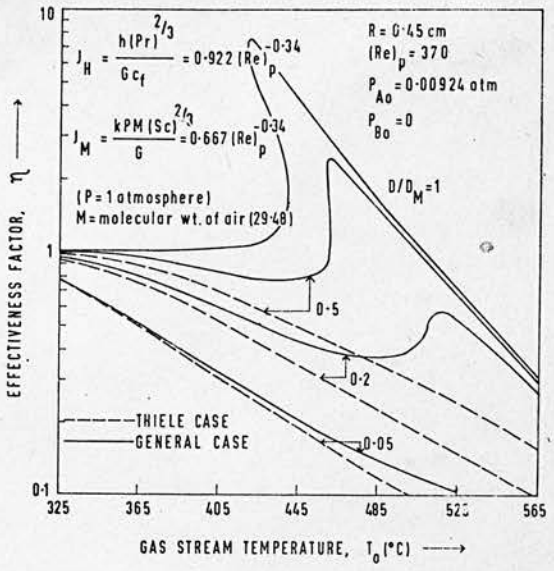

Fig. 1. Influence of internal diffusion coefficient on catalyst effectiveness factor. Comparison with the Thiele case.

their interactions with the reaction kinetics produce a variety of effects.

The solutions obtained show a marked dependence upon the internal diffusion coefficient, stressing the need for a more precise estimate of this parameter. For small values of the diffusion coefficient, the rate of disappearance of *o*-xylene is controlled by internal diffusion. The predictions of effectiveness and selectivity factors are in good agreement with those realised for a simpler model (the Thiele case), neglecting heat and mass transfer at the external surface. In this case, low effectiveness combined with reduced selectivity leads to greatly reduced yields of anhydride in comparison with those obtained in the absence of internal transport restriction.

As the diffusion coefficient is increased towards its maximum value, $D = D_M$, gas film transport becomes appreciable in relation to internal diffusion in influencing reaction rates, as shown by the significant differences in effectiveness and selectivity values with those of the Thiele model. Indeed, gas film mass transfer may become the rate-controlling process, as a result of large film heat transfer resistance. Selectivity is now greatly reduced, becoming independent of D at

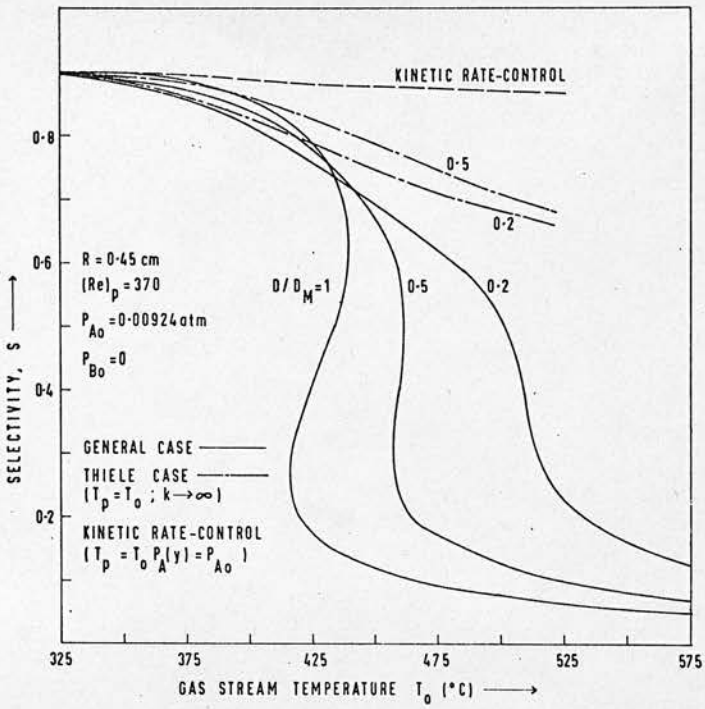

Fig. 2. Influence of internal diffusion on catalyst selectivity.

the higher temperatures. However, in some cases, it is possible to balance low selectivity with high effectiveness (> 1) to give yields of anhydride comparable to, or even greater than those of the Thiele model (Fig. 3).

The temperature difference across the external film as a function of gas temperature is displayed in Fig. 4 for several values of the internal diffusion coefficient, D. At relatively low temperatures, the pellet is operating at essentially the gas stream temperature. With increasing temperature, marked gradients occur across the gas film until at high temperatures all the curves approach the asymptote given by

$$T_{p,\max} - T_0 = \frac{k}{h}\{(-\Delta H_3)p_{A0} + (-\Delta H_2)p_{B0}\}. \quad (15)$$

Equation (15) is calculated from Eq. (11) on the assumption of complete combustion to by-products C on the external surface of the catalyst pellet. It should be remarked, here, that the upper part of these curves may be considerably in error, because radiation between solid and gas will become important at the higher temperatures.

(ii) *Film transport*

The considerable scatter in experimentally determined j-factor correlations for heat and mass transfer at a solid surface leave one in considerable doubt over the choice of a suitable correlation. Strictly speaking, these correlations are specific to the given system and provide no means for extrapolation to other conditions. In the absence of direct measurement, the only practicable approach is to employ transport data taken from a similar system.

Figure 5 compares effectiveness factor curves for two j-factor correlations due to Thodos [8] and Satterfield and Resnick [9]. The precision required in the data depends on the operating region. At the lower temperatures, changes in the transport data have little effect, since the reaction rate is either controlled by kinetics or inter-

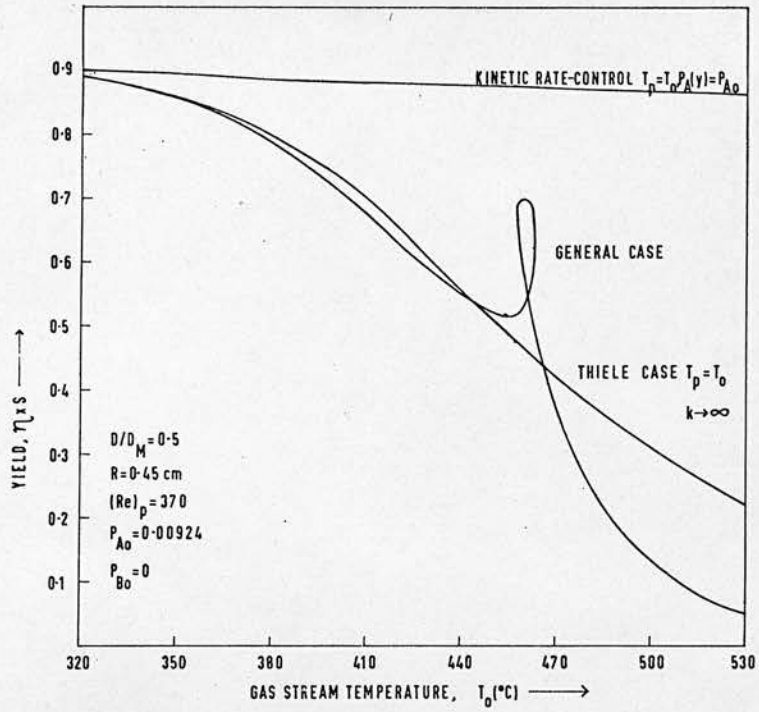

Fig. 3. Yield as affected by internal diffusion (Thiele case) and by both internal diffusion and film heat and mass transfer (general case).

nal diffusion. With increasing temperature, changes in the film coefficients exert their greatest influence in the region of steep rise in the effectiveness factor. This region may even be non-unique, in which case three steady state solutions are found, although not all are stable. Operation in this peaked region is undesirable, however, not only from stability considerations but also because of low yields, which arise as a consequence of greatly reduced selectivity (Fig. 2).

(iii) *Multiple steady states*

Multiple steady state solutions are obtained, but only over a narrow temperature range and for relatively large values of the internal diffusion coefficient (cf. Figs. 1–3, 5). Calculations with p_{A0} reduced, but p_{B0} increased from zero, showed the disappearance of multiple steady states, indicating that their occurrence is largely due to the interactions of the physical transport rates with the rate of the partial oxidation step $A \rightarrow B$.

In a packed-bed reactor, the choice of "local" gas stream temperature and composition is not arbitrary; rather, the admissable values only follow as a result of solving the conservation equations for the entire system—both intraparticle and interparticle fields. Whether this constraint is sufficient to remove the combinations of gas stream temperatures and composition, which lead to multiple steady states within the individual catalyst particles, can only be legitimately decided by further analysis on the reactor. In the present instance, it seems unlikely that multiple steady states will occur at any point within the reactor.

INFLUENCE OF INTERNAL TRANSPORT ON REACTOR PERFORMANCE

The set of descriptive equations for the catalyst pellet can be combined with the appropriate equations for the flowing gas stream to produce a

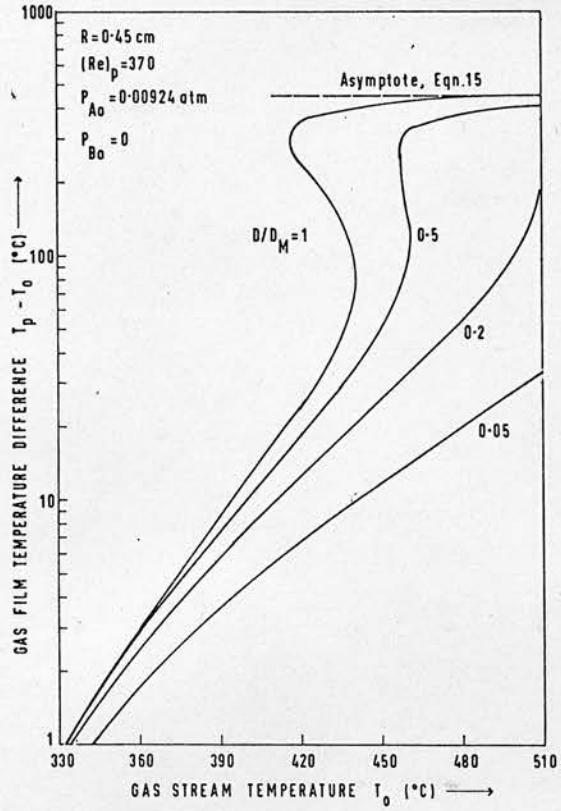

Fig. 4. Influence of internal diffusion on gas film temperature rise.

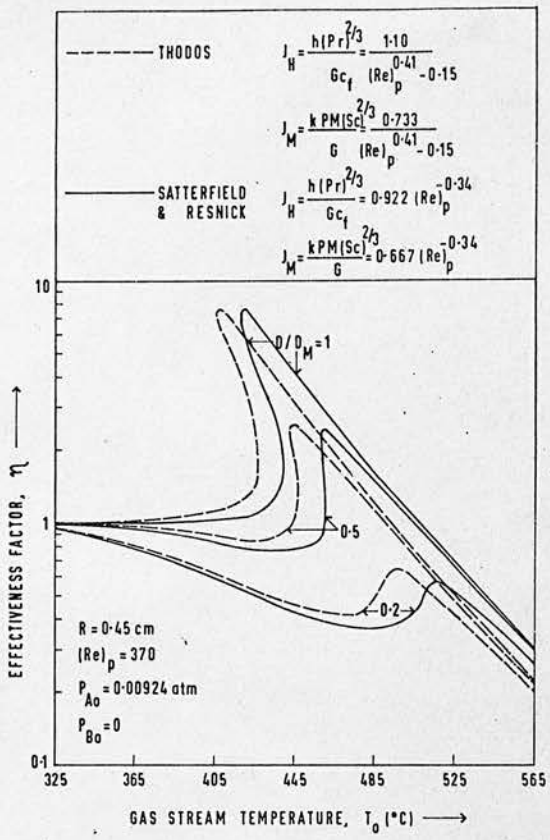

Fig. 5. Influence of film heat and mass transfer coefficients on catalyst effectiveness factor.

mathematical model of the packed-bed reactor [10, 11].

Froment [2] demonstrated "parametric sensitivity" of this reaction in a cooled tubular reactor from calculations based on a quasi-homogeneous reactor model, neglecting internal and film transport restrictions. The existence of an undesirable temperature "run-away" prevented operation at near-optimal conditions, thereby leading to reduced productivity and unfavourable economics.

With this economic factor in mind, we shall investigate whether or not the explosive character of the reaction is not to a large extent limited by physical transport, particularly the internal diffusion rate. Operation at a higher average bed temperature may then permit some improvement in yield, even at the expense of an impaired selectivity due to over-exposure of intermediate within the porous catalyst.

Operation below the "run-away" limit

It is useful, first of all, to examine the added refinements in the model for operating conditions outside the critical range, if only to show their possible redundancy. This assertion is, in fact, borne out by the results in Table 1, which compares conversion and yield as predicted from a simple one-dimensional quasi-homogeneous model (with radial heat transfer resistance lumped at the wall) and a similar one-dimensional model accounting for internal and film transport.

Also shown are the predictions from a more refined two-dimensional quasi-homogeneous model, accounting for restricted radial diffusivity both for heat and mass. The results indicate the adequacy of the simple one-dimensional quasi-homogeneous model in the sub-critical operating

Table 1. Conversion and yield comparisons from the various models. Feed temperature = 355°C. Other data as in Table 2

	% conversion of *o*-xylene	% yield of phthalic anhydride
1-D quasihomogeneous	76	63
1-D heterogeneous		
$D/D_M = 0{\cdot}2$	75	62
$D/D_M = 0{\cdot}1$	73	61
2-*D* quasihomogeneous (mean radial values)	72	61
2-*D* heterogeneous		
$D/D_M = 0{\cdot}2$	71	60
$D/D_M = 0{\cdot}1$	69	59

range, at least for the small tube diameter (1 in.) employed in the calculations.

Operation at "run-away" conditions

Figure 6 shows the effect on the axial temperature profile of operating in the "run-away" region with decreasing rates of internal diffusion. For sufficiently small values of D, within the range of study, uncontrolled temperature rise is prevented. However, we might still expect a "run-away" situation to develop by operating at a sufficiently high inlet temperature. The magnitude of this temperature increase is clearly of importance in the implementation of optimal operating conditions.

As an example, consider the case for $D = 0{\cdot}04D_M$. Calculations on the one-dimensional model, incorporating pellet effects, show a "run-away" at 390°C. Further, operation at an inlet temperature above 375°C proves to be uneconomic because of reduced selectivity. A comparison is made in Fig. 7 of the effect of operating a 3-meter reactor at 375°C, with appreciable internal transport restrictions, as opposed to operation at 350°C (also at 15°C below respective "run-away" limit) with no internal transport limitation. The results show an actual improve-

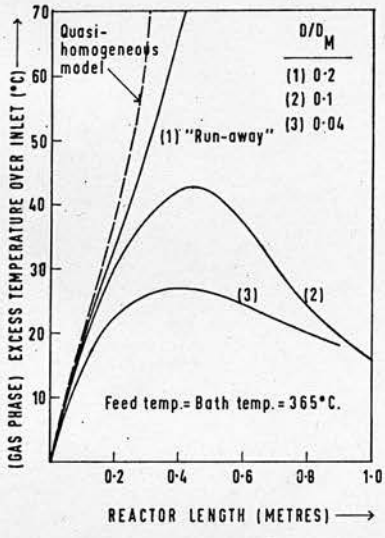

Fig. 6. Influence of internal diffusion coefficient on axial temperature profile from a one dimensional reactor model.

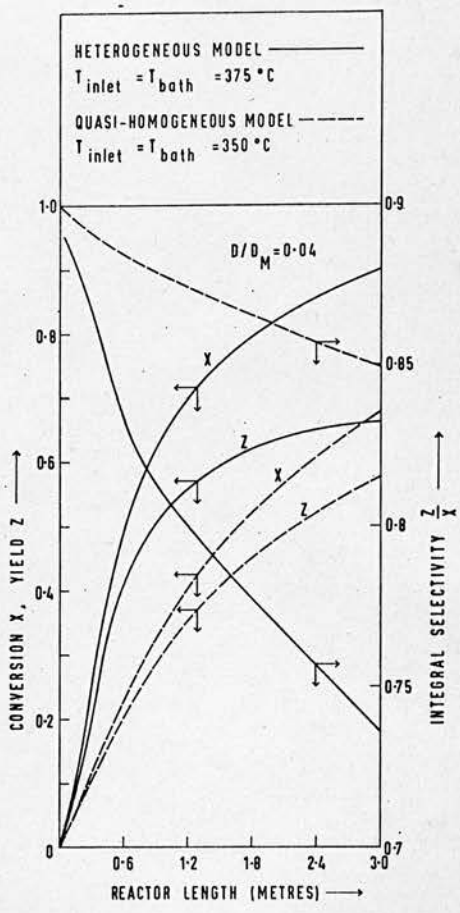

Fig. 7. Influence of internal diffusion on reactor performance.

ment in yield from 57·5 to 66 per cent even though an appreciable reduction of selectivity has occurred through internal transport effects. Even if it were possible to operate the latter reactor in the critical region (i.e. at an inlet temperature of 360°C) the yield would still be less than 66 per cent.

This rather striking instance of physical transport actually leading to improved reactor performance again serves to indicate the need for continuing research on mass transfer in porous catalyst pellets.

Table 2. Summary of data for the reactor models (see Ref. [2])

Parameter	Meaning	Value
G	Superficial mass flow rate	4684 kg/m²/hr
c_f	Specific heat of air	0·25 cal/g°C
P_A, in	*o*-xylene feed partial pressure	0·00924 atm.
P_{O_2}	Partial press. of O_2 (in excess)	0·208 atm.
d_p	Particle diameter	0·3 cm
d_t	Tube diameter	2·5 cm
L	Reactor length	3 m
ρ_B	Bed density	1·3 g/cc
Pe_{hR}	Peclet number for radial heat transfer (2-D model)	5·25
Pe_{mR}	Peclet number for radial mass transfer (2-D model)	10
α_w	Wall heat transfer coefficient	134 k cal/m² hr °C
U	Overall heat transfer coefficient (1-D models)	82·7 k cal/m² hr °C
$(Re)_p$	Reynolds number (based on pellet dia.)	123
Sc	Schmidt number	2
Pr	Prandtl number	0·69

NOTATION

A, B, C reactant, desired product, by-products

D effective diffusivity of *o*-xylene and phthalic anhydride in the porous catalyst

D_M binary molecular diffusion coefficient of *o*-xylene (or phthalic anhydride) in air

h gas film heat transfer coefficient

k gas film mass transfer coefficient of *o*-xylene and phthalic anhydride

k_1, k_2, k_3 reaction rate constants

K_p effective thermal conductivity of catalyst particle

p_A, p_B, p_{O_2} point intraparticle partial pressures of *o*-xylene, phthalic anhydride and oxygen

R particle radius

R_g gas constant

S selectivity (Eq. (13))

T_0 bulk gas stream temperature, °K

T_P catalyst particle temperature, °K

$T_{P,\max}$ maximum particle temperature, °K, (Eq. (15))

y particle radial variable

$-\Delta H_1$, $-\Delta H_3$ heats of reaction of *o*-xylene to phthalic anhydride and complete combustion products respectively

$\Delta T_{\max}$ maximum intraparticle temperature rise (Eq. (2))

Greek symbols

ϵ particle void fraction

η effectiveness factor (Eq. (12))

ρ apparent particle density

τ tortuosity factor

REFERENCES

[1] McGUIRE M. L. and LAPIDUS L., *A.I.CH.E.Jl* 1965 **11** 85.
[2] FROMENT G. F., *Ind. Engng Chem.* 1967 **59** (2) 18.
[3] PRATER C. D., *Chem. Engng Sci.* 1958 **8** 284.
[4] BUTT J. B., *Chem. Engng Sci.* 1966 **21** 275.
[5] SATTERFIELD C. N. and SHERWOOD T. K., *The Role of Diffusion in Catalysis*. Addison-Wesley 1963.
[6] ARIS R., *Introduction to the Analysis of Chemical Reactors*. Englewood Cliffs 1965.
[7] *International Critical Tables*. McGraw-Hill 1926.
[8] DEACETIS J. and THODOS G., *Ind. Engng Chem.* 1960 **52** 1003.
[9] SATTERFIELD C. N. and RESNICK H., *Chem. Engng Prog.* 1954 **50** (10) 504.
[10] McGREAVY C. and CRESSWELL D. L., *4th European Symp.* on *Chemical Reaction Engineering*, Brussels, Sept. 1968.
[11] CARBERRY J. J. and WHITE D., *Ind. Engng Chem.* 1969 **61** (7) 27.

Résumé—Les influences de la diffusion "dans les pores" et du transfert de masse et de chaleur d'un film sur l'effectivité et la sélectivité d'un catalyseur sont examinées pour un système de réactions parallèles et consécutives hautement exothermiques, catégorisées, par exemple, par l'oxydation partielle d'o-xylène en anhydride phtalique. Les tests de sensitivité paramétrique révèlent une dépendance marquée à la fois du facteur d'effectivité et du facteur de sélectivité sur le coefficient de diffusion "dans les pores", soulignant la nécessité d'une estimation plus précise de ce paramètre.

L'effet des taux restreints de diffusion "dans les pores" sur une température "passante" dans un réacteur hautement exothermique à couches garnies est également étudié, et l'on montre que le rendement d'un produit spécifique peut être considérablement amélioré en favorisant un effet appréciable de diffusion entre les particules, malgré la réduction de sélectivité.

Zusammenfassung—Die Einflüsse "inner-poröser" Diffusion sowie der Wärme- und Stoffübertragung in Filmen auf die katalytische Wirksamkeit und Selektivität werden für ein System hochexothermer Parallel- und Folgereaktionen, ein typisches Beispiel stellt die Teiloxydation von o-Xylol zu Phtalsäureanhydrid dar, untersucht. Parametrische Empfindlichkeitsproben deuten eine ausgesprochene Abhängigkeit sowohl des Poren ausnutzungs grades als auch der Selektivität von dem "inner-porösen" Diffusionskoeffizienten an, wodurch die Notwendigkeit einer genaueren Bewertung dieses Parameters betont wird.

Die Wirkung beschränkter "inner-poröser" Diffusionsraten auf das "Durchgehen" der Temperatur in einem hochexothermen Füllkörperbett-Reaktor wird ebenfalls untersucht, und es wird gezeigt, dass die Ausbeute an Sollprodukt beträchtlich verbessert werden kann wenn ein nennenswerter Diffusionseffekt unter den Teilchen hervorgerufen wird, jedoch auf Kosten einer verminderten Selektivität.

REFERENCES

1. Churchill S.W., "The Interpretation and Use of Rate Data: The Rate Concept", Scripta, Washington D.C., 1974.

2. Box G.E.P. and Hunter W.G., Technometrics 7,1,23 (1965)

3. Reported in: Thomson S.J. and Webb G., "Heterogeneous Catalysis", Oliver and Boyd, Edinburgh, 1968.

4. Hougen O.A. and Watson K.M., "Chemical Process Principles, Part 3, Kinetics and Catalysis", Wiley, N.Y., 1947.

5. Wilhelm R.H., Pure Appl. Chem., 5, 403 (1962).

6. Beek J., in "Advances in Chemical Engineering, Vol 3", edited by Drew T.B., Hoopes J.W. and Vermeulen T., Acad.Press, N.Y., 1962.

7. Kjaer J, "A General Calculation Method for Fixed-Bed Catalytic Reactors on a Digital Computer", Akademisk Forlag, Copenhagen, 1963.

8. Froment G.F., Ind.Eng.Chem. 59,2,18 (1967).

9. Hlavacek V., Ind,Eng,Chem, 62,7,8 (1970).

10. Karanth N.G. and Hughes R., Cat.Rev.Eng.Sci. 9,2,169(1974).

11. Smith J.M., "Chemical Engineering Kinetics", 2nd edition, McGraw Hill, N.Y., 1970.

12. Satterfield C.N., "Mass Transfer in Heterogeneous Catalysis", M.I.T. Press, 1970.

13. Sehr R.A., Chem.Eng.Sci. 9,145 (1958).

14. Weekman V.W., J.Catal. 5,44 (1966).

15. Bell W.K. and Brown C.F., J.Chem.Phys. 59,7,3566 (1973).

16. Petersen E.E., "Chemical Reaction Analysis", Prentice-Hall, Englewood Cliffs, N.J., 1965.

17. Stoll D.R. and Brown L.F., J.Catal. 32,37 (1974).

18. Smith J.M., Can.J.Ch.E. 48, 142 (1970).

19. Kadlec B., Hudgins R.R. and Silveston P.L., Chem.Eng.Sci. 28,935 (1973).

20. Hawtin P., Chem.Eng.Sci., 26, 2783 (1971).

21. Raja Rao M. and Smith J.M., A.I.Ch.E.Jl., 10,293 (1964).

22. Wakao N. and Nardse Y., Chem.Eng.Sci. 29, 1304 (1974).

23. Toei R., Okazaki M., Nakanishi K., Kondo Y., Hayashi M. and Shiozaki Y., J.Ch.E.Japan, 6,1,50 (1973).

24. Abed R. and Rinker R.G., J.Catal, 34,246 (1974).

25. Carberry J.J., A.I.Ch.E.Jl., 6,460 (1960).

26. Barker J.J., Ind.Eng.Chem. 57,4,43 (1965).

27. Whitaker S., A.I.Ch.E.Jl. 18,2,361 (1972).

28. Balakrishnan A.R. and Pei D.C.T., I.E.C.Proc.D. and D.13,4,441 (1974).

29. Petrovic L.J. and Thodos G., I.E.C. Funds, 7,2,275 (1968).

30. Satterfield C.N. and Resnick H., C.E.P. 50,504 (1954).

31. Korbach P.F. and Stewart W.E., I.E.C. Funds, 3,24 (1964).

32. Calderbank P.H., Caldwell A.C. and Ross G., Chemie et L'Industrie-Genie Chimique 2, 215 (1969).

33. Chambers R.P. and Boudart M., J.Catal. 6,141 (1966).

34. Carberry J.J., Ind.Eng.Chem. 56,11,39 (1964).

35. Brisk M.L., Day R.L., Jones M. and Warren J.B., Trans.Inst.Chem.Engrs. 46,T3 (1968).

36. Pereira J.R. and Calderbank P.H., Chem.Eng.Sci. 30,167 (1975).

37. Tho N-X and Rouleau D., Can.J.Ch.E. 51,761(1973).

38. Berty J.M., C.E.P. 70,5,78 (1974).

39. Mahoney J.A., J.Catal. 32,247 (1974).

40. Mezaki R. and Hill W.J., Brit.Ch.E. 13,3,358 (1968).

41. Boudart M., "The Kinetics of Chemical Processes", Prentice-Hall, Englewood Cliffs N.J., 1968.

42. Sawyer D.N., Ph.D. Thesis, Univ.Wisconsin, 1969.

43. Hofmann H.: Proc 5th European, 2nd International Symp.Chem.Rn.Engng., Amsterdam 1972, p.A 2-1.

44. Happel J., Cat.Revs.Eng.Sci. 6,2,221 (1972).

45. Mezaki R. and Happel J., Cat.Revs.Eng.Sci. 3,241 (1970).

46. Mulla T.H.A., Ph.D. Thesis, Univ.Strathclyde, 1970.

47. Weller S., A.I.Ch.E.Jl. 2,1,59 (1956).

48. Podolski W.F. and Kim Y.G., I.E.C. Proc.D. & D. 13,4,415 (1974).

49. Boudart M., A.I.Ch.E.Jl. 2,1,62 (1956).

50. Edelson D. and Allara D.L., A.I.Ch.E.Jl. 19,3,639 (1973).

51. Nault L.G., Bolme D.W. and Johanson L.N., I.E.C. Proc.D.&D. 1,4,285 (1962).

52. Buzzi Ferraris G., Donati G., and Rejna F., Chem.Eng.Sci. 29,1621 (1974).

53. Pritchard D.J. and Bacon D.W., Can.J.Ch.E. 52,103 (1974).

54. Galeski J.B. and Hightower J.W., Can.J.Ch.E. 48,151 (1970).

55. Blanton W.A., Byers C.H. and Merrill R.P., I.E.C. Funds 7,611 (1968).

56. Yates J.T., Chem. & Eng.News, 52,34,19 (1974).

57. Orlickas A., Hoffman T.W., Shaw I.D. and Reilly P.M., Can.J.Ch.E. 50,628 (1972).

58. Petersen E.E., Friedly J.C. and Devogelaere R.J., Chem.Eng.Sci. 19,683 (1964).

59. Baddour R.F. and Yoon C.Y., C.E.P. Symp.Ser. 57,32,33 (1961).

60. Paris J.R. and Stevens W.F., Can.J.Ch.E. 48,1,100 (1970).

61. Smith J.M., Chem.Eng.Jl. 5,109 (1973).

62. Young L.C. and Finlayson B.A., I.E.C. Funds, 12,4,412 (1973).

63. Froment G.F. in Bischoff K.B. (ed), "Chemical Reaction Engineering", Adv. in Chem.Ser. 109, A.C.S., 1972.

64. Olbrich W.E., Agnew J.B. and Potter O.E., Trans.Inst.Chem.Engrs. 44, T207 (1966).

65. Deans H.A. and Lapidus L, A.I.Ch.E.Jl. 6,663 (1960).

66. Caldwell L., Ph.D. Thesis, University of Edinburgh, 1971.

67. Gunn D.J. and Pryce C.E., Trans.Inst.Chem.Engrs. 47,T341 (1969).

68. Rosenbrock H.H. and Storey C., "Computational Techniques for Chemical Engineers", Pergamon, Oxford, 1966.

69. Greenspan D., "Discrete Models", Addison-Wesley, Reading, Mass., 1973.

70. Himmelblau D.M. and Bischoff K.B., "Process Analysis and Simulation: Deterministic Systems", Wiley, 1968: p.59.

71. Aris R., Ch .Eng.Educ. 8,1,19 (1974).

72. Carberry J.J., Chem.Eng.Sci. 17,675 (1962).

73. Frank-Kamenetskii,D.A.,"Diffusion and Heat Exchange in Chemical Kinetics", 1st edition, Princeton Press, N.J. (1955). 2nd edition, Plenum Press, N.Y. (1969)

74. Hatfield B. and Aris R., Chem.Eng.Sci. 24,1213 (1969).

75. Yu K.M. and Douglas J.M., Chem.Eng.Sci. 29, 163 (1974).

76. Gavalas G.R., "Nonlinear Differential Equations of Chemically Reacting Systems", Springer-Verlag, N.Y., 1968.

77. McGreavy C. and Thornton J.M., Chem.Eng.Jl. 1,296 (1970).

78. Michelsen M.L. and Villadsen J., Chem.Eng.Sci. 27,751 (1972).

79. Jackson R., Chem.Eng.Sci. 28, 1355 (1973).

80. Cresswell D.L., Chem.Eng.Sci. 25,267 (1970).

81. Luss D., Chem.Eng.Sci. 26,1713 (1971).

82. Varma A. and Amundson N.R., Chem.Eng.Sci. 28,91 (1973).

83. Pis'men L.M. and Kharkhats Yu.I., Dokl.Acad.Nauk,S.S.S.R. 178, 901 (1968); reported in (84).

84. Bailey J.E., Chem.Eng.Sci. 27, 1055 (1972).

85. Horn F.J.M., Jackson R., Martel E. and Patel C., Chem.Eng.Jl. 1,79 (1970).

86. Jackson R. and Horn F.J.M., Chem.Eng.Jl. 3,82 (1972).

87. Yang R.Y.K. Padmanabhan L. and Lapidus L., Chem.Eng.Jl. 2,218 (1972).

88. Yang R.Y.K. and Lapidus L., Chem.Eng.Sci. 28,875 (1973).

89. Aronson D.G. and Peletier L., Arch.Rat.Mech.Anal. 54,175 (1974).

90. Koh H.-P., Hughes R. and Harriot P., Chem.Eng.Sci. 29,2189 (1974).

91. Jackson R., Chem.Eng.Sci. 29,1413 (1974).

92. Hlavacek V., Kubicek M. and Marek M., J.Catal. 15,17 (1969).

93. Hansen K.W., Chem.Eng.Sci. 26,1555 (1971).

94. Carberry J.J., Ind.Eng.Chem. 58,10,40 (1966).

95. Cresswell D.L., Ph.D. Thesis, Univ.Leeds, 1969.

96. Beek J., A.I.Ch.E.Jl. 7,337 (1961).

97. Carberry J.J., A.I.Ch.E.Jl. 7,350 (1961).

98. Liu S.-L., A.I.Ch.E.Jl. 16,5,742 (1970).

99. Jouven J.G. and Aris R., A.I.Ch.E.Jl. 18,2,402 (1972).

100. Rajadhyaksha R.A. and Vasudeva K., J.Catal. 34,321 (1974).

101. Goto S. and Morita N., J.Chem.Eng.Japan 3,2,192 (1970).

102. Schilson R.E. and Amundson N.R., Chem.Eng.Sci. 13,226 (1961).

103. Tinkler J.D. and Pigford R.L., Chem.Eng.Sci. 15,326 (1961).

104. Petersen E.E., Chem.Eng.Sci. 17,987 (1962).

105. Gunn D.J., Chem.Eng.Sci. 21, 383 (1966).

106. Hlavacek V. and Marek M., Chem.Eng.Sci. 23, 865 (1968).

107. McGreavy C. and Cresswell D.L., Can.J.Ch.E. 47,583 (1969).

108. McGreavy C. and Cresswell D.L., Proc. European Reaction Engineering Symposium, Brussels, 1968: 2nd session p.1.

109. Ruthven D.M., J.Catal. 25,259 (1972).

110. Bird R., Stewart W. and Lightfoot E., "Transport Phenomena", Wiley, N.Y., 1960, p.502.

111. Kehoe P., Chem.Eng.Sci. 29,315 (1974).

112. Lee E.S., "Quasilinearization and Invariant Imbedding", Academic Press, N.Y., 1968.

113. McGinnis P.H., C.E.P. Symp. Ser. 61,55,2 (1965).

114. Finlayson B.A., "The Method of Weighted Residuals and Variational Principles", Academic Press N.Y., 1972.

115. Acton F.S., "Numerical Methods That Work", Harper & Row, N.Y., 1970.

116. Villadsen J. and Stewart W.E., Chem.Eng.Sci., 22,1483 (1967). Errata, ibid, 23,1515 (1968).

117. Villadsen J, "Selected Approximation Methods for Chemical Engineering Problems", Instituttet for Kemiteknik, Numerisk Institut, Danmarks Tekniske Højskole, Lyngby, Denmark, 1970.

118. Ferguson N.B. and Finlayson B.A., A.I.Ch.E.Jl. 18,5,1053 (1972).

119. Ferguson N.B. and Finlayson B.A., Chem.Eng.Jl. 1,327 (1970).

119a. Stewart W.E. and Sorensen J.P.; Proc 5th Europ/2nd Intern.Symp. Chem.Rn.Eng.,Amsterdam, 1972.

120. Michelsen M.L. and Villadsen J., Chem.Eng.Jl., 4,64 (1972).

121. Ramkrishna D., Chem.Eng.Sci. 28, 1362 (1973).

122. Finlayson B.A., Cat.Rev.Sci.Eng., 10,1,69 (1974).

123. Prater C.D., Chem.Eng.Sci. 8,284 (1958).

124. Cox M.G., Computer Jl. 13,101 (1970).

125. Broyden C.G., Computer Jl. 12,94 (1969).

126. Paterson W.R. and Cresswell D.L., Chem.Eng.Sci. 26,605 (1971).

127. Karanth N.G. and Hughes R., Chem.Eng.Sci. 27,2107 (1972).

128. Karanth N.G., Koh H.-P. and Hughes R., Chem.Eng.Sci. 29, 451 (1974).

129. Van den Bosch B. & Padmanabhan L., Chem.Eng.Sci. 29,1217 (1974).

130. Hlavecek V., and Kubicek M., Chem.Eng.Sci. 26,1737 (1971).

131. Van den Bosch B. and Padmanabhan L., Chem.Eng.Sci. 29,805 (1974).

135. Villadsen J., "Applications of the Collocation Method", D.T.H., Lyngby, Denmark, 1973.

136. Sredni J., Ph.D. Thesis, Univ.Wisconsin, 1970.

137. Box G.E.P. and Newbold P., J.Roy.Stat.Soc., Ser A, 134, 229 (1971).

138. Mandel J., "The Statistical Analysis of Experimental Data", Interscience, N.Y., 1964.

139. Peterson D.L., C.E.P. Symp.Ser. 42,59,8 (1963).

140. Box M.J., Technometrics 12,219(1970).

141. Correspondence between Churchill S.W., and Mezaki R., Draper N. and Johnson R.A., I.E.C. Funds 12, 491 (1973).

142. Box G.E.P. and Tiao G.C., "Bayesian Inference in Statistical Analysis", Addison-Wesley, Reading, Mass., 1973.

143. Tukey J.W., Ann.Math.Stat. 33,1 (1962).

144. Eykhoff P., Automatica, 4,205 (1968).

145. Nieman R.E., Fisher D.G. and Seborg D.E., Int.Jl.Control 13,209 (1971).

146. Kendall M.G. and Stuart A., "The Advanced Theory of Statistics", Griffin, London,Volume 1, 1958; Volume 2, 1961.

147. Personal communication; Professor D.J. Finney, Department of Statistics, University of Edinburgh. (1973).

148. Draper N.R. and Smith H., "Applied Regression Analysis", Wiley, N.Y., 1966.

149. Deutsch R., "Estimation Theory", Prentice-Hall, Englewood Cliffs, N.J., 1965.

150. Box G.E.P. and Draper N.R., Biometrika, 52,355 (1965).

151. Slin'ko M.G., Spirak S.I., and Timoshenko V.I., Kinetika i Kataliz 13,6,1570 (1972).

152. Nieman R.E. and Fisher D.G., Can.J.Ch.E. 50,802 (1972).

153. Gerald C.F., "Applied Numerical Analysis", Addison-Wesley, Reading, Mass, 1970.

154. Box G.E.P., Hunter W.G., MacGregor J.F. and Erjavec J., Technometrics 15,33 (1973).

155. Behnken D.W. and Draper N.R., Technometrics 14,101 (1972).

156. Kittrell J.R. and Mezaki R., Brit.Chem.Eng. 11, 1538 (1966).

157. Hershey H.C., Zakin J.L. and Simha R., I.E.C. Funds. 6,413 (1967).

158. Anderrsen R.S. and Bloomfield P., Numer.Math. 22, 157(1974).

159. Cuenod M. and Sage A.P., Automatica 4,235 (1968).

160. Powell M.J.D., Comp.Jl. 7, 155 (1964).

161. Nelder J.A. and Mead R., Comp.Jl. 7,308 (1965).

162. Seinfeld J.H. and Lapidus L, "Mathematical Methods in Chemical Engineering, Volume 3; Process Modelling, Estimation and Identification", Prentice-Hall, Englewood Cliffs, N.J., 1974.

163. Bellman R., Jacquez J., Kalaba R. and Schwimmer S., Math.Biosciences 1, 71(1967).

164. Schlossmacher,E.J,A.I.Ch.E.Jl. 18, 870 (1972).

165. Hwang M., and Seinfeld J.H., A.I.Ch.E.Jl., 18,90 (1972).

166. Berger A.J., A.I.Ch.E.Jl. 19,365 (1973).

167. Medler C.L. and Hsu C-C., I.E.E.E.Trans.Auto.Control, 14,726 (1969).

168. Leonides C.T. and Paine G., Jl.Opt.Theory and Appl. 2,316 (1968).

169. Ramaker B.L., Smith C.L. and Murrill P.W., I.E.C.Funds, 9,28 (1970).

170. Donnelly J.K. and Quon D., Can.J.Ch.E. 48,114 (1970).

171. Shah P.S., Erickson L.E., Fan L.T. and Prokop A., Biotech and Bioeng. 14,533 (1972).

172. Dalla Lana I.G., McGregor D.E., Liu C.L. and Cornode A.E. Proc.5th European/2nd International Symp. on Chem.Rn. Eng., Amsterdam, 1972.

173. Bremermann H., I.E.E.E.Symp. - Adaptive Processes, Decision and Control, Houston; 23,2,3 (1970).

174. Seinfeld J.H., Lapidus L. and Hwang M., I.E.C. Funds. 9,226 (1970).

175. Denis G.H. and Daubert T.E., A.I.Ch.E.Jl. 20,720 (1974).

176. Broekhoven L.H. and Watts D.G., Department of Mathematics, Queen's University, Kingston, Ontario; Mathematical Pre-print No. 1972-26 (1972).

177. Roth R.S. and Roth M.M., Math.Biosciences 5,57 (1969).

178. Box M.J. in Watts D.G. (ed.), "The Future of Statistics", Academic Press, N.Y., 1968.

179. Hosten L.H., Chem.Eng.Sci. 29,2447 (1974).

180. Paynter J.D. and Schuette W.L., I.E.C.Proc.D. and D. 10,250 (1971).

181. Bischoff K.B., Chem.Eng.Sci. 27,1193 (1972).

182. Gay I.D., J.Phys.Chem. 75, 1610 (1971).

183. Tang Y.P., I.E.C. Funds, 10, 321 (1971).

184. Himmelblau D.M., Jones C.R. and Bischoff K.B., I.E.C. Funds, 6,539 (1967).

185. Foss S.D., Chem.Eng.Sci. 26,485 (1971).

186. Tanner R., I.E.C. Funds, 11,1 (1972).

187. Tanner R., A.I.Ch.E.Jl. 18,385 (1972).

188. Buzzi Ferraris G. and Donati G., Chem.Eng.Sci. 29,1504 (1974).

189. Van den Bosch B. and Hellinckx L., A.I.Ch.E.Jl. 20,250 (1974).

190. Gavalas G.R., A.I.Ch.E.Jl. 19,214 (1973).

191. Wei J. and Prater C.D., Adv.Catalysis 13,203 (1962).

192. Bodenstein M., Z.Physik.Chem. 100, 68 (1922).

193. Himmelblau D., "Process Analysis by Statistical Methods", Wiley, N.Y., 1970.

194. Hunter W.G., I.E.C. Funds, 6, 461 (1967).

195. Davis J.D. and Byrne J.F., J.Amer.Ceram.Soc. 7,809 (1924).

196. Schmidt J.P., Mickley H.S. and Grotch S.L., A.I.Ch.E.Jl. 10,149 (1964).

197. Shabaker R.H., Ph.D. Thesis, Univ.Wisconsin, 1965.

198. Fredlein R.A. and Lauder I., Aust.J.Chem., 22,33 (1969).

199. Dyne S.R., Glasser D. and King R.P., Rev.Sci.Inst. 38, 209 (1967).

200. Ferron J.R. in "Efficient Computer Methods for the Practising Chemical Engineer", Inst.Chem.Engrs., London, 1967.

201. Williams R.D., Chem.Eng.Educ. 8,1,28 (1974).

202. Chen H. H.-Y. and Aris R., Automatica 2,41 (1964).

203. Ray W.H. and Aris R., Automatica 3, 53 (1965).

204. Furusawa T., Nishimura H. and Miyauchi T., J.Ch.E.Japan 2,95 (1969).

205. University of Edinburgh, Undergraduate Research Project under the supervision of D.L. Cresswell (1975).

206. Kittrell J.R. in Drew T.B. et al (editors), Adv.Chem.Eng. 8,97-183, Acad.Press., N.Y., 1970.

207. Glasser D. and Williams R.D., I.E.C. Funds, 10,516 (1971).

208. Seinfeld J.H. and Chen W.H., Chem.Eng.Sci. 26,753 (1971).

209. King R.P., South African Jl.Sci. 63,91 (1967).

210. Neuman C.P. and Casasayas F.G., Trans.ASME, Jl.Dynamic Systems, Measurement and Control 94, 310 (1972).

211. Kagiwada H.H., "System Identification - Methods and Applications", Addison-Wesley, Reading, Mass., 1974.

212. Diamesis J.E., Proc.I.E.E.E. 53, 205 (1965).

213. Garnett J.R. and Eisenberg L., Proc.I.E.E.E. 61,490(1973).

214. Cresswell D.L., University of Edinburgh; unpublished paper.

215. Personal Communications from S.W. Elliott, Institute of Nuclear Medicine (1974 and 1975).

216. Calderbank P.H. and Pogorski L.A., Trans.Inst.Chem.Engrs. 35, 195(1957).

217. Grassman P., "Physical Principles of Chemical Engineering", Pergamon, Oxford, 1971.

218. De Wasch A.P. and Froment G.F., Chem.Eng.Sci. 27,567 (1972).

219. Olbrich W.E. and Potter O.E., Chem.Eng.Sci. 27, 1723 (1972).

220. Marivoet J., Teodoroiu P. and Wajc S.J., Chem.Eng.Sci. 29, 1836 (1974).

221. Gunn D.J. and Khalid M., Chem.Eng.Sci. 30, 261 (1975).

222. Valstar J.M., Bik J.D., and Van der Berg P.J., The Chemical Engineer (London) 227, CE 136 (1969).

223. Ellis S.N., Ph.D. Thesis, University of Edinburgh (1973).

224. Ramirez G., Ph.D. Thesis, University of Edinburgh (1975).

225. Agnew J.B. and Potter O.E., Trans.Inst.Chem.Engrs. 48, T15 (1970).

226. Olbrich W.E., Proc.Chemeca '70 Conference, Session 6A, p.101; Inst.Chem. Engrs.Symp.Ser., No.33, Butterworths of Australia and Inst.Chem.Engrs., 1971.

227. Olbrich W.E. and Potter O.E., Chem.Eng.Sci. 27, 1733 (1972).

228. Carslaw H.S. and Jaeger J.C., "Conduction of Heat in Solids", O.U.P., 1959.

229. Bunnell D.G., Irvin H.B., Olson R.W. and Smith J.M., Ind.Eng.Chem. 41, 1977 (1949).

230. Benenati R.F. and Brosilow C.B., A.I.Ch.E.Jl. 8, 359 (1962).

231. Roblee L.H.S., Baird R.M., and Tierney J.W., ibid 4, 460 (1958).

232. Blum E.H. and Wilhelm R.H. in "Application of Mathematical Models in Chemical Engineering Research, Design and Production", Proc.Symposium No.4, A.I.Ch.E.-I.Chem.E. Joint Meeting, London, June 1965, p.21.

233. Ridgway K. and Tarbuck K.J., J.Pharm.Pharmac. 18, Supplement, 168S (1966).

234. Watson J.T.R., "Viscosity of Gases in Metric Units", H.M.S.O., 1972.

235. Fahien R.W. and Smith J.M., A.I.Ch.E.Jl. 1, 28 (1955).

236. Yagi S. and Kunii D., A.I.Ch.E.Jl., 3, 373 (1957).

237. Kunii D. and Smith J.M., A.I.Ch.E.Jl. 6, 71 (1960).

238. Yagi S. and Wakao N., A.I.Ch.E.Jl., 5, 79 (1959).

239. Hilsenrath J. et al "Tables of Thermodynamic and Transport Properties", Pergamon, Oxford, 1960.

240. Olbrich W.E., Agnew J.B. and Potter O.E., Trans.Inst.Chem.Engrs. 44, T207 (1966).

241. Duncan P., "Heat Transfer in Packed Beds", E.U. Department of Chemical Engineering, Final Year Research Report, 1975.

242. Davies W.E.R. and Unger J.I., Institute for Aerospace Studies, Univ. Toronto, January 1973. UTIAS Technical Notes numbers 184, 185.

243. Priestley A.J. and Agnew J.B., I.E.C. Proc. D. and D. 14, 171 (1975).

244. Aris R., "The Mathematical Theory of Reaction and Diffusion in Permeable Catalysts", O.U.P., 1975.

245. Marek M. and Stuchl I., Chem.Eng.Sci. 30, 555 (1975).

246. Ha K-D and Hanna O.T., paper submitted to Chem.Eng.Sci.

247. Carey G.F. and Finlayson B.A., Chem.Eng.Sci. 30, 587 (1975).

248. Hite R.H. and Jackson R., Chem.Eng.Sci. 30, 641 (1975).

249. Hsiang T.C. and Reilly P.M., Can.J.Ch.E. 52, 830 (1974).

250. Pritchard D.J. and Bacon D.W., Chem.Eng.Sci. 30, 567 (1975).

251. Paterson W.R., an unpublished experimental investigation into the kinetics of the oxidation of o-xylene over Vanadia catalyst, in a spinning catalyst basket reactor.

252. Calderbank P.H. in: Advances in Chemistry Series, Number 133, "Chemical Reaction Engineering II", A.C.S., 1974.

253. Joly C., Andrianne J., Ginoux J.J. and Thiry F., Int.Jl.Heat and Mass Transfer, 17,803 (1974).